2009-01-01

Toxicity assessment of single-walled carbon nanotubes

Eva Herzog
Technological University Dublin

Recommended Citation

Herzog, Eva. (2009). *Toxicity assessment of single-walled carbon nanotubes*. Technological University Dublin. doi:10.21427/D7459K

Toxicity assessment of single-walled carbon nanotubes

by

Eva Herzog, B. Sc. (Hon.)

A thesis submitted to the Dublin Institute of Technology in partial fulfillment for the degree of

Doctor of Philosophy

Supervisors: Dr. Hugh J. Byrne

Dr. Maria Davoren

Radiation and Environmental Science Centre / School of Physics,

Focas Institute, Dublin Institute of Technology

January 2009

"Es ist durchaus richtig und alle geschichtliche Erfahrung bestätigt es, daß man das Mögliche nicht erreichte, wenn nicht immer wieder in der Welt nach dem Unmöglichen gegriffen worden wäre."

Max Weber (1864 – 1920)

Dedicated to my mum

Abstract

The objective of this study was to investigate the potential adverse health effects of occupational exposure to SWCNT dust using various *in vitro* approaches. Lung epithelium (represented by A549 and NHBE cells) was chosen as target cell model and exposed to minimally processed particle samples under submerse conditions and effects were compared to that of carbon black and crocidolite asbestos exposure. Cytotoxicity studies indicated low acute cytotoxicity of SWCNT. Morphological changes included decreases in microvilli and increased numbers of surfactant storing lamellar bodies and changes in cytoskeleton. Due to interactions of SWCNT and toxicity indicator dyes, the clonogenic assay was chosen as an alternative to quantify cytotoxicity and showed that long-term exposure lead to decreased cell proliferation. This effect was not only attributed to direct particle effects but also secondary SWCNT toxicity due to medium depletion. Intracellular reactive oxygen species (ROS) could only be detected in the absence of foetal bovine serum (FBS) supplements. An inflammatory mediator response was never observed. In contrast, suppression of lipid and inflammatory mediators was seen as characterised by the downregulation of interleukin-8 (IL-8) and cyclooxygenase-2 (COX-2) gene expression, inhibition of IL-8 and IL-6 promoter activation and decreased protein release of IL-8, IL-6 and macrophage chemoattractant protein-1 (MCP-1). The same response was found for cells immunologically induced by tumour-necrosis factor-α (TNF-α). Suppressive effects were partly due to TNF-α adsorption onto SWCNT surfaces. Dispersion of SWCNT in dipalmitoylphosphatidylcholine (DPPC) solution decreased particle agglomerate sizes and increased both cytotoxicity and oxidative potential.

Declaration

I certify that this thesis which I now submit for examination for the award of Doctor of Philosophy (PhD), is entirely my own work and has not been taken from the work of others, save and to the extent that such work has been cited and acknowledged within the text of my work.

This thesis was prepared according to the regulations for postgraduate study by research of the Dublin Institute of Technology and has not been submitted in whole or in part for another award in any Institute.

The work reported on in this thesis conforms to the principles and requirements of the Institute's guidelines for ethics in research.

The Institute has permission to keep, lend or copy this thesis in whole or in part, on condition that any such use of the material of the thesis be duly acknowledged.

Signature 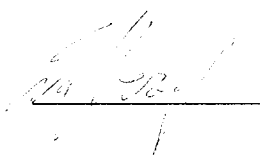 Date 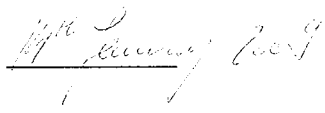

Acknowledgements

I would like to sincerely thank the following people without whom the completion of this thesis would not have been possible.

First of all I would like to thank my supervisor Hugh. J. Byrne. It wouldn't have been possible to do this work without all his ideas and advice. A special thanks also to my supervisor Dr. Maria Davoren who encouraged me throughout my studies, always offering support and never loosing her positivity. Thanks to both of you for letting me do my own thing whenever I wanted to, I really appreciate it.

I also would like to thank everyone who assisted me with my experiments throughout this project. First of all thanks to Dr. Alan Casey for his work and help with the spectroscopy and particle characterisation. Thanks to Prof. Albert Duschl and Dr. Geja Oostingh from the Department of Molecular Biology at the University of Salzburg for the opportunity to collaborate and a special thanks to Geja for her supervision during that time. A big thanks to Dr. Konrad L. Maier, Dr. Anke G. Lenz, Dr. Ingrid Beck-Speier, Helga Hinze-Heyn and Barbara Oswald for the advice and assistance during my stay at the Institute of Inhalation Biology at the Helmholtz Zentrum München. Thanks also to Dr. Marion Frankenberger and everyone of the Clinical Cooperation Group for allowing me to work in their labs and supervise me throughout the experiments carried out in Gauting. Thanks to Dr. Fiona M. Lyng for her help with the cell microscopy and clonogenic assay and thanks to Dr. David Cottell for his assistance with the TEM studies.

Finally of course a huge thanks to everyone at the Focas Institute and the RESC to make my time here so enjoyable. A special thanks to Elaine, Karina and Co., I wouldn't have had such a great time in Ireland without you. I'll miss you all.

Vielen Dank an Prof. Helmers für seine Unterstützung, vor allem während meiner Zeit in Athlone. Und ein großes Dankeschön Dir, Stefan, dass du während der letzten drei Jahre für mich da warst, und ich mich immer auf Dich verlassen konnte, warst mir wirklich eine große Hilfe. Letztendlich natürlich noch ein extra grosses Danke an meine Mama, ohne die es nie moglich gewesen wäre, überhaupt zu studieren und nach Irland zu kommen, bist die Beste.

Abbreviations

5-LO	5-lipoxygenase
A549	Human alveolar type II carcinoma cell line
A549-IL6	A549 cell line transfected with eh IL-6 promoter region
A549-IL8	A549 cells line transfected with the IL-8 promoter region
A549-NF-κB	A549 cell line transfected with the NF-κB binding sequence
A549-TNF-α	A549 cell line transfected with the TNF- α promoter region
AB	Alamar Blue™
ACEA	European Association of Car Makers
Ad-Mol	Adhesion molecules
AFM	Atomic force microscopy
AK	Adenylate kinase
ALB	Aggregation of lamellar bodies
AM	Alveolar macrophage
ANOVA	Analysis of variances
AP-1	Activator protein 1
ApoE	Apolipoprotein E
Apop	Apoptotic cells
ArcD SWCNT	Arc discharge produced SWCNT
ATCC	American type culture collection
BEAS-2B	Normal human bronchial epithelial cell line
BLAF	Bronchoalveolar lavage fluid
BSA	Bovine serum albumin
C_{60}	Fullerene
Ca	Calcium

Carboxy-DCF	6-carboxy-2', 7'-dichlorofluorescein, oxidised form
Carboxy-DCFH	6-carboxy-2', 7'-dichlorofluorescein, oxidised form
Carboxy-H_2DCFDA	6-carboxy-2',7'-dichlorodihydrofluorescein diacetate
CB	Coomassie Blue
CD	Cluster of differentiation
cDNA	Copy DNA
CLSM	Confocal laser scanning microscope
CNT	Carbon nanotubes
Co	Cobalt
CO_2	Carbon dioxide
CI	Confidence interval
COX-2	Cyclooxygenase-2
COPD	Chronic obstructive pulmonary disease
$cPLA_2$	Cytosolic phospholipase A_2
DAPI	4' ,6-Diamidino-2-phenylindol
DEP	Diesel exhaust particles
DJ	Desmosome junction
DLS	Dynamic light scattering
DMEM-F12	Dubecco's modified essential medium-F12 nutrient mix
DMSO	Dimethylsulfoxide
DNA	Deoxyribonucleic acid
DPPC	Dipalmitoylphosphatidylcholine
DPX	chlorimuron ethyl
EC	European Commission
EC_{50}	Effective concentration leading to a 50% response

ECACC	European collection of cell cultures
EDTA	Ethylenediaminetetraacetic acid
EIA	Enzyme immunosorbant assay
ELB	Extracellular lamellar body
ELISA	Enzyme linked immunosorbant assay
EPA	Environmental Protection Agency
EPITH	Epithelial cells
ERK	Extracellular signal-regulated kinases
E-selectin	Endothelial adhesion molecule 1
EtOh	Ethanol
F12K	Kaighn's modification cell culture medium
FACS	Fluorescence associated cell sorter
FBS	Foetal bovine serum
Fe	Iron
FITC	Fluorescein isothiocyanate
FP	Filopodia
FP6	6th Research Framework Programme
FP7	7th Research Framework Programme
f-SWCNT	Functionalised SWCNT
FU	Fluorescent units
GSH	gluathione
H	Hours
H_2O_2	Hydrogen peroxide
HaCaT	Normal human keratinocyte cell line
HiPco® SWCNT	High pressure carbon monoxide produced SWCNT
HRP	Horseradish peroxidise

HT	High density tubes
ICAM-1	Intercellular adhesion molecule 1
IgG	Immunglobulin G
IL	Interleukin
iNOS	Inducible nitric oxide synthase
IκB	Inhibitor of κB
L	Lipid droplet
LAL	Limulus amobocyte lysate
LB	Lamellar bodies
LPS	Lipopolysaccharide
LPS-PA	Lipopolysaccharide derived from *Pseudomonas aeruginosa*
LTB4	Leukotriene B4
LUC	Luciferase
LYM	Lymphocytes
M	Metaphase
MAP	Mitogen-activated protein
MARCO	Macrophage receptor with collagenous structure
MCP-1	Macrophage-chemoattractant protein-1
M-CSF	Macrophage-colony stimulating factor
MdM	Monocyte derived macrophages
Mg	Magnesium
MHC	Major histocompatibility complex
MIP	Macrophage inflammatory protein
MKK	Mitogen-activated protein (MAP) kinase kinase
MMD	Mass median diameter
Mo	Molybden

mRNA	Messenger RNA
Mt	Mitochondria
MTT	3-(4,5-Dimethylthiazol-2-yl)-2,5-diphenyltetrazoliumbromid
Mv	Microvilli
MVB	Multivesicular body
MWCNT	Multi-walled carbon nanotubes
NAC	N-acetyl-l-cysteine
NADPH	reduced nicotinamide adenine dinucleotide phosphate
Nec	Necrotic cell
NEUT	Neutrophils
NF-κB	Nuclear factor-κ-B
NHBE	Primary normal human bronchial epithelial cell line
Ni	Nickel
NP	Nanoparticle
NR	Neutral Red
Nuc	Nucleus
OECD	Organisation for Economic Development
P90	Printex 90 carbon black
PAH	Ployaromatic hydrocarbon
PBMC	Peripheral blood monocytic cells
PBS	Phosphate buffered saline
PCR	Polymerase chain reaction
$Pd(N)_6$	Random hexamer
PE	Phycoerythrin
PGE_2	Prostaglandin E_2
PI	Propidum iodide

PLA_2	Phospholipase A_2
PM	Particulate matter
$PM_{0.1}$	Particulate matter < 0.1 μm
$PM_{2.5}$	Particulate matter < 2.5 μm
PP	Pseudopodia
RBM	Radial breathing modes
RER	Rough endoplasmic reticulum
RLT buffer	RNeasy lysate buffer
RLU	Relative light units
RNA	Ribonucleic acid
ROS	Reactive oxygen species
RPMI 1640	Roswell Park Memorial Instiute developed culture medium
RT	Room temperature
RT-PCR	Reverse transcriptase PCR
SD	Standard deviation
SDBS	Sodium dodecyl benzene sulfonate
SDS	Sodium dodecylsulphate
SF	Single fibre
SiO_2	Quartz
$sPLA_2$	Secretory phospholipase A_2
SWCNT	Single-walled carbon nanotubes
TEM	Transmission electron microscopy
TF	Tonofilaments
TiO_2	Titanium dioxide
TLR	Toll-like receptor
TMB	Tetramethylbenzidine

TNF-α	Tumour-necrosis-factor-α
TRITC	Tetramethyl rhodamine iso-thiocyanate
Triton-X	$C_{14}H_{22}O(C_2H_4O)_n$
Tween	Polysorbate
UICC	Union interanation contre le cancer
UV	ultraviolet
VCAM-2	Vascular cell adhesion molecule 2
WST-1	2-(2-methoxy-4-nitrophenyl)-3-(4-nitrophenyl)-5-(2,4-disulfophenyl)-2H tetrazolium
Y	Yttrium
ZnO	Zinc oxide

Table of Contents

Page

Chapter 1

Chapter 2

Table of Figures

Page

Table of Tables

Page

Chapter 1

Introduction

1.1 Objectives

Nanotechnology, identified as one of the key technologies of the 21st century, is attracting increased funding and investment world-wide, ultimately leading to a rise in development and production of nanoparticles (size: 1-100 nm) [1]. Carbon nanotubes (CNT) are an example of a carbon-based nanomaterial [2] which has generated enormous popularity in nanotechnology due to their unique properties, offering a wide range of potential applications within commercial, medical and environmental sectors and have been one of the most extensively studied nanoobjects [3, 4]. Consequently, occupational and public exposure to carbon nanotubes will increase dramatically in the near future [5]. In an ideal scenario, the potential human and environmental impacts of these nanomaterials should be thoroughly investigated prior to such exposure so that the appropriate safety actions (if warranted) can be put in place. However, very little is currently known about the potential health risks associated with this new material. Carbon nanotubes (CNT) have a large surface area for potential interactions. In addition, they are long and thin fibres as shown in Figure 1.1 and are often compared to asbestos so that there is particular concern about their safety. The primary objective of this study is therefore to investigate the potential occupational health risks of single walled carbon nanotube (SWCNT) exposure using various *in vitro* techniques, including cellular and molecular endpoints such as cytotoxicity, clonal survival, formation of reactive oxygen species (ROS) and lipid and inflammatory mediator release. As lung epithelium represents one of the first tissues coming into contact with aerosolised carbon nanotubes, the study focused on the assessment of

pulmonary toxicity and therefore human lung epithelium was chosen as target cell model.

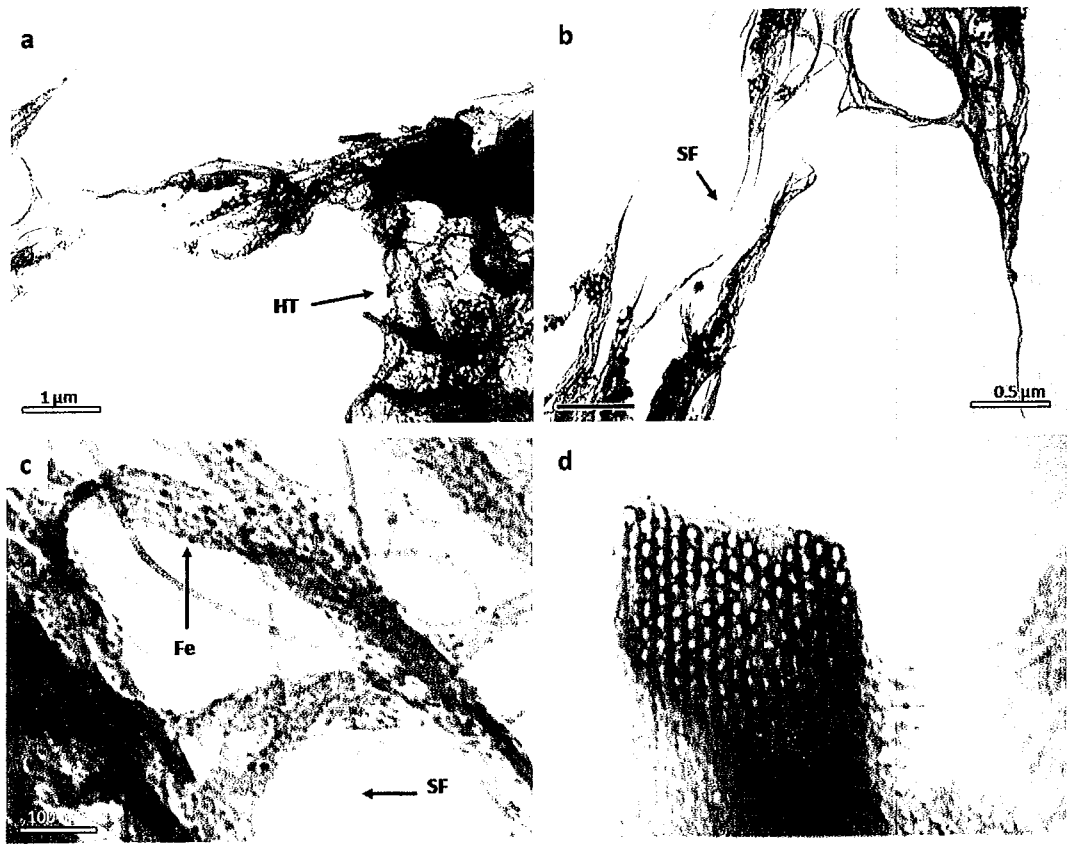

Figure 1.1:(a-c) Transmission electron microscopy (TEM) images of HiPco® SWCNT (as purchased) showing high density tubes (HT), single nanotube fibres (SF), and iron catalyst residues (Fe) obtained using a Jeol 100CX TEM. Image (d) shows a SWCNT bundle as grown during synthesis [6].

The degree of dispersion ultimately determines the way in which particles are presented to exposed tissue. In order to mimic the occupational exposure to SWCNT dust as closely as possible, this study aimed to employ minimal processing of SWCNT samples by avoiding synthetic surfactants or functionalisation. Furthermore, the influence of dispersion medium on SWCNT reactivity was

investigated with the objective of choosing the most relevant vehicle for pulmonary toxicity assessment.

Carbon nanotubes represent a novel material which also present novel challenges for toxicity testing. It is well established that SWCNT and other carbon-based nanomaterials interact strongly with many molecular species including small organic molecules [7, 8], polysaccharides [9, 10], proteins and deoxyribonucleic acid (DNA) [11, 12]. Consequently, SWCNT may also interact and interfere with organic molecules that are present or frequently employed during toxicity assessment. In addition, SWCNT are highly insoluble in aqueous media used in biological systems. As a result, evaluating the effects of SWCNT exposure poses a great challenge. Investigating and characterizing any potential interactions of SWCNT is of utmost importance for the interpretation of toxicity data obtained following SWCNT exposure studies. Furthermore, the identification and development of alternative test methods may be required in order to replace methods and endpoints that are not suitable for evaluating SWCNT toxicity. Therefore, this study not only aims to assess cellular and molecular effects of SWCNT exposure on lung epithelium *in vitro* but also to investigate the compatibility of SWCNT and various test systems used for toxicity assessment in order to develop strategies for accurate risk assessment of carbon nanomaterials.

1.2 Study design

The overall design of this study is illustrated in Figure 1.2 including the characterisation of physical/chemical properties and interactions of the test

particles with their molecular environment using various spectroscopic techniques. The *in vitro* toxicity of SWCNT was assessed on both, the cellular and molecular level. In addition, morphological changes and particle uptake were assessed using microscopic evaluation.

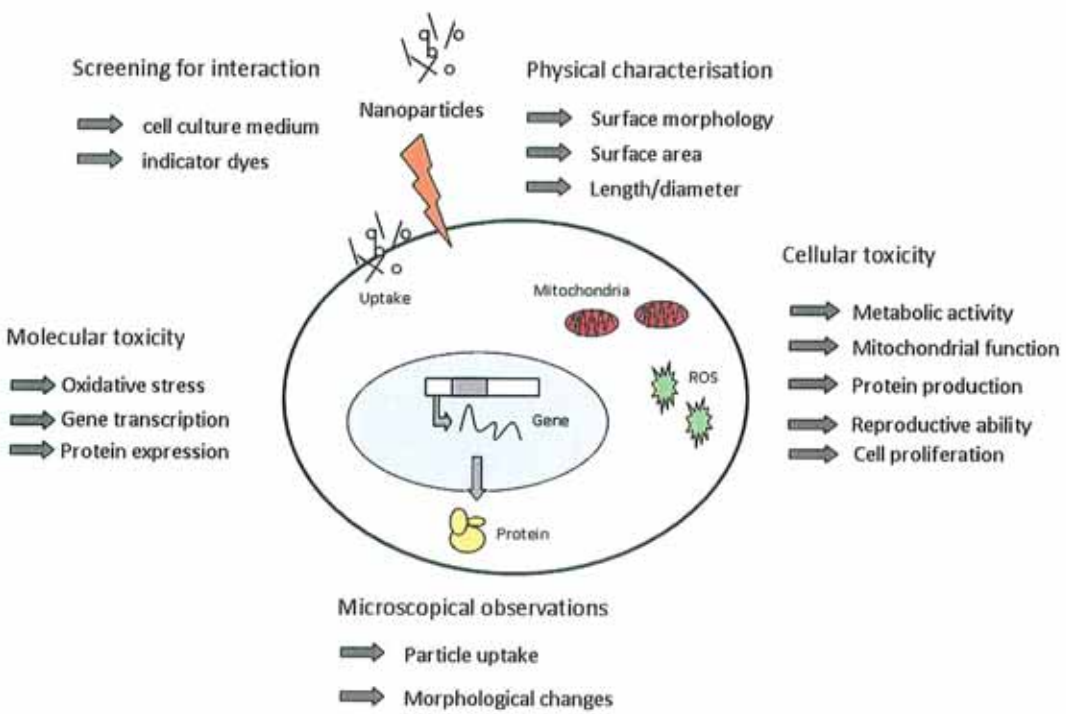

Figure 1.2: Schematic presentation of the project design.

1.2.1 Target tissue

The lungs are regarded as one of the main portals of entry for nanoparticles, which emphasises the importance of pulmonary toxicity evaluation. The first barrier that confronts inhaled particles that deposit on conducting airways or the alveolar region is the epithelium [13] as illustrated in Figure 1.3. Furthermore, epithelial cells of the respiratory tract are regarded as regulators of airway inflammation in

addition to alveolar macrophages and fibroblasts [14]. They play a key role in the modulation of inflammatory processes by releasing inflammatory cytokines [15, 16] and are affected in asthma, bronchitis, pulmonary fibrosis and lung cancer [17].

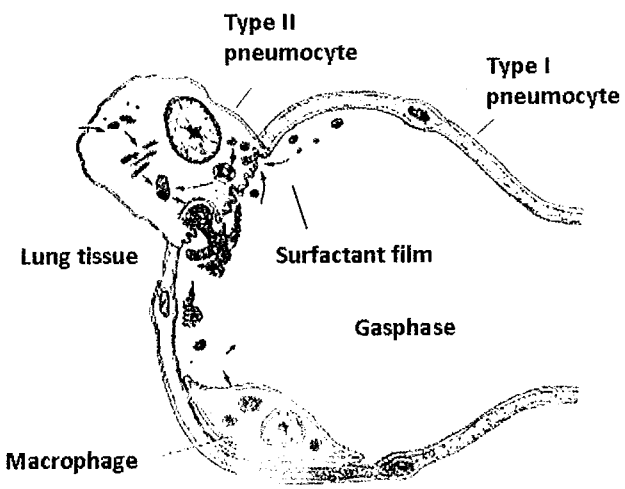

Figure 1.3: Schematic illustration of lung tissue including type I and II pneumocytes and macrophages covered by a lung surfactant film [18].

The lung epithelial surface area is mainly made of type I cells. However there is no reliable human *in vitro* model available for this cell type and therefore alveolar epithelial type II cells are commonly used as a substitute [19]. This is reasonable since type II cells are able to proliferate and transdifferentiate into type I cells when the existing type I cell population is damaged in the lung alveoli [20]. The epithelial type II carcinoma cell line A549 (shown in Figure 1.4a) was thus chosen as appropriate target cells throughout this study. Cell lines should preferably be freshly-derived, non cancerous cells. Otherwise, responses should be thoroughly compared with those of normal cells to ensure that effects on cancer cells do not

differ greatly [21]. Therefore, in addition to A549 cells, the normal human bronchial epithelial cell line BEAS-2B (Chapter 4) and the primary human bronchial epithelial cells NHBE as shown in Figure 1.4b (Chapter 5 and 6) were included.

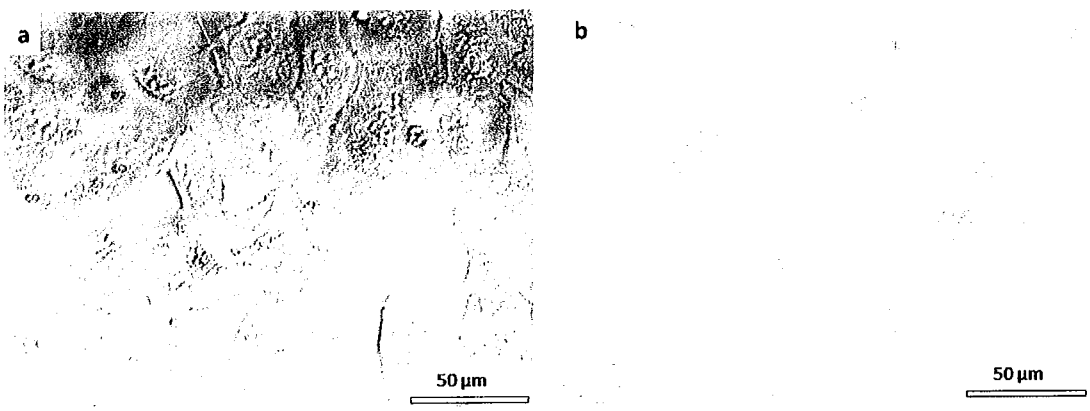

Figure 1.4: Micrographs of (a) A549 and (b) NHBE cell monolayers.

Macrophages play another key role in the cellular response to particles inhaled into the lungs [22] and alveolar macrophages play an indisputable role among the pulmonary host defence mechanisms in the innate immune system. They clear the alveolar region from inhaled particles and cellular debris [23]. Early responses by the macrophages to inhaled foreign material, including airborne particles, are essential for a proper activation of the pulmonary immune system and seem to play a key role in the response to toxicants [24]. Therefore, including macrophages (Chapter 7) in addition to lung epithelial cells would aid in creating a more complete picture of the pulmonary response to SWCNT as shown in Figure 1.3.

Mononuclear cells in the circulation have the capacity for phagocytosis and propensity to differentiate to macrophages under certain circumstances [25, 26].

In the alveoli, there are macrophages present that have migrated from blood and are similar in properties to monocytic cells [27-29]. Therefore, monocyte derived macrophages (MdM) can serve as a model for alveolar macrophages and were chosen as an additional cell model in this study (Chapter 7).

The skin with its large surface area is another potential route for occupational and environmental exposure to nanomaterials and serves as one of the principal portals of entry for nanoparticles [30]. Dermal keratinocytes play an important role in the cell renewal system and in maintaining skin integrity and are commonly used as a model for testing dermal toxicity [31, 32]. Therefore, in Chapter 3 and 4, the immortalized non-tumorigenic human dermal keratinocyte cell line HaCaT was included as dermal cell model in order to evaluate the specificity or universality of cell responses and to validate test methods used for particle toxicity assessment.

1.2.2 Test particles and concentrations

The high pressure carbon monoxide (CO) disproportionation (HiPco®) method is the most commonly used technique to produce SWCNT of high purity [33-35]. Therefore, HiPco® SWCNT were chosen as the most relevant SWCNT candidates for toxicity testing. In addition, SWCNT synthesised using electric arc discharge (ArcD), the first and still one of the most widely used methods [2, 36], were selectively included (Chapter 4, 5 and 7) in order to determine the role of production method on SWCNT toxicity. A more extensive description of SWCNT synthesis will be given in Chapter 2, 2.3.1. Particles were left unrefined in order to assess toxic responses to the SWCNT samples in its entirety, including impurities.

It is without question that the toxicity obtained for SWCNT samples may contain contributions from contaminants such as transition metal residues present. However, the the effects of individual contaminants were not centre of this study and may be explored as part of future investigations.

Carbon black represents one of the most studied ultrafine particles and thus a wide range of toxicity data is available [37-40]. Furthermore, it is closely related to SWCNT on a chemical basis. This led to the choice of including nanoparticulate Printex 90 (P90) carbon black as control particles allowing the assessment of chemistry and morphology on particle toxicity (Chapter 4 and 7).

Quartz (SiO_2) is one of the most widely used positive control particles as it has been proven to lead to cytotoxic and inflammatory reactions in exposed tissues [41-43]. Therefore, quartz was chosen as a control particle of known toxicity in Chapter 3.

The structural resemblance to asbestos fibres has put SWCNT in a particularly critical position [44]. Therefore, quartz was replaced by crocidolite asbestos as control particle of choice in selected studies in order to determine whether CNT have the potential of being asbestos-like. Crocidolite asbestos is a member of the amphibole asbestos group that is often considered as the most pathogenic and oncogenic type of asbestos [45-47].

Exposure concentrations were chosen to be comparable to previous studies investigating the toxicity of carbon nanotube material [31, 48-52] so that 1.56 to 800 μg/ml were identified to be appropriate for the assessment of SWCNT cytotoxicity. The effects of SWCNT exposure on the molecular level (Chapter 5-7)

were assessed for concentrations outside the cytotoxic range. Therefore, studies were carried out for SWCNT concentrations ranging between 1.56 and 50 µg/ml only.

Carbon particles in solution behave very differently to molecules so that following sonication and exposure, the main particle fraction tends to settle onto the bottom of the culture vessels. Therefore, it was decided to express the exposure doses as mass of particles per exposed surface area (µg/cm^2) in addition to mass per volume (µg/ml). However, due to the wide length distribution of nanotube samples and varying surface areas depending on the degree of aggregation, exact characterisation of exposure doses was still difficult [48] and the expression of particle concentration as particle number per cell was not applicable to this study.

1

1.2.3 Particle characterisation

Studies on nanoparticles, asbestos and other fibres have shown that dimension, durability and dose are key parameters for determining the toxicity of particles [53]. With respect to the generation of ROS and development of fibrosis and cancer, particle surface characteristics are of utmost importance, as seen with quartz particles [21]. Thus, for evaluating the effects of CNT *in vivo* or *in vitro*, characterisation of the physico-chemical properties of the test material, including size distribution, mass, concentrations and particle numbers present, shape, crystal structure, chemical composition, surface area, surface chemistry, surface charge, and porosity is critical. Carbon nanomaterials are difficult to disperse as an aerosol and tend to clump into large masses, so that the agglomeration state also

needs to be determined. This information is necessary to ensure that all potentially significant characteristics are known to allow retrospective interpretation of toxicity and inter-study comparisons. Ideally, materials should be characterised as they are supplied or produced, at the point of administration, and afterwards. This would help to identify any changes in the material due to physisorption or chemisorption of biomolecules, changes in surface chemistry due to biochemical events or other physicochemical changes following interaction with surrounding biological systems, which might have influence on aggregation state and/or solubility [21]. However, due to its physical properties, the characterisation of SWCNT material is highly challenging and many common characterisation and detection methods are not applicable for SWCNT dispersions, e. g. dynamic light scattering (DLS).

1

Transmission Electron Microscopy (TEM), considered as the gold standard in many cases for nanoparticle characterisation, Raman spectroscopy, BET and AFM were employed for characterisation of SWCNT powders used in this study. Raman, UV-vis and fluorescence spectroscopy as well as optical microscopy were used for the description of SWCNT following dispersion in biological media.

1.2.4 Particle dispersion

As a means to reduce the formation of SWCNT bundles, researchers have employed numerous carrier solvents including media with varying percentages of FBS, other sera or organic synthetic surfactants as further discussed in Chapter 2, 2.3.5.2.1.3). In order to mimic occupational exposure to SWCNT dust in this study, test particles

were suspended in cell culture growth medium using short-term sonication, without the use of synthetic surfactants. Due to their highly adsorptive nature, it is most likely that during human exposure, particles such as CNT would come into contact with a variety of different molecules leading to coating by various components present within a biological system [54, 55], therefore it was decided to use foetal bovine serum (FBS) as a supplement in cell culture medium. Furthermore, cells are routinely grown in FBS supplemented culture medium so that removal of FBS may have negative consequences on cell performance. However, it has been previously demonstrated that the toxicity of particles may differ in the presence of FBS compared to FBS free environments [56-58]. Therefore within the first experimental study (Chapter 3), exposures were carried out in the presence and absence of FBS in order to identify the role of FBS on particle toxicity. Consequently, this information was taken into account for further investigations.

Upon inhalation, it is hypothesised that particles may deposit in the lung and come in contact with lung surfactant which consists of lipids and specific proteins that line the air-liquid interface of the alveolar surface and bronchioles [59, 60]. Lung surfactant is synthesized and secreted by alveolar type II cells where it is stored in lamellar bodies [61, 62] and it is physiologically important for lowering the surface tension of the pulmonary alveolar hypophase surface [63]. Furthermore it protects against pathogens by opsonising bacterial, fungal and viral surface oligosaccharides through surfactant protein binding [64-66]. Experiments by Schürch *et al.* (1990) demonstrated that surfactant may aid in the displacement of particles from air to the aqueous phase and towards the lung epithelium [67]. In

addition, studies showed that when particles were present in peripheral airways and alveoli they exist in a completely immersed, wetted state below the surfactant film [67]. Approximately 90% of bronchoalveolar lavage fluid (BALF) consists of phospholipids with DPPC being the most abundant and the substance mainly responsible for the surface tension lowering properties [68]. Therefore, the use of DPPC dispersed into physiological saline has been used as a simple model of lung surfactant. Over the course of this study, international consensus evolved towards the need for more realistic exposure models so that DPPC was employed as dispersant in Chapter 5 and 6 in order to increase the biological relevance of the toxicity studies carried out and in order to assess whether DPPC has any influence on particle toxicity [69, 70].

Initially, an ultrasonic tip was employed for dispersing SWCNT in cell culture medium as it appeared to be the most effective method. However, over the course of this study, a method using an ultrasonic bath as described by Kreyling *et al.* (personal communications) was preferred due to the reduced risk of sample contamination.

1.2.5 Toxicity assessment

Toxicity evaluations started with the assessment of cytotoxicity using a battery of assays that determine multiple endpoints including metabolic viability (Alamar Blue™ reduction), protein content (Coomassie Brilliant Blue staining), lysosomal viability (Neutral Red uptake), mitochondrial activity (MTT and WST-1 reduction) and membrane integrity (Adenylate kinase release). In order to overcome and

avoid potential interferences of SWCNT with these endpoints, a more qualitative approach to toxicity assessment was included and morphological changes post SWCNT exposure were assessed using light, fluorescence and transmission electron microscopy.

The clonogenic assay was used as an alternative to dye based assays and allowed direct quantification of SWCNT toxicity. The toxicity of two forms of SWCNT which were synthesised by different production methods (HiPco® and ArcD SWCNT) was compared and furthermore, the responses were compared to the effects of nano-sized carbon black (P90). By taking into account colony size in addition to colony number, the effects of particle exposure on both cell proliferation and clonal survival could be determined. The universality of this novel application of the clonogenic assay including the use of both colony number and size was assessed by including HaCaT and BEAS-2B cells as additional cell models.

In addition to cytotoxicity assessment, the effects of SWCNT on a sub-cellular level were investigated by including a variety of molecular endpoints. Since oxidative stress represents one of the most central paradigms of nanoparticle toxicity [71] as further discussed in Chapter 2, 2.2.4.3, the formation of intracellular ROS was assessed following exposure of A549 and NHBE cells as a further part of this study. Formation of ROS was compared following HiPco® and ArcD SWCNT, P90 carbon black and crocidolite asbestos treatment. Furthermore, the role of dispersion vehicle, including FBS and DPPC, on the oxidative potential of test particles was investigated (Chapter 5).

Antioxidant depletion due to excess oxidative stress is believed to ultimately lead to inflammatory responses as illustrated in Chapter 2, Figure 2.3 [71, 72]. Therefore, following ROS measurements, the effects on inflammatory mediator release were assessed including the endpoints interleukin-8 (IL-8) gene expression and IL-8, interleukin-6 (IL-6), tumour-necrosis factor-α (TNF-α) and macrophage-chemoattractant protein-1 (MCP-1) release (Chapter 6). As for ROS formation, effects were compared between cancerous and primary epithelial cells and the role of DPPC dispersion was determined. In parallel, cells were induced by treatment with human recombinant TNF-α before particle exposure in order to compare the inflammatory responses of normal, healthy cells with those of cells in an immunologically induced state as present during infections. The SWCNT type most effective in inducing intracellular ROS was chosen as test particle together with crocidolite asbestos which has been reported to affect cell signalling cascades including inflammatory responses as will be further described in Chapter 2, 2.3.4.2.

1

Finally, the effect of SWCNT exposure on the propensity of macrophages to release inflammatory and lipid mediators was assessed in the presence and absence of the bacterial toxin lipopolysaccharide (LPS). Ultrafine carbon particles have been shown to affect lipid mediator release of exposed cells [39] so that the arachidonic acid pathway including COX-2 gene expression and prostaglandin E_2 (PGE_2) synthesis were included as further endpoints in this study and effects were compared between MdM and A549.

1.2.6 Method validation

Due to their highly adsorptive nature, SWCNT interact with a wide range of small organic molecules [8-11]. Thus, the interactions between SWCNT and the constituents of cell culture medium were investigated within this study. This was essential in order to be able to interpret any toxicity data obtained using cell culture models and assure the validity of test methods. Furthermore, it is conceivable that SWCNT might be able to absorb essential cell nutrients present in growth medium, making them unavailable for cultured cells, resulting in an indirect, secondary toxicity due to nutrient deprivation which was consequently included as a study endpoint. Protein adsorption by SWCNT was also considered for the interpretation of data resulting from protein analysis and inflammatory mediator response.

1

Common toxicity assays frequently employ the use of colorimetric or fluorescent indicator dyes. For that reason, in parallel to the cytotoxicity assessment, spectroscopic characterisation using UV-vis and Raman spectroscopy was carried out in order to determine whether SWCNT interact with the emission or absorbance measurements and therefore have the potential to interfere with assay endpoints leading to the risk of data misinterpretation (i.e. false positive or negative results). Quantifying the degree of interaction between SWCNT and indicator dyes used in biological studies is essential for the estimation and validation of their applicability for SWCNT toxicity assessment.

1.2.7 Thesis outline

The first part of Chapter 2 will give an overview on nanotechnology and nanomaterials with special regard to mechanisms of toxicity and single walled carbon nanotubes including their toxicological characteristics. The second part will present a summary of the recent literature available on SWCNT toxicity including a summary of cell uptake studies and frequently used CNT dispersion methods. A more comprehensive version of this information is also available in table form in Appendix C, Table C.1 to C3.

Due to the rapidly evolving nature of the field of nanotoxicology, experimental procedures varied depending on the type and stage of investigations carried out. Therefore, procedures and protocols are presented for every corresponding study. For lucidity purposes, a condensed summary of the respective study is given at the beginning of each experimental chapter.

The cytotoxicity studies carried out on SWCNT together with particle characterisation and a spectroscopic investigation into the interactions between SWCNT and commonly used colorimetric indicator dyes are described in Chapter 3. This study also determines the role of FBS supplements on particle toxicity and presents qualitative SWCNT toxicity assessment as a first step to overcome the interferences with indicator dyes and confirm cytotoxicity of test particles. Chapter 4 then introduces the clonogenic assay as an alternative way to quantify particle cytotoxicity avoiding the use of indicator dye based assays. Furthermore, it describes the indirect toxicity of SWCNT in terms of medium depletion.

Chapter 5 to 7 consecutively show investigations carried out to determine whether SWCNT also affect cells on the molecular level. As an initial response to particle exposure, Chapter 5 evaluates intracellular ROS formation following exposure of A549 and NHBE cells to HiPco® and ArcD SWCNT, P90 carbon black and crocidolite asbestos both in the presence and absence of DPPC dispersion.

Studies on whether HiPco® SWCNT are also able to induce an inflammatory response of lung epithelial cells (A549 and NHBE) are described in Chapter 6. In addition, this study further investigated the role of DPPC dispersion and immunological stimulation on inflammatory cell responses and compared the exposure to HiPco® SWCNT with that of crocidolite asbestos. Data not presented in the main text including time-point comparisons are illustrated in Appendix D. All investigations carried out on macrophages and lipid mediator responses are included in Chapter 7. The responses of individual MdM batches are illustrated in Appendix E.

Finally, conclusions on the pulmonary toxicity of SWCNT together with the challenges associated with nanotoxicity testing and recommendations are discussed in Chapter 8.

Chapter 2

Background on SWCNT toxicity

2.1 The field of Nanotechnology/ Nanoscience

Nanoscience is defined as "the study of phenomena and the manipulation of materials at atomic, molecular, and macromolecular scales, where properties differ significantly from those at larger scale" [1], and nanotechnologies as the manipulation, precision placement, measurement, modelling or manufacture of sub-100 nanomatre scale matter [73]]. Richard P. Feynman (1918-1988) was the first to mention the concept of nanoscience during his key lecture at the annual American Physical Society meeting in 1959 [74]. The Japanese researcher, Norio Taniguchi, spoke about "precision machining with tolerance of a micrometer or less" in 1974 and Eric Drexler first introduced the word nanotechnology in his book "Nanosystems" in 1986 predicting productivity growth and personal wealth due to nanotechnology [75].

Nanotechnology is widely perceived as one of the key technologies of the 21st century and accordingly there has been increased investment from government and industry worldwide. In 2005, nanotechnology research attracted around US$ 9.6 billion [76]. The European Commission (EC) has become the largest funding body in the field of nanotechnology worldwide. The scientific output in nanoscience increased at a compound annual growth rate of nearly 16% over the last decade [77]. The number of nanotechnology products and devices is growing rapidly with more than 300 already on the market [78]. The application of nanotechnology is believed to hold solutions to a number of environmental challenges including energy conservation, pollution prevention and remediation and disease prevention, detection and treatment. However, new technologies are also associated with new risks and there is great uncertainty regarding the

behaviour of nanoparticles in the environment and the human body. Therefore, the EC aims to develop a policy framework for the integrated, safe and responsible development of nanotechnology and the funding of research. Nearly € 1.4 billion were provided to nanoscience and nanotechnologies projects under the 6th Research Framework Programme (FP6) and more than double that funding is proposed to fund nanotechnology research up to 2013 under FP7 [79].

2.2 Nanoparticles

2.2.1 Ultrafine vs. engineered nanoparticles

The term "engineered nanomaterial" is used to describe materials that are deliberately created such that they are composed of discrete functional parts which have one or more dimensions of the order of 100 nm or less [80]. The size range of interest is typically from 100 nm down to the atomic level of around 0.2 nm [1]. The typical length scales is illustrated in Figure 2.1. Thin films and surface coatings, as used within features on computer chips, are examples of nanomaterials with one dimension in the nanoscale, whereas nanowires, nanotubes, and some biopolymers possess two nanoscaled dimensions. Other nanoparticles, such as fullerenes (C_{60}), dendrimer precipitates, colloids, quantum dots, or nanocrystalline materials are made up of three dimensions ranging within the nanoscale [1]. All of these materials are specifically designed to meet certain chemical and physical requirements which are very important in terms of their performance during application.

In contrast, non-engineered nanomaterials are unintentionally generated, such as ultrafine atmospheric particles formed during combustion processes. They are chemically heterogeneous and polydisperse, making comparisons with engineered nanomaterials problematic [81].

2.2.2 Physical characteristics of engineered nanomaterials

Materials in the nano-size range exhibit specific behaviours, resulting in different or enhanced properties, leading to a new range of possible applications compared to the same materials at a larger scale. Particularly towards the smaller end of this range, changes are due to both the increased surface area and the dominance of quantum effects [82, 83]. The smaller the particle, the greater the surface area per unit mass (relative surface area), so that chemical reactivity increases due to higher numbers of chemical reactions occurring at the surface. This is also the reason why some nanomaterials are likely to be useful as catalysts. The occurrence of quantum effects changes the optical, magnetic or electrical properties. For materials such as crystalline solids, small size causes a greater interface area within the material which has influence on both, mechanical and electrical properties [84, 85].

Tension affects physical and chemical properties at the larger end of this size range. Brownian motion, the random movement of larger particles and molecules due to the interaction with smaller molecules and atoms also has an influence, so that the control of individual atoms or molecules in these environments is very difficult [86].

2.2.3 Applications of engineered nanomaterials

Because of the wide range of potential applications of newly developed nanomaterials, there are great expectations into nanotechnology research. At present, nanoparticles are added to sunscreens and cosmetics or are used as composites, clays, coatings and surfaces to make tougher and harder cutting tools [87]. For example titanium and zinc oxide (TiO_2, ZnO) nanoparticles are used as UV filters in sunscreens, there are TiO_2 coated self-cleaning windows, and buckminster fullerenes (C_{60}) which have potential as drug delivery systems [88]. In the near future it is intended that nanoparticles will commonly be used in paints, environmental remediation, fuel cells, displays, batteries, fuel additives, and catalysts. Potential long-term applications include nanotube composites, low friction lubricants, magnetic material, medical implants, machinable ceramics, nanoengineered membranes for more energy efficient water purification or desalination, and enhancement of data storage [1].

2

A main area of interest is bio-nanotechnology and nanomedicine. Here, nanomaterials could be used as cellular engineering scaffolds, molecular motors, biomolecules for sensors in drug delivery and prosthetics [89]. Quantum dots could be used in solar energy or as fluorescent labels that can be tuned to emit or absorb particular colours of light, among other things useful in cancer diagnostics and treatment [88].

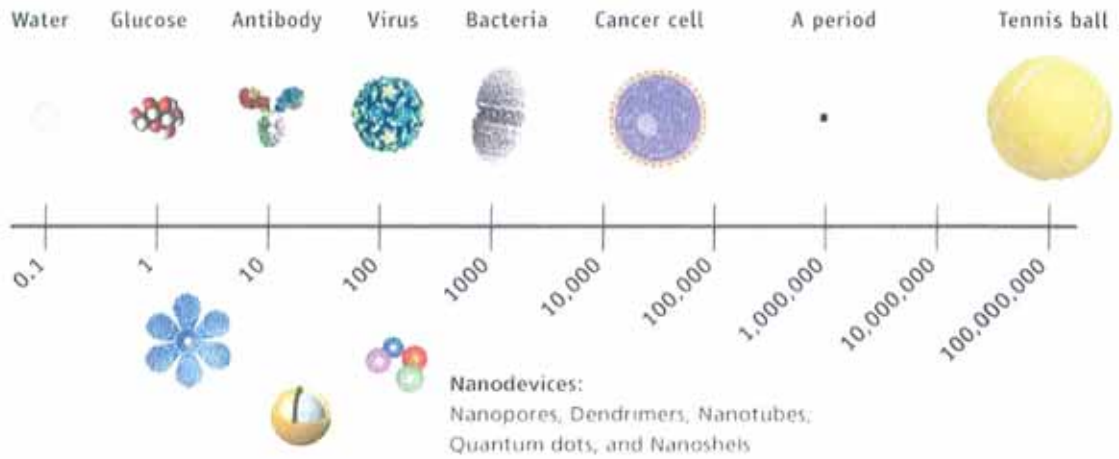

Figure 2.1: Length scale showing the nanometer in context [90].

2.2.4 Toxicological risk of engineered nanomaterials

Before novel materials can be incorporated into new and existing devices, their toxicity and biocompatibility needs to be investigated and before the use of nanomaterials becomes widespread, the potential occupational exposure hazards need to be acknowledged [91]. With an increasing number of consumer and industrial products containing engineered nanoparticles, the risk of human exposure increases and these materials may become a threat to the environment [92].

A gap currently exists in EU regulations for registering new chemical hazards, as particle size is not taken into account. Once a material has been accepted on the bulk scale, there is currently nothing to stop the same material being used as nanoparticle [88]. Almost nothing is known about uptake, distribution and toxicity, so that nanomaterials can potentially be toxic even if the bulk material is not [89]. The same physical and chemical properties that make these materials so attractive

may be associated with potentially harmful effects on cells and tissues. Their increased reactivity and their potential for unrestricted mobility make them commercially attractive for drug delivery into poorly accessible compartments of the body such as the brain but may also lead to cellular toxicity.

2.2.4.1 *Routes of exposure*

As illustrated in Figure 2.2, there are various exposure routes for manufactured nanomaterials, the main sources being occupation and the environment. They may become suspended in the air during fabrication, distribution, use and disposal and can enter the body through inhalation, ingestion, and dermal absorption. For therapeutic purposes, they might be directly injected into the body.

Even though it is unknown whether human exposure to nanomaterials is sufficient to cause health effects comparable with air pollution, under certain workplace conditions, they may be inhaled in significant amounts. Furthermore, nanoscaled particles may more easily enter the body than larger particles [93].

The lungs represent the primary route of exposure for any airborne particles which deposit on the airway or alveolar epithelium and encounter mucus or epithelial lining fluid. They may then interact with macrophages, resulting in clearance, or they can enter the interstitium where they may make contact with fibroblasts, endothelial cells and/or cells of the immune system [94]. Stober and Harris developed a mathematical model to estimate the aerodynamic diameter of a particle [95]. This aerodynamic diameter is defined as the diameter of a virtual sphere of unit density which would have the same penetration in the human

respiratory tract as the particle under consideration. The aerodynamic diameters depends on variables such as particle density, size, and form, whereas the outer diameter is the main determinant, and can be used to predict where a particle deposits in the respiratory tract which ultimately helps to identify the relevant target tissue [95].

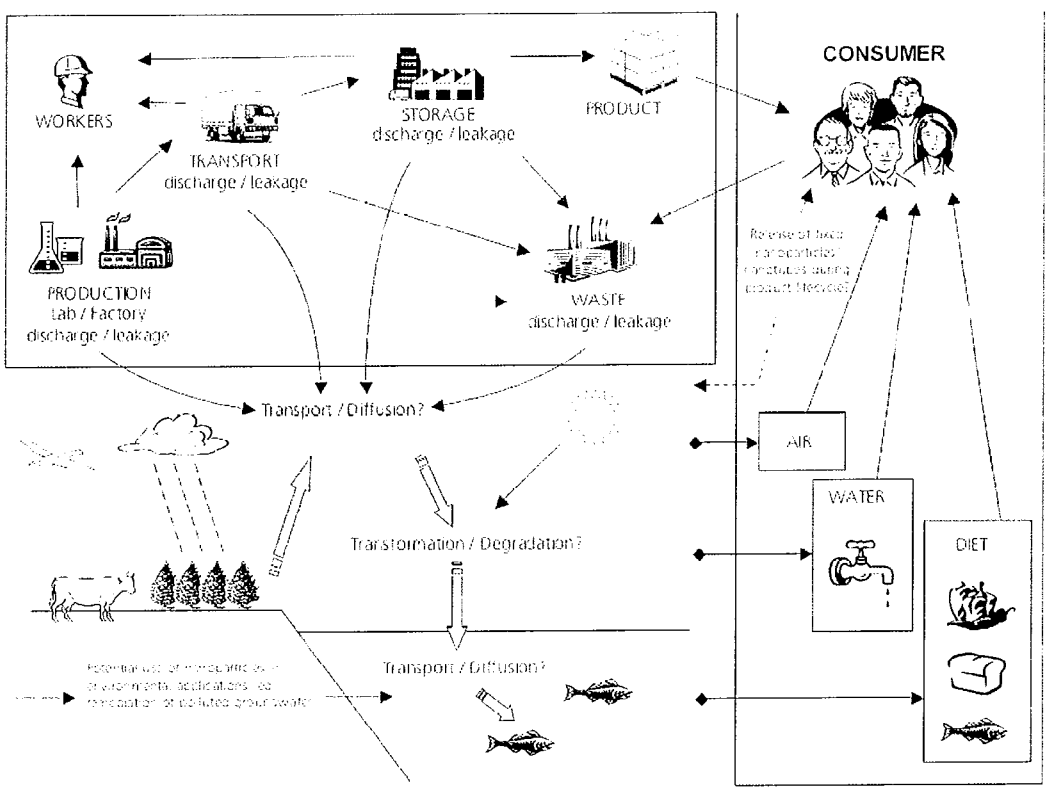

Figure 2.2: Potential exposure routes for nanoparticles [1].

The skin is the largest organ of the body with a huge surface area and is unique because it represents an important route for both occupational and environmental nanomaterial exposure, particularly during manufacture. Within the avascular epidermis, particles might lodge and not be removed by phagocytosis. Zinc and titanium oxide particles, as used in cosmetics have already been shown to penetrate the stratum corneum of rabbit skin [96]. Highest absorption occurs from

water and oily vehicles [50]. In addition, limited studies indicate that nanoparticles may also be able to access the body via the gut [44].Determinants of nanomaterial toxicity

Size, surface area, surface chemistry, solubility and shape are all paramters that can determine particle toxicity [53]. A large surface area allows a greater contact area with cellular membranes, greater capacity for absorption and transport of toxic substances and greater area available for chemical reactions [97]. The chemical reactivity of the surface area, including surface components (e.g. transition metals, coatings) and the inherent toxicity of these chemicals are important as they may initiate toxic reactions such as the release of free radicals [98, 99]. The physical dimensions of a particle determine whether it is able to penetrate organs or cells and whether it can be removed by macrophages [100, 101]. Particle clearance together with their solubilityinfluences the retention time of particles in tissues and cells and therefore its biopersistence. The longer a particle stays in contact with cellular membranes, the greater the probability of a toxic reaction and damage [44, 102, 103].

2.2.4.2 *Mechanisms of nanomaterial toxicity*

Oxidative stress is one of the best developed paradigms to explain nanomaterial toxicity and the effects of nanoparticle exposure seen in animal studies also indicate a role of oxidative stress in the production of inflammatory cytokines and cytotoxic cellular responses [21, 22, 39, 44, 71]. The generation of ROS through Fenton and Haber-Weiss reactions or following phagocytosis has been directly related to particle toxicity [55, 104], leading to lipid peroxidation, oxidative stress

and changes in cell morphology [31, 105]. Other consequences of oxidative injury include effects on cellular signalling, nuclear factor activation, gene transcription and protein translation, DNA damage and oncogene expression [106, 107].

The sequential response of cells to increasing levels of oxidative stress can be explained by using the hierarchical oxidative stress model as shown in Figure 2.3 [71, 72]. In the presence of low ROS concentrations, anti-oxidants and detoxification enzymes such as glutathione (GSH) are induced which are able to neutralize ROS. As soon as these enzymes become depleted and the antioxidant defence is overstrained, an inflammatory response is initiated through mitogen-activated protein (MAP) kinase and nuclear factor-κB (NF-κB) signalling leading to the release of cytokines and chemokines. Further excess ROS consequently lead to the release of apoptotic factors and in turn cell death [71].

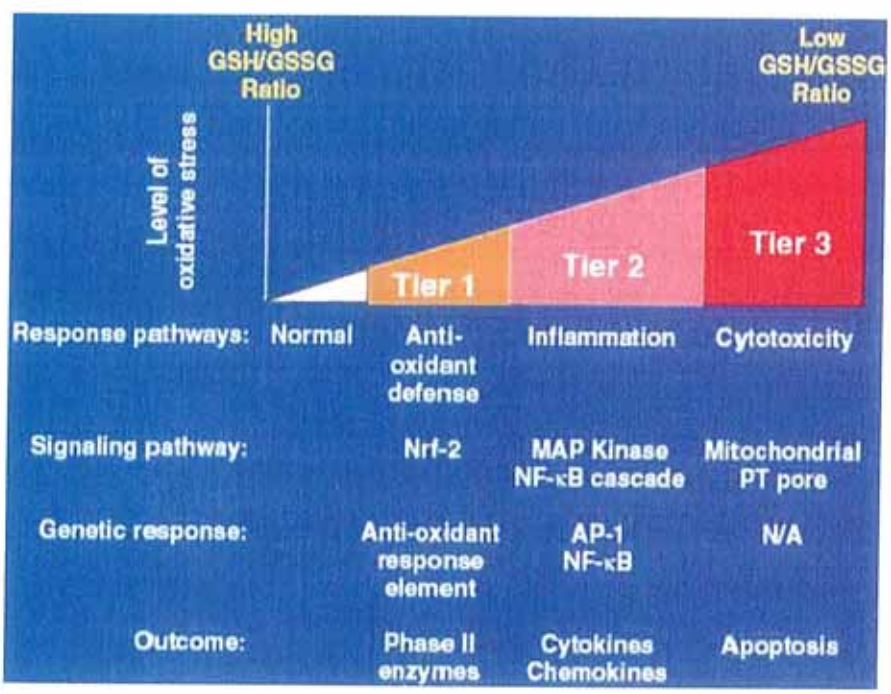

Figure 2.3: The hierarchical oxidative stress model [71].

Figure 2.4 shows the fate of an inhaled particle and the biological processes associated with fibre induced lung injuries. Following inhalation, particles can either translocate, persist or be cleared. Upon reaching the surface of the alveolar epithelium, alveolar macrophages can be stimulated and epithelial cells (EPITH) start to produce oxidants and proteases to attract leucocytes such as neutrophils (NEUT) and lymphocytes (LYM) . Excess ROS may activate redox sensitive transcription factors such as NF-κB which can in turn lead to the transcription and formation of pro-inflammatory mediators including early response cytokines, such as IL-1 and TNF-α which leads to the activation of epithelial cells, fibroblasts and endothelial cells which consequently respond by releasing further inflammatory signalling molecules such as IL-8, IL-6, TNF-α or monocyte chemoattractant protein-1 (MCP-1) [24, 104, 108-110]. Oxidants can also induce cellular and DNA damages leading to cancer [111]. . Growth factors and cytokines produced by leukocytes stimulate the proliferation of fibroblasts with a subsequent accumulation of extracellular matrix. The net result is an expansion of mesenchymal cells and an accumulation of connective tissue matrix which characterise lung fibrosis [112, 113].

In *in vitro* studies, diesel exhaust particles (DEP) were shown to cause the induction of IL-8 and granulocyte macrophage colony stimulating factor (GM-CSF) production of bronchial epithelial cells [114], as well as the induction of IL-8 and TNF-α and generation of ROS in macrophages and bronchial epithelium. Furthermore, they were reported to induce phase I and II metabolic enzymes in the above cell lines [115, 116]. In addition, DEP stimulated the expression and production of eotaxin, an important chemokine involved in airway eosinophil recruitment, via a NF-κB dependent pathway [117]. There is also evidence that

redox cycling chemicals containing particulate matter (PM) can induce MAP kinase and NF-κB activation. These signalling cascades play important roles in the transcriptional activation of cytokines, chemokines including interleukins (IL-4, IL-5, IL-6, IL-8, IL-10, IL-13), macrophage chemoattractant proteins, adhesion molecules, GM-CSF and macrophage inflammatory proteins (MIP-1 α) and adhesion molecules that impact PM-induced airway inflammation [118, 119].

Another mechanism of the effects of particles on alveolar macrophages as proposed by Beck-Speier *et al.* (2005) is illustrated in Figure 2.5 and includes uptake of particles by cells and particle interference with cell membranes leading to the activation of phospholipases through MAP kinase kinase (MKK)-1, extracellular signal-regulated kinases (ERK 1 and ERK 2) and cytosolic and secretory phospholipase-A_2 ($cPLA_2$ and $sPLA_2$) signalling. These enzymes in turn hydrolyse phospholipids resulting in the production of arachidonic acid. Arachidonic acid can activate the respiratory burst NADPH oxidase in the plasma and phagolysosomal membrane leading to ROS formation, lipid peroxidation and/or oxidative stress. Furthermore, non-enzymatic oxidation of arachidonic acid can lead to the formation of isoprostanes which are also indicators for oxidative stress [120-122]. However, arachidonic acid can also serve as a substrate for cyclooxygenase (COX) and 5-lipoxygenase (5-LO) leading to the formation of the lipid mediators prostaglandins and leukotrienes, respectively (Figure 2.5).

The study by Beck-Speier *et al.* (2005) showed that particles with low oxidative potential trigger the formation of arachidonic acid, prostaglandin E_2 (PGE_2) and ROS, whereas particles with high oxidative potential additionally stimulate the generation of leukotriene B4 and 8-isoprostane. Following exposure to ultrafine

carbon particles, PGE_2 formation was elevated at lower particle concentrations than LTB4 or 8-isoprostane. This indicates the high sensitivity of PGE_2 as a marker for the effects of xenobiotics on the arachidonic acid pathway. In contrast to the proinflammatory leukotrienes, PGE_2 can act as an immuno-suppressive leading to attenuation of the inflammatory responses [39]. It has been reported to lead to the suppression of proinflammatory cytokines including IL-1 and TNF-α [123, 124]. Furthermore PGE_2 has been reported to be elevated in alveolar macrophages following recovery of rats exposed to silica particles and lead to the decrease of TNF-α [125]

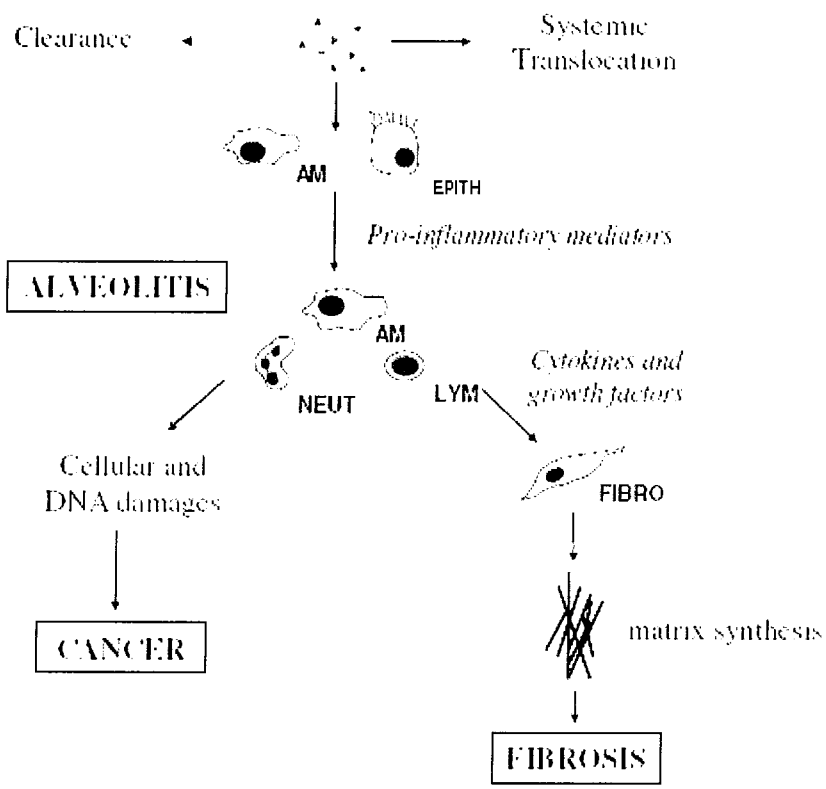

Figure 2.4: Major biological processes associated with particle-induced lung injuries [113].

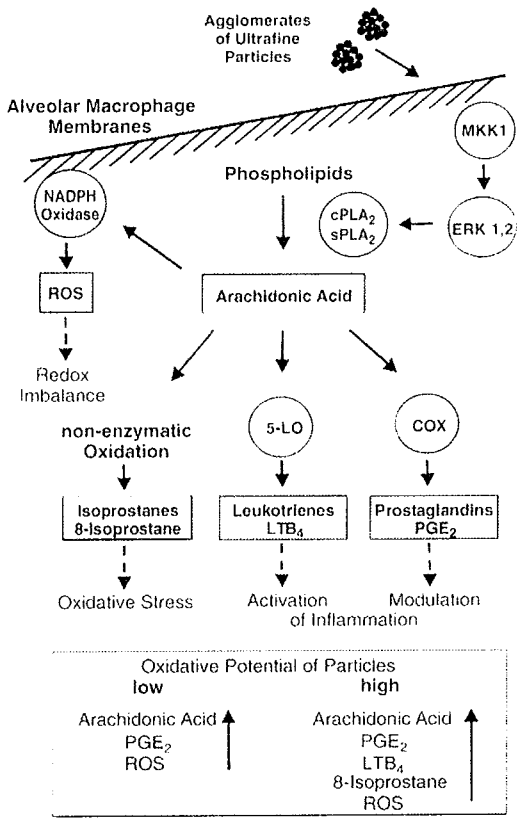

Figure 2.5: Summary scheme of ultrafine particle-induced effects on arachidonic acid-related signalling [39].

2.3 Single-walled carbon nanotubes

Carbon nanotubes (CNT) were first observed by Sumio Iijima in 1991 and have sparked an abundance of research since their discovery [2]. They are unique nanoobjects with two-dimensions of the order of 100 nm or less, comprising entirely of carbon. They consist of extended rolled up tubes of sp^2-hybridised graphene sheets, capped on both ends with a bisected fullerene. Due to the number of ways that exist to roll and close graphene sheets, there is a large variety of possible helical geometries with different diameters and chiralities [126]. Two types of CNT can be differentiated by their structures, single-wall carbon

nanotubes (SWCNT) and multiwall carbon nanotubes (MWCNT) as shown in Figure 2.6. Whereas SWCNT consist of a singular graphene cylindrical wall (diameter 0.7 - 2 nm), MWCNT have walls made up of several coaxial graphene cylinders, so that the diameter of MWCNT is about ten nanometres or more, depending on the number of layers. Both types of CNT can reach up to several micrometres in length [85].

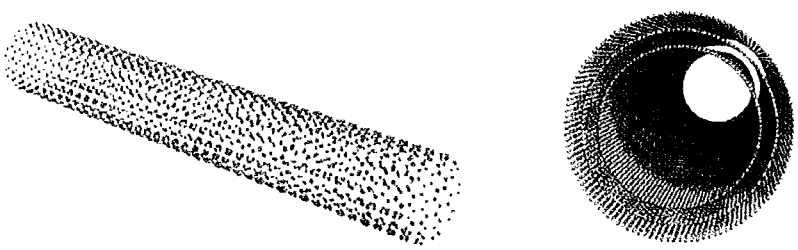

Figure 2.6: Schematic of a SWCNT (left) and a MWCNT (right) [1].

2

2.3.1 Synthesis of carbon nanotubes

In 2004, the annual production of SWCNT was 9 tonnes [44]. Due to their outstanding properties which permit a huge range of novel applications, and the annual global production of single-walled tubes was 9 tons in 2004 [127]. . In 2007, Bayer MaterialScience alone increased its production capacity for carbon nanotubes to 60 tonnes per year [128]. Several methods, as shown in Figure 2.7, have been developed for the synthesis of CNT, including electric arc-discharge [36, 129, 130], pulsed laser vapourisation [6, 131, 132], and the catalytic vapour deposition (CVD) method including the high pressure decomposition of carbon monoxide also referred to as the HiPco® process [34].

The arc discharge (ArcD) technique was the first and most widely used method by which SWCNT were produced and is based on electric arc discharge generated between two graphite electrodes under an inert atmosphere of helium or argon [2, 36]. The purity of the samples is in the region of 60%, amorphous carbon and turbostratic graphite being the principle impurities.

Laser ablation was the first technique to produce SWCNT on a mass scale. Here, CNT are produced by the vaporisation of graphite under an inert atmosphere such as argon [6]. The use of pure graphite leads to the formation of MWCNT whereas the addition of transition metal catalysts leads to the formation of SWCNT [133].

The HiPco® process is the most commonly used technique to yield high purity (≥ 90%) SWCNT and uses a gas-phase catalytic process. The resulting SWCNT have an average length of 1 μm and contain 3 – 5 nm sized metal catalyst particle impurities that are encased within the carbon shells and distributed throughout the sample [33-35].

The production method ultimately determines the type of catalyst present in raw SWCNT samples. In order to obtain SWCNT using the electric ArcD, cobalt (Co) and nickel (Ni) are added as catalyst metals whereas the HiPco® process mainly uses iron (Fe) catalysts. The different methods also produce SWCNT of varying diameters and lengths, matted in bundles or ropes, in varying yields, which contain varying degrees of other impurities including amorphous carbon and turbostratic graphite.

At present, it is still difficult to guarantee specific dimensions and physical properties. Furthermore, the separation of tubes from tangles (or bundles) in

which they emerge from the production process is still problematic [88]. In addition, it is often necessary to remove catalyst or amorphous carbon residues present after synthesis. Ultrasonication or acid washing is frequently employed to purify SWCNT samples, but these methods increase the risk of damaging or chemically altering the tubes [44].

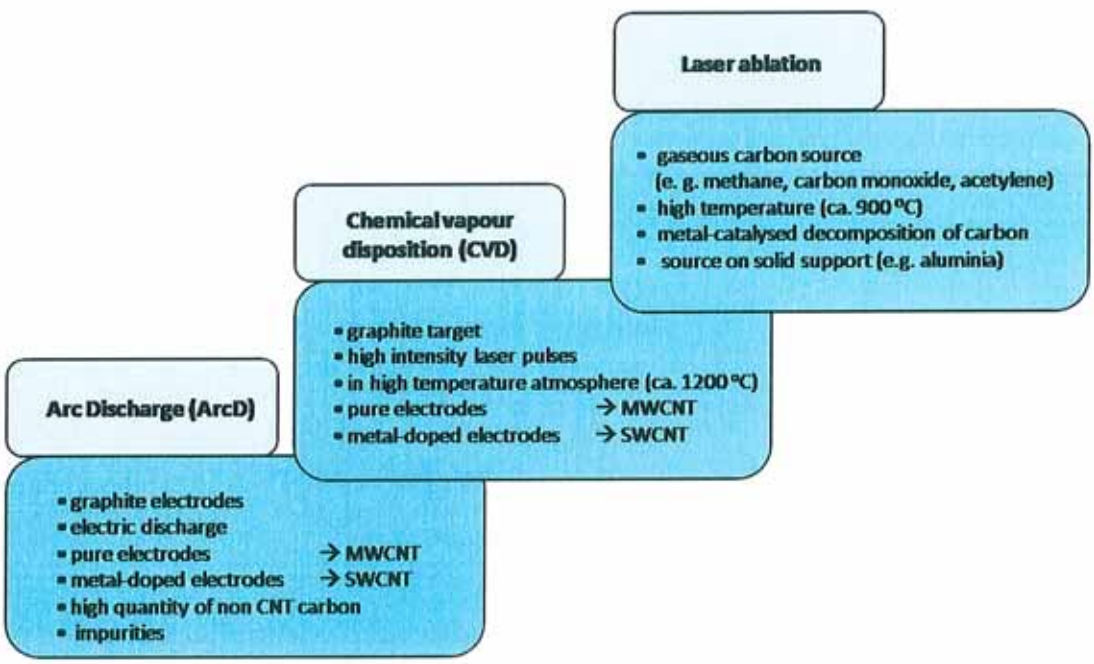

Figure 2.7: Common methods used to synthesize CNT (modified from [44]).

2.3.2 Applications of single-walled carbon nanotubes

Nanotubes are of ultra-light weight and are mechanically very strong with a Young's modulus of over one terra Pascal which makes them as stiff as diamond. Furthermore, they have excellent thermal and chemical stability, and can conduct electricity extremely well [134, 135]. Depending on the helicity of the rolled graphene sheets, they show semiconductor or metallic properties leading to a

plethora of proposed applications in electronics, computer and aerospace industries, for example as superconductor material, molecular switch or quantum computers [1, 48, 89].

Another major area of research is in the field of biomedical devices, including nanomaterial-based molecular imaging techniques and nanosensors. Complexed with single-stranded DNA, SWCNT can exhibit certain conductivity properties depending on the presence of complementary DNA sequences, allowing the identification of a single nucleotide polymorphism, by measuring the change in conductivity as the consequence of altered DNA association with the nanotube. Another innovative area of nanomedicine is the development of nanodevices that facilitate molecular repair mechanisms in macromolecules such as DNA, or the musclepowered "Biobots" and excitable vesicles that can be used for devices with the potential to replace lost biological functions [136].

2

To improve the mechanical properties of existing polymeric materials as well as ceramics and metal-matrix composites, SWCNT can be used as nano-sized fillers, creating anisotropic nanocomposites. Selective adhesion and enhanced function of osteoblasts, as well as an increase in nerve cell functions and decreased astrocyte adhesion on composites containing nanometre scaled carbon fibres have been demonstrated. Due to their electrical conductivity, electrically conductive polymers and electrically stimulatable tissue engineering constructs could be created [91, 137].

Wong Shi Kam and his colleagues (2004) demonstrated that CNT can be exploited as molecular transporters to carry cargoes into cells [138]. They can be filled with

targeted DNA molecules or peptides, to deliver them into special tissue regions [138].

The proposed applications of these novel materials are numerous and they may form a cornerstone of many technological advances. However, before such materials can be incorporated into new and existing biomedical devices, it is imperative that the toxicity and biocompatibility of CNT is thoroughly investigated [91].

2.3.3 Exposure to SWCNT

The growing interest in development and production of CNT may ultimately lead to increased risk of human exposure. The greatest potential for CNT exposure over the next few years will be in the workplace, such as industry and laboratory environments. Owing to their extremely light weight, dry CNT could become airborne and be easily inhaled [137]. Preliminary studies suggest that using the current manufacturing techniques, CNT are difficult to disperse as an aerosol and may exist as single entities but mainly as aggregates or agglomerates, so called nanoropes or bundles [48, 95, 113, 139]. The only real exposure data on SWCNT aerosols formed under laboratory conditions and potential dermal loading during material handling in the field estimated 0.7 to 53 $\mu g/m^3$ of nanotubes in air samples and 217 to 6020 μg on individual gloves worn during handling of samples. In this study, SWCNT were mainly found as aggregates or bundles but there is evidence that single SWCNT entities may potentially enter the workplace air [139].

2.3.4 Toxicological characteristics of SWCNT

As for nanomaterials in general, the main determinants of toxicity of SWCNT include total and relative surface area, chemical reactivity, physical dimensions, and solubility [44]. Carbon nanotubes have generally low chemical reactivity,only the end-caps and defects due to missing carbon atoms are significantly reactive [140]. However, SWCNT can change their behaviour due to functionalisation, for example by introducing carboxylic acid residues during purification. Metal, organics and other support material present in SWCNT samples can also influence their toxicity [44, 49].

Due to their physical dimensions, SWCNT have a very large surface area which is determined by length, diameter, and degree of bundling. Theoretically, SWCNT surface area accounts for 1300 m^2/g and can be lowered to about 300 m^2/g by bundle formation [44, 141].

Key parameters for the induction of adverse pulmonary effects are particle dose and dimensions [53]. These two values are linked because the geometry of a particle determines the dose reaching the respiratory tract. The fibre dimension determines its ability to penetrate into the centri-acinar region of the lungs. Even long fibres (>15 μm) can be respired if they are thin enough (< 5 μm) [91].

There is only limited information available on the respiratory effects of engineered nanomaterials like SWCNT, so that it might be useful to look at studies performed on ultrafine particles. Relevant information has been provided by studies on the minerals quartz and asbestos, as well as air pollution particles which have been studied for many years [142].

2.3.4.1 *Ultrafine particle aspect*

Humans have always been exposed to different types of nanomaterials arising from natural sources, such as atmospheric photochemistry, volcanic activity and forest fires. Since the Industrial Revolution in Europe at the end of the 19th century, air pollution has become of global concern. An increase in respiratory diseases due to air pollution has been reported previously, e.g. following smog episodes in Meuse Vally (1930) and London (1950). Epidemiological studies consistently related increases in particulate matter (PM) concentrations and increases in morbidity and mortality [87, 143-145]. As a result air quality standards have been introduced in many countries. Particulate Matter (PM) is used to describe a heterogeneous mixture of substances including carbon, metals, nitrate, sulphates, and volatile and particulate matter [146]. Regulations aimed mainly at PM sized smaller than 10 um (PM10) but it was shown, that fine ($PM_{2.5}$) and ultrafine ($PM_{0.1}$) fractions are the most toxic [53, 93, 147, 148]. Oberdörster (1996) showed that fine particles of titanium dioxide or carbon black are more toxic than the same particle at a larger scale. Very small particles, of a size similar or smaller than molecules, might not be detected by phagocytes, could act as haptens or modify protein structures [53, 93].

Combustion derived nanoparticles mainly induce lung injury via generation of oxidative stress resulting in cell injury and inflammation. The large surface area and reactive metal and organic molecules are mainly responsible for these effects [149]. Lung inflammation can eventually lead to airway diseases, cardiovascular diseases, fibrosis or cancer. Cardiovascular effects are due to potential translocation into the bloodstream. The inflammatory effects of carbon black

particles have been demonstrated *in vivo* and in a number of *in vitro* models [150-155]. Low exposure to quartz in the micrometre range has also been shown to cause severe lung inflammation, cell death, fibrosis and tumours in rats related to the highly reactive quartz surface, generating free radicals [107].

It has also been demonstrated that inhaled ultrafine particles can gain access to the central nervous system, via both the blood brain barrier and the olfactory nerve from deposits on the nasal olfactory mucosa [137].

2.3.4.2 *Fibre aspect*

Information on the toxicological potential of fibres has been derived from studies on asbestos which is a family of chemically and physically distinct fibres classified by morphology into two major groups, serpentine such as chrysothile, and amphibole, such as crocidolite. Crocidolite asbestos [$(Na_2(Fe^{3+})2(Fe^{2+})_3Si_8O_22(OH)_2$] has a high iron content and is often considered the most pathogenic and oncogenic type of asbestos [45-47]. It consists of long, rigid, rod-like fibres that are more difficult to be broken down in tissue compared to chrysotile forms [156].

Lung inflammation, asbestosis, lung cancer and mesothelioma are the most common health effects associated with the exposure to asbestos. Cytotoxicity, oxidative stress, inflammation and both direct and indirect genotoxicity have been proposed as mechanisms of toxicity [157-161].

Asbestos fibres mainly act through an oxidative stress/NF-κB pathway, whereas crocodilite's toxicity is mainly associated with its bioavailable transition metals leading to ROS and consequently inflammation and DNA damage [44]. As illustrated in Figure 2.8, asbestos has been shown to induce ROS and consequently activation of NF-κB and activator protein-1 (AP-1) and inactivation of p53 [162]. This has further been linked to proto-oncogene expression (c-fos and c-jun) and the release of inflammatory cytokines and chemokines, such as TNF-α, IL-6, IL-8, and macrophage inflammatory proteins [163-165]. Furthermore, asbestos was shown to affect enzymes such as iNOS, the arachidonic acid pathway including PLA_2 (PLA-2), 5-LOS and COX-2 and a variety of adhesion molecules (ICAM-1, VCAM-2, E-selectin) [166].

Fibre morphology and chemical composition are believed to be crucial determinants of bioreactivity of asbestos, so that the same might be true for nanoparticles such as SWCNT. Asbestos consists of fibres narrower than about 3 μm, so that their aerodynamic properties allow them to reach the gas-exchanging part of the lung following inhalation. The fibres with the highest biopersistence remain in the lung for the longest period of time, increasing the risk of chronic toxic responses such as fibrosis and cancer. The length of a fibre is the main determinant of its persistence [91] and studies showed that fibres longer than 20 μm have the greatest toxic and carcinogenic potential, because these particles are too long to be phagocytosed and cannot be rapidly cleared from the lung. The mean diameter of the alveolar macrophage is 10.5 to 13 μm for the rat and 14 to 21 μm for humans which represents the limit above which fibres cannot be removed via the mechanism of phagocytosis [95]. The build-up of fibres in the lung may

possibly lead to inflammation, eventually causing fibrosis and lung cancer [167]. In studies by Donaldson *et al.* (1989) and Ye *et al.* (1999), only the longer fibre fractions of asbestos and glass were seen to initiate inflammation or cause mesothelioma formation [141, 168]. The reactive surface area of fibres or the release of reactive ions such as transition metals is reputedly responsible for their inflammatory effects [21].

The development of SWCNT production techniques means that they are being made increasingly longer so that they satisfy the requirements of being fibre-like. Their insolubility in neutral or mild acid pH makes them potentially biopersistent. In addition, metal residues present in the samples can increase their inflammatory potential [44]. Carbon nanotubes can be longer than 20 μm and therefore potentially biopersist after inhalation. As with asbestos, pulmonary fibrosis, lung cancer, mesothelioma, and other pleuropulmonary disorders could be a consequence of CNT exposure [169]. The role of metal and carbon impurities requires further investigation as these particles might increase the reactivity of SWCNT surfaces or simply be toxic in their own right. Also the effect of SWCNT diameter on toxicity is not yet known as no exposure to this degree of thinness has been evaluated in humans thus far. The degree of rigidity and flexibility and therefore the ability of SWCNT to bend or curl could influence their toxicity and may be different to the effects of other fibres [44]. A recent report by Zheng and colleagues (2005) described unusual redox features of SWCNT themselves, and thus whether CNT unique electronic and redox properties can cause unusual or even unknown effects on cells and tissues requires further elucidation [136, 170].

Similar to the synergistic (more than additive) interactions of cigarette smoke and asbestos exposure, it is possible that CNT could exhibit similar synergisms with other ultrafine materials, such as polyaromatic hydrocarbons (PAH), cigarette smoke or diesel particulates [167].

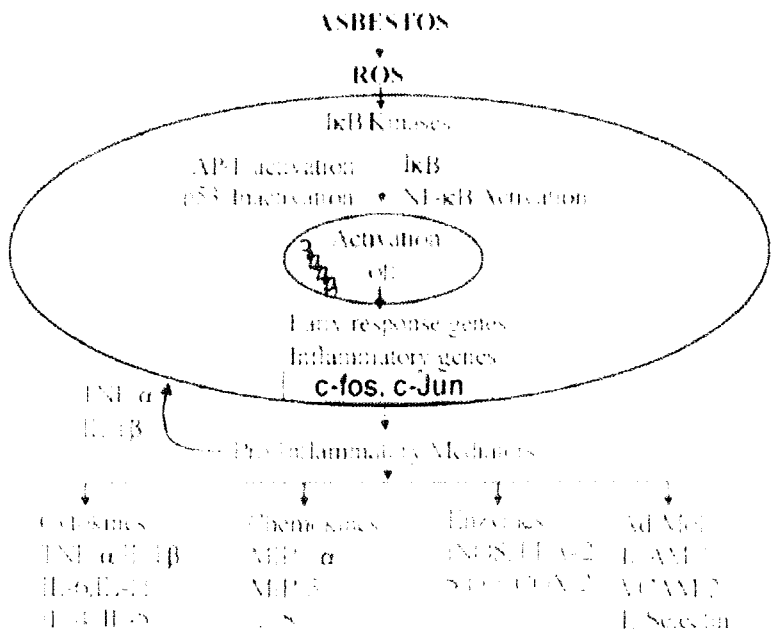

Figure 2.8: Activation of transcription factors and related gene expression by asbestos [166].

2.3.4.3 *Sample impurities*

As described in 2.3.1, the manufacture of nanomaterials, particularly carbon nanotubes, is commonly associated with the use of different transition metals as catalysts. The most commonly used metals are cobalt (Co), molybden (Mo), iron (Fe), nickel (Ni) and yttrium (Y). Decorating iron or nickel levels can reach up to 40 percent and 25 percent by weight, respectively. These metals can be encapsulated and therefore coated with carbon, or attached to the outside of the tubes so that a

metal oxide layer will form around them. As the size of the metal particle determines the diameter of the tube that grows from it, metal residues are mostly nano-sized, as long as no aggregates are formed [44]. The type and content of residual metal may be important in terms of relative toxicity. The health risk associated with CNT prior to removal of catalyst material may be due to both the carbonaceous and metallic components. Transition metals can interact with oxidative species generated, triggering cascades of redox cycling and depleting endogenous reserves of antioxidants. The resultant free radical reactions can damage macromolecules and mediate tissue damage. The development of pathological conditions such as certain cancers, skin, liver and heart diseases, diabetes, hormonal abnormalities, and immune system dysfunctions might follow. Thus, there is a significant risk of synergistic effects [31, 136].

The purification processes to remove these contaminants are of unequal efficiency, so that the final chemical composition of nanotube samples often varies [95]. Even purified SWCNT may contain some amount of catalyst residues. Variable amounts of inert synthesis support, such as silicates (e.g. zeolites), aluminia or magnesium oxide can also be present inside and/or at the extremities of CNT. With the exception of magnesium oxide, strong acids or bases are needed to remove these residues. Furthermore, amorphous carbon black and various graphite sheet structures can be present in SWCNT samples [44, 95, 113].

2.3.4.4 *Aggregation*

Carbon nanotubes are usually synthesized as bundles and their high molecular weights and strong intertubular forces, both van der Waals and electrostatic, promote further formation of bundles and ropes. Therefore, the degree of aggregation ultimately determines how CNT are presented to exposed cells or tissue. Furthermore, their lung deposition characteristics can change, as aggregates have a greater aerodynamic diameter than single particles of beyond the range that can be respired (> 5 μm), and can be less easily inhaled deep into the lung. It might be easier for macrophages to detect and clear a large bundle compared to a single nanotube [171]. New techniques have been developed to enable CNT to remain separate, which would lead to more applications, but could increase the risk of inhalation exposure [1, 112, 113]. Lung surfactant might also help to separate single fibres [48].

2

2.3.5 Review on the pulmonary toxicity of SWCNT

To date pulmonary toxicity is one of the main areas of carbon nanotube studies. A summary of a wide range of *in vivo* and *in vitro* studies performed on CNT is presented in Appendix C, Table C1. As illustrated in Figure 2.9, the number of studies published each year has been growing linearly between the year 2000 to the present day. To date, there are more than 200 publications describing the toxicity of CNT (based on PubMed http://www.ncbi.nlm.nih.gov), indicating the great need for and interest in the safety assessment of these materials.

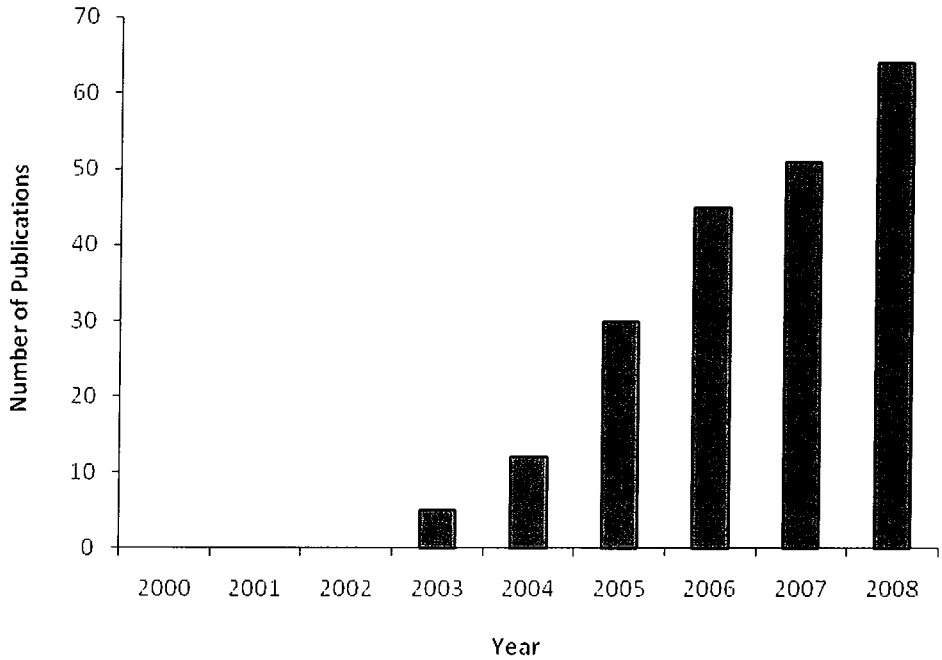

Figure 2.9: Number of publications appearing on http://www.ncbi.nlm.nih.gov using the search criteria "nanotube + toxicity" for the publications dates 200 to 2008.

2

2.3.5.1 *In vivo exposure*

As can be seen in Appendix C, Table C.1, more than half of all *in vivo* studies performed on CNT material have been carried out using rodent models with mice being used two times more than rats. Furthermore, CNT was most frequently dispersed in saline solution with or without the addition of polysorbate (Tween). In order to investigate pulmonary effects, particles were administered by intratracheal instillation [113, 172-179] or pharyngeal aspiration [180-185].

Nearly all *in vivo* studies using intratracheal instillation have found histological evidence of inflammation [113, 172, 173, 179], pneumonia-like reactions [173,

174] and granuloma formation [172, 176, 179] and Muller *et al.* (2008b) suggested that the intrinsic toxicity of CNT is mainly mediated by the presence of defective sites in the carbon framework [178]. On the contrary, other studies did not report any abnormalities in pulmonary function or inflammation [175]. As an additional endpoint, Muller *et al.* (2008a) also investigated the genotoxicity of SWCNT and found dose-dependent increases in micronucleated pneumocytes following administration of a single dose [177]. Unfortunately, an important limitation to all tests using intratracheal administration is the fact that a single dose of CNT is directly introduced into the trachea of anaesthesized animals, resulting in a less realistic situation compared to natural inhalation exposure. Artefacts are possible due to the non-physiological rapid delivery of particles. In addition, the study suffers from the problem that CNT form aggregates in aqueous solutions, despite the use of surfactants and sonication [1, 91]. By injecting a bolus dose of aggregated material, foreign-body granulomas can be induced that are non-specific and may not reflect the intrinsic effects of the test material. Therefore, even the investigators themselves questioned the toxicological relevance of their findings. The absence of dose-response relationships noted by some authors might have been the consequence of SWCNT clumped into large masses instead of evenly distributed throughout the lung [113].

2

Alternatively, pharyngeal aspiration of CNT samples was used for exposure purposes [186, 187] resulting in aortic mitochondrial DNA damage, increased progression of atherosclerosis in apolipoprotein E (ApoE)-deficient mice and accelerated plaque formation. Manugum *et al.* (2006) reported fibrotic lung lesions, bridging of alveolar macrophages and increased platelet-derived growth

factor expression [187]. Four consecutive studies on the *in vivo* effects of pharyngeal aspiration of HiPco® SWCNT were carried out by Shvedova and colleagues [181, 183-185]. Rapid progressive fibrosis, granuloma formation, increased pulmonary resistance [183], decrease in antioxidant levels of vitamin E-deficient mice [184] and elevated apoptosis and inflammatory responses of reduced nicotinamide adenine dinucleotide phosphate (NADPH)-oxidase-deficient mice [185] could be shown. In addition, sequential exposure to SWCNT and bacteria lead to enhanced pulmonary inflammation and delayed bacterial clearance suggesting increased susceptibility to lung infection in SWCNT exposed populations [181]. In contrast, co-stimulation of mice to MWCNT and ozone did not result in synergistic or additive effects but attenuated inflammatory and cytotoxic responses [180].

Although pharyngeal aspiration results in some exposure to single CNT fibres, it still cannot mimic a real exposure situation, as it results in bypassing the nose and delivery of a bolus dose. To avoid exposure artefacts, Mitchell and collegues (2007) carried out a whole-body inhalation exposure to MWCNT which in turn resulted in immunosuppression and no inflammatory responses [188].

Regrettably, the degree of purity of CNT preparations has not been reported in several experiments [176, 179, 189] is that so that it remains unclear whether the toxicological findings observed could be influenced by the presence of graphite and metal contaminants present in CNT samples [137]. Overall, *in vivo* studies showed that there is the risk of developing lung lesions following CNT exposure even though studies were solely based on rodents and guinea pigs and there is a lack of real inhalation studies. Extrapolating rodent data to the human situation has

proven to be difficult and inhalation in rats has been shown to differ greatly from that of larger mammals, particularly humans [190].

Dermal *in vivo* toxicity has only been evaluated by a few studies including that of Huczko and Lange (2001) who used the patch and modified Draize rabbit eye test and showed no sign of health hazards [189]. Subcutaneous implantation was reported to result in no acute toxicity [191] but the activation of major histocompatibility complex (MHC) and oedematous reactions [192].

A number of studies exist which explore biodistribution and clearance of CNT following intravenous injections of functionalised CNT. Water-soluble CNT have been shown to be rapidly excreted via the biliary pathway [193] with high clearance rates without any negative side effects [193-195]. Other studies on functionalised CNT reported excretion via the renal pathway [194]. In contrast, non-functionalised CNT seemed to reside in the body over a long period and tend to accumulate mainly in the liver with no or low signs of toxicity [196-198]. However, some authors did report adverse effects of intravenously injected CNT including acceleration of thrombosis development and platelet activation [199].

A study by Bardi *et al.* (2008) investigated the effects of MWCNT injection into the cerebral cortex of mice with the conclusion that MWCNT do not cause degeneration/apoptosis of cortical neurons [200].

Due to their structural resemblance to asbestos, two studies have been carried out to investigate whether CNT show any sign of asbestos-like pathogenic behaviour [201, 202]. These studies injected CNT samples into the peritoneal cavity of mice and results showed signs of asbestos-like toxicity in both cases as seen by foreign

body giant cell and granuloma formation on the peritoneal side of mouse diaphragms [201] as well as mesothelioma formation [202].

2.3.5.2 *In vitro studies*

In contrast to *in vivo* tests, *in vitro* studies facilitate the identification and specification of biological pathways and mechanisms involved in toxic reactions observed *in vivo*. The test material can be studied under controlled conditions and individual pathways can be isolated, which is not feasible in the *in vivo* situation. *In vitro* assays can be used for a very rapid determination of dose levels and important parameters influencing toxicity and translocation potential of nanomaterials, such as size, surface area and reactivity [53]. In addition, performing *in vivo* studies is costly, particularly regarding the assessment of valuable nanomaterials. However, disadvantages include lack of validation against *in vivo* effects, mismatch in doses that are commonly very high, over-simplification, and non-involvement of the complete biological response.

2.3.5.2.1 *Factors influencing the outcomes of* in vitro *studies*

2.3.5.2.1.1 *Role of cell model*

As can be seen in Appendix C, Talbe C.1, *in vitro* studies have been carried out on a wide range of different cell models including lung epithelium [51, 203-211], macrophages [48, 49, 167, 169, 212-216], monocytic cells [151], erythrocytes

[217], neutrophils [218], fibroblasts [3, 52, 219-221], keratinocytes [30, 31, 205, 222-225], mesothelial cells [226, 227], kidney cells [228]; osteoblasts [219], endothelium [229], hepatoma cells [230], smooth muscle cells [231] and neuronal cells [232]. The cell models employed originated from a wide range of tissues. Therefore, they may also behave and respond differently so that it is understandable that exposure to CNT has led to conflicting results in the published literature.

2.3.5.2.1.2 *The role of CNT type*

There are additional factors that contribute to the discrepancies observed between *in vitro* studies, including the great diversity of CNT types, produced in varying bundle sizes, different diameters and lengths. This highlights the importance of detailed sample characterisation in order to allow and facilitate inter-study comparisons. In turn, multidisciplinary expertise is required to carry out particle characterisation [91].

Overall it was concluded that cellular responses strongly depended on morphology and aggregation state of particles, with high aspect ratio carbon material being most toxic [151, 204, 222]. However, some studies showed that intact CNT are less active than ground CNT due to their high level of agglomeration making them less bioavailable [95]. Soto *et al.* (2007) and Simon-Deckers *et al.* (2008) also concluded that the effects seen following MWCNT exposure were independent of particle morphology or length [169, 209].

The use of different types of catalyst metals for synthesis, as shown in Figure 2.7, together with the varying degrees of sample purification employed ultimately increases the number of CNT types with different toxicological characteristics and may therefore account for some of the discrepancies observed between *in vitro* studies. The majority of authors agreed on the dependence of biological CNT effects on catalyst contaminants, making them more reactive, particularly in terms of oxidative stress and inflammatory response [31, 49, 51, 206, 213]. Therefore, purified CNT are believed to be less toxic than un-purified samples [206]. In contrast, some authors report the effects to be independent of impurities including catalyst effects [169, 209, 227] or have found refined CNT to be even more toxic than unrefined ones [52]. Depending on proposed applications, it has to be decided whether it is best to remove metal contaminants, or whether it is more relevant to assess the biological effects of CNT/contaminant mixtures.

2

2.3.5.2.1.3 *The role of dispersion*

Another common problem in all studies of CNT is their hydrophobic surface which makes them hardly soluble in aqueous solutions and leads to the formation of bundles and ropes. This occurs particularly in saline, media or serum solutions as commonly used in toxicity testing [91]. Additionally, some materials settle rapidly hindering the formation of a homogenous suspension [233]. The wide range of dispersion media employed for CNT suspensions are listed in Appendix C, Table C.2. This list also indicates that culture medium is by far the most popular vehicle for *in vitro* studies. As CNT are insoluble in aqueous solutions including PBS or cell culture medium they tend to clump into large masses, so that a number of different

methods have been employed for nanotubes dispersion in order to obtain homogenous dispersions. Sonication appears to be the most commonly used method for suspending CNT agglomerates with the advantage that any chemical modification can be avoided. However, many researchers still observed CNT agglomeration or re-aggregation following sonication and prolonged sonication may cause defects on CNT surface structure leading to altered reactivity [234].

The use of organic solvents [44] such as dichlorobenzene, chloroform, carbon disulphide sodium dodecylsulphate (SDS) [174, 235, 236] or DMSO [167, 169, 228] is frequently the method of choice to achieve improved CNT dispersion. Only the use of surfactants such as pluronic surfactants [187, 212, 215, 221, 223, 225], Triton-X or polysorbate [223, 227], can help to disperse SWCNT in water or cell culture medium, causing them to exfoliate into individual or small bundles and coating them hydrophillically. A drawback associated with these methods is that some processing conditions can result in surfactant dissociation and toxic effects observed during studies can be largely due to surfactant residues [223]. Furthermore, fibres treated with salt solution similar to those found in biological systems change their durability and some undergo dissolution, break up into smaller fragments or dissolve entirely. Other types resist dissolution completely, like amphibole asbestos [44, 237, 238].

2

The various methods employed to disperse the CNT samples lead to further discrepancies in toxicity data due to differences in dispersion vehicles, sample preparation and handling [91]. Well-suspended CNT bundles have been shown to be less toxic than rope-like agglomerates [225, 227].

Another frequently used technique to improve solubility, particular with regards to biomedical applications, is functionalisation of CNT, typically attaching peptide, acid, amine, or polymer molecules covalently to the sidewalls of nanotubes, making them water-soluble. Cells exposed to functionalised, watersoluble CNT usually do not show any signs of cytotoxicity [221]. However, they may still have the potential to induce inflammatory responses [225].

Overall, there is much controversy about the best method for solubilising nanotubes in biologically relevant media as some methods result in uneven surface coverage, or inter CNT coupling, changing the intrinsic toxicity of nanotube material [21].

The ideal vehicle would lead to homogenous SWCNT dispersions without alterations of surface chemistry and/or CNT sizes and at the same time would have minimal cell toxicity. In addition, it needs to be relevant for the exposure situation of interest and may therefore differ between studies regarding biomedical applications or occupational risk assessment. For assessing the risk of occupational exposure to CNT dust it is most practical to mimic the degree of aggregation occurring in workplace air and Maynard *et al.* (2004) reported that workers might be exposed to both, bundled and single SWCNT [139].

Over the course of this study, due to the fact that inhaled particles are most likely to deposit on the alveolar wall which is lined by lung lining fluid [59, 67, 239], BALF or dipalmitoylphosphatidylcholine (DPPC), the main component of lung lining fluid, were identified as suitable dispersant for the assessment of pulmonary exposure to CNT material [240, 241].

2.3.5.2.2 *The* in vitro *effects of purified SWCNT*

As displayed in Appendix C, Table C.1, the most commonly investigated endpoints of *in vitro* studies included cytotoxicity, oxidative stress and inflammatory responses. The most common findings following exposure to purified CNT material included good biocompatibility [219] as characterised by low cytotoxicity [206, 210, 213, 219, 229], little or no oxidative stress [49, 51, 213, 219, 235] and absence of inflammatory responses [51, 213, 219]. However, there are studies showing cytotoxic effects of purified CNT [48, 52, 215, 218, 227], decreases in cell growth [231] and cell adhesion [210], inflammatory responses or oxidative stress [218], impaired phagocytosis [48] and complement activation [217].

2.3.5.2.3 *The* in vitro *effects of un-purified SWCNT*

2

The effects of unpurified, raw material have been seen to be generally more detrimental leading to cell death [3, 31, 50, 167, 204, 205, 222, 226-228], decreased cell proliferation and cell cycle arrest [3, 50, 228, 232], decreased cell adhesion [52, 204, 228], oxidative stress [31, 49, 51, 205, 222, 226, 242], inflammatory responses [3, 50, 223, 243], alteration of gene transcription and protein formation [50, 172, 203, 205, 224, 226, 242], genotoxicity [50, 172, 177, 178, 203, 205, 224, 226, 242, 244-247], decreased trans-epithelial resistance [207, 211], decreased phagocytic ability [248], increased antigen presentation of macrophages [214] and airway hyper-responsiveness [214]. Nevertheless, there are studies reporting no decreases in cell viability [52, 207, 211, 220] or anti-

inflammatory responses following unpurified CNT exposure [212, 214] and no genotoxic effects [249].

2.3.5.2.4 *Cellular uptake of CNT*

The ability of CNT to enter exposed cells is also an endpoint of frequent interest as it ultimately determines whether particles have the potential to interact with intracellular components such as DNA leading to genotoxic effects. Cellular uptake has primarily been described for functionalised CNT [225, 248, 250] but also for purified [51, 209, 210, 214] and un-purified CNT samples [50, 51, 209, 216]. However, as shown in Appendix C, Table C.3, findings were inconsistent as there are also studies that could not detect any intracellular particles [31, 52].

2

2.4 Conclusions

Starting with identifying the relevant background on the toxicity of nanomaterials including the role of physical and chemical characteristics, applications, routes of exposure and potential mechanisms of toxicity with special focus on SWCNT, the present chapter reviewed and discussed existing studies on the *in vitro* and *in vivo* toxicity of CNT material. Furthermore, factors influencing the outcomes of CNT toxicity assessment were identified. This information was subsequently used for the following chapters which describe the investigations into the toxicity of unpurified SWCNT as carried out within the course of this study.

Chapter 3

Effects of SWCNT on cell viability

This chapter is based on the following publications:

***In vitro* toxicity evaluation of single-walled carbon nanotubes on human A549 lung cells**

Maria Davoren, Eva Herzog, Alan Casey, Benjamin Cottineau, Gordon Chambers, Hugh J. Byrne, Fiona M. Lyng.

Toxicology *In Vitro*, 2007, Volume 21, Issue 3, pages 438-448

Spectroscopic analysis confirms the interaction between single-walled carbon nanotubes and various dyes commonly used to assess cytotoxicity

Alan Casey, Eva Herzog, Maria Davoren Fiona M. Lyng, Hugh J. Byrne, Gordon Chambers

Carbon, 2007, Volume 45, Issue 7, pages 1425-1432

Probing the interaction of single-walled carbon nanotubes within cell culture medium as a precursor to toxicity testing

Alan Casey, Maria Davoren, Eva Herzog, Fiona M. Lyng, Hugh J. Byrne, Gordon Chambers

Carbon, 2007, Volume 44, Issue 1, pages 34-40

3.1 Chapter summary

This Chapter describes the *in vitro* cytotoxicity assessment of SWCNT on A549 cells. A dermal cell model (HaCaT) was used for comparison purposes. Cellular viability was determined by evaluating metabolic, lysosomal and mitochondrial activity as well as protein content and revealed the SWCNT to have very low acute toxicity to the A549 cells. However, cytotoxicity increased with prolonged exposure times. To investigate the interactions between serum components in the test medium and the test materials, exposures were conducted both in serum containing (5%) and serum-free medium. Serum supplements appeared to have low influence on SWCNT toxicity but significantly decreased the toxicity of quartz particles. Overall cell responses were the same between A549 and HaCaT cells. Considerable variation was found in the toxicity of SWCNT depending on the indicator dye employed. Therefore, a comprehensive spectroscopic study was carried out to investigate the interactions between colorimetric dyes and SWCNT as used in this study which revealed interactions in all cases, resulting in the reduction of the associated absorption/fluorescent emission. As a first step to overcome the risk of data misinterpretation, qualitative toxicity assessment was carried out. Trypan Blue staining confirmed the findings of low acute toxicity of SWCNT. Propidium iodine (PI) staining revealed that cell necrosis only occurred in proximity to SWCNT agglomerates. Studies employing TEM confirmed that there was no intracellular localization of SWCNT in A549 cells following 24 h exposure. However, increased numbers of surfactant storing lamellar bodies were observed in exposed cells. Immunostaining showed disruption of actin and tubulin organisation and the tendency of cells to grow around SWCNT bundles.

3.2 Introduction

The objective of this study was to perform a comprehensive *in vitro* cytotoxicity assessment of SWCNT in order to investigate the potential of these particles to induce adverse pulmonary effects. Quartz was tested in parallel exposures to provide a benchmark of particle toxicity. Particle exposures were conducted both in serum containing (5 %) and serum-free cell culture medium in order to evaluate the role of serum supplements on particle toxicity. Cytotoxicity parameters evaluated in this study, following 24 h exposure to both materials, included the metabolic, lysosomal, and mitochondrial activities of the cells. In addition total protein content, cell membrane integrity and inflammation responses were also measured. Metabolic activity of cells was also quantified following longer exposure periods of up to 96 h. Qualitative toxicity assessment was carried out using Trypan Blue and PI staining as well as immunohistochemistry. The present study also employed TEM to characterise the SWCNT pre exposure, to investigate if the SWCNT were internalised by these lung cells and to examine any ultrastructural changes in cell morphology post exposure.

Literature has revealed that the interactions of SWCNT and other carbon based nanomaterials with various molecular species such as proteins, enzymes and DNA [12, 251, 252] and commonly used cytotoxicity assays which may result in interference with absorption/fluorescence data [30, 210, 225]. Therefore, a spectroscopic analysis was carried out as part of this study in order to gain more knowledge about the degree of interaction between SWCNT and the specific dyes used in this study in order to be able to interpret the toxicity data obtained.

3.3 Materials and Methods

3.3.1 Test Materials

HiPco® derived SWCNT were purchased from Carbon Nanotechnologies, Inc. (Houston, TX) who reporter the material to contain 10-wt % iron. The diameter distribution of these HiPco® tubes was previously determined to be 0.8-1.2 nm by Raman spectroscopy. Atomic force microscopy (AFM) revealed HiPco® SWCNT in their "as produced" state to be on average 800 nm long and estimated bundle sizes of 2.6×10^{-14} m^2 [253, 254] . Samples were employed as purchased, with no further purification.

Cristalline quartz (SiO_2; Certified Reference Material, BCR No 66) with a particle distribution of 0.35 to 3.50 μm was employed as a positive control and obtained from Sigma Aldrich Ltd. (Dublin, Ireland). This standard quartz sample was mined in Frechen, Germany and is mostly silicon dioxide with trace amounts of iron (0.4 mg g^{-1}), titanium (0.26 mg/g), sodium (0.09 mg/g) and calcium (0.06 mg/g).

3

3.3.2 Reagents

3-(4,5-dimethylthiazol-2-yl)-2,5-diphenyltetrazolium bromide (MTT), Coomassie Brilliant Blue 250 (CB), Neutral Red (NR) and Trypan Blue were all purchased from Sigma Aldrich Ltd. (Dublin, Ireland). The viability dye 2-(4-iodophenyl)-3-(4-nitrophenyl)-5-(2,4-disulfophenyl)-2H-tetrazolium (WST-1) was purchased from Roche (UK).

The ToxiLight™ kit for Adenylate Kinase (AK) analysis was purchased from Cambrex BioScience (Wokingham Ltd, UK). Alamar Blue™ (AB) was purchased from Biosource (UK). Cell culture media and supplements and the trypsinisation solution were purchased from Biosciences (Dublin, Ireland).

3.3.3 Cell culture

A549 cells (ATCC, CCL-185) a human lung carcinoma epithelial cell line and the normal human keratinocyte cell line HaCaT (kindly provided by Prof. Dr. Petra Boukamp, Heidelberg) were employed for testing. Both cell lines were cultured in Kaighn's medium (F12K) and Dubeccos's modified minimum essential medium (DMEM, Cambrex), respectively which was supplemented with 2 mM L-glutamine, 10% foetal bovine serum (FBS), 45 IU/ml penicillin and 45 IU/ml streptomycin, at 37°C in a 5% CO_2 humidified incubator.

3

3.3.4 Dispersion of nanomaterials

Stock suspensions of SWCNT and quartz were prepared both in serum containing (5%-F12K) and serum-free (0%-F12K) medium. An ultrasonic tip (Ultra sonic processor VCX-750 watt) at an amplitude of 40% for a total time of 30 seconds carried out in 10 second sequential steps was employed to disperse the suspensions prior to preparation of test concentrations. TEM studies on samples prepared in an identical fashion have indicated that the SWCNT remain bundled after dispersion [255]. Working concentrations were prepared by dispersing an

initial concentration of 800 µg/ml of each material by sonication. Each stock concentration was then serially diluted on a 96-well plate with each type of medium to prepare test concentrations. Cells were then exposed to the same concentration range of SWCNT and quartz (1.56, 3.12, 6.25, 12.5, 25, 50, 100, 200, 400, 800 µg/ml, in other terms, cells were exposed to 0, 0.32, 1.30, 5.20, 20.79 and 83.16 µg of test material per cm^2 of cell monolayer) prepared in both 5%-F12K and 0%-F12K medium. Transmission Electron Microscopy (TEM) was performed using a Jeol 100CX TEM, on raw as purchased HiPco® SWCNT by dispersing 1 mg of SWCNT in 10 ml ethanol with the aid of a sonic tip. The dispersion was then dropcast onto 200 nm formvar coated copper grids for examination.

Figure 3.1: Confocal laser scanning microscope (Zeisse LSM 510 META).

For spectroscopic analysis of the SWCNT and cytotoxicity indicator dyes, SWCNT were dispersed within the dye under study at initial concentrations of 800 µg/ml with the aid of an ultrasonic tip as described before. The SWCNT concentration was then reduced by 1:2 serial dilution with sonication to a final concentration of 1.56 µg/ml.

3.3.5 Quantitiative cytotoxicity assessment

For cytotoxicity assays, cells were seeded in 96-well microplates (Nunc, Denmark) at a density of 1 x 10^5, 7 x 10^4, 3 x 10^4 and 2 x 10^4 cells/ml in F12K medium containing 10% FBS for 24, 48, 72 and 96 h studies, respectively. These seeding densities were found to be optimal to achieve 80% confluency for each cell line at the end of each respective exposure period. After 24 h of cell attachment, plates were washed with 100 µl/well phosphate buffered saline (PBS) and the cells were treated with increasing concentrations of each nanomaterial prepared in either 5 or 0%-F12K for 24 h. Culture medium supplemented with 5% FBS was used for 48 h to 96 h exposures. Six replicate wells were used for each control and test concentration per microplate. Cytotoxicity was assessed using five assays as outlined below.

3

3.3.5.1 *Alamar Blue™, neutral red, coomassie blue assays*

For 24 h studies, the AB, NR and CB assays were conducted consecutively on the same set of plates. The AB assay was performed first. The bioassay was carried out according to manufacturer's instructions. Briefly, control media or test exposures were removed; the cells were rinsed with PBS and 100 µl of an AB/NR medium (5% [v/v] solution of AB and 1.25% [v/v] of NR dye) prepared in fresh media (without FBS or supplements) were added to each well. Following 3 h incubation, AB fluorescence was quantified at the respective excitation and emission wavelength of 540 and 595 nm using a microplate reader (Tecan GENios, Grödig, Austria). Wells containing medium and AB without cells were used as blanks. The

mean fluorescent units for the six replicate cultures were calculated for each exposure treatment and the mean blank value was subtracted from these. Viability and protein determination of the cells following exposure to each chemical were then subsequently investigated using the NR and CB assays according to Liebsch and Spielmann (1995) with the modification of Coomassie Brilliant Blue dye being employed in place of Kenacid Blue R dye [256].

3.3.5.2 *Tetrazolium dye based assays*

The plates for the MTT and WST-1 assays were seeded and exposed identically to the first series of plates prepared for the AB, NR, and CB assays. Following nanomaterial exposure, control medium or test exposures were removed (medium from each control/treatment was pooled and frozen at -80°C for subsequent AK analysis), the cells were rinsed with PBS and 100 µl of fresh medium (without FBS or supplements) were added to each well. For the MTT assay, 10 µl of MTT (5 mg/ml) prepared in PBS were then added to each well and the plates were incubated for 3 h at 37°C in a 5% CO_2 humidified incubator. After this incubation period the medium was discarded, the cells were washed with 100 µl of PBS and 100 µl of DMSO were added to each well to extract the dye. The plates were shaken at 240 rpm for 10 min and the absorbances were measured at 570 nm using a microplate reader (Tecan GENios, Grödig, Austria).

The WST-1 assay was carried out following 24 h to 96 h exposures after which the test medium was removed, the cells were rinsed with PBS and 100 µl of fresh medium were added to each well. WST-1 dye was then added at a working

concentration of 9.1% [v/v] in PBS. In contrast to the MTT assay, the reduced form of WST-1 is water soluble so that absorbance could be determined directly at 450 nm after conversion.

3.3.5.3 *Measurement of adenylate kinase (AK) release*

The bioluminescent ToxiLight™ kit (Cambrex BioScience, Wokingham Ltd, UK) was employed to measure the concentration of AK present in the supernatants collected as described above. This kit quantitatively measures the release of AK from damaged cells and the assay was performed according to manufacturer's instructions.

3.3.5.4 *Trypan Blue staining*

3

Trypan Blue staining was carried out following 24 h exposure to SWCNT in serum free medium. Control medium or test exposures were removed, rinsed with PBS and harvested using trypsin/EDTA solution. Cells were then taken up in culture medium without serum supplemented with 0.4% [v/v] Trypan Blue and incubated for 5 min. Cell numbers were then determined using a Neubaur improved haemoctyometer and the number of Trypan Blue stained cells were recorded so that the proportion of dead cells could be calculated.

3.3.6 Qualitative cytotoxicity assessement

3.3.6.1 *Propidium Iodine staining*

Exposures were conducted in 35 mm petri dishes (Nunc, Denmark) that were seeded with 2 ml of cell suspension prepared in 10%-F12K at a density of 2 x 10^5 cells/ml. Cells were allowed to attach for 24 h and were then exposed to selected concentrations of SWCNT (0, 400, 800 µg/ml) prepared in 0%-F12K medium for 24 h. Control medium and test concentrations were removed, cells were rinsed twice with PBS and stained with 1.5 ml of PI at final concentrations of 1 µg/ml prepared in PBS. After 10 min incubation, the dye was removed, the cells were rinsed with PBS and images were recorded using a confocal laser scanning microscope (CLSM; Zeiss LSM 510 META) using a HeNe laser at 543 nm excitation and 650 nm emission as shown in Figure 3.1. Propidium iodine is only able to enter necrotic cells which could therefore be detected.

3

3.3.6.2 *Immunostaining*

A549 cells were grown on glass coverslips placed within 6-well plates by adding 1 ml of cell suspension of a density of 2.5 x 10^4 cells/ml for 96 h studies onto each coverslip, respectively. Cells were allowed to adhere for 3 h after which 4 ml culture medium were added to each well. Following 24 h incubation at 37°C, the cell medium was removed, the cells were rinsed with PBS and exposed to SWCNT solutions for 96 h. At the end of the exposure, test concentrations were removed and the cells were washed twice with warmed (37°C) PBS supplemented with

Ca^{2+}/Mg^{2+}. Cells were then fixed using 1.5 ml of paraformaldehyde (4% in PBS) for 10 minutes at room temperature. Following fixation, cells were again washed twice with PBS Ca^{2+}/Mg^{2+} and then permeabilized with 1.5 ml of 0.1% Triton-X-100 in PBS for 4 min at room temperature. Slides were again washed twice with PBS Ca^{2+}/Mg^{2+} and blocked with 1 ml of 1% sterile bovine serum albumin (BSA) in PBS for 15 min at room temperature with agitation. The solution of BSA was removed and 250 µl of primary antibody (monoclonal mouse IgG anti b-tubulin, clone TUB 2.1, T4026 Sigma) diluted 1:100 in 1% BSA-PBS were added to the coverslips. One of the coverslips to which 250 µl of 1% BSA-PBS without primary antibody was added, served as the negative control. Cells were then incubated for 1 h at 37°C with humidity after which they were washed 5 times for 5 min each using 1.5 ml 1% BSA-PBS with agitation. This was followed by addition of 250 µl of the mixture consisting of goat anti-mouse-IgG-fluorescein isothiocyanate (FITC) conjugate (whole molecule, F-0257 Sigma) 1:50 in 1% BSA-PBS and phalloidin tetramethyl rhodamine iso-thiocyanate (TRITC) labelled (P1951 Sigma) 1:40 in 1% BSA-PBS, to each coverslip. Cells were then incubated for 45 min at 37°C with humidity in the dark. Afterwards, cells were again washed 5 times for 5 min each using 1.5 ml PBS with agitation. Coverslips were transferred on to aluminium foil and 100 µl of 0.5 µg/ml DAPI (4',6-diamidino-2-phenylindole, D8417 Sigma) in PBS were added. After 15 min incubation at room temperature in the dark, excess dye was drained and the coverslips were mounted upside-down on glass microscope slides using 40 µl Mowiol®-DABCO (Mowiol 4-88 Calbiochem, DABCO, Diazabicyclooctane, D 2522 Sigma) and sealed with nail polish. Samples were then analysed using a CLSM (Zeiss LSM 510 META) or stored at 4°C in the dark until subsequent analysis. An excitation at 543 nm excitation and an emission at 560 nm using a HeNe laser were

used for actin detection. In parallel, 488 nm excitation and 525 nm emission using an argon ion laser were employed for tubulin analysis.

3.3.6.3 *Optical and Transmission Electron Microscopy*

Exposures were conducted in 35 mm petri dishes (Nunc, Denmark) that were seeded with 2 ml of cell suspension prepared in 10%-F12K at a density of 2 x 10^5 cells/ml. Cells were allowed to attach for 24 h and were then exposed to selected concentrations of SWCNT (0, 400, 800 µg/ml) and quartz (0, 400, 800 µg/ml) prepared in both 5%-F12K and 0%-F12K medium for 24 h. Following exposures, cells were washed with 0.1 M Sorensen's phosphate buffer (see Table 3.1) and then fixed in 2.5 % glutaraldehyde in 0.1 M phosphate buffer for 1 h, washed 3 times for 1 min each in 0.1 M phosphate buffer and post-fixed in 1% OsO_4 in 0.1 M phosphate buffer for 30 minutes. After washing 3 times for 1 min each in 0.1 M phosphate buffer, samples were stained with 0.1% toluidine blue solution (in dH_2O) for 10 min and again washed 3 times for 1 min each in 0.1 M phosphate buffer. This was followed by dehydration using increasing concentrations of ethanol and the samples were subsequently embedded in epoxy resin. First, cells were incubated twice in 70% ethanol for 10 min each, followed by two 90% ethanol incubations for 10 min. Finally, cells were exposed to 100% ethanol 3 times for 20 min each. To infiltrate cells with epoxy, samples were incubated for 1 h in 100% ethanol:epoxy resin (1:1). Fresh epoxy resin was added and cells were incubated for a further 2 h at 37°C. Finally, fresh epoxy resin was added again and the samples were incubated for 24 h at 60°C.

Table 3.1: Protocols for solutions used in qualitative toxicity assessment

Solution	Constituents	Volumes/Amounts
10x PBS	Na_2HPO_4	12g (8.4 mM)
	NaH_2PO_4	2.0g (1.6 mM)
	NaCl	85g
	Bring up to 1 litre using dH_2O and adjust pH to 6.7-6.8.	
Ca^{2+}/Mg^{2+} PBS	dH_2O	249 ml
	$CaCl_2$ (1M)	0.5 ml
	$MgSO_4$ (1M)	0.5 ml
	Mix the two solutions (50 ml 10xPBS + 200ml dH_2O)	
Paraformaldehyde (4%)	dH_2O	25ml
	Paraformaldehyde	2g
	Heat slowly up to 50°C	
BSA; 1%	BSA (A-7906 Sigma)	0.5 g
	PBS	50ml
	Filter using a polyethersulfone (PES)-membrane syringe filter (0.2 µm pore size)	
Phalloidin TRITC-labelled (stock solution)	Phalloidin TRITC-labelled	100 µg
	Methanol	580 µl (0.132 mM)
	Store at -20°C in the dark	
Sorensen's buffer	Na_2HPO_4 (Solution A)	0.2 M
	$NaH_2PO_4 \times 2H_2O$ (Solution B)	0.2 M
	40.5 ml solution A + 9.5 ml solution B + 50 ml dH_2O = 0.1 M Sorensen's phosphate buffer	

Optical microscopy sections (1 µm) were cut en face with a glass knife, stained with 1% toluidine blue and mounted with DPX (Sigma Aldrich, Dublin, Ireland). These sections were examined using a Nikon Eclipse E600 microscope and images were recorded using a Spot RT digital camera. Ultra thin sections (80 nm) were cut en face with a diamond knife, stained with uranyl acetate and lead citrate and examined using an FEI Tecnai G2 TEM.

3.3.7 Spectroscopic characterisation

Absorption and fluorescence spectroscopy were performed on the dispersed nanotubes in 0%-F12K, 5%-F12, 5% AB [v/v], 1.25% NR [v/v], 5 μg/ml MTT and 9.1% [v/v] WST-1 as used for cytotoxicity studies. Solutions were characterised following a 24 h settling period after which the solutions were decanted, centrifuged and characterised using Perkin Elmer Lambda 900 Absorption and LS55B Luminescence spectrometers, respectively. Vibrational analysis was carried out with an Instruments S.A. LabRam 1B Raman microscope using 514.5 nm laser excitation on dropcast films [257].

3.3.8 Statistics

Fluorescence as fluorescent units (FU), luminescence as relative light units (RLU) and absorbance were all quantified using a microplate reader (TECAN GENios, Grödig, Austria). Experiments were conducted in at least triplicate (three independent experiments). Test treatments for each assay (AB, NR, MTT, CB) were expressed as percentage of the unexposed control ± standard deviation (SD). Control values were set at 100%. For the AK assay, cytotoxicity was expressed as mean percentage increase relative to the unexposed control ± SD. Control values were set at 0% cytotoxicity. Cytotoxicity data (where appropriate) was fitted to a sigmoidal curve and a four parameter logistic model used to calculate the 50 % effective concentration (EC_{50}), which was the concentration of nanomaterial which caused a 50% inhibition in comparison to untreated controls. The EC_{50} values are reported ± 95 % Confidence Intervals (± 95% CI). This analysis was performed

using Xlfit3™ a curve fitting add-in for Microsoft® Excel (ID Business Solutions, UK). Statistical analyses were carried out using one-way analyses of variance (ANOVA) followed by Dunnett's multiple comparison tests.

3.4 Results

3.4.1 Initial characterisation of SWCNT

Carbon nanotube samples were characterised using electron microscopy and Raman spectroscopy. The TEM images obtained for HiPco® nanotubes (as purchased) tested in this study are shown in Figure 1.1. An area of what is termed high density tubes can be seen in Figure 1.1a. Bundles or agglomerates of varying lengths and diameters can be clearly seen which is typical of raw HiPco® SWCNT. In Figure 1.1b individual SWCNT and remnant catalytic iron particles resultant from the fabrication process are evident.

Raman spectroscopy was employed to probe the effects of culture medium dispersion on SWCNT as described in Casey *et al.* (2007a) [255]. The Raman spectrum of pristine nanotubes consists primarily of three main features, the radial breathing mode (RBM), the D line and the G line which are shown in Figure... [258]. These modes are very sensitive to any perturbation to the local environment of the nanotube and are therefore a good indication of complex formation and/or agglomerate debundling [259-262]. Changes were observed in the G-line region of the spectrum positioned at ~1580 cm^{-1} which were consistent with the coating of the SWCNT with molecular components of the medium and or the serum through van der Waals physisorption [10, 255, 258, 262].

3

The frequency positionings of the radial breathing modes (RBM) of pristine nanotubes are inversely related to the diameters of the nanotubes and using this relationship, the diameter range of the raw SWCNT sample was calculated to range

between 0.8 nm - 1.4 nm [263-265]. The RBM spectrum is significantly influenced by the local environment and spectral changes are interpreted as due to de-bundling or selective solubilisation [7, 84, 261]. Even though significant changes in terms of reduced mode intensity could be observed between the spectra of SWCNT dispersed in serum supplemented culture medium and that of raw SWCNT soot, there was no indication of selective solubilisation or de-bundling as all modes were still present within the spectrum [255, 263]. Therefore, it was concluded that over the concentration range tested, the nanotubes remain as bundles rather than being dispersed as individual tubes [255].

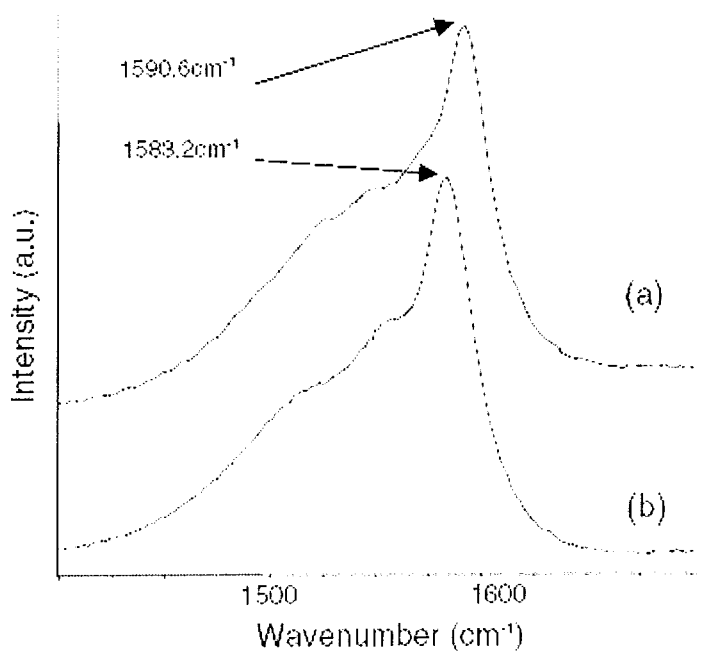

Figure 3.2: G line region for 514.5 nm excitation (a) 100 ug/ml HiPco SWCNT dispersed in 5%-F12K medium and containing (b) raw SWCNT soot [255].

3.4.2 Cytotoxicity assessment of SWCNT

3.4.2.1 *Quantititatve dye-based cytotoxicity assays*

3.4.2.1.1 *Alamar Blue™ assay*

The Alamar Blue™ (AB) assay is designed to quantify the proliferation of various cell lines and is widely utilized to measure cytotoxicity. Viable proliferating cells cause a reduction of the dye causing a colour change from a non-fluorescing indigo blue (oxidised) to a fluorescent pink species (reduced). One main advantage of this assay lies in its water solubility. It therefore requires no solvent extraction step and hence cellular viability is unaffected allowing multiple tests to be carried out on the cells. Measurements may be made by absorbance monitoring of AB supplemented cell culture medium or alternatively fluorescent measurements can be made. The absorbance spectra of the oxidised and the reduced forms overlap. Therefore the absorbance measurements must be made at the absorbance maxima of each form, namely 570 nm and 600 nm. Fluorescent measurements can be made by exciting from 530 to 560 nm and recording emission at 590 nm [266]. In this study, 540 and 595 nm were used as excitation and emission wavelengths, respectively.

3

Following 24 h exposures, significant cytotoxicity ($P \leq 0.05$) was recorded at 400 and 800 µg/ml SWCNT tested in the presence of serum for the AB assay, with approximately 33 and 53% inhibition demonstrated respectively in comparison to untreated controls. The EC_{50} ± 95% CI value was determined as 744 ± 91 µg/ml SWCNT for serum exposures. In serum free media, significant cytotoxicity was

again recorded at 400 and 800 µg/ml SWCNT where a 42 and 51% inhibition in AB fluorescence was recorded in comparison to unexposed controls (Figure 3.2a). In the absence of serum, the EC_{50} was found to be > 800 µg/ml SWCNT.

Following exposure of the A549 cells to quartz in serum containing medium, significant cytotoxicity was observed at 200 and 400 µg/ml which resulted in an 18 and 23% inhibitory effect respectively in comparison to controls. At the top concentration tested (800 µg/ml), however, only a 2% inhibition was measured in comparison to untreated controls. Hence no EC_{50} value was derived for this exposure. For quartz exposures in the absence of serum, significant cytotoxicity was observed at 25, 50, 100, 400, and 800 µg/ml. Approximately 50 and 90% inhibition was recorded in comparison to untreated controls at 400 and 800 µg/ml of quartz, respectively (Figure 3.2b). An EC_{50} of 397 ± 159 µg/ml for quartz exposure without serum was determined.

3

Culturing of cells in the absence of serum for increased periods of time significantly affects cell performance. Therefore, exposure periods exceeding 24 h were carried out using 5%-F12K. As displayed in Figure 3.3a, exposure of A549 cells to SWCNT resulted in a time-dependent decrease in AB reduction to as low as 5% compared to control levels following 96 h exposures. In contrast, reductions in cell viability following quartz exposure never exceeded 27%, even after 96 h Figure 3.3 b.

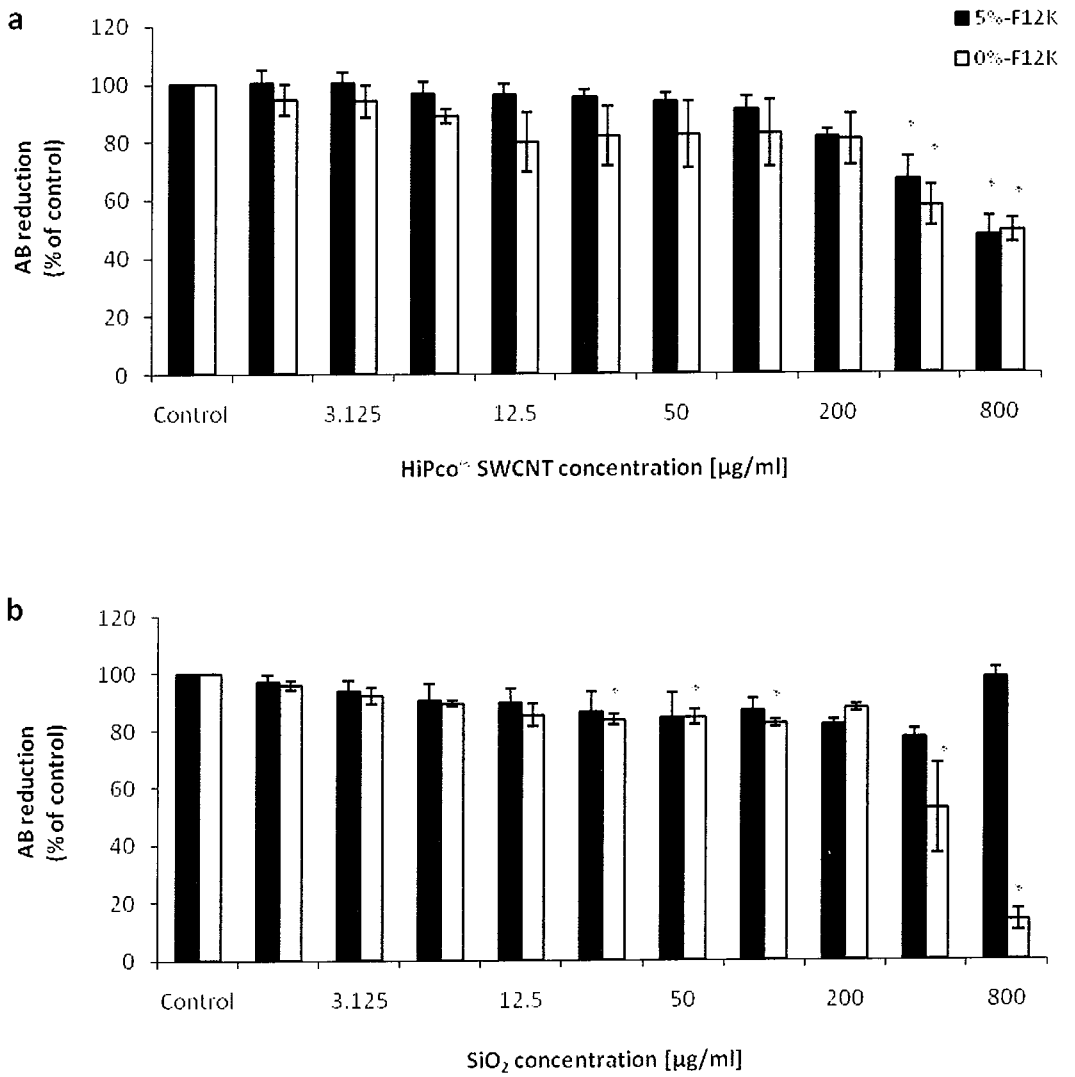

Figure 3.3: Cytotoxicity of HiPco® SWCNT (a) and quartz (b) to A549 cells after 24 h exposure determined by the AB assay. Exposures were conducted in media containing 5% serum (black) and serum free media (grey). Data are expressed as percent of control mean +/- SD of three independent experiments. *Denotes a significant difference from the control (P≥0.05).

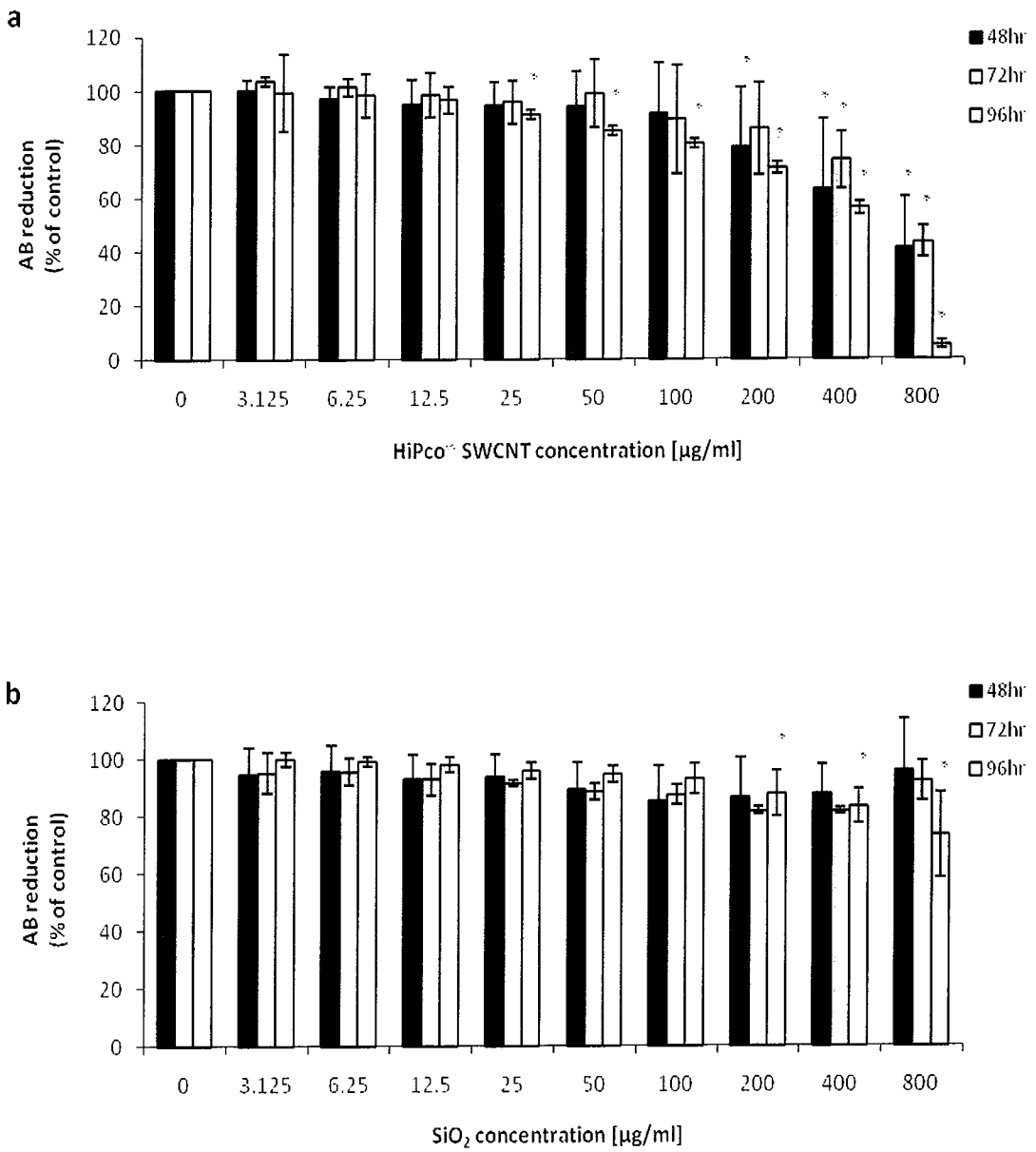

Figure 3.4: Cytotoxicity of (a) HiPco® SWCNT and (b) quartz dispersed in 5%-F12K to A549 cells after 48 h to 96 h exposure determined by the AB assay. Data are expressed as percent of control mean +/- SD of three independent experiments. *Denotes a significant difference from the control (P≥0.05).

3.4.2.1.2 *Coomassie Blue Assay*

The protein content of cells after exposure to a suspected toxicant is often used as a measure of cytotoxic effects *in vitro*. Different spectroscopic methods are routinely available, including measurement of protein's intrinsic UV absorbance, and methods generating a protein-dependent colour change, namely the Lowry-Bronsted assay and the Smith copper/bicinchoninic assay are well established. The simplest and most sensitive test is the Bradford assay, introduced in the mid 1970s, which is based on the equilibrium between three forms of Coomassie Brilliant Blue-G250 (CB) dye, which binds specifically to tyrosine side chains of protein molecules but not to other cellular constituents. Within the linear range of the assay (approximately 5 to 25 μg/ml), the more protein present, the more CB binds due to hydrophobic and ionic interactions [267, 268].

SWCNT in serum containing medium produced significant cytotoxicity at concentrations of 400 (25% inhibition) and 800 (32% inhibition) μg/ml using the CB assay. In the absence of serum, significant cytotoxicity was also observed at these concentrations (Figure 3.4a). No EC_{50} values were determined for the CB assay for both serum and serum free exposures, as maximum cytotoxicity determined in both instances was less than 50%.

For quartz exposures in serum containing media (Figure 3.4b), significant cytotoxicity was determined at 200, 400 and 800 μg/ml, with approximately 18, 30 and 34 % inhibition compared to untreated controls recorded, respectively. Therefore, the EC_{50} value was greater than the top concentration tested. In the absence of serum, a slight but non-significant increase in CB absorbance over controls was recorded for concentrations up to and including 200 μg/ml quartz.

Significant cytotoxicity was recorded at 400 (22% inhibition) and 800 (52% inhibition) μg/ml quartz (Figure 3.4b). An EC_{50} of 753 ± 187 μg/ml for quartz exposure without serum was determined with this assay.

3.4.2.1.3 *MTT Assay*

The MTT colorimetric assay determines the ability of viable cells to reduce the soluble yellow tetrazolium salt MTT into an insoluble purple formazan precipitate [269, 270]. Addition of solvent destroys the cell membrane and results in liberation and solubilisation of the crystals. The number of viable cells is thus directly proportional to the level of the initial formazan product created and can be quantified by measuring the absorbance at 570 nm [269].

For the MTT assay, exposure in serum containing medium resulted in significant cytotoxicity from 12.5 μg/ml SWCNT upwards and a maximum of 32% inhibition was recorded at 800 μg/ml SWCNT in comparison to the control. For exposures in the absence of serum, significant cytotoxicity was recorded from 3.125 μg/ml SWCNT upwards and 800 μg/ml SWCNT resulted in approximately 45% inhibition in comparison to the control (Figure 3.5a). Therefore, no EC_{50} values were determined for the MTT assay for both serum and serum free exposures to SWCNT, as maximum cytotoxicity determined in both instances was less than 50%.

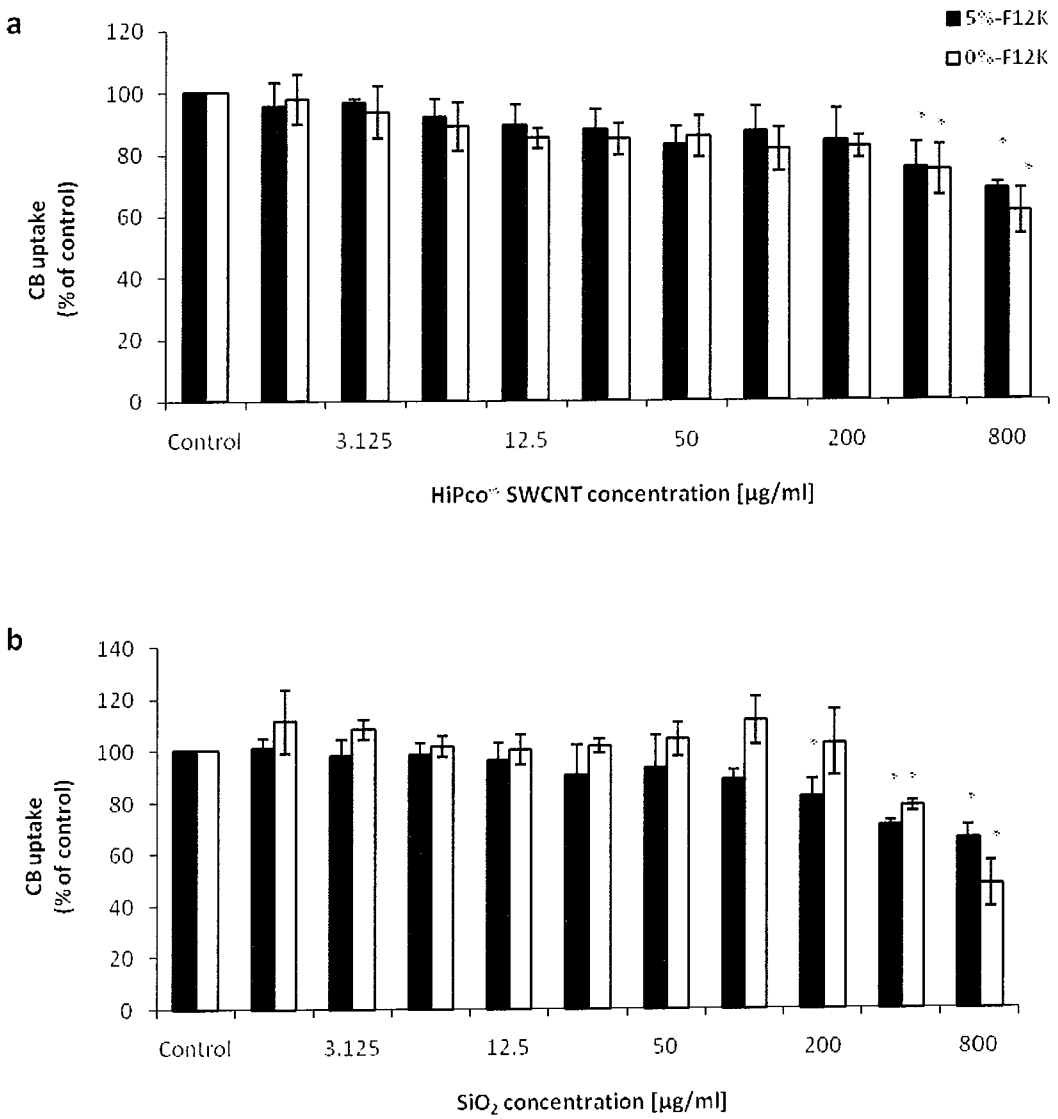

Figure 3.5: Cytotoxicity of HiPco® SWCNT (a) and quartz (b) to A549 cells after 24 h exposure determined by the CB assay. Exposures were conducted in media containing 5% serum (black) and serum free media (grey). Data are expressed as percent of control mean +/- SD of three independent experiments. *Denotes a significant difference from the control (P≥0.05).

No significant cytotoxicity was determined following 24 h exposure of the A549 cells to quartz in serum containing media. For the majority of the concentrations tested (except 400 µg/ml) a stimulatory or hormetic response was recorded but none of these were found to be statistically significant when compared to untreated controls. In the absence of serum in the test medium, significant cytotoxicity was determined at 100, 400 and 800 µg/ml quartz, with approximately 80% inhibition recorded at the top concentration (Figure 3.5b). An EC_{50} of 465 ± 130 µg/ml for quartz exposure without serum was determined with the MTT assay.

3.4.2.1.4 *WST-1 Assay*

The WST-1 assay is very similar to the MTT assay. The tetrazolium salt WST-1 is reduced by cellular mitochondrial hydrogenases at the same structural position when compared to MTT [271, 272]. The resulting product, in contrast to the MTT assay, is water-soluble and can be spectroscopically quantified at 450 nm without the requirement of an extraction step [271, 272].

The WST-1 assay was only carried out for SWCNT dispersed in serum-free medium at concentrations between 1.56 and 400 µg/ml. The highest SWCNT concentration resulted in a decrease in cell viability by 20% following 24 h. Prolonged exposure up to 96 h showed time-dependent decreases reaching viability levels as low as 40% compared to control cells (Figure 3.6a). The toxicity of quartz particles seemed to be time-independent leading to reductions of 20 to 40% at 400 µg/ml (Figure 3.6b).

3.4.2.1.5 *Neutral Red assay*

The NR cytotoxicity assay is based on the ability of viable cells to incorporate and bind neutral red, a weak cationic dye that readily penetrates cell membranes by non-ionic diffusion [273]. It accumulates in the lysosomes of cells where it binds to the sensitive lysosomal membrane. Cells damaged by xenobiotic action have decreased ability to take up and bind NR, so that viable cells can be distinguished from damaged or dead cells.

In this study, inconsistent fluorescent readings were repeatedly acquired when using the NR dye as can be seen from the error bars in the data presented (Figure 3.7a). A dose-response curve of this nature can be interpreted as a hormesis effect. However, the large data variation makes interpretation problematic. For the toxicity of quartz particles (Figure 3.7b), the NR assay did show good correlation with the MTT assay (Figure 3.5b).

3

3.4.2.1.6 *Adenylate Kinase*

Analysis of cell supernatants for the release of adenylate kinase (AK) following quartz exposure for 24 h showed significant increases in AK at 200 to 800 µg/ml with 400 µg/ml showing the most pronounced response (Figure 3.8). Following SWCNT exposure, AK release was surprisingly reduced in a dose-dependent fashion reaching a decrease of more than 40% at a dose of 800 µg/ml. In contrast, quartz did result in significant increases in AK release reaching a maximum at a concentration of 400 µg/ml.

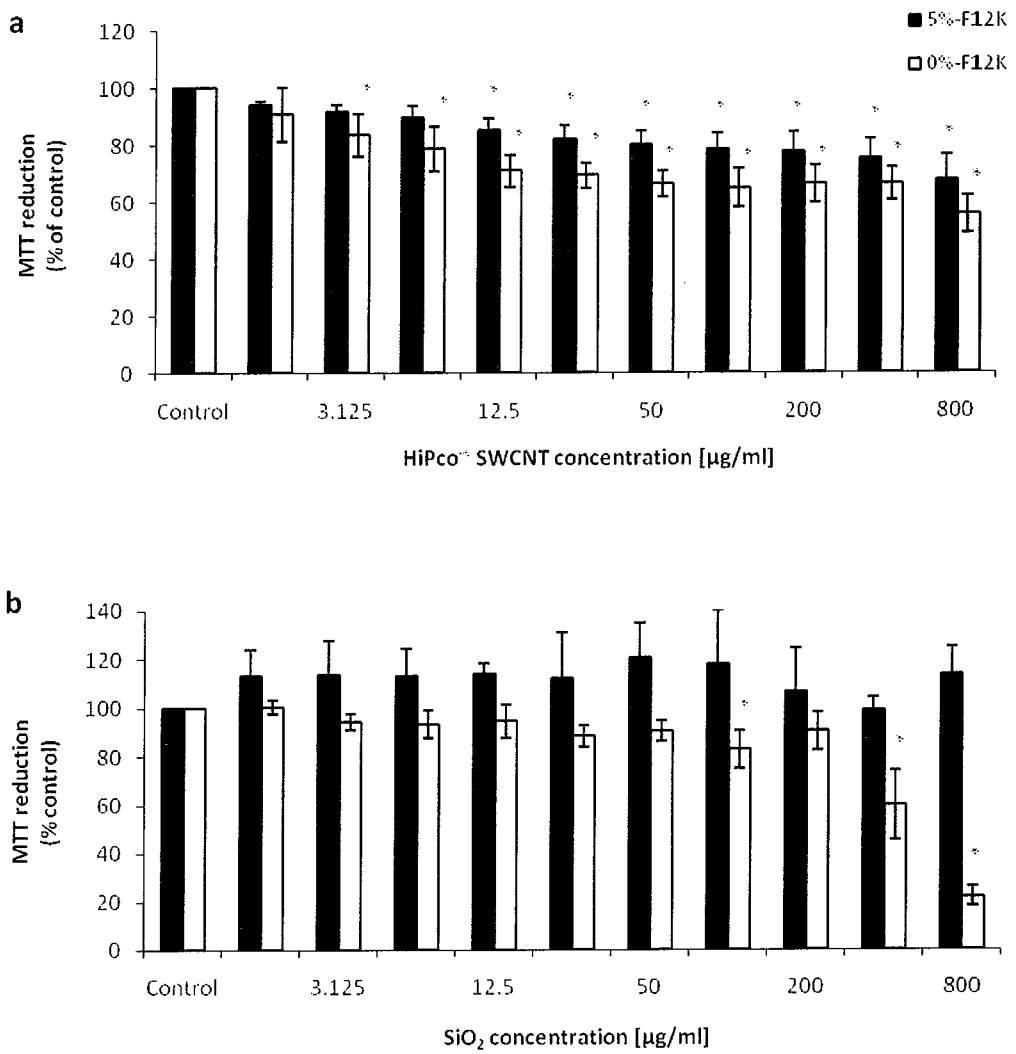

Figure 3.6: Cytotoxicity of HiPco® SWCNT (a) and quartz (b) to A549 cells after 24 h exposure determined by the MTT assay. Exposures were conducted in media containing 5% serum (black) and serum free media (grey). Data are expressed as percent of control mean +/- SD of three independent experiments. *Denotes a significant difference from the control (P≥0.05).

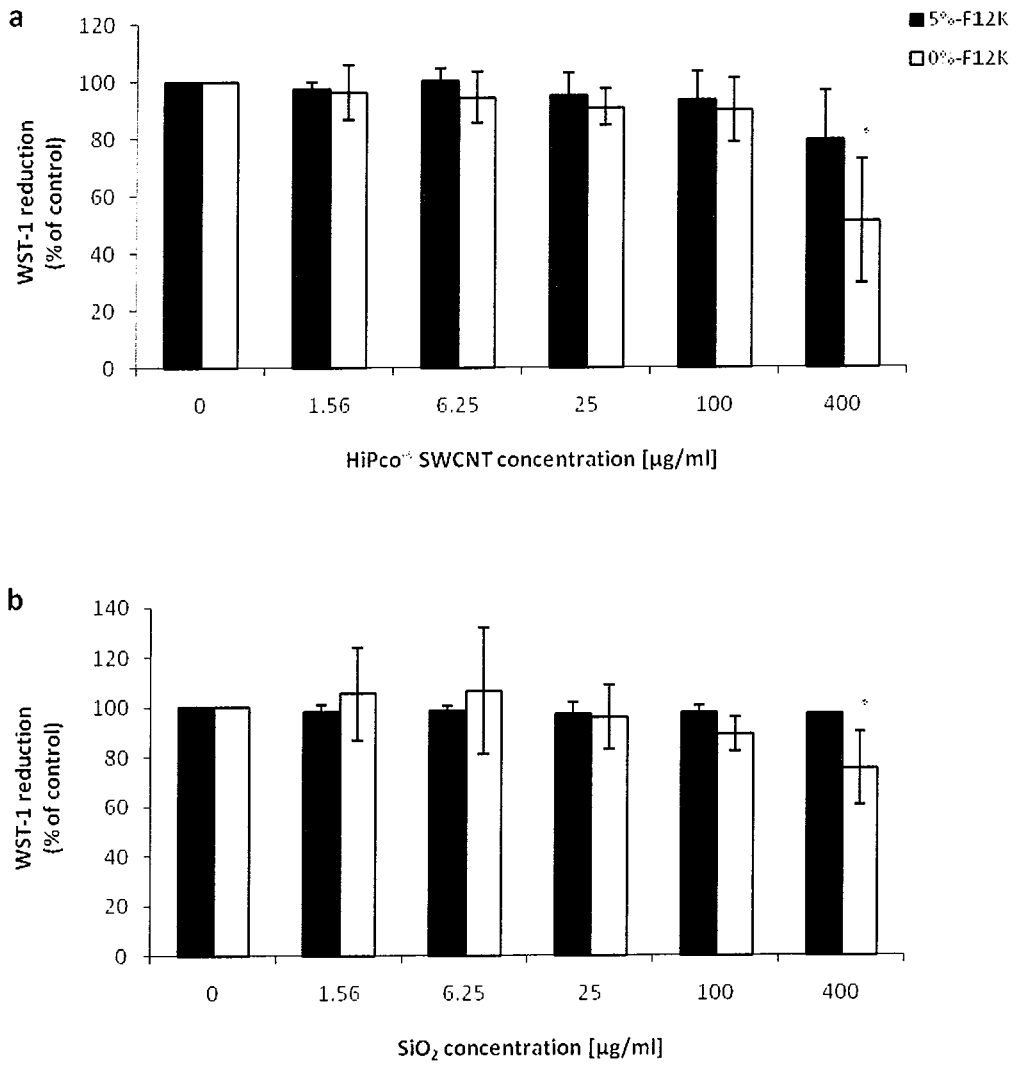

Figure 3.7: Cytotoxicity of HiPco® SWCNT (a) and quartz (b) to A549 cells after 24 h exposure determined by the WST-1 assay. Exposures were conducted in media containing 5% serum (black) and serum free media (grey). Data are expressed as percent of control mean +/- SD of three independent experiments. *Denotes a significant difference from the control (P≥0.05).

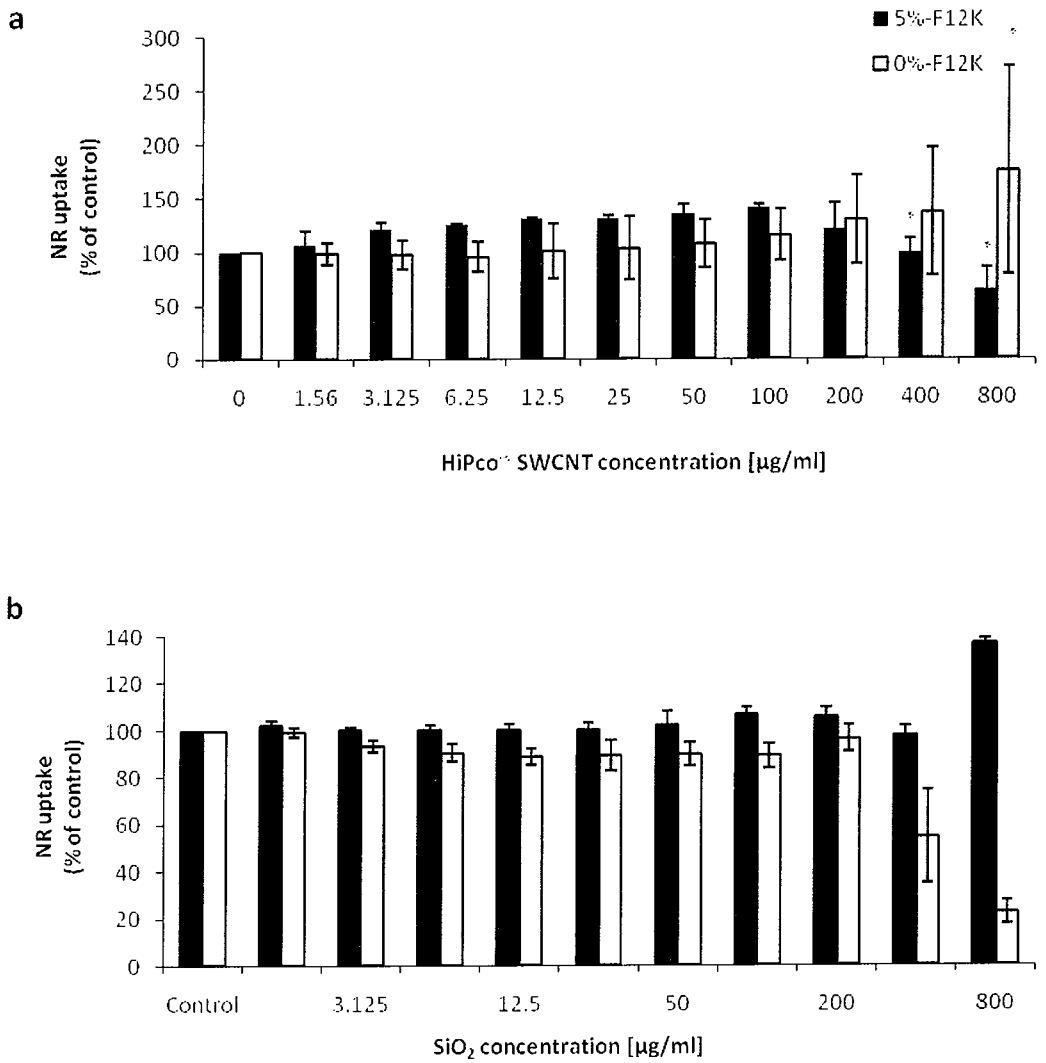

Figure 3.8: Cytotoxicity of SWCNT (a) and quartz (b) to A549 cells after 24 h exposure as determined by the NR assay. Exposures were conducted in media containing 5% serum (black) and serum free media (grey). Data are expressed as percent of control mean +/- SD of three independent experiments. *Denotes a significant difference from the control (P≥0.05).

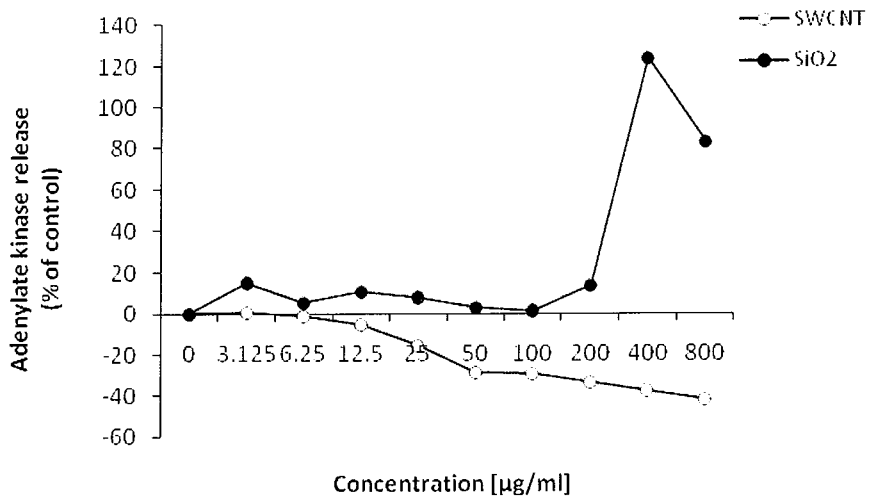

Figure 3.9: Adenylate kinase (AK) release by A549 cells following 24 h exposure to SWCNT (white) and quartz (black). Data are expressed as percent of control mean of three pooled independent experiments.

3.4.2.1.7 *Comparison to other cell lines*

3

In order to assess whether the responses to SWCNT were specific to A549 cells, effects were compared to that of a dermal model using keratinocyte cells (HaCaT). Cell responses were compared based on AB reduction (Figure 3.9) and AK release (Figure 3.10). As seen for A549 cells, cell viability of HaCaT cells decreased dose-dependently with increasing concentrations of SWCNT as shown in Figure 3.9a. However, the decrease was less pronounced than that seen for A549 cells (Figure 3.3) with maximum reductions of 49% compared to control levels following 24 h exposure. Even after 96 h, levels did not exceed a 50% reduction (Figure 3.9a). In contrast, HaCaT cells were more sensitive to quartz toxicity compared to A549 cells. Significant decreases in AB reductions were only observed following 96 h

exposures of A549 cells, whereas a time- and dose-dependent decrease in AB reduction, reaching levels of up to 53% compared to control cells, could be observed for HaCaT cells (Figure 3.9b). However, overall, both cell models, pulmonary and dermal, did show significant decreases in cell viability only at high SWCNT concentrations which became more pronounced following longer exposure periods.

In addition, AK release was also decreased following exposure of both cell types indicating that cell responses are not specific to cell type but might be common mechanisms of SWCNT toxicity. For both cell lines, AK release reached its maximum at quartz concentrations of 400 μg/ml (Figure 3.10). However, HaCaT cells appeared more sensitive to particle exposure, leading to increases in AK release by up to 287% following quartz exposure. Exposure of A549 cells resulted in increases by only 124%. HaCaT cells were also more sensitive to the effects of SWCNT exposure which caused decreases in AK by 74%.

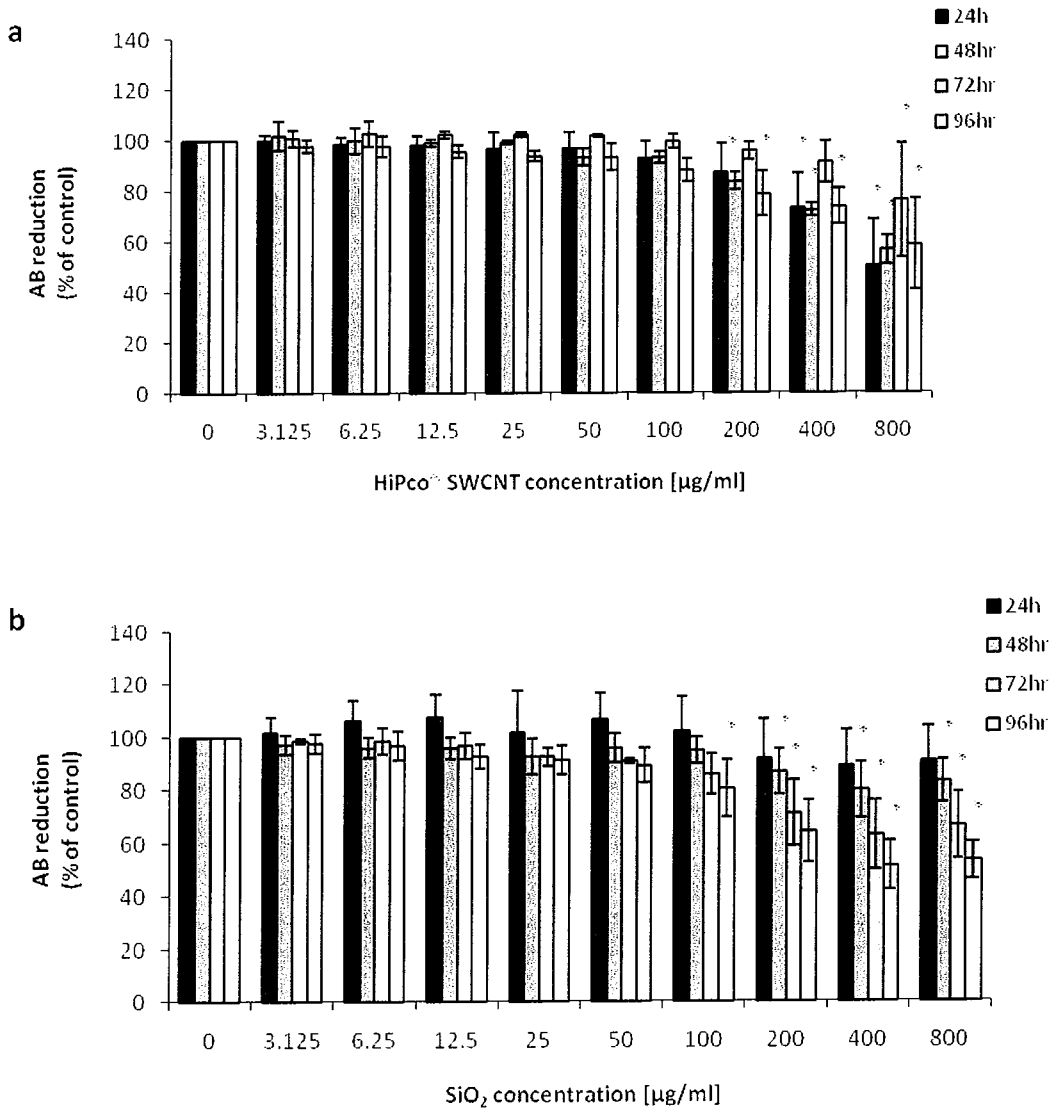

Figure 3.10: Cytotoxicity of HiPco® SWCNT (a) and quartz (b) to HaCaT cells after 48h – 96h exposure determined by the AB assay. Exposures were conducted in media containing 5% serum. Data are expressed as percent of control mean +/- SD of three independent experiments. *Denotes a significant difference from the control (P≥0.05).

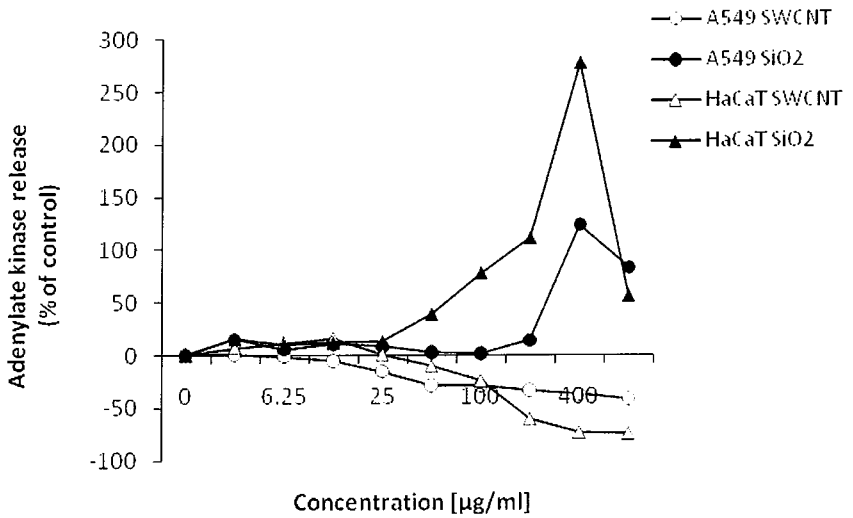

Figure 3.11 Adenylate kinase (AK) release by A549 and HaCaT cells following 24 h exposure to SWCNT (white) and quartz (black). Data are expressed as percent of control mean of three pooled independent experiments.

3.4.3 Spectroscopical study

As shown in Figure 3.7, the measurement of NR uptake following SWCNT exposure did result in large data variation. Furthermore, AK release decreased below control levels indicating decreased cytotoxicity with increasing SWCNT concentrations which would stand in contrast to any previously obtained results. During cytotoxicty studies it was noted that agglomerates of SWCNT adhere to cell surfaces and remain adhered even after several washes with PBS as shown in Figure 3.11. Therefore, some SWCNT were still present during cell incubations with the different toxicity indicator dyes used in this study so that the question was raised whether SWCNT may interact with some of these colorimetric and fluorescent dyes, resulting in unexpected absorption/fluorescence data. In order to

investigate and characterize any potential interactions, a spectroscopic study was carried out as described by Casey *et al.* (2007b) [257].

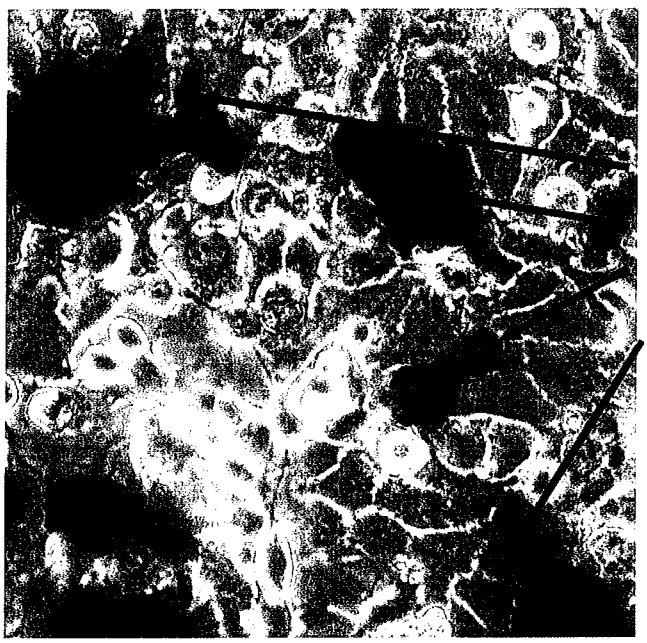

Figure 3.12: Phase contrast micrograph (200 x) of A549 cells following 24 h exposure to 800 µg/ml SWCNT with 5% serum showing black agglomerates of SWCNT (arrows) on cell surface.

3

As illustrated in Figure 3.12, colour changes could be observed in AB, NR, MTT and WST-1 solutions following addition of SWCNT leading to colour quenching. Therefore, spectroscopical studies were carried out in order to characterise the interactions between SWCNT and the dye molecules observed.

In order to investigate whether there was an interaction between the indicator dyes employed for cytotoxicity assessment, the respective dye solutions were incubated with stock concentrations of SWCNT as would be present during toxicity testing [257]. During the 24 h exposure period, the particles settled and the supernatants were used for spectroscopical analysis. Therefore, absorbance or

emission values were plotted against SWCNT concentration. The resulting curve was then compared to the emission/absorbance behaviour of control solutions that were prepared in parallel and without the addition of SWCNT.

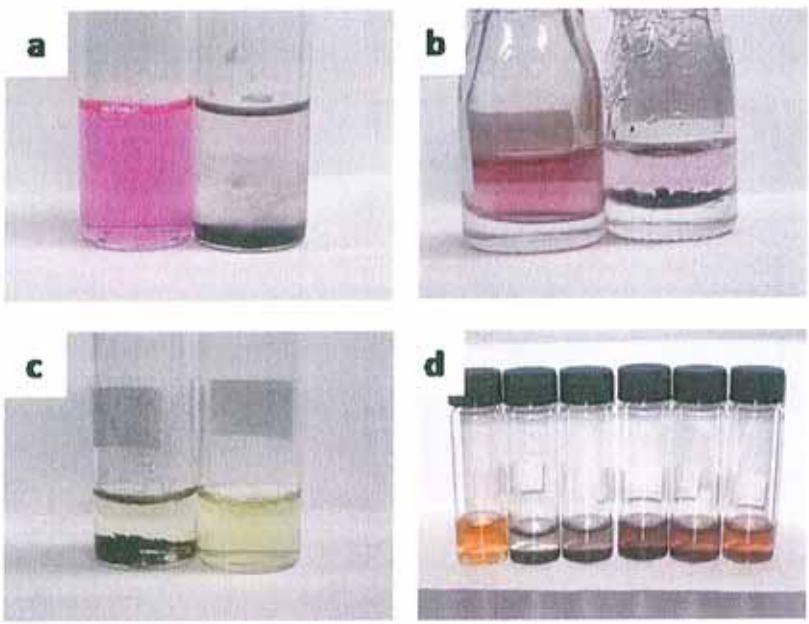

Figure 3.13: (a) converted AB (b) NR (c) unconverted MTT and (d) WST-1 solution before (left) and after addition of HiPco® SWCNT (right).

For investigating interactions with the CB dye, stock CB solution as used for cytotoxicity assessment were incubated with 400 µg/ml SWCNT and serially diluted with acetic acid buffer solution to final concentrations of 2.34 µg/ml. Plotting the absorbance data (615nm), a linear relationship was observed with significant differences between control and SWCNT exposed solutions. The associated slope was reduced from 2.5 to 1.4 upon the addition of SWCNT. While the reduction in an absorbance feature of this nature provides little information about the type of the interaction between the two species, it verifies the existence of an interaction. Furthermore, the fact that reduction in CB absorbance could be

observed at all SWCNT concentrations and became significant above 25 μg/ml, could make the evaluation of SWCNT toxicity based on CB binding measurements problematic.

Before the interaction of SWCNT with the AB dye could be studied, confluent cells had to be exposed to AB solutions in order to allow reduction into its reduced, pink form. This reduced AB solution was then exposed to SWCNT and serially diluted down using the same solution. The pink AB solution immediately lost its characteristic colour and total quenching of fluorescent emission at 595nm by 540nm excitation was observed. Therefore, the procedure was repeated using a lower initial SWCNT concentration of 80 μg/ml (10 % of highest toxicity test concentration), which was serially diluted to a final SWCNT concentration of 3.9 x 10^{-2} μg/ml. The initial SWCNT concentration of 80 μg/ml again resulted in total quenching of emission at 595nm. Monitoring this quenching as a function of SWCNT concentration and plotting it as a ratio of the SWCNT free AB solution's emission at 540nm excitation, showed a dose-dependent behaviour. At the lowest SWCNT concentration of 3.9 x 10^{-2} μg/ml, fluorescent quenching was observed with a reduction to approximately 68% compared to the SWCNT free solution.

3

Similar behaviour was observed for the NR, MTT and WST-1 dye solutions. To elucidate interactions with NR, SWCNT were dispersed in a NR deionised water solution in an initial 1:1 concentration ratio of 6.25 μg/ml and the solution was then serially diluted with deionised water, to reduce both the NR and the SWCNT concentration equally to a final concentration of 9.5 x 10^{-4} μg/ml and the emission was recorded.

To investigate the interactions with the MTT dye, confluent cells were exposed to MTT solutions at a concentration of 0.5 mg/ml and the system was allowed to undergo the reduction process to form the purple formazan precipitate. This was then extracted with 0.04N HCl prepared in isopropanol and then decanted and centrifuged to remove any remaining cells. Solutions containing SWCNT were then prepared with this at an initial concentration of 800 µg/ml and serially diluted. At SWCNT concentrations above 0.05 mg/ml the solutions underwent a colour change from the characteristic purple of the converted form of MTT to a pale yellow similar to that of the unconverted MTT. This colour change may indicate the presence of MTT, which was not converted by the cells and did not interact with the SWCNT. The absorbance spectra were recorded and the reduction of the formazan feature at 570 nm was monitored as a function of SWCNT concentration. No noticeable spectroscopic differences were observed at concentrations below 6.25 µg/ml. Above this concentration, a reduction in absorption was observed and this reduction was seen to increase with increasing SWCNT concentration.

3

In contrast to the MTT assay, the product of WST-1 reduction is water-soluble. This is also the reason why this dye was recommended by Wörle Knirsch *et al.* (2006) as no binding of crystals to SWCNT could be observed microscopically leading the authors to conclude that no interaction would take place [210]. Within the course of this study, potential interactions were characterised spectroscpically. The WST-1 dye was allowed to undergo the conversion process by exposing it to confluent cells for a period of 3 h followed by decanting and centrifugation to remove any remaining cells as described for the MTT dye. Initial SWCNT concentrations of 400 µg/ml were then added and the solution was serially diluted using the converted

WST-1 dye. A reduction in the WST-1 associated absorbance was noted at concentrations above 12.5 µg/ml, which further reduced with increasing SWCNT concentrations.

Overall, the spectroscopic studies showed that there are indeed interactions taking place between SWCNT and all indicator dyes used resulting in interferences with absorbance and fluorescent measurements. Given the amount of SWCNT agglomerates which remain adhered to the cells even after repeated washing, accurate quantification of SWCNT is not guaranteed using these dyes. In order to evaluate whether there is any cytotoxicity of SWCNT or whether the effects seen are solely due to SWCNT interactions, qualitative toxicity assessment was carried out using microscopic evaluation.

3.4.4 Qualitative toxicity assessment

3.4.4.1 *Trypan Blue staining*

Cells with an intact membrane are able to exclude the Trypan Blue dye [274]. Therefore, cells damaged due to SWCNT toxicity will take up the dye and stain blue. In this study, the Trypan Blue assay was used to quantify cytotoxicity but also qualitatively observe membrane damage by microscopical observations. As shown in Figure 3.13, 19% of A549 cells were stained with Trypan Blue and therefore displayed signs of cytotoxicity following exposure to 400 µg/ml SWCNT in the absence of serum.

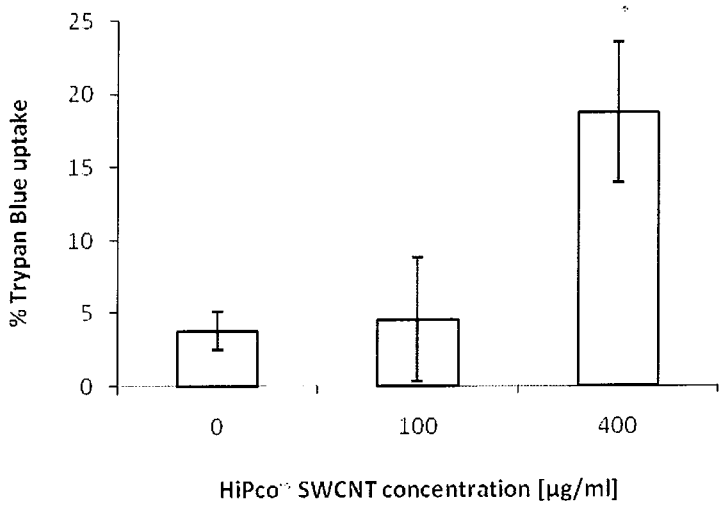

Figure 3.14: Trypan Blue uptake by A549 cells following 24 h exposure to 0-400 µg/ml HiPco® SWCNT dispersed in 0%-F12K. Data are expressed as percent of control mean +/- SD of three independent experiments. *Denotes a significant difference from the control (P≥0.05).

3.4.4.2 *Propidium iodine staining*

Propidium iodide (PI) can also be used for cytotoxicity evaluation. It is able to penetrate the nucleus of necrotic cells and it is possible to detect them at an excitation wavelength of 540 nm and emission of 650 nm [213, 248]. Following 24 h exposure to SWCNT, the number of PI stained control A549 cells was very low (Figure 3.14 a). Exposure to SWCNT in the absence of serum did result in increased PI uptake indicating cytotoxicity. The dye was preferably taken up by cells in close proximity to (Figure 3.14 b) and even underneath SWCNT agglomerates (Figure 3.14 c), indicating cell necrosis around these areas. This was seen independently of the SWCNT concentrations used. Furthermore, it was noted that around SWCNT, A549 cells tended to grow out of plane (Figure 3.14 d) towards SWCNT bundles

which might ultimately lead to cell detachment. Therefore, SWCNT in the absence of serum supplements do have the potential of being cytotoxic to A549 cells.

3.4.4.3 *Immunostaining*

Actin-tubulin staining was used in order to assess effects of particle exposure on the cytoskeleton of A549 cells. Exposures were carried out for 96 h in the presence of FBS. Figure 3.15 and Figure 3.16 show typical images obtained for A549 control cells in areas of low and high cell density, respectively. As can be seen, control cells did not show any significant irregularities in their cytoskeleton. In contrast, following SWCNT exposure, tubulin filaments appeared to accumulate and actin became more unstructured around SWCNT agglomerates (Figure 3.17 and Figure 3.18). In addition, cells appeared to grow towards and around SWCNT agglomerates as shown in Figure 3.18. By taking images along the z-axis it was possible to obtain information on the 3-dimensional behaviour of exposed cells. As can be seen in Figure 3.19, following the slices through the exposed cell monolayer starting at the bottom of the culture dish, this aggregation of both tubulin and actin filaments, around SWCNT agglomerates could be confirmed. No effects could be observed on cells growing distant from SWCNT. This indicates that over longer exposure periods in the presence of FBS, SWCNT are not acutely cytotoxic to A549 cells.

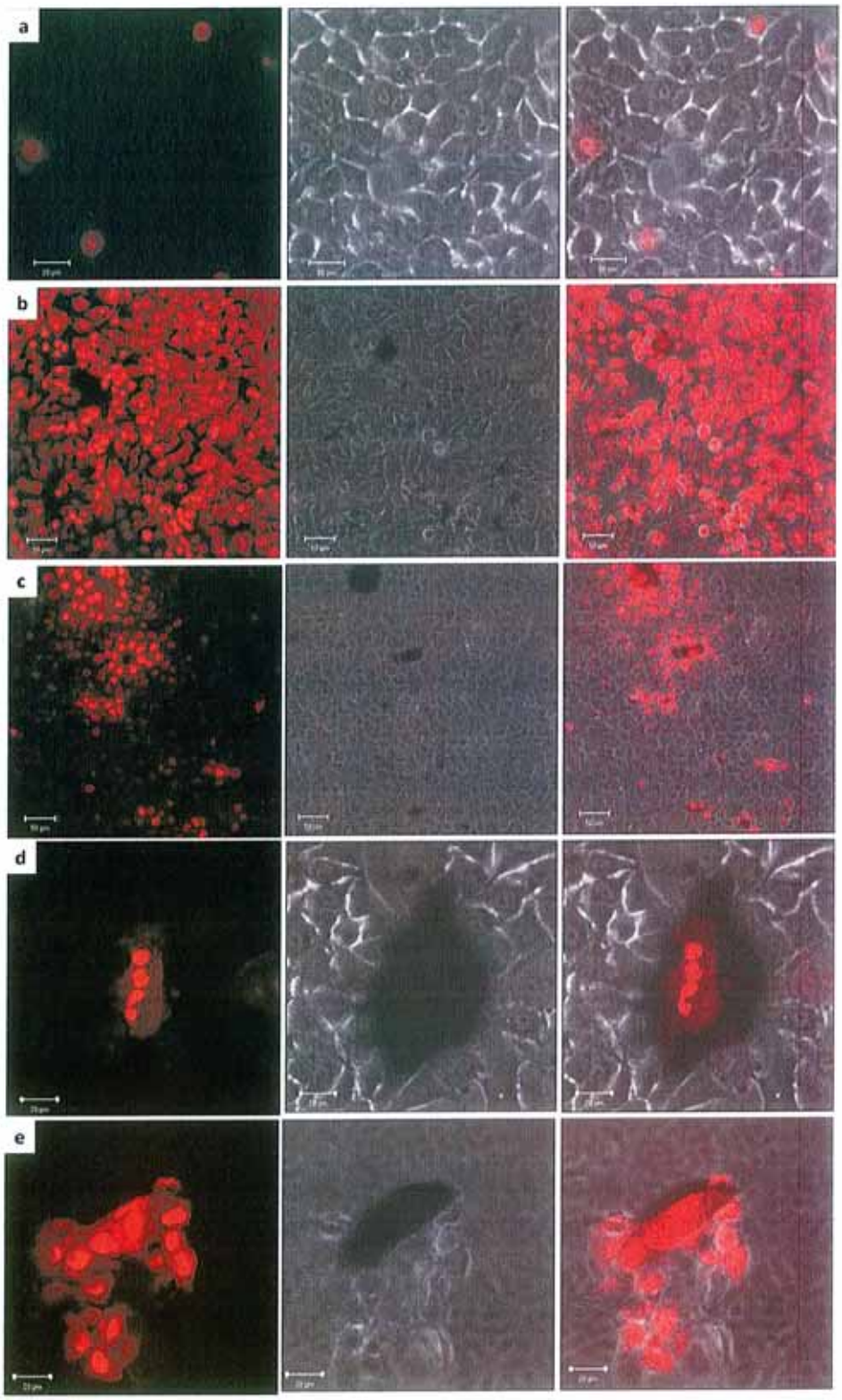

Figure 3.15: PI staining of A549 cells following 24h exposure to (a) control culture medium or (b) 800 µg/ml HiPco® SWCNT followed by cell fixation using formaldehyde, (c) 50 µg/ml and (d and e) 800 µg/ml of HiPco® SWCNT

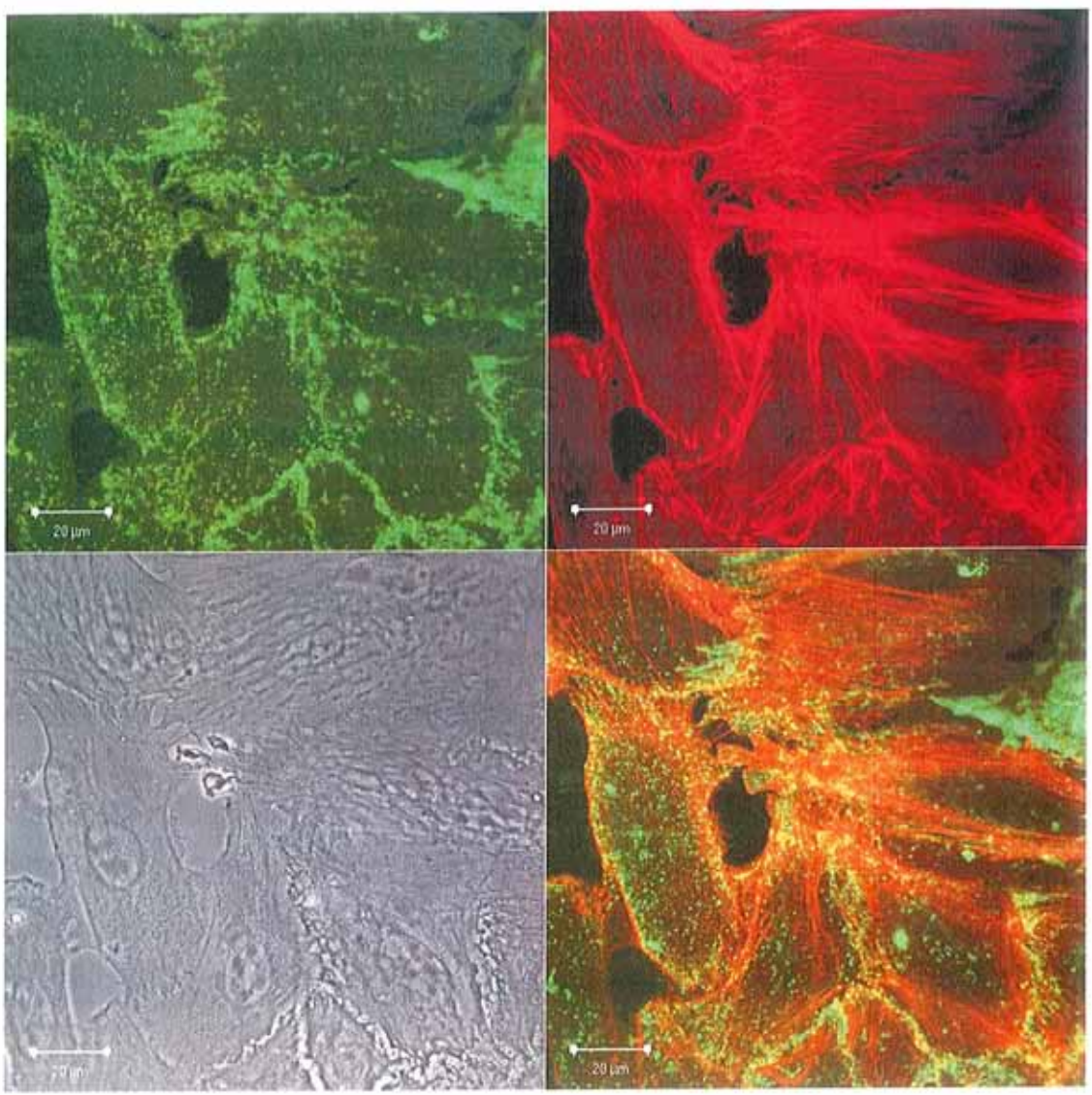

Figure 3.16: Low cell density area of A549 cells following 96 h exposure to control culture medium.

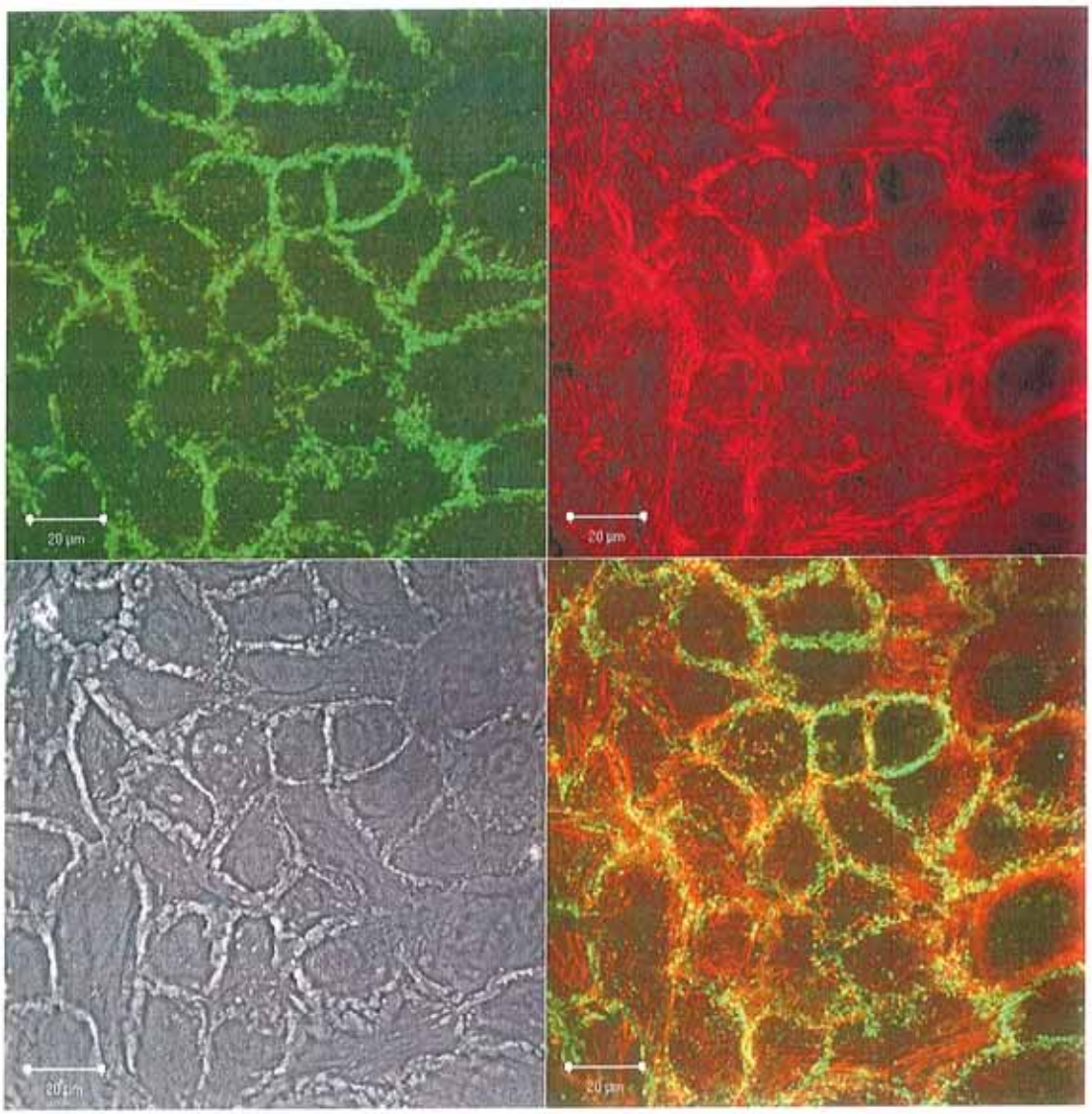

Figure 3.17: High cell density area of A549 cells following 96 h exposure to control culture medium.

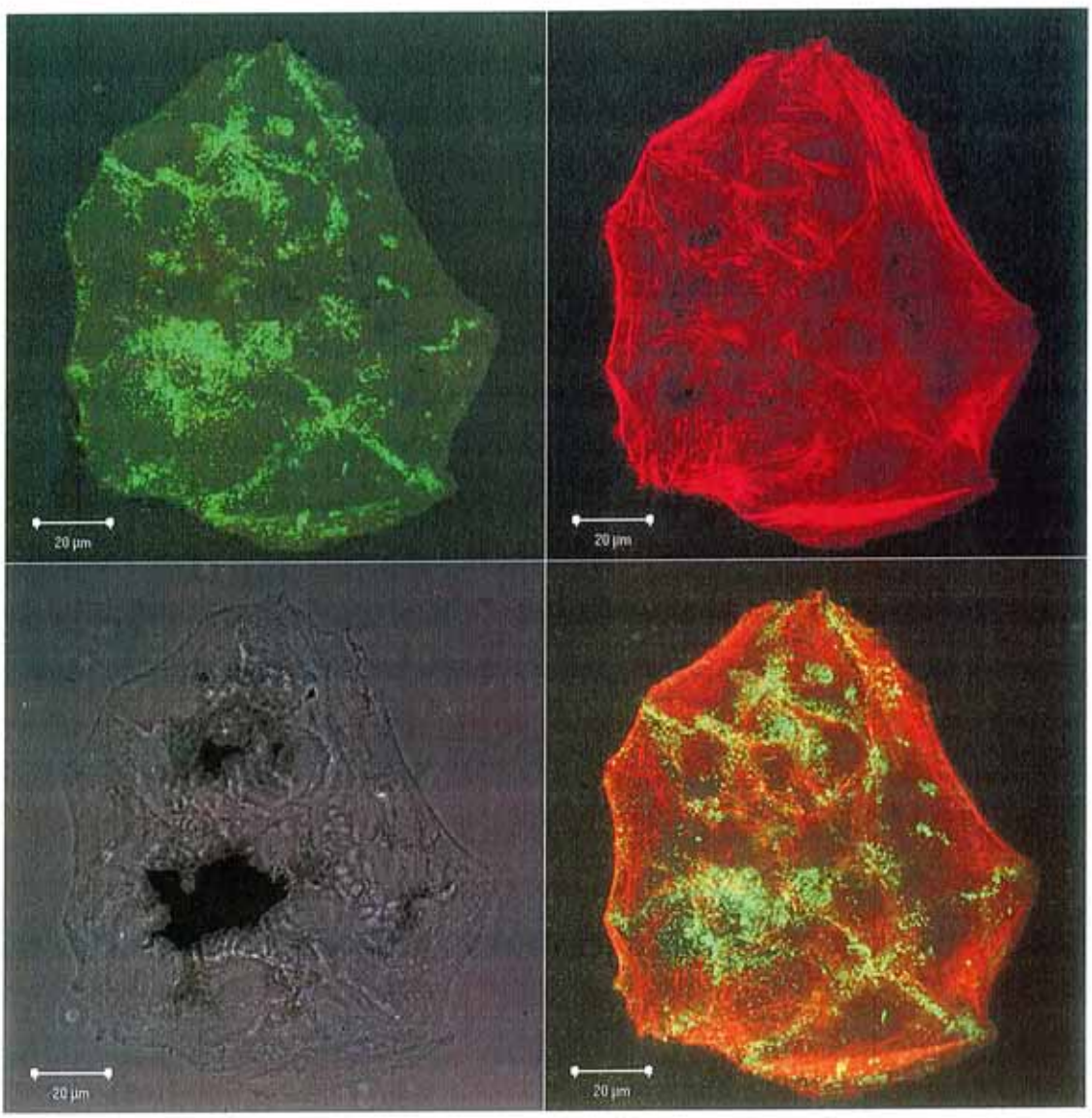

Figure 3.18: A549 cells following 96 h exposure to 400 µg/ml of HiPco® SWCNT.

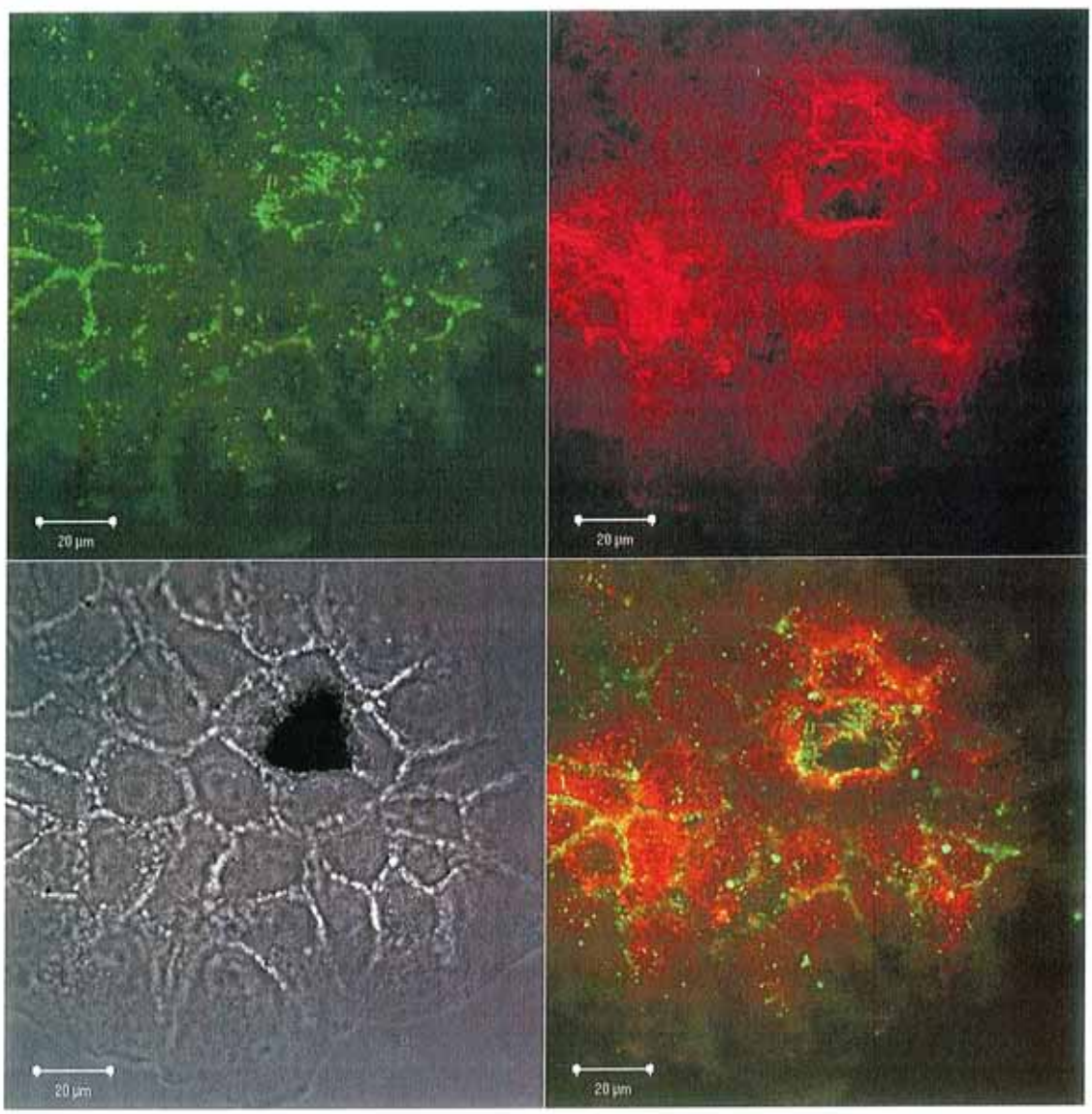

Figure 3.19: A549 cells following 96 h exposure to 25 µg/ml of HiPco® SWCNT.

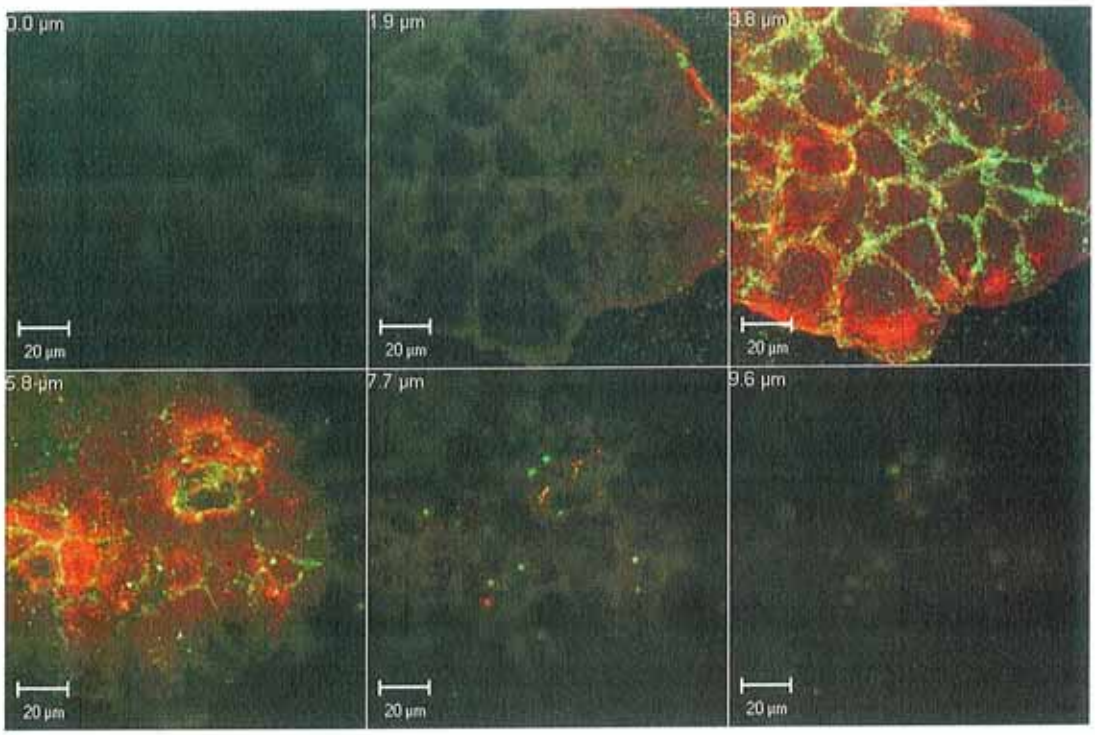

Figure 3.20 Z-stack series of A549 cells following 96 h exposure to 25 µg/ml of HiPco® SWCNT.

3.4.4.4 *Optical and Transmission Electron Microscopy*

Optical micrographs of the A549 cells following exposure to selected concentrations of SWCNT and quartz in serum containing medium are presented in Figure 3.20. Control A549 cells were of typical cuboidal shape, indicative of type II pulmonary morphology (Figure 3.20a). Exposure to the positive control quartz (800 µg/ml) resulted in extensive cell mortality as evidenced by the cell debris seen in Figure 3.20b Cells exposed to SWCNT exhibited altered morphology and necrotic and apoptotic cells were observed (Figure 3.21 a and b)..

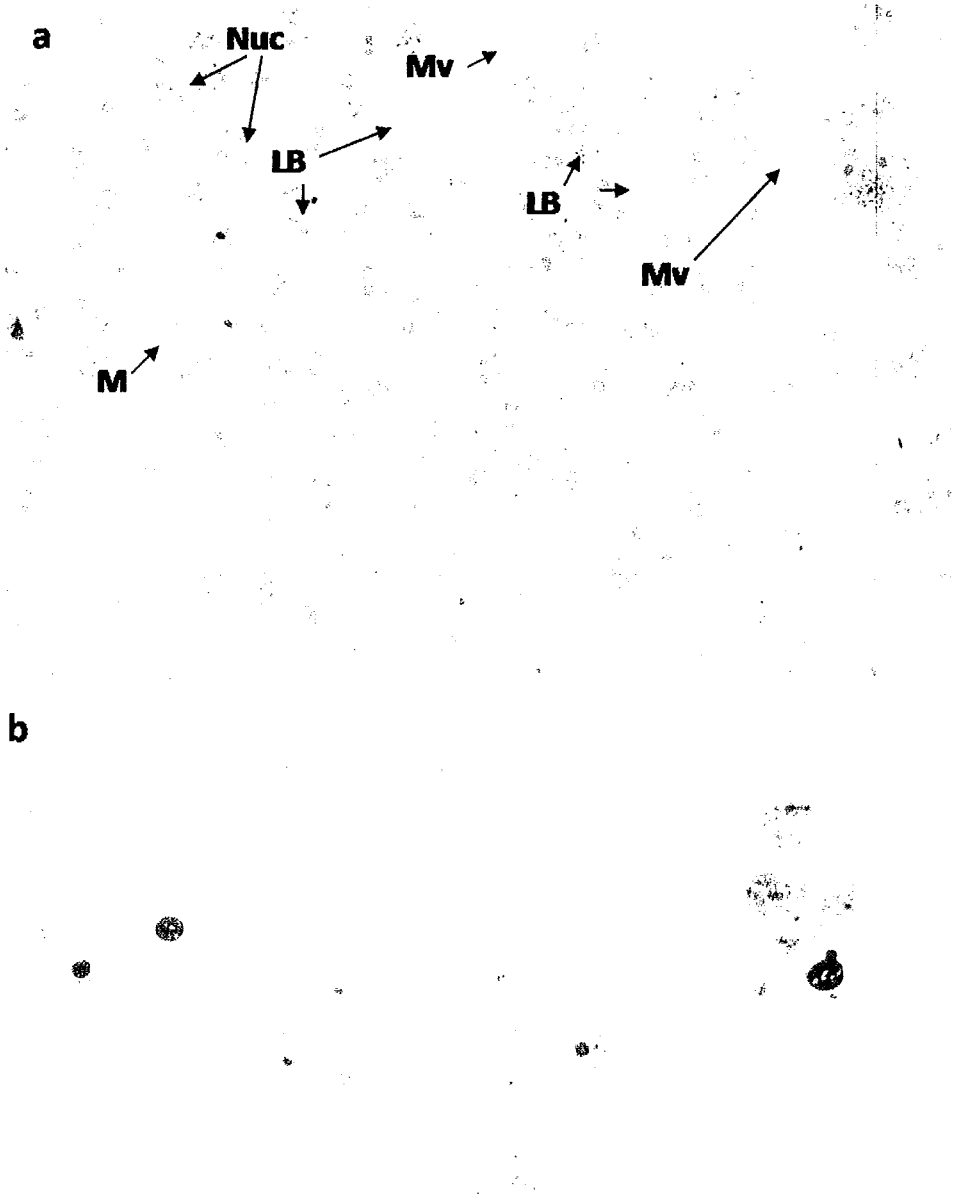

3

Figure 3.21: Optical micrographs of A549 (a) control cells showing nucleus (Nuc) and cells in metaphase (M), lamellar bodies (LB) and microvilli (Mv);(b) cells exposed to 800 μg/ml quartz showing cell debris. Magnification of 400 x.

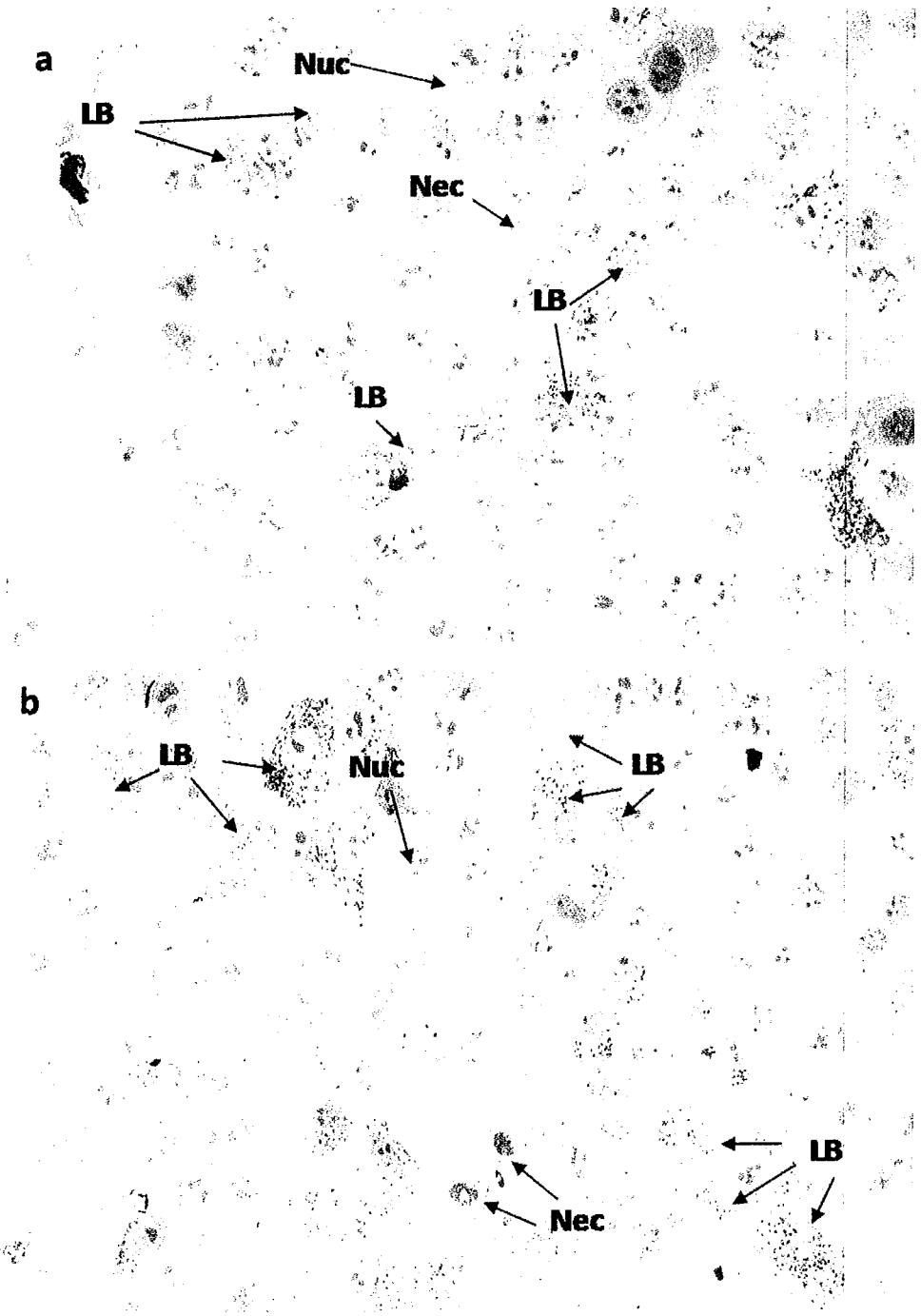

Figure 3.22: Optical micrographs of A549 (a) cells exposed to 400 µg/ml SWCNT with serum showing nucleus (Nuc), necrotic cells (Nec) and lamellar bodies (LB); (b) cells exposed to 800 µg/ml SWCNT with serum showing nucleus (Nuc) and lamellar bodies (LB). Magnification of 400 x.

Morphological features such as lamellar body structures, microvilli, tonofilaments, desmosome junctions, characteristic of alveolar epithelial type II cells were observed in TEM images of control cell cultures (Figure 3.21). Following exposure to 400 μg/ml SWCNT, an increase in lamellar bodies was recorded (Figure 3.22a-c); multivesicular bodies were also observed (Figure 3.22b) and the presence of extracellular (excreted) lamellar bodies was noted (Figure 3.21c). Following exposure to the highest test concentration of SWCNT, substantial increases in lamellar bodies were observed compared to untreated controls, although this observation was not quantified (Figure 3.22d-e). A reduction in microvilli and an increase in lipid droplet numbers were also evident compared to control cultures. Multivesicular bodies were observed at the cell surface (Figure 3.22f).

No evidence of SWCNT internalisation (either in serum containing or serum free media) was found for this lung epithelium model. Due to the crystalline nature of quartz it was not possible to section the exposed cell cultures for subsequent TEM imaging.

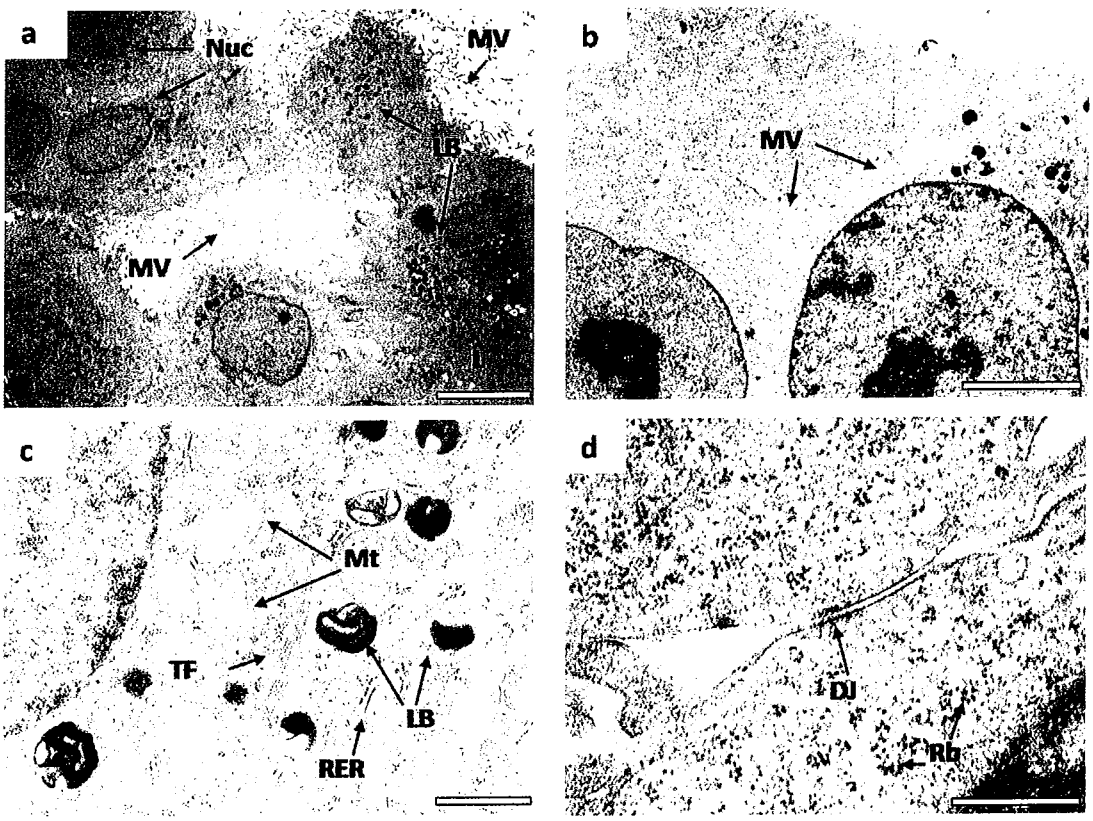

Figure 3.23: TEM of A549 control cells showing (a) nucleus (Nuc), lamellar bodies (LB), lipid droplets (L) and extensive microvilli (Mv); (b) intercellular microvilli (Mv), (c) mitochondria (Mt), lamellar bodies (LB), tonofilaments (TF) and rough endoplasmic reticulum (RER); (d) desmosome junction (DJ) and free ribosomes (Rb). Scale bars indicate (a) 10 μm, (b) 5 μm, (c) 1 μm and (d) 500 nm.

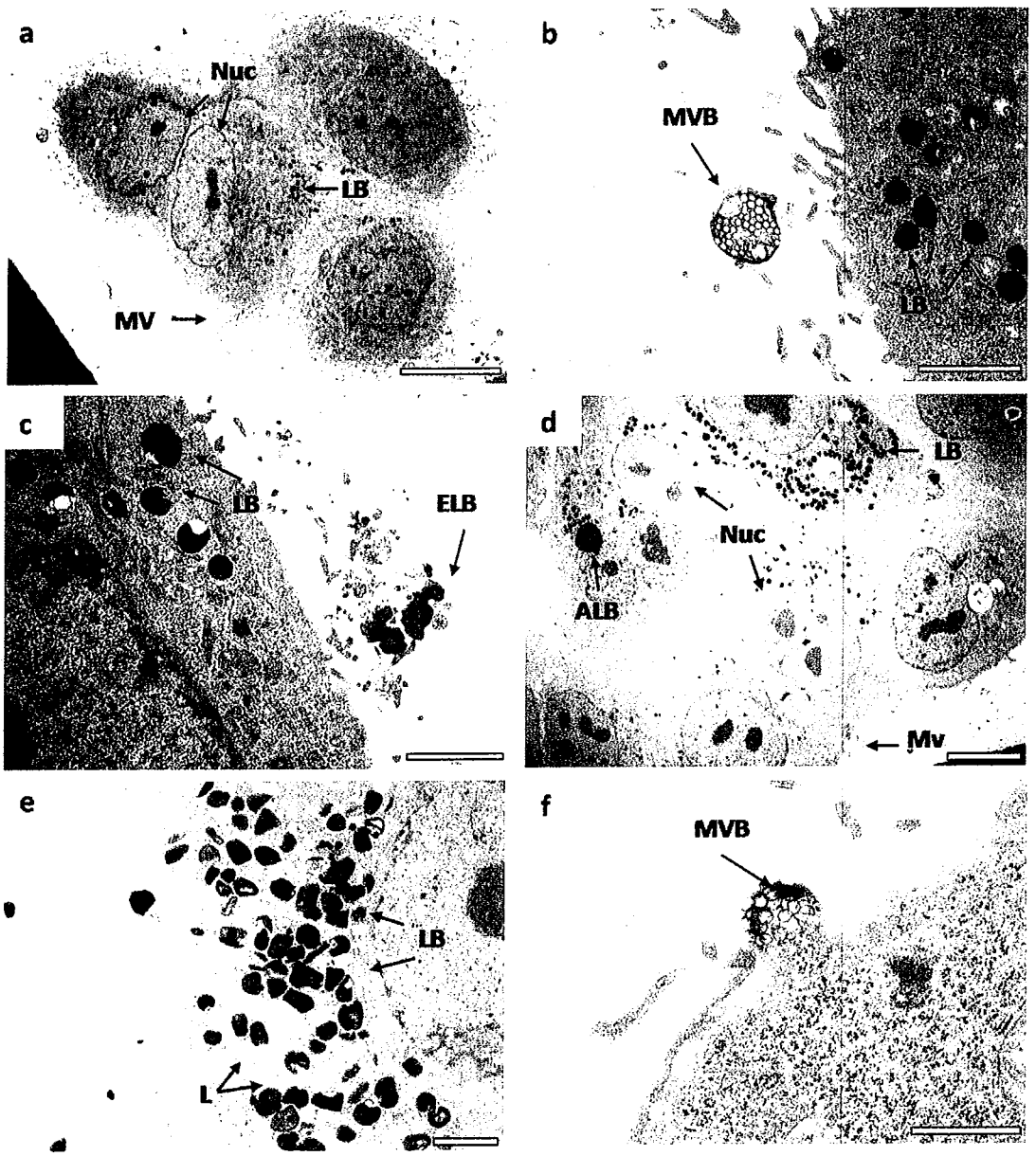

Figure 3.24: TEM of A549 cells treated with 400 μg/ml SWCNT (a–c) showing (a) nucleus (Nuc), lamellar bodies (LB), and microvilli (Mv), (b) lamellar bodies (LB) and multivesicular body (MVB), (c) lamellar bodies (LB) and extracellular lamellar bodies (ELB) and A549 cells treated with 800 μg/ml SWCNT; (d–f) showing (d) nucleus (Nuc), lamellar bodies (LB), and reduced microvilli (Mv), and an aggregation of lamellar bodies (ALB), (e) lamellar bodies (LB) and an accumulation of lipid droplets (L) and (f) a multivesicular body (MVB) associated with the plasma membrane. A549 cells were exposed to SWCNT either with serum (a, b and d, e) or without serum (c and f). Scale bars indicate (a) 10 μm, (b; c; e) 2 μm, (d) 10 μm and (f) 1 μm.

3.5 Discussion

This chapter describes a comprehensive *in vitro* cytotoxicity assessment of SWCNT on the alveolar type II carcinoma cell line A549. Parameters evaluated included the metabolic, lysosomal, and mitochondrial activities, in addition to total protein content and cell membrane integrity. Furthermore, the present study employed qualitative methods for cytotoxicity assessment in order to overcome the risk of data misinterpretation due to the existence of interferences between test particles and toxicity indicator dyes. Therefore, light, fluorescence and transmission electron microscopy were carried out to investigate whether the SWCNT were internalised by exposed lung cells and to examine for any structural or morphology changes post exposure.

3.5.1 Particle dispersion

One of the main problems in the toxicity evaluation of SWCNT is the propensity of the nanotubes to agglomerate owing to substantial van der Waals attractions. A phase contrast micrograph of A549 cells following 24 h exposure to 800 μg/ml SWCNT revealed large aggregates of SWCNT on the cell surface (Figure 3.11). In addition to dispersion in serum containing (5%) medium, SWCNT were suspended in serum-free medium in order to investigate the role of serum supplements on particle toxicity. Visual observation of the SWCNT prior to cell exposure revealed that nanotubes appeared to be dispersed more readily by serum containing medium.

In parallel studies to the *in vitro* cytotoxicity assessment, spectroscopic techniques were employed to assess the interaction of the SWCNT and the various media components and significant interaction between the SWCNT and FBS was found [255]. Over the concentration range studied, Raman spectroscopy indicates that although the nanotubes are dispersed by the medium, they remain as bundled aggregates of larger diameter similar to those of the "as produced" samples [255].

Monteiro-Riviere *et al.* (2005) found that different synthetic surfactants showed increased dispersion and reduced aggregation of MWCNT, but they also noted that the presence of surfactant did not alter the cytotoxicity of the MWCNT to a human keratinocyte cell line (HEK) as determined by the NR assay [50]. In the results reported here, slightly greater toxicity was generally found with SWCNT in the absence of serum (Figure 3.4a, Figure 3.5a, Figure 3.6a). Serum components may potentially coat the nanotubes and therefore rendering them less toxic.

3

3.5.2 Cytotoxicity of SWCNT and quartz

From the results obtained for quartz, it can be concluded that cell metabolism (AB assay), and mitochondrial activity (MTT) are negatively impacted at concentrations lower than that required for cell detachment (CB). Cytotoxicity tests revealed the SWCNT to have very low acute toxicity to the A549 cells, as all but one of the reported 24 h EC_{50} values exceeded the top concentration tested (800 μg/ml). The AB assay was found to be the most sensitive endpoint as the greatest cytotoxicity (approximately 50% in both 5% serum and serum free media) was recorded at the top concentration of SWCNT. The AB assay was also

the most sensitive and reproducible endpoint based on EC_{50} values obtained following quartz exposures. Therefore it was the assay of choice for the assessment of the effects of long-term exposure to SWCNT and quartz. Both particles were able to dose- and time-dependently reduce cell viability over 96 h.

The presence of serum significantly reduced quartz toxicity as can be seen in Figure 3.2b, Figure 3.4b, Figure 3.5b, Figure 3.6b Figure 3.7b. Even following 96 h, quartz exposure had only small effects on cell viability, indicating that the presence of serum remains to provide protection from toxic insults and does not diminish over time (Figure 3.3b). Gülden and Seibert (2005) reported that the bioavailability of chemicals *in vitro* can be reduced due to partitioning into lipids and binding to serum proteins [275]. The 'protective' effect of serum in silica toxicity has also been well documented [276, 277]. Antonini and Reasor (1994) demonstrated, that coating of silica with a commercially available bovine pulmonary surfactant afforded short-term protection against its toxicity when tested both *in vitro* on rat alveolar macrophages and *in vivo* following intratracheal instillation [278, 279]. Antonini *et al.* (1994) also demonstrated that pre-treatment of rats with amiodarone, a drug that significantly increases the concentration of total phospholipids in whole lung resulted in reduced toxicity of silica dust following subsequent intratracheal instillation [279].

However, the addition of FBS had only minimal effects on SWCNT toxicity indicating that serum only plays a minor role for the cytotoxicity of this type of particle. Therefore, FBS supplements were included for further SWCNT toxicity studies. This could avoid impaired cell performance due to removal of serum and increase the studies' biological relevance as particles are most likely to encounter a

variety of proteins and molecules following inhalation exposure as described in Chapter 1, 1.2.4.

In parallel to A549 exposures, cytotoxicity was determined using a dermal cell model in order to evaluate whether SWCNT effects are specific to lung epithelial cells. Based on the AB and AK assays, it was concluded that cell responses only differ slightly between A549 and HaCaT cells and exposure to SWCNT *in vitro* appears to result in common effects including decrease in AB reduction and AK release. Casey *et al.* (2007a) reported interactions between SWCNT and cell culture medium components and this phenomenon is further discussed in Chapter 4 [255]. Consequently, the type of culture medium used for particle dispersion may influence particle toxicities which may contribute to the differences in sensitivities observed between A549 and HaCaT cell lines.

3

3.5.3 Dye interaction

Due to unexpected cyototoxicity data and the persistence of SWCNT agglomerates adhered to cell monolayers, it was hypothesized that SWCNT may interact with the toxicity indicator dyes leading to interferences with absorbance and fluorescence readings. Recent literature has revealed interactions of SWCNT and other carbon based nanomaterials with various commonly used cytotoxicity assays [30, 210, 225] and Hurt *et al.* (2006) addressed this confounding issue and advised caution when performing even established toxicity assays in the presence of significant quantities of fine carbon [280]. Monteiro-Rivere and Inman (2006) reported absorptive interferences between carbon black nanoparticles and the NR dye

resulting in false readings. The carbon black was found to adsorb to the NR dye and trigger a signal in the dye implying high cell viability when in fact the cells were not even present [30]. The increase in lamellar bodies in the exposed cells compared to unexposed controls could also contribute to the inconsistencies shown here with the NR dye, as secretion vacuoles like lamellar bodies are secondary lysosomes [281]. Another recent study has reported SWCNT interference with the MTT assay due to binding of formazan precipitates onto SWCNT resulting in decreased absorbance measurements [210] and the adsorbing properties of the carbon nanotubes are also suspected to potentially interfere with the AK assay in the present study which may explain the decreases in AK observed following SWCNT exposures.

No attempts to quantify the interferences between carbon nanoparticles and indicator dyes have been realised to date. Therefore, a full spectroscopic study, namely Raman, UV-Vis absorption and fluorescence spectroscopy, was carried out in order to assess the interactions of the SWCNT and the various dye markers employed in this study. Interactions between indicator dyes and SWCNT could be observed in all cases, even for WST-1 which was previously recommended by other authors [210]. The presence of SWCNT resulted in quenching of the absorbance and fluorescence signals which has severe implications for toxicity evaluations using these assays, potentially resulting in false positive toxicity evaluations being made as a result of the interaction of the SWCNT with the dye molecules. Therefore, the likelihood of the toxicity curves obtained using the AB, MTT, WST-1 or CB assays being a true representative of SWCNT toxicity is questionable and the cytotoxicity of SWCNT might have even been overestimated

as some of the reductions in absorbance/fluorescence observed following exposure are partly due to SWCNT interactions instead of real cell responses.

3.5.4 Qualitative cytotoxicity

As a first step to overcome this problem, alternative cytotoxicity assays, mainly of a qualitative nature that are independent of SWCNT interactions, were carried out in order to further assess the effects of SWCNT.

Firstly, the Trypan Blue cell viability assay was performed to assess cytotoxicity in a qualitative and quantitative manner. Trypan Blue is only able to enter and stain dead cells which can therefore be distinguished from viable cells by microscopical evaluation. As shown in Figure 3.13, SWCNT exposure did result in approximately 20% cytotoxicity following 24 h exposure in the absence of serum. In comparison, the AB assay revealed reductions in cell viability by around 40% (Figure 3.2) indicating that interaction between AB dye and SWCNT does play a role and may lead to overestimation of cytotoxicity of SWCNT. However, the Trypan Blue assay could confirm low acute toxicity of SWCNT exposure.

Optical, fluorescence and transmission electron microscopy were employed to assess for nanomaterial interaction/localisation within the A549 cells and to establish evidence of dose related morphological changes (Figure 3.14 to Figure 3.22). Cells were also exposed to the same concentrations of quartz without serum and optical microscopy sections confirmed the extensive cell death demonstrated in the viability assays.

In this study, no evidence of internalisation of SWCNT in lung epithelium was found. Similarly, whilst Shvedova *et al.* (2003) reported ultrastructural changes in cell morphology of HaCaT cells, TEM imaging did not reveal intracellular localization of these particles [31]. However, it is difficult to identify nano-sized carbon structures using TEM and complementary methods such as electron energy loss spectroscopy (EELS) would help to verify the absence of particle uptake. Other studies have shown that internalization of various nanoparticles can occur as discussed in 2.3.5.2.4. Wörle-Knirsch *et al.* (2006) reported that SWCNT could be found as bundles of thousands inside A549 cells and postulated that they were mostly encapsulated in endosomes and infrequently found inside mitochondria [210]. Monteiro-Riviere *et al.* (2005) demonstrated MWCNT were primarily located within the intracytoplasmic vacuoles of human epidermal keratincotyes (HEKs) and demonstrated different morphology between control cells and those exposed to MWCNT [50]. In the concurrent spectroscopic study, Raman and fluorescence emission analysis indicated that no debundling or reduction in aggregation state occurred upon the dispersion of SWCNT in the media over the concentration range studied. Typically these aggregates can be of the order of microns therefore reducing the likelihood of internalization.

While no evidence of SWCNT internalization in the A549 cells was found, ultrastructural changes in the cell morphology following SWCNT exposure could be observed (Figure 3.21, Figure 3.22). It is worth noting however, that any obvious qualitative morphological differences between those exposures conducted with and without serum could not be distinguished. Propidium iodine staining was used to detect cells undergoing necrosis following SWCNT exposure. Following 24

h, overall only a small number of necrotic cells was observed confirming results obtained by the AB and Trypan Blue assays. However, necrosis did take place around areas where SWCNT bundles attached to the cell monolayer (Figure 3.14). In the same areas, A549 cells showed the tendency to grow out of plane, towards SWCNT agglomerates (Figure 3.14d) This was also seen by Tian *et al.* (2006) and Wörle-Knirsch *et al.* (2006) and may explain the granuloma formation seen *in vivo* (Chapter 2, 2.3.5.1) [52, 210].

The PI dye has the advantage that its fluorescence is significantly higher compared to that of AB or NR. Furthermore, very short incubation of cells with PI dye is needed to sufficiently stain cell nuclei, so that the time available for SWCNT to quench PI fluorescence is significantly reduced. An automated *in vitro* technique for drug toxicity testing using PI has been described by van Lambalgen and Lelieveld (1987) using a 96-well microplate format [282]. A linear relationship was obtained between cell number and fluorescence intensity and reproducible dose-response curves for six tested drugs were reported. However, the extent of cell toxicity following SWCNT exposure was to low for automatic analysis using a multi-well fluorescence reader.

Actin-tubulin staining also revealed alterations of cytoskeleton around areas of SWCNT attachment indicated by disruption of actin and tubulin organisation and aggregation of tubulin (Figure 3.17 and Figure 3.18) around SWCNT. Using 3-dimensional fluorescence analysis it could be shown that tubulin aggregation was a real cellular response and not due to antibody binding to SWCNT. This would indicate that over extended exposure periods, SWCNT may be incorporated within cell monolayers and are therefore not acutely cytotoxic. As seen using PI staining,

cytoskeleton staining showed that cells tend to grow out of plane towards SWCNT agglomerates (Figure 3.19).

Using TEM it was seen that the A549 cells have retained the main properties of alveolar epithelial type II cells, i.e. pulmonary surfactant secretory functions [283] and within these cells the lamellar bodies are recognised as storage vessels from which surfactant is released into the alveolus [284]. After secretion, alveolar forms of surfactant include these lamellar bodies, highly organised structures termed tubular myelin, and monolayered and multilayered, phopholipid-rich sheets and vesicles [285]. While the principal function of this pulmonary surfactant is the regulation of surface tension in the lungs [286], it is also postulated that increased production of this surfactant may play a role in defending the lungs against chemical and particulate damage [59, 287]. Following exposure to both 400 and 800 μg/ml SWCNT, an increase in lamellar bodies compared to untreated controls was observed within exposed cells (Figure 3.22 a-c). In addition, the presence of extracellular lamellar bodies, which appeared to have exocytosed their contents, was recorded at 400 μg/ml SWCNT (Figure 3.22 c). Multivesicular bodies were also observed following cell exposure to both 400 and 800 μg/ml SWCNT (Figure 3.22 b). It was thus surmised that these vesicles were most likely the phospholipid-rich multivesicular bodies as mentioned above, which are involved in the surfactant synthesis and recycling. Interestingly, a very similar plasma membrane projection to that identified in Figure 3.22f was shown by Stearns *et al.*, (2001), in an electron micrograph following exposure of A549 cells to 40 μg/ml ultrafine titanium dioxide [288]. Stearns *et al.* (2001) also reported that aggregates of TiO_2, which entered the A549 cells by ingestion, were later found in membrane-bound

vacuoles and enmeshed within lamellar bodies [288]. In an *in vivo* study, Shvedova *et al.* (2005) also observed increased numbers of AE2 cells expressing cytoplasmic lamellar bodies in TEM sections of mouse lung following SWCNT exposure via pharyngeal aspiration [183]. It was therefore hypothesized that the increased presence of these lamellar bodies and the concurrent surfactant secretion is a protective response of the lung cells to reduce the cytotoxic effects of SWCNT. Hook (1993) postulated that one possible mechanism that might account for the protective effects is the quenching of free radicals by the unsaturated phospholipids of pulmonary surfactant [59]. This theory seems quite plausible, considering that surface modification of silica with phospholipids can markedly reduce its toxicity. Previous research has also shown that direct mechanical stretching of the AE2 cells can trigger the release of surfactant [289]. As can be seen in Figure 3.11, SWCNT aggregates were found on the cell surface and remained attached even after several washes with PBS. Hence another possible stimulus for this enhanced secretion of surfactant may be due to the physical stress of the SWCNT aggregates on the cell surface.

3.6 Conclusion

For toxicity assessment, minimal processing of the SWCNT samples was employed to mimic exposure to the raw, as-produced powder. Although the nanotubes were dispersed in culture medium, they remained as large diameter bundled aggregates. In conclusion, exposure of A549 cells to a wide dose range of SWCNT (1.56-800 μg/ml) for 24 h revealed the SWCNT to have low acute toxicity. Only slight variations in SWCNT toxicity were observed in the absence of serum indicating a minor role of serum supplements on the effects of SWCNT exposure. In contrast, quartz toxicity was significantly decreased following the addition of FBS. Whereas quartz seemed less cytotoxic than SWCNT in the presence of FBS, it appeared more cytotoxic when FBS was removed. Of the multiple cytotoxicity assays used, the AB assay was found to be the most sensitive and was therefore used for the assessment of long term exposures which showed dose- and time-dependent behaviour. The origin of cells (lung or skin) did not affect overall cell responses. However, the SWCNT were found to interfere with a number of the dyes used in the cytotoxicity assessment (CB, AB, NR, MTT and WST-1) as shown by a comprehensive spectroscopic study. This raises questions about the validity of cytotoxicity data based on the absorption/fluorescent emission of these dyes. Any toxicity data obtained using SWCNT needs to be corrected for any such interactions. Morphological observations have the advantage of being more independent of SWCNT interferences and TEM studies confirmed that there were morphological alterations in exposed cells including cytoskeletal changes and an increased numbers of surfactant storing lamellar bodies. It was therefore surmised that the increased presence of these lamellar bodies was a defensive response of

these lung cells to SWCNT exposure and it is concluded that the protective function of the pulmonary surfactant following nanomaterial exposure warrants further investigation.

Chapter 4

Effects of SWCNT on clonogenic survival and cell proliferation

This chapter is based on the following publications:

A new approach to the toxicity testing of carbon nanomaterials – the clonogenic assay.

Eva Herzog, Alan Casey, Fiona M. Lyng, Gordon Chambers, Hugh J. Byrne, Maria Davoren

Toxicology Letters, 2007, Volume 134, Issues 1-3, pages 49-60

Single-walled carbon nanotubes induce indirect cytotoxicity by medium depletion in A549 lung cells.

Alan Casey, Eva Herzog, Fiona M. Lyng, Hugh J. Byrne, Gordon Chambers, Maria Davoren

Toxicology Letters, 2008, Volume 179, Issue 2, pages 78-84

Probing the interaction of single walled carbon nanotubes within cell culture medium as a precursor to toxicity testing.

Alan Casey, Maria Davoren, Eva Herzog, Fiona M. Lyng, Hugh J. Byrne, Gordon Chambers

Carbon, 2007, Volume 44, Issue 1, pages 34-40

4.1 Chapter summary

The cellular toxicity of three types of carbon nanomaterials, namely HiPco® SWCNT, ArcD SWCNT and Printex 90 carbon black, was studied on three different cell models including A549, BEAS-2B and HaCaT cells using the clonogenic assay. Due to the interactions observed between carbon nanomaterials and toxicity indicator dyes, the clonogenic assay allowed a more reliable method for the *in vitro* toxicity assessment of carbon-based nanomaterials. It was demonstrated that the toxicity of "as produced" SWCNT samples differed between cell lines and the SWCNT production method used, with HiPco® SWCNT samples being more reactive compared to ArcD produced SWCNT samples. Both SWCNT types were found to elicit a stronger cytotoxic response than carbon black. Furthermore, it was possible to distinguish between effects on cell viability and cell proliferation by including colony size as an additional endpoint in the clonogenic assay. Whereas colony number correlated well with colorimetric endpoints, colony size measurements appeared more sensitive. All three particle types were highly effective in inhibiting cell proliferation in all three cell lines, whereas only HaCaT and BEAS-2B cells also showed decreased cell viability. In addition, the ability of HiPco® and ArcD SWCNT to induce an indirect cytotoxicity in A549 lung cells by means of medium depletion was investigated. Spectroscopic analysis confirmed the ability of SWCNT to induce an indirect cytotoxic effect by altering the culture medium and hence depletion of essential media constituents required for cellular growth. This indirect effect may contribute for up to 50% of the reductions seen in cell proliferation following direct SWCNT exposure over 96 h or 10 days and up to 10% of the cytotoxicity seen following 24 h.

4.2 Introduction

In the previous chapters, *in vitro* cytotoxicity assessment of carbon-based nanomaterials has been shown to be problematic due to their adsorptive nature. Interactions of SWCNT and other carbon-based nanomaterials with a number of cytotoxicity indicator dyes, as demonstrated in Chapter 3, 3.4.3 [30, 210, 225, 257, 280] potentially leads to false readings and misinterpretation of particle toxicity, making these assays unreliable for quantitative assessment of carbon nanomaterial toxicity and highlighting the urgent need for the development and application of alternative screening techniques [56, 257]. The development and validation of methods to evaluate the toxicity of engineered nanomaterials is also regarded as one of the main future challenges relevant to the safety of nanotechnology [290].

In this study, the clonogenic assay is used as an alternative method which avoids the use of any colorimetric or fluorescent indicator dye, thus eliminating the risk of interactions and allowing the assessment of true cytotoxicity. The clonogenic assay, also called colony formation assay, is an *in vitro* cell survival based assay measuring the ability of a single cell to form a colony. It was first described in 1956 by Puck and Markus (1956) [291]. Since this time, it has been used in a variety of studies with many different cell types to detect cells that retained the capacity for producing a large number of progeny after treatments that can cause reproductive death as a result of damage to chromosomes, apoptosis, etc. [292]. Furthermore, the clonogenic assay has been reported to be more sensitive than colorimetric cytotoxicity assays since dying, abortive cells can still be metabolically active and

thus give misleading results in non-clonogenic assays. So far, it is the method of choice in the area of oncological research to determine reproductive cell death post radiation [293, 294]. However, it has also been proposed as a method to determine the cell survival following exposure to other classes of xenobiotics [295, 296]. Both lung and dermal cell models were chosen as test systems in order to assess the validity and universality of the clonogenic assay.

Effects were compared between HiPco® and ArcD produced SWCNT in order to evaluate the role of production method and corresponding sample contaminants on particle toxicity. Furthermore, P90 carbon black was included, on the one hand as control particle of known toxicity [37-40], and on the other hand in order to assess the applicability of the clonogenic test system to other carbon-based nanomaterials. In contrast to quartz, P90 carbon black has the advantage of being chemically related to SWCNT and having particle sizes in the nanometre range.

Particle exposures were carried out in the presence of FBS. This was considered valid as previous studies showed FBS to play only a minor role in SWCNT cytotoxicity (Chapter 3, 3.4.2.1). Furthermore, serum supplements were required for healthy cell performance over extended time periods employed during the clonogenic assay.

Spectroscopic analysis of a commercial cell culture medium, commonly used in toxicity studies also revealed significant interaction of the constituent components with SWCNT (3.4.3) [255]. The question was thus raised that if the SWCNT interact with the medium and adsorb nutrient constituents, does the medium still have the same capability to maintain healthy cells? Furthermore, can the toxicological data

collected on experiments performed in this way (dispersion of SWCNT in a cell culture medium) be affected? If this is the case, SWCNT may induce an indirect toxicity due to the reduction in the availability of the medium components to the cells due to interaction with the SWCNT. Therefore, a second part of this study investigated this hypothesis of an indirect toxicity by medium depletion.

4.3 Materials and methods

4.3.1 Test materials

In addition to HiPco® derived SWCNT as described in Chapter 3, ArcD synthesized SWCNT were obtained from Sigma–Aldrich, product number 519308 (Dublin, Ireland) containing 50–70 % SWCNT and trace amounts (<1 wt %) of nickel and yttrium catalysts, the dominant impurity being amorphous carbon and turbostratic graphite. Arc discharge tubes ranged from 1.2 nm to 1.5 nm in diameter and 2–5 μm in length, occurring in bundles of around 20 μm in length [254]. AFM showed estimated bundle sizes 4.1×10^{-14} m^2 for ArcD SWCNT samples which were therefore bigger than that of HiPco® SWCNT (Chapter 3, 3.3.1).

Printex 90 (P90) carbon black particles were kindly provided by Degussa AG (Frankfurt am Main, Germany) and had a mean diameter of 14 nm.

4.3.2 Cell culture

A549 cells (Chapter 3), BEAS-2B (ECACC, 95102433) immortalised human bronchial epithelial cells and HaCaT cells were all grown in DMEM medium (Cambrex). All media were supplemented with 10 % FBS and 45 IU/ml penicillin and 45 IU/ml streptomycin and cells were maintained at 37 °C in a 5 % CO_2 humidified incubator. In order to allow direct comparisons between cell types and to avoid contributions of culture medium type to particle toxicity, all cell lines were grown and exposed using DMEM medium.

4.3.3 Dispersion of nanomaterials

Nanomaterials were dispersed as described in Chapter 3 using an ultrasonic tip using initial stock concentrations of 400 μg/ml.

4.3.4 Characterisation of SWCNT exposed culture medium

To investigate the interactions of SWCNT with cell culture medium components, SWCNT solutions were prepared by dispersing an initial concentration of 1000 μg/ml of SWCNT in both the serum containing (5%) medium, and the serum free medium (0%) by sonication. By subsequent dilution with medium the concentration of SWCNT was reduced to obtain a range of solutions varying from the initial concentration down to a final concentration 0.97 μg/ml [255].

For characterising indirect effects, SWCNT exposed culture medium was prepared as described by Casey *et al.* (2008) [54]. Initial concentration of 800 μg /ml of both types of SWCNT were dispersed in cell culture medium supplemented with 5% FBS using an ultrasonic tip. Each stock concentration was then serially diluted with culture medium and sonicated as before to prepare test concentrations. After dispersion, the test concentrations were refrigerated for 24 h and then centrifuged (3000RPM/1800g for 20 minutes) and filtered (using 0.2μm cellulose acetate filters) to remove the dispersed nanomaterials. The resultant filtrate was termed depleted medium. Cells were then exposed to the depleted medium that was previously exposed to a concentration range of nanomaterials (1.56 - 800 μg/ml) [54]

4.3.5 Spectroscopic characterisation of test particles

For cytotoxicity evaluation, fluorescence and absorbance were all quantified using a microplate reader (TECAN GENios, Grödig, Austria). Absorption and fluorescence spectroscopy were performed on the dispersions of nanotubes in all solutions after a 24 h settling period after which they were characterised using absorption, luminescence and Raman analysis as described in Chapter 3 [54]. Elemental analysis was performed by Atomic Absorption spectroscopy on media suspensions post SWCNT removal with the aid of a Varian SpectrAA 200.

4.3.6 Alamar Blue™ assay

The AB assay was carried out as described in 3.3.5.1 and treated with 100 µl depleted medium (previously containing test nanomaterial concentrations of 1.56 to 800 µg/ml). Upon exposure for 24, 48, 72 or 96 h, cell viability was assessed according to the manufacturer's guidelines. At least three independent experiments were performed.

4.3.7 Clonogenic assay

The procedure for the clonogenic assay was adopted from Puck and Markus (1956) and Franken *et al.* (2006) and cells were treated after plating [291, 295]. Exponentially growing cells were harvested and seeded in six-well microplates (Nunc, Denmark) at a density of 250 cells/well for A549 cells and 300 cells/well

for HaCaT and BEAS-2B cells. Each well contained 2 ml of cell culture medium. The average plating efficiencies, the percentage of individual cells that give rise to colonies, were 74.8% for A549 cells, 39.8% for HaCaT and 32.0% for BEAS-2B cells.

Cells were allowed to attach for approximately 14 h. This attachment period was shorter than the population doubling time of these cell lines which is reported to be around 22 h for A549 cells (ATCC, CCL-185), 23 h for HaCaT [297] and 27 h for BEAS-2B cells (Reddel, personal communication, 7 Aug 2007). Therefore, it can be assumed that mostly single cells were present at the time of exposure. Cells were then washed with 2 ml of PBS and treated with 2 ml of test material prepared in cell culture medium to final concentrations of 0, 1.56, 25, 100 and 400 μg/ml. Cells were exposed to nanomaterials over the time period they needed to form colonies, a colony being defined as at least 50 clones of one cell. Both A549 and BEAS-2B cells were incubated for 10 days, whereas HaCaT cells had formed sufficiently large colonies after only 7 days. Therefore, cells were exposed for 10 or 7 days, dependent on cell type. Due to the extended exposure periods investigated using the clonogenic assay, the highest concentration of particles tested was reduced from 800 down to 400 μg/ml compared to previous studies. Furthermore, moving away from high exposure concentrations increases biological relevance of the study.

Before colonies were counted, particle solutions were removed, cells were washed with PBS and finally fixed and stained using a 20% carbol fuchsin in formalin solution (BDH, Poole, UK). In addition to colony number as the classical clonogenic assay endpoint, surface area was chosen as an additional endpoint to evaluate the

effects of nanomaterials on colony formation [298]. Digital photographs were taken from each six-well microplate and the Java based image processing program ImageJ (http://rsb.info.nih.gov/ij/) was used to measure colony surface areas.

For indirect toxicity assessment, A549 cells were exposed to depleted culture medium as described for the AB assay (2.6).

4.3.8 Statistics

At least three independent experiments were conducted for each cell line and type of nanomaterial. Test results for each assay were expressed as percentage of the unexposed control +/- SD. Control values were set as 100 %. Differences between samples and the control were evaluated using the statistical analysis package SPSS 14.0. Statistically significant differences were set at $P \leq 0.05$. Normality of data was confirmed with Q–Q percentile plots and Kolmogorov–Smirnov tests. Equality of variances was evaluated using Levène tests. One-way analysis of variances (ANOVA) followed by Dunnett's multiple comparison tests were carried out for normally distributed samples with homogeneous variances. Non-parametric tests, namely Kruskal–Wallis followed by Mann–Whitney-U-tests were applied to samples without normal distribution and/or inhomogeneous variances. Cytotoxicity data was fitted to a normal log or exponential growth model in order to calculate the EC_{50} values which were determined using REGTOX-EV6.xls (Eric Vindimian, http://eric.vindimian.9online.fr/) and were confirmed using Xlfit3™ (ID Business Solutions, UK), both curve fitting add-ins for Microsoft® Excel. EC_{50} values are reported ± SD.

4.4 Results and discussion

4.4.1 Direct effects of carbon nanomaterial exposure

4.4.1.1 *Toxicity of carbon nanomaterials using pulmonary cell models*

As demonstrated in Figure 4.1 for A549 cells, after prolonged exposure to carbon nanomaterials, aggregates of particles tend to selectively adhere to the cell colonies rather than the substrate. This was the same for all cell lines tested. Several consecutive washing steps with PBS and water were not able to remove these aggregates from the cell surfaces similar to the effects seen in Chapter 3, Figure 3.11. Aggregates of SWCNT seemed to be consistently larger compared to those formed by P90 carbon black nanoparticles.

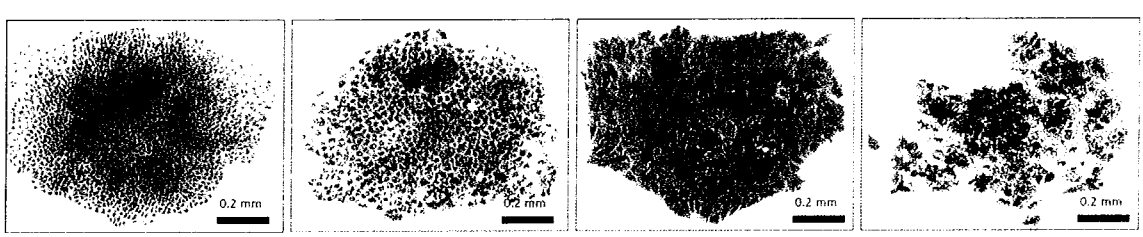

Figure 4.1: Colonies of A549 cells after 10-day exposure to 400μg/ml of carbon nanomaterials ×20 magnification (left to right: control, Printex 90, ArcD SWCNT, HiPco® SWCNT exposed colonies).

As shown in Figure 4.2a, after a 10-day exposure of A549 cells to carbon nanomaterials, colony numbers were reduced to around 72.0, 57.7 and 72.6 % for carbon black, ArcD and HiPco® produced SWCNT compared to the control, respectively. HiPco® SWCNT and P90 carbon black could only elicit a statistically significant ($P \leq 0.05$) reduction in colony number at the highest concentration

tested. This confirms the results from previous studies showing toxicity in A549 cells exposed to HiPco® SWCNT at concentrations of 400 and 800 μg/ml as shown in Chapter 3, 3.4.4.4. Arc discharge produced SWCNT caused a significant increase in the number of colonies of ca. 5.8 and 3.5 % after exposure to 1.56 and 6.25μg/ml. From 100μg/ml on, a significant reduction could be determined.

In contrast to the relatively small effects identified on colony numbers of A549 cells, a greater effect was observed when looking at colony surface areas. Cells seemed to form much smaller colonies when exposed to carbon nanomaterials, also demonstrated in Figure 4.3. These reductions in colony sizes were due to fewer cells being present within the exposed colonies whereas individual cell sizes remained unchanged. It is clear that although the colony number is not dramatically affected by the exposure to the test materials, their capacity to grow and proliferate is significantly reduced. It is therefore proposed that colony size is a valid endpoint to monitor the effect of the nanparticles and other nanomaterials. Using colony size as an additional endpoint for toxicity assessment, significant effects could be observed for all particles at concentrations as low as 25 μg/ml (Figure 4.2b). Size reduction after P90 carbon black and ArcD SWCNT exposure were even significant at concentrations of 1.56 μg/ml, HiPco® SWCNT from concentrations of 6.25 μg/ml upwards. A dose-dependent reduction in colony size could be determined for all three particle types tested with size inhibitions down to only 13.6, 6.2 and 7.5 % compared to control for P90 carbon black, ArcD and HiPco® produced SWCNT, respectively.

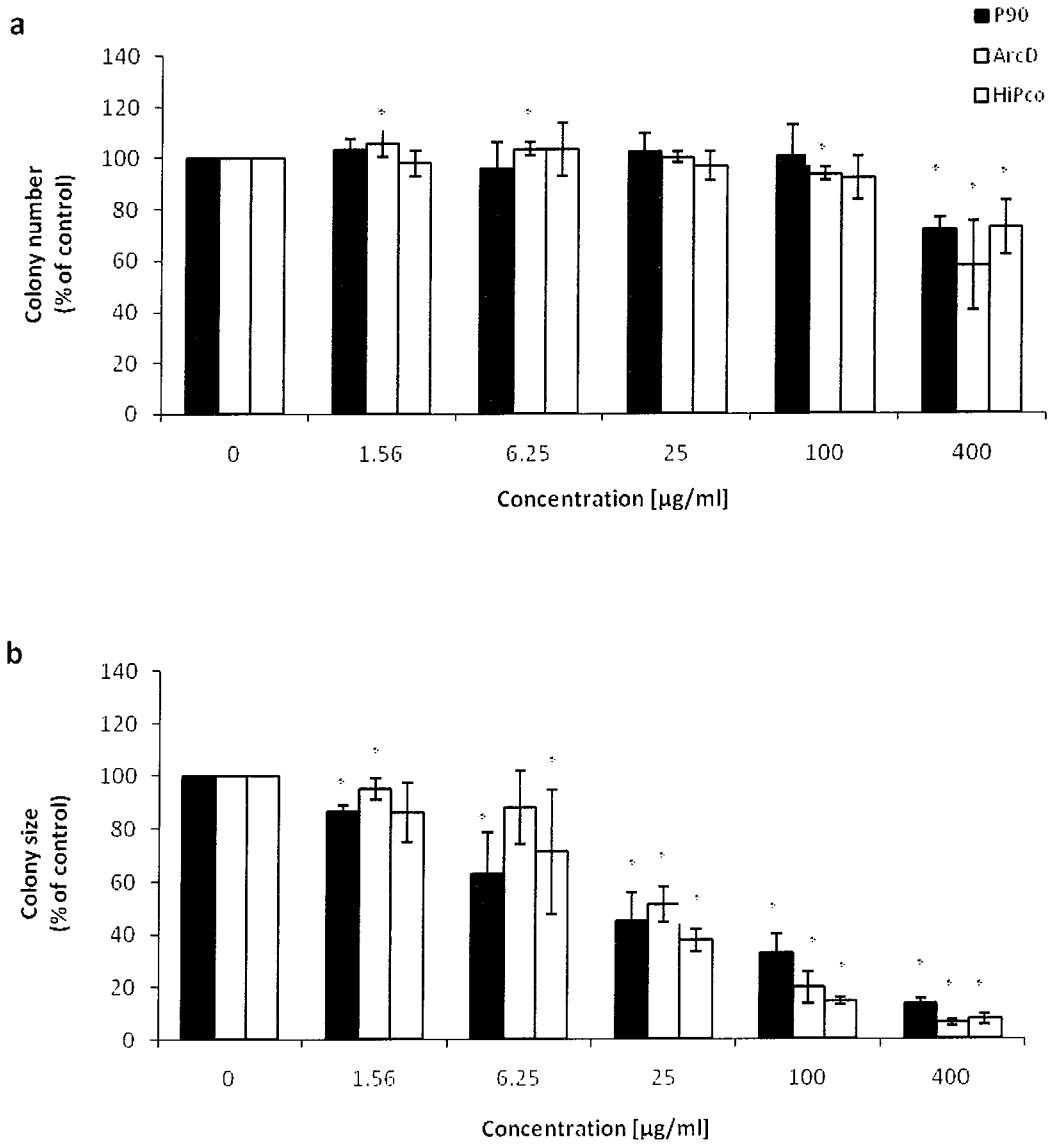

Figure 4.2 Effects of carbon nanomaterial exposure on colony formation, (a) effects on colony number, (b) effects on colony size of A549 cells. Bars showing colony numbers/size as determined following 10 days exposures to P90 carbon black (black), ArcD SWCNT (grey) and HiPco® SWCNT (white). Results are expressed as percent of control mean ± SD of three independent experiments each carried out in triplicate. * Denotes a significant difference from the control (P≥0.05).

Considering both endpoints, colony number and size, it could be concluded that all types of carbon nanomaterials tested were able to significantly decrease clonogenic survival and cell proliferation in a dose-dependent fashion when exposed constantly over 10 days. As illustrated in Figure 4.2, colony surface area measurements seemed to be significantly more sensitive as an endpoint compared to the classically performed colony number counts when assessing the effects of all three types of carbon nanomaterials on A549 lung cells.

To be able to compare and rank the toxicity of the particles tested, EC_{50} values were calculated for both the effects on colony numbers and colony sizes, as shown in Table 4.1 and Table 4.2. EC_{50} values of A549 cells in terms of colony number were determined to be greater than the highest concentration of 400 µg/ml for all particles tested. However, the EC_{50} values in terms of colony size were all considerably less, ranging between 15 µg/ml and 28 µg/ml with HiPco® SWCNT being most toxic. Transformed cell lines such as A549 cells are frequently referred to as being more resistant to toxic insults compared to cells derived from normal tissue, possibly due to higher glutathione and catalase antioxidant activities activities [299, 300]. Therefore, in addition to the A549 cell line, the clonogenic assay was also carried out on BEAS-2B cells, an immortalisedbronchial epithelial cell model derived from normal human tissue.

As illustrated in Figure 4.4, exposure of BEAS-2B cells to carbon nanomaterials over 10 days resulted in a dose-dependent reduction in colony number, being statistically significant at all concentrations tested. At the highest concentration, BEAS-2B cells were no longer able to form colonies, indicating a high degree of cell toxicity. Unfortunately, no colony surface area measurements were possible for

this cell line due to the high motility of cells resulting in widely spread, ill-defined colonies. Comparing EC_{50} values of the effects of nanomaterial exposure on colony numbers, HiPco® SWCNT appeared to be more than three times as toxic to BEAS-2B cells compared to ArcD SWCNT and P90 carbon black (Table 4.4.1).

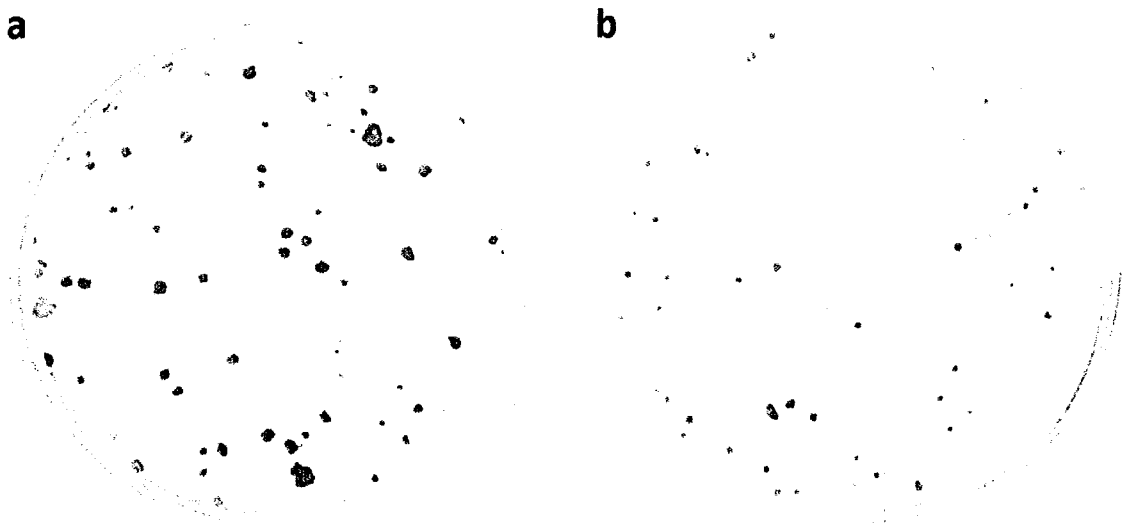

Figure 4.3: Colonies of A549 cells after 10 days incubation with (a) DMEM cell culture medium only and (b) 400 µg/ml HiPco® SWCNT dispersed in DMEM cell culture medium.

Compared to A549 lung carcinoma cells, the normal lung cell line seemed to be significantly more sensitive to nanomaterial exposures. It should be noted that BEAS-2B cells were grown in DMEM growth medium in contrast to the recommended LHC-8 culture medium. Due to interactions observed between culture medium components and SWCNT, using the same type of culture medium for all three cell lines made it possible to compare the effects of SWCNT on these three cell lines. However, the use of DMEM rather than LHC-8 may influence the characteristics of BEAS-2B cells.

Table 4.1: EC_{50} [μg/ml] values for inhibition of colony number of A549, BEAS- 2B and HaCaT cell lines following exposure to P90 carbon black, ArcD SWCNT and HiPco® SWCNT

	Carbon black	ArcD SWCNT	HiPco® SWCNT
A549	> 400 ± 0.41	> 400 ± 1.05	> 400 ± 1.79
BEAS-2B	14.66 ± 1.74	13.70 ± 1.95	4.39 ± 0.99
HaCaT	180.90 ± 0.68	106.23 ± 2.18	40.29 ± 2.42

Results are EC_{50} values ± SD

Table 4.2: EC_{50} [μg/ml] values for inhibition of colony size of A549 and HaCaT cell lines following exposure to Printex 90 carbon black, ArcD SWCNT and HiPco® SWCNT

	Carbon black	ArcD SWCNT	HiPco® SWCNT
A549	20.63 ± 2.81	28.38 ± 4.47	15.04 ± 1.89
HaCaT	78.78 ± 1.53	27.35 ± 2.20	23.28 ± 1.81

Results are EC_{50} values ± SD

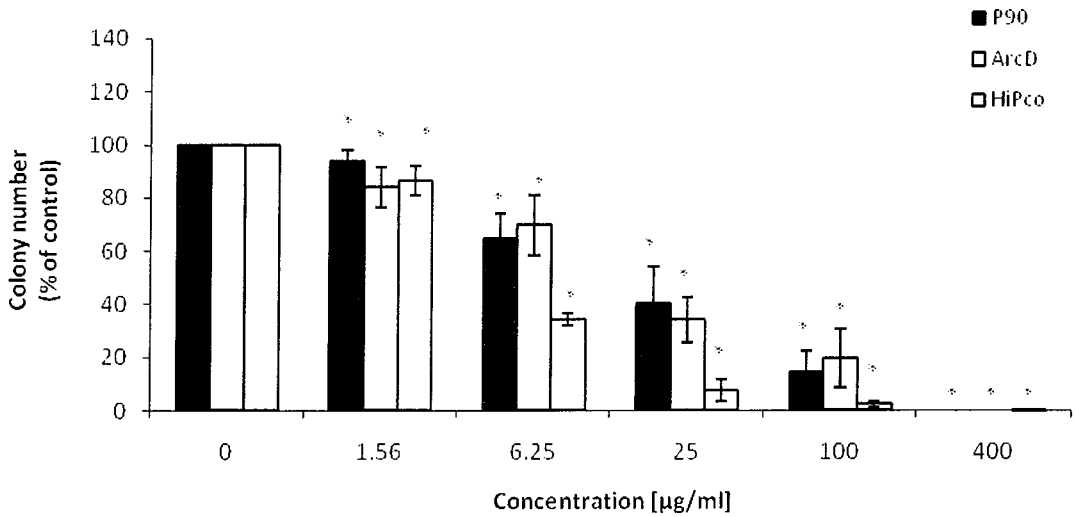

Figure 4.4: Effects of carbon nanomaterial exposure on colony formation of BEAS-2B cells. Bars showing colony numbers as determined following 10 days exposures to P90 carbon black (black), ArcD SWCNT (grey) and HiPco® SWCNT (white). Results are expressed as percent of control mean ± SD of three independent experiments each carried out in triplicate. * Denotes a significant difference from the control (P≥0.05).

4.4.1.2 *Toxicity of carbon nanomaterial using a dermal cell model*

The keratinocyte cell line HaCaT formed colonies after only 7 days of incubation compared to the 10 days needed for the lung cells tested. Therefore, cells were constantly exposed to carbon nanomaterials for 7 days and results are shown in Figure 4.5. All three types of carbon particles exhibited dose-dependent effects on the clonogenic survival of HaCaT cells. At concentrations of 400 µg/ml, colony numbers were reduced by 89 %, 86 % and 85 % following P90 carbon black, ArcD and HiPco® SWCNT exposures, respectively. Furthermore, colony size was demonstrated to decrease by more than 80% compared to control colonies following exposure to all three types of particles at this concentration. For all three

particles tested, significant reductions in colony number and size could be observed at concentrations starting at 25 μg/ml. SWCNT were able to significantly decrease colony sizes at concentrations as low as 6.25 μg/ml. Comparing EC_{50} values for the clonogenic survival of HaCaT cells, as shown in Table 4.4.1 and Table 4.4.2, it can be concluded that SWCNT are significantly more toxic compared to P90 carbon black. In terms of colony number, HiPco® SWCNT appeared more than twice as toxic as ArcD produced SWCNT. However, only a small difference between the toxicity of the two types of SWCNT was noted in terms of colony size.

Both the colony number and colony surface area endpoints, as illustrated in Figure 4.5, appear to correlate very well for HaCaT cells. Colony surface area appeared to be slightly more sensitive and more reproducible, resulting in smaller data variability. In contrast, for A549 cells, surface area measurements and colony number differed greatly. This might indicate increased cell death of HaCaT cells following exposure to carbon nanomaterials whereas A549 cells appeared more resistant, still forming colonies at very high concentrations, only responding with decreased cell proliferation.

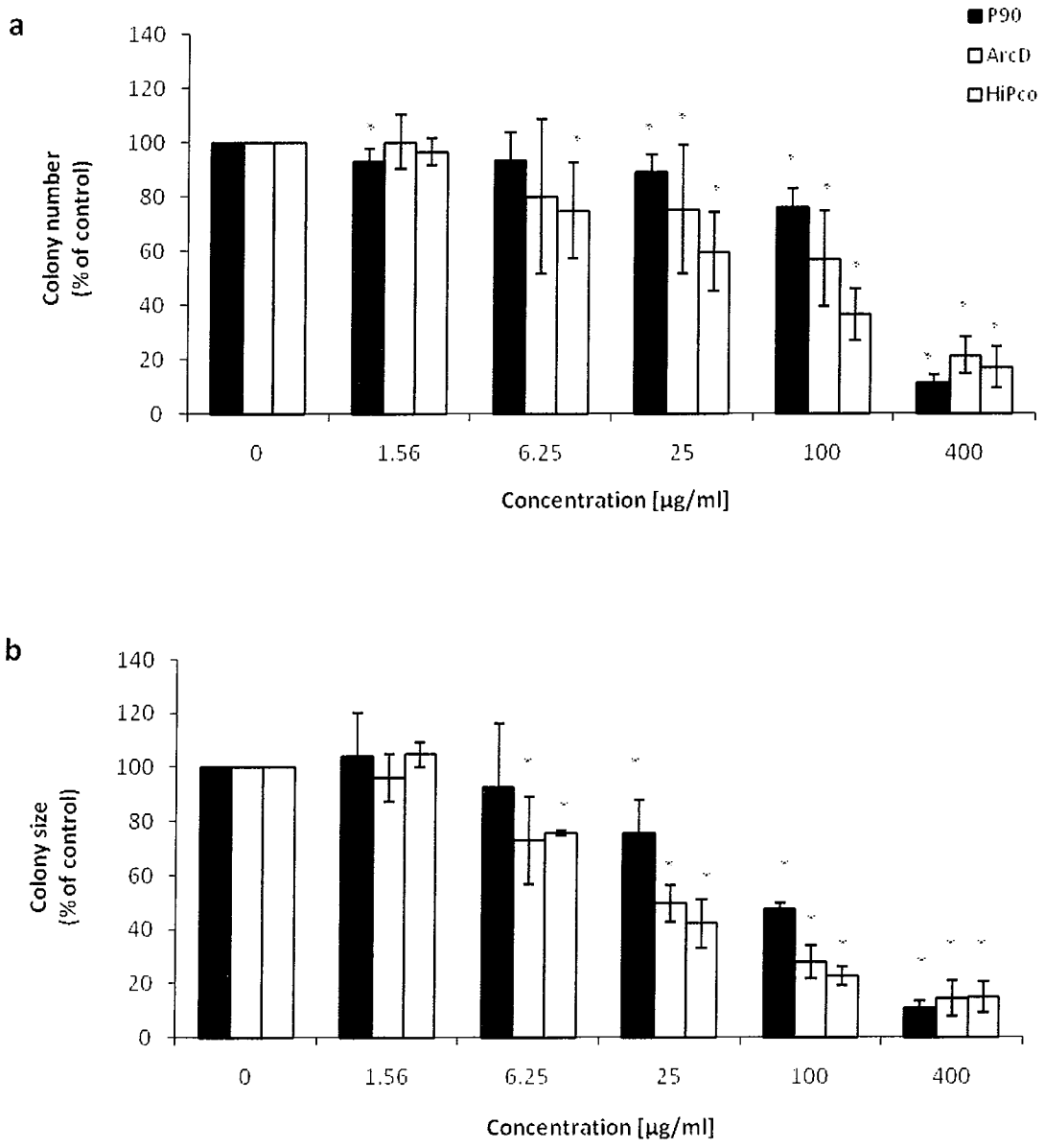

Figure 4.5: Effects of carbon nanomaterial exposure on colony formation, (a) effects on colony number, (b) effects on colony size of HaCaT cells. Bars showing colony numbers as determined following 7 days exposures to P90 carbon black (black), ArcD SWCNT (grey) and HiPco® SWCNT (white). Results are expressed as percent of control mean ± SD of three independent experiments each carried out in triplicate. * Denotes a significant difference from the control (P≥0.05).

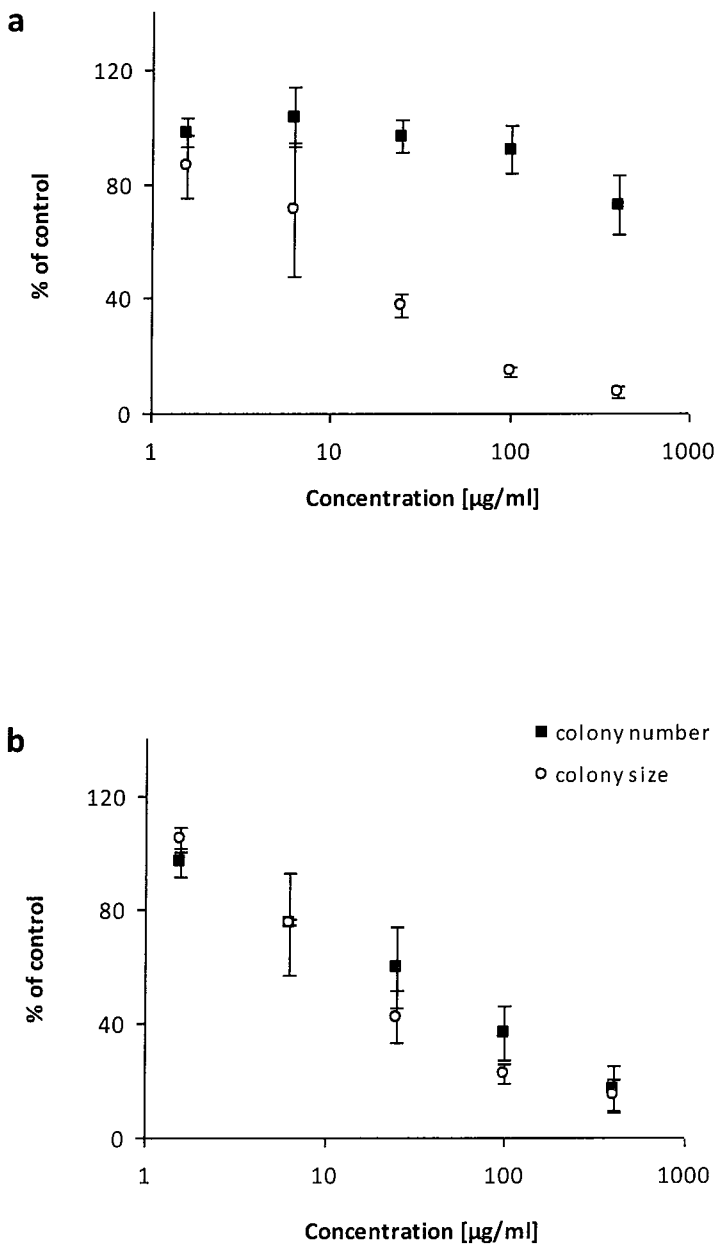

Figure 4.6 Effects of HiPco® SWCNT exposure on colony number (black) vs. colony size (grey) of (a) A549 and (b) HaCaT cells. Results are expressed as percent of control mean ± SD of three independent experiments each carried out in triplicate.

4.4.1.3 *Particle toxicity comparison*

To date, toxicity studies are based on mostly non-standardized CNT material making it complicated to perform comparisons between studies [210]. Overall, the findings on the cytotoxicity of carbon nanomaterials appear to be contradictory. Discrepancies between studies may be explained by differences in sample preparation, sample composition and/or assay system used as described in 2.3.5.2.1. There are only limited studies available imitating the occupational exposure situation to carbon nanomaterials by avoiding the use of any surfactants, functionalisation of SWCNT or acid treatment. With the current state of the art production methods, occupational exposure and therefore potential toxicity is to the SWCNT dust sample in its entirety, therefore, this study compares "as produced", commercial carbon nanotube samples including impurities. The potential role of these impurities is discussed further in Section 4.4.1.3.2.

Results of the clonogenic assay suggest that both SWCNT samples produced by HiPco® and ArcD as well as nanosized carbon black exhibit cytotoxicity and reduce cell proliferation in a dose-dependent fashion in the cell lines tested. The lowest EC_{50} values, as illustrated in Table 4.4.1 and Table 4.4.2, were determined for HiPco® SWCNT exposures for all three cell lines and both endpoints, colony number and colony size. This indicates HiPco® SWCNT to be the most cytotoxic of the particles tested. Pulskamp *et al.* (2007) also exposed A549 cells to SWCNT for 24–96 h and concluded no acute toxicity, indicating the importance of long-term studies for the identification of SWCNT toxicity [206].

4.4.1.3.1 *SWCNT versus carbon black*

Carbon black nanoparticles were effective in reducing clonogenic survival but to a lesser extent compared to the two types of SWCNT. As ArcD SWCNT do not contain iron residues or significant amounts of other transition metals, this may indicate that nanotube material is intrinsically more bioreactive compared to amorphous carbon nanoparticles such as carbon black. In contrast, carbon black particles seemed more toxic compared to MWCNT to lung tumour cells following exposure for 24 h up to 5 days in a study by Magrez *et al.* (2006) [204]. The high toxicity of carbon black was suspected to be due to the presence of highly reactive dangling bonds present at a high density in carbon black but only present at lattice defects and end caps of carbon nanotubes [204]. Some authors even reported higher toxicity of carbon black compared to SWCNT was also reported by other authors [206]. However, dye-based assays were employed for cytotoxicity assessment in these studies, making interpretation difficult. In this study, carbon black particles had a very similar effect to SWCNT when assessing colony size but were much less toxic when assessing colony number as the endpoint.

Murr *et al.* (2005) reported cytotoxic responses of murine lung macrophages to carbon nanotube aggregates to be essentially identical to nanoparticle carbon black aggregates as well as chrysotile asbestos fibril aggregates [167]. The authors concluded that it is unlikely that cytotoxicities are morphologically specific. This would correlate well with the effects on A549 cells seen in this study, where no significant difference between the effects of the three types of carbon nanomaterials could be determined. However, treatment of HaCaT and BEAS-2B cells did show differences in particle toxicities. Also Jia *et al.* (2005) concluded that

nanomaterials with different geometric structures exhibit different cytotoxicities and bioactivities *in vitro* following comparisons between SWCNT, MWCNT and fullerenes [48].

4.4.1.3.2 *ArcD SWCNT versus HiPco® SWCNT samples*

No studies have been published to date that directly compare the toxic effects of SWCNT produced by the HiPco® and ArcD method. In this study, ArcD and HiPco® SWCNT seemed to exhibit different effects on colony numbers and therefore clonogenic survival of HaCaT and BEAS-2B cells. These discrepancies may be due to differences in metal catalyst residue type and metal and carbon residue content of the samples. The microstructure of SWCNT consists of bundles of SWCNT which are aggregated with residual catalyst nanoparticles or other nanomaterial contamination, particularly graphite residues. The HiPco® SWCNT sample tested contained 10 wt% iron residues whereas ArcD SWCNT contained a high amount of amorphous carbon impurities and very small residues of nickel and yttrium. Transition metal components of ultrafine particles (PM_{10}), such as iron, are highly oxidative and reactive in biological systems and have been demonstrated to cause deleterious effects [301]. There is strong evidence that they are able to stimulate proinflammatory responses *in vivo* and *in vitro* and have been postulated to play an important role in the toxicity of HiPco® SWCNT [4, 49]. The toxicity of catalytic metals may hide the real toxic effects of CNT [52] or may interact in a positive manner to generate inflammation [40]. This might explain the higher toxicity of HiPco® SWCNT compared to ArcD or carbon black as seen in this study. In

contrast, Tian *et al.* (2006) reported refined SWCNT to be more cytotoxic to human dermal fibroblasts compared to unrefined SWCNT, active carbon, carbon black, MWCNT and carbon graphite [52].

Due to their geometry and hydrophobic surface, CNT have a tendency to form agglomerates with bundle-like form. Extensive efforts have been made to disperse CNT. However, extensive use of surfactants, organic solvents or functionalisation leads to CNT material that cannot be considered representative for occupational exposure assessments [227]. As described for the previous studies, no surfactant was used in order to aid the dispersion of nanomaterials in cell culture medium in this study so that the real exposure situation was mimicked as closely as possible. Raman and fluorescence emission analysis indicated no debundling or reduction in aggregation state upon dispersion of HiPco® SWCNT in the media over the concentration range studied [255]. However, bundle sizes of ArcD and HiPco® SWCNT as present in organic media are different with an average of ca. 4.1×10^{-14} m^2 for ArcD SWCNT and only about 2.6×10^{-14} m^2 for HiPco® produced SWCNT. The smaller bundle size of HiPco® SWCNT may therefore be an alternative explanation for their increased effect on cell viability.

Differences in colony number, relatable to cell viability, after exposure to the different SWCNT samples may be ascribed to either different impurity content or bundle size. The colony size measurements did not reveal substantial differences between the two types of carbon nanotubes. This might point to a common toxic effect of SWCNT on the rate of cell division and proliferation. The differences in catalyst residues and sample impurity content do not seem to play a role in this

mechanism pointing towards a dependence of this effect on intrinsic SWCNT properties, as fundamentally the chemical composite of the nanotubes is the same.

4.4.1.4 *Cell line comparison*

It was demonstrated that sensitivity to carbon nanomaterial differs between cell lines. However, accurate comparisons between cell lines was not applicable as exposure times varied depending on cell type. Comparing EC_{50} values (Table 4.4.1, Table 4.4.2), the human carcinoma lung cell line A549 was found to be much more resistant compared to the two normal human cell lines tested when assessing effects on colony number. The normal lung cells BEAS-2B were the most sensitive, followed by HaCaT cells. However, none of the particles tested was able to exhibit 50% reduction in colony numbers of these cells. Based on colony size, in contrast, A549 cells appeared more sensitive than HaCaT cells when exposed to carbon black, whereas SWCNT exposures had nearly the same effect on colony sizes for both cell lines, leading to maximum reductions of 85–93% compared to control colonies. As illustrated for the example of HiPco® SWCNT exposures in Figure 4.6, significant discrepancies exist between the responses in colony number and colony size for A549 cells, whereas both endpoints correlated well for HaCaT cells. This was true for all three types of carbon nanomaterials tested.

The ability of cells to form colonies has been widely used to screen xenobiotics for potential toxic activity [295]. Only mitotically viable cells are capable of producing clones and therefore colonies. As a result, the number of colonies formed after or during treatment indicates cell viability as these cells are able to stay attached to

the culture vessel surface and are able to undergo a certain amount of cell divisions. Colony size is a more sensitive endpoint measuring the number of cells per colony which can be used to estimate the rate of division and proliferation of treated cells [302]. Therefore, the results presented indicate that both cell lines respond similarly in decreasing cell proliferation but very differently regarding cell death. Due to the high rate of cell migration of BEAS-2B cells during exposure and colony formation, no accurate measurement of colony sizes could be carried out. However, it was noted that the number of cells per colony decreased with exposure to increased particle concentrations. It also appeared that A549 cells' main response to carbon nanomaterial exposure is reduction of their rate of proliferation while maintaining their viability. HaCaT cells, in contrast, responded equally in loss of cell viability and decreased cell proliferation. Manna *et al.* (2005) also reported inhibition of cell proliferation upon treatment of HaCaT cells with SWCNT particles following 72 h exposure and reported similar findings using A549 cells suggesting a common toxicity mechanism [205]. Yet, in their study, SWCNT were dissolved in dimethylformamide, making direct study comparisons difficult.

Including both colony number and colony size measurements in the clonogenic assay enables distinction between effects on general cell viability and cell proliferation, making it a highly useful tool in cytotoxicity testing. Furthermore, the clonogenic assay has been reported to be more sensitive than colorimetric proliferation assays which measure the numbers of viable cells. Colorimetric assays fail when synthesis of protein, DNA, RNA, lysosomal or mitochondrial enzymes is induced in an arrested cell population without any change in cell numbers [302]. Some cells that are scored as healthy by colorimetric methods may

actually be injured and are destined to die at some later time [8, 10-12, 303]. Therefore, the clonogenic assay offers the possibility of long-term toxicity assessment at a sub-lethal level. In addition, it does not involve any fluorescence or absorbance measurements as indicators for cell viability. Therefore, it provides a more realistic and reliable estimate of the toxicity of carbon-based nanomaterials compared to colorimetric dye-based assays, as any interactions between carbon nanomaterials and indicator dyes can be avoided.

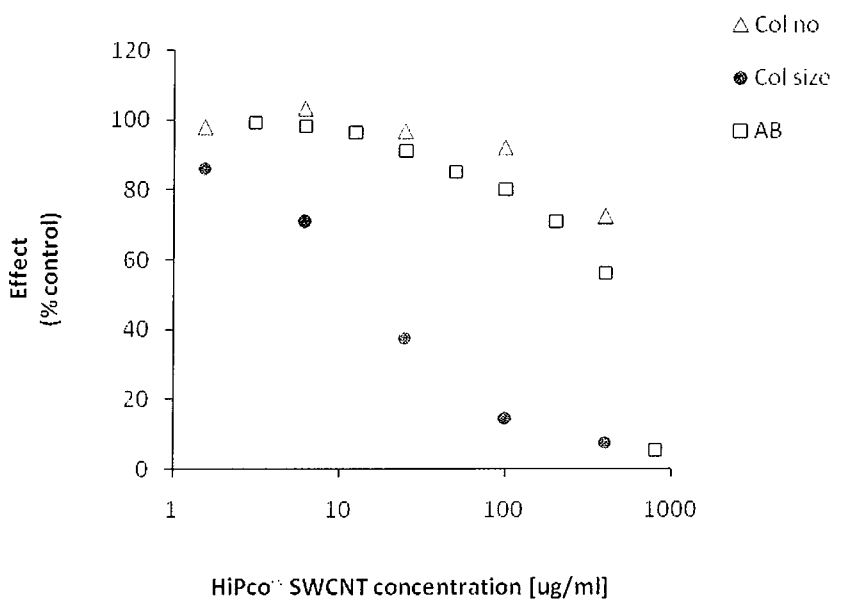

Figure 4.7: Association between clonogenic and colorimetric assay endpoints.

Comparing the results obtained using the clonogenic assay with the cytotoxicity dose-response curve obtained by the AB assay following 96 h exposures (as described in Chapter 3, 3.4.2.1.1), the colony size endpoint appeared to be the most sensitive endpoint followed by AB reduction as shown in Figure 4.7. Colony number seemed to be the least sensitive endpoint as the same dose-response could

be observed for colony numbers following exposure over 10 days as was seen for AB reduction following exposure over only 96 h.

4.4.1.5 *Interaction with cell culture media*

Ultrafine carbon black as well as SWCNT are known to interact and bind to a variety of organic molecules including sugars, proteins and cytokines [7, 9, 304]. This adsorptive nature of carbon-based nanomaterials may potentially lead to indirect, secondary toxicity by depleting cell growth media due to the binding of essential nutrients, cytokines and growth factors to particle surfaces. This nutrient depletion as a result of carbon particle exposure may affect cell viability and therefore colony formation, but more particularly colony sizes. It is well known that cells in nutrient deficient environment respond by reduced cell proliferation, ultimately leading to reduced colony sizes [305, 306]. The fact that catalyst residues did not seem to significantly affect SWCNT toxicities, as indicated by similar EC_{50} values calculated by colony size, may also point to the conclusion that the effects of SWCNT on cell growth and proliferation may be a result of such an indirect toxicity.

This secondary toxicity must also be kept in mind when undertaking comparison studies as different types of cell culture media may be more prone to SWCNT interactions than others. In this study, all three cell lines tested were maintained and exposed using the same type of culture medium. Therefore, it was possible to disregard any differences in cell line toxicity due to variations between growth media components. However, carbon nanomaterials may have tendencies to

selectively bind certain types of cytokines or growth factors which might differ between the three cell lines tested. Therefore, interactions between SWCNT and components of cell culture medium as well as the effects of culture medium that has previously been exposed to carbon nanomaterials need to be investigated.

4.4.1.5.1 *Spectroscopic characterisation of indirect effects*

Spectroscopic studies were conducted by Casey *et al.* (2007a) in order to demonstrate and elucidate the interactions of HiPco® SWCNT with cell culture medium and its components. Upon addition of raw SWCNT to the medium a noticeable colour change was observed [255]. UV/Vis absorption spectroscopy revealed a dramatic reduction in the absorption attributable to the phenol red, a pH indicator within the medium, without an associated change in pH. Reductions were also observed in absorbance features attributed to various components of the medium indicating an interaction with the SWCNT. Fluorescence spectroscopy revealed reductions in emission features associated with riboflavin and FBS, giving further support to an interaction [255].

In order to investigate the proposed mechanism of an indirect rather than a direct toxic effect of SWCNT, all nanotube species were removed from the exposure medium by centrifugation and filtration in order to be able to fully discriminate between direct and indirect effects. Raman spectroscopy (514.5 nm laser excitation) was employed to verify the removal of SWCNT from medium. The absence of SWCNT features from the recorded spectra provided a good indication that the SWCNT were successfully removed from the medium. The Raman analysis

also showed no evidence of amorphous carbon as present in ArcD SWCNT samples, although it is plausible that trace amounts remained within the media and were not detected by the Raman method. Atomic absorption analysis was carried out in order to detect any catalytic iron particles that might have leached from HiPco® SWCNT into the media. While a slight increase in iron levels were observed in the media following the filtration and centrifugation of the SWCNT, it should be noted that iron is an essential element for organisms and the levels present in the depleted medium were found to be two orders of magnitude less than those demonstrated to elicit genotoxic and cytotoxic effects in human cells [307].

The UV/visible absorption spectrum of FBS-supplemented culture medium consists of four features at 270, 360, 410 and 560 nm [255]. Upon addition of SWCNT considerable reductions of the intensity of these features was observed. The features at 270 and 410 nm were assigned to the added 5% FBS, whereas the two remaining features at 360 and 560 nm originate from the components of the medium itself, namely riboflavin [308, 309] and phenol red pH indicator, respectively. Furthermore a colour change of the medium was registered in the region of high SWCNT concentrations but only slight alterations in pH. This was interpreted as evidence that the SWCNT altered the chemical "composition" of the medium by interaction without adversely affecting the pH. The spectral changes observed are attributable to an adsorption of the molecular components of the medium to the π-electron surface of the nanotubes. This adsorption, coupled with the removal of SWCNT by filtration and centrifugation, would in turn cause a reduced effective concentration of these components in the medium facilitating the indirect toxic effect of SWCNT due to medium depletion to occur.

Due to the reductions observed in the absorbance of the characteristic medium features, it was expected that there would also be a reduction in their associated fluorescence emission features. Excitation of 5% FBS medium by three wavelengths, namely 268, 360 and 410 nm, each corresponding to the absorbance of an individual component of the medium, yielded emission spectra centered at 360 nm, 450 nm and 450 nm respectively. These excitation wavelengths were used here to study the filtered medium to assess the effect of SWCNT removal and the degree of SWCNT-medium interactions as previously described for indicator dyes by plotting the quenching of emission as a function of particle concentration. In all tested samples a dose-dependent reduction in emission of culture medium features was observed following SWCNT removal which gives further supportive evidence for the alteration of the medium upon interaction with SWCNT.

A similar quenching/interaction behaviour was observed for both types of SWCNT tested. However, the highest maximum degree of quenching was observed for all emission features at a HiPco® SWCNT concentration of 800 μg/ml. The relative equivalence of the responses indicates that SWCNT impurities play a negligible role in the depletion of culture medium. As reported previously, bundles of HiPco® SWCNT present a larger surface area when compared to that of ArcD SWCNT [254]. A larger surface area would in turn lead to increased nutrient adsorption onto HiPco® SWCNT bundles compared to ArcD SWCNT bundles, ultimately leading to a more effective depletion of culture medium by HiPco® SWCNT. This may explain the higher maximum degree of quenching observed for HiPco® SWCNT compared to ArcD SWCNT.

4.4.1.5.2 *Cytotoxicity due to indirect effects of SWCNT*

Due to the reported interaction between organic indicator dyes and SWCNT, employing such dyes for cytotoxicity screening of carbon nanomaterials is not recommended [30, 210, 257, 280]. However, the absence of SWCNT in the tested medium made it possible to employ the highly sensitive AB assay. Figure 4.8 displays the cytotoxicity response curves obtained for HiPco® SWCNT and the ArcD SWCNT using the AB assay following exposure to depleted culture medium (previously containing SWCNT). Concentrations quoted are those of the nanomaterials in the medium pre-filtration. As can be seen, there is a clear dose- and time dependent decrease in cell viability starting at HiPco® SWCNT concentrations of 400 μg/ml following 48 h exposure (Figure 4.8a). However the effect only fell within statistical significance at the highest test concentration of 800 μg/ml.

A slightly different behaviour was observed for the ArcD SWCNT filtered medium (Figure 4.8b). Data variability was larger than seen for HiPco® SWCNT filtered medium and a clear dose- and time-dependent effect was only noted at the highest concentrations tested. However, it is clear for example from the 96 h response that the ArcD SWCNT exposed medium elicits a smaller response than that for the corresponding HiPco® medium irrespective of statistical significance. This is consistent with the greater degree of quenching observed for the HiPco® medium. Again the greater surface area reported for HiPco® bundles compared to those of ArcD tubes could explain the higher toxicity observed for medium previously exposed to HiPco® SWCNT than ArcD SWCNT filtered medium.

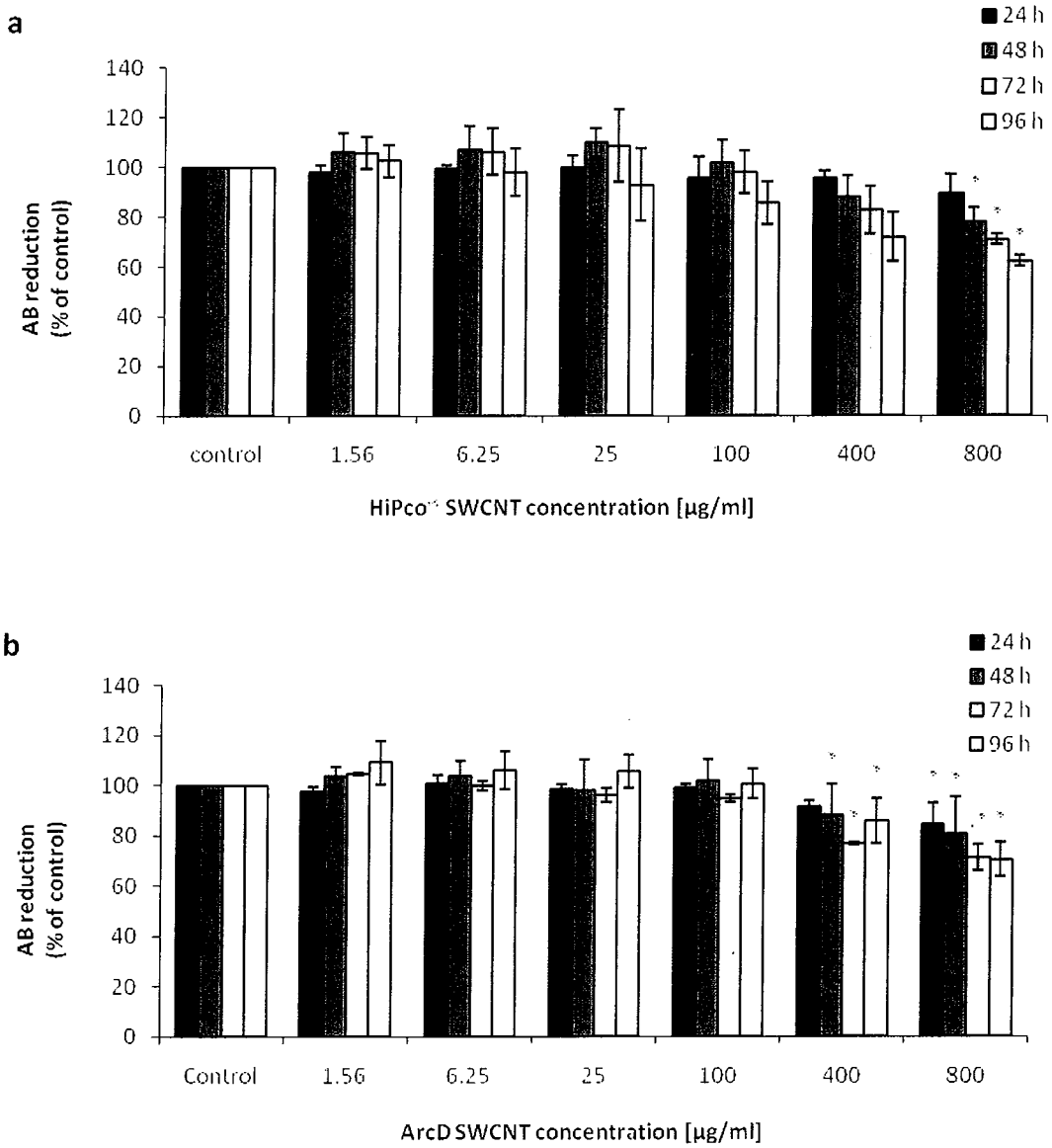

Figure 4.8: Cytotoxicity of (a) HiPco® SWCNT and (b) ArcD SWCNT filtered medium to A549 cells after 24, 48, 72 and 96 hour exposures determined by the AB assay. Data are expressed as percent of control mean ± SD of four independent experiments. *Denotes significant difference from control ($p \leq 0.05$).

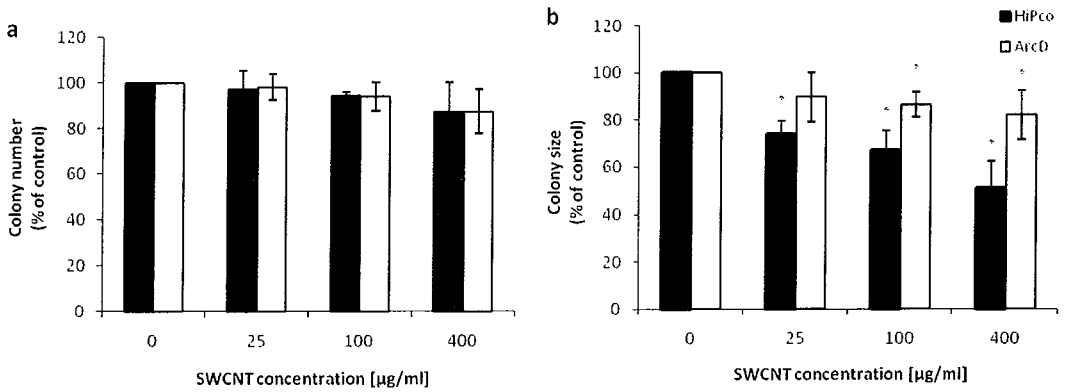

Figure 4.9: (a) Colony number and (b) colony sizes of A549 cells following 10 days exposure to SWCNT depleted culture medium. Data are expressed as percent of control mean ± SD of three independent experiments. *Denotes significant difference from control ($p \leq 0.05$).

The clonogenic assay was employed in addition to the AB assay for the assessment of indirect SWCNT toxicity. As can be seen in Figure 4.9a, the ability of A549 cells to form colonies during incubation in depleted culture medium was only slightly reduced when the medium was previously exposed to the highest SWCNT concentration of 400 µg/ml. Treatment with any other SWCNT concentrations did not show any effects. This was the same for HiPco® and ArcD SWCNT samples. However, when determining colony sizes, significant, dose-dependent reductions were observed following HiPco® SWCNT treatment where colonies reached sizes of only 51% of that of controls grown in normal culture medium (Figure 4.9b). Already at the lowest HiPco® SWCNT concentration tested, colony size was reduced by more than 26%. This lends further support to the possibility of an indirect toxicity by means of nutrient depletion resulting from SWCNT interaction with the culture medium.

During the clonogenic assay, on average 8 µl of culture medium was available for one cell during the 10 days of exposure. In contrast, during the AB assay, only 0.002, 0.003, 0.007 and 0.01 µl was available for 24, 48, 72 and 96 h exposures, respectively. Therefore, the total of available nutrients was higher in the clonogenic assay compared to the AB assay. This could explain why cells were still able to form colonies at numbers comparable to cells grown in control medium. However, medium depletion did inhibit the rate of cell proliferation and metabolism as indicated by reduced AB reductions and smaller colony sizes. As the amount of nutrients available to cells during the AB assay was 99.9% lower compared to the clonogenic assay, greater effects of medium depletion could be seen in the AB assay which can explain the discrepancies seen between the two assay systems employed in this study. This may also explain why 96h AB reduction appeared to be the more sensitive endpoint compared to colony formation following direct particle exposures as seen in Figure 4.7.

The clonogenic assay showed that medium depletion has long-term effects on A549 cells on a sub-lethal level. HiPco® SWCNT samples were always more effective compared to ArcD SWCNT samples indicating the importance of surface area in the mechanism of medium depletion. The data presented in this study has implications for studies on the cytotoxicity of SWCNT following direct exposure. Figure 3.2a and Figure 3.3a in 3.4.2.1 display the obtained cytotoxic response curve of A549 cells following direct exposure to SWCNT as evaluated by the AB assay. Data of this nature would obviously contain a contribution from the demonstrated indirect effect of medium depletion coupled with absorptive interferences [257, 280] which needs to be considered when evaluating long-term

exposures to high SWCNT concentrations. Regarding the measurements of colony size following 10 days and AB reduction following 96 h exposure to HiPco® SWCNT, up to 50% of the effects observed following direct exposure may be due to indirect particle effects. Following 24 h exposures, indirect effects account for only 10% of the overall effect observed.

Protein binding of SWCNT has also been described by other authors including Monteiro-Riviere and Inman (2006) who reported binding of the pro-inflammatory cytokine IL-8 to nanoparticle carbon black; Salvador-Morales *et al.*, (2006) who have demonstrated the binding of lung surfactant proteins onto SWCNT; Dutta *et al.* (2007) who have shown albumin adsorption by SWCNT and Hirano *et al.* (2008) who reported interactions between MWCNT and macrophage receptors with collagenous structure (MARCO) [12, 30, 212, 215, 243]. Indirect effects in terms of nutrient depletion have also been shown by Guo *et al.* (2008) which described dose-dependent adsorption of over 14 different amino acids and vitamins from cell culture medium onto SWCNT leading reductions in cell viability [230]. Folate supplements were reported to restore cell performance and its absence due to CNT adsorption was therefore identified as one of the factors responsible for the adverse effects observed. In the study presented here, it was seen that SWCNT can lead to decreased cell viability due to such indirect mechanisms causing depletion of cell culture media. Medium depletion caused reduced metabolic activity, as seen by the AB assay, as well as inhibited colony formation as shown by the clonogenic (colony forming) assay. The dominant effect, as indicated by the colony size endpoint, is a reduction of the proliferative capacity of the cells in the depleted medium.

4.5 Conclusion

By employing the clonogenic assay as an alternative to the commonly used absorbance or fluorescence-based assays, any adsorptive interactions between nanomaterial and indicator dyes could be overcome, allowing a more realistic and accurate toxicity determination. Even though the use of the clonogenic assay as a high-throughput assay is limited, this assay offers the possibility for the *in vitro* assessment of long term toxicity including sub-lethal endpoints, making it highly sensitive and valuable. In this study, it could be illustrated that including measurements of colony surface area as an additional endpoint makes the assay even more sensitive and allows distinction between effects on cell viability and cell proliferation as two separate endpoints. Therefore, the clonogenic assay can be recommended for the toxicity evaluation of carbon-based nanomaterials on colony forming cell lines.

It was possible to show differences in cytotoxicity between two types of carbon nanomaterials, SWCNT and carbon black with nanotube material being intrinsically more reactive compared to amorphous carbon nanoparticles. Different cell lines manifested specific cytotoxic responses in terms of cell viability and proliferation, highlighting increased sensitivity of normal cell lines compared to carcinoma cell lines and differences in tissue sensitivity. It was shown that the toxicity of SWCNT differs according to the production method used, with HiPco® SWCNT being more reactive compared to ArcD produced SWCNT. The effects on colony numbers indicate that residual metal catalyst particles may contribute to the primary toxic response. In terms of proliferative capacity, however, the

different types of SWCNT had similar effects, indicating a common, possibly secondary mechanism which might be partly the result of the adsorptive interaction between SWCNT bundles and the molecular components of the medium.

Cytotoxicity assessment coupled with spectroscopic analysis could verify the proposed hypothesis of an indirect toxicity as a result of the interaction of SWCNT with cell culture medium. It is without question that upon their dispersion and subsequent removal, both types of SWCNT tested in this study did alter the composition of the medium, as evidenced by the spectroscopic analysis. The removal of SWCNT impurities confirms that this is an intrinsic effect of the adsorption by the nanotubes of molecular components of the cell growth medium resulting in medium depletion. This in turn resulted in an adverse effect on cellular growth as verified by the cytotoxicity data presented for both the clonogenic and the AB assay. The clonogenic endpoints give a clear indication that the principal effect of SWCNT exposure is one of reduced proliferative capacity rather than viability. Once again cellular effects were higher for the nanomaterial with the larger surface area.

Overall, this study highlights the fact that not only the direct but also indirect effects contribute to the toxicity profile of carbon based nanomaterials.

Chapter 5

Effects of SWCNT on intracellular ROS formation

This chapter is based on the following publications:

Oxidative stress response of human lung epithelial cells upon carbon nanoparticle exposure depends on the dispersion media

Eva Herzog, Hugh J. Byrne, Maria Davoren, Alan Casey, Maria Schmittner, Albert Duschl, Gertie Janneke Oostingh

Toxicology and Applied Pharmacology, submitted October 2008

SWCNT suppress inflammatory mediator responses in human lung epithelium *in vitro*

Eva Herzog, Hugh J. Byrne, Alan Casey, Maria Davoren, Anke-Gabriele Lenz, Konrad L. Maier, Albert Duschl, Gertie Janneke Oostingh

Toxicology and Applied Pharmacology, accepted on 29th October 2008

doi:10.1016/j.taap.2008.10.015

5.1 Chapter summary

Following assessing the cytotoxicity of SWCNT, this study investigated whether SWCNT have the potential of inducing ROS and may therefore initiate tier 1 to 3 responses in exposed cells as described in Chapter 2, 2.2.4.3. As in the previous study, effects were compared between HiPco® and ArcD SWCNT in order to further investigate the role of production method and particle contaminants on SWCNT toxicity. Due to the structural resemblance of SWCNT to asbestos fibres, crocidolite asbestos was included as additional control particle to P90 carbon black. Intracellular ROS were measured following short-term exposure of NHBE and A549 cells using the redox sensitive probe 6-carboxy-2',7'-dichlorodihydrofluorescein diacetate (carboxy-H_2DCFDA). In order to investigate the role of dispersion vehicle on particle toxicity, the oxidative potential was compared following particle dispersion in cell culture medium with and without FBS supplement and dispersion in DPPC. It was demonstrated that *in vitro* exposure of lung epithelial cells to carbon nanomaterials resulted in only moderate or low oxidative stress under the exposure conditions employed. Cell responses were found to be strongly dependent on the medium used for particle dispersion. Whereas the presence of DPPC increased intracellular ROS formation, FBS seemed to protect the cells from oxidative insult.

5.2 Introduction

As described in Chapter 2, 2.2.4.3, the potential mechanisms of nanomaterial toxicity are very diverse, involving cytotoxicity and a variety of cell signalling responses including inflammatory and lipid mediators, all of which may be included within the hierarchical oxidative stress paradigm (Chapter 2, 2.2.4.3 and Figure 2.3). Previous studies on SWCNT have mainly focused on tier 3, the last level of cellular responses characterised by cytotoxicity (Chapter 3 and 4). However, these studies revealed that cell death or decreased proliferation only takes place at very high particle concentrations or following long exposure periods indicating low acute cytotoxicity of SWCNT exposure. Therefore, the following studies were aimed at investigating whether SWCNT have the potential of inducing earlier cell responses including tier 1 or 2. The small size of CNT may not only allow them to gain access to cells and tissues, it also leads to large specific surface area which may render them highly interactive. In addition, some types of nanomaterials contain transition metals as trace impurities which are known to generate ROS in biological systems [310].

The fluorogenic carboxy-H_2DCFDA was used as ROS indicator in this study. As illustrated in Figure 5.1, the dye permeates live cells where it is deacetylated by nonspecific intracellular esterases. In the presence of ROS, including hydrogen peroxides, peroxyl radicals and peroxynitrite anions, the reduced carboxydichlorofluorescin (carboxy-DCFH) is oxidised to a green fluorescent compound (carboxy-DCF) [311].

The carboxy derivative carries additional negative charges that improve its cellular retention compared to noncarboxylated forms of 2', 7'-dichlorofluorescein (DCF) [312].

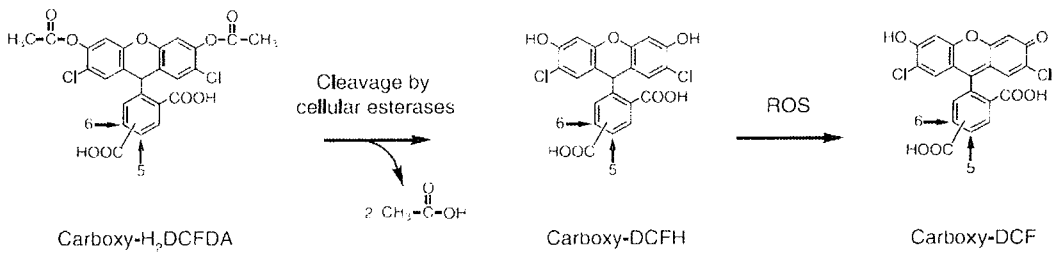

Figure 5.1: Principle of the carboxy-H2DCFDA assay [313].

The high biopersistence and structural resemblance of CNT to asbestos has put SWCNT in the spotlight in terms of their potential toxicity as described in Chapter 2, 2.3.4.2 [44]. The parallels drawn in terms of aspect ratio and fibrous nature highlight the need for further investigations of the comparative toxicity of CNT and asbestos fibres. Cytotoxicity, oxidative stress and pro-inflammatory and fibrogenic factors released by lung target cells are all believed to play a key role in the pathogenesis of asbestos toxicity [156, 314, 315]. Thus a systematic comparison of SWCNT bundles and asbestos fibres is advantageous and was therefore conducted in this study.

Upon inhalation, it is hypothesised that particles may deposit in the lung and come in contact with lung surfactant as described in Chapter 1, 1.2.4. Interaction between CNT and pulmonary surfactant following inhalation exposure may lead to particle coating and modification of the surface chemistry [69]. In turn, this may have consequences for the oxidative potential of the particles. In addition, lung

surfactant can influence particle dispersion which would ultimately lead to changes in particle size distribution, agglomeration state or surface area, all factors that are believed to play an important role in the toxicity and oxidative potential of carbon nanomaterials [92]. Therefore, DPPC dispersed into physiological saline has been used as a simple model of lung surfactant (Chapter 2, 2.3.5.2.1.3) in order to mimic the real world exposure situation more closely and increase biological relevance [69, 70]. To study whether lung surfactants can alter the extent of dispersion and thereby the toxicity of SWCNT samples, all exposures were carried out using medium suspended particles in parallel.

In order to assess whether A549 cells are representative of primary cells regarding the aspects studied here, normal bronchial epithelial cells (NHBE) were also tested in parallel.

The objective of this study was therefore to investigate the oxidative stress response of human lung epithelial cells upon exposure to three different types of nanomaterials: HiPco® SWCNT, ArcD produced SWCNT and P90 carbon black. The results are compared to those observed for crocidolite asbestos fibres. In addition, three different vehicles were used for particle suspension in order to assess the influence of dispersant media on the potential of nanomaterials to induce oxidative stress.

5.3 Materials and Methods

5.3.1 Cell Culture

5.3.1.1 *A549 human lung epithelium*

A549 cells were cultured in RPMI 1640 (Gibco, Karlsruhe) supplemented with L-glutamine, penicillin and streptomycin (Gibco) and 10% FBS (Biochrom, Berlin) in a humidified atmosphere containing 5% CO_2 at 37 °C. In contrast to previous studies (Chapter 3 and 4), a new batch of A549 cells was employed for the studies described in the following chapters. This new batch was routinely grown in RPMI 1640 medium which was therefore employed instead of Kaighn's or DMEM media.

5.3.1.2 *Normal human primary bronchial epithelial cells*

Normal human primary bronchial epithelial cells (NHBE) were obtained from Clonetics™ (Lonza, Switzerland) and were maintained in bronchial epithelial cell basal medium (BEBM®) plus SingleQuots® supplements as recommended by the supplier. Cells were used between passages 3-7.

5.3.2 Test Particles

HiPco® SWCNT, ArcD SWCNT and P90 carbon black as described in 3.3.1 and 4.3.1, respectively and standard reference crocidolite asbestos (UICC), obtained from SPI Supplies (Structure Probe Inc., West Chester, USA) and characterised as described

by Bowes and Farrow (1997), were used as test particles [316]. Crocidolite asbestos was reported to have a mean length of ≤ 5 µm and a mean width of < 0.5 µm [317]. BET surface area was reported to be 5.6 m^2/g [318].

5.3.3 Dispersion of test particles

5.3.3.1 *Dispersion of SWCNT in cell culture medium*

Particle dispersion was carried out according to Kreyling *et al.* (personal communication). The use of an ultrasonic bath was preferred over sonication via an ultrasonic tip due to reduced risk of sample contamination.

A stock concentration of 500 µg/ml of SWCNT was prepared in glass vials using the appropriate culture medium by vortexing the solution three times for 5 seconds each and subsequently sonicating it for 1 min (Sonorex RK52, Bandelin, Berlin, Germany) with constant tapping of the glass vial onto the bottom of the ultrasonic bath. This procedure was repeated three times.

5.3.3.2 *Dispersion of SWCNT in DPPC*

A DPPC (Sigma Aldrich, P0763) solution of 2.5 mg/ml was prepared in PBS by sonication for 10 minutes at 37°C using an ultrasonic bath. A 500 µg/ml stock concentration of SWCNT was prepared in DPPC/PBS solution followed by vortexing three times for 5 seconds each and subsequently sonicating for 1 min

(Sonorex RK52, Bandelin, Berlin, Germany). This procedure was repeated three times.

5.3.3.3 *Dispersion of crocidolite asbestos*

Stock concentrations of 500 μg/ml crocidolite asbestos [$(Na_2(Fe^{3+})2(Fe^{2+})_3Si_8O_22(OH)_2$] were prepared by diluting in the appropriate cell culture medium or DPPC/PBS. As asbestos was easily dispersible in aqueous solutions, no ultrasonication was required but short-term vortexing was used in order to disperse the samples.

5.3.4 Characterisation of SWCNT suspensions

5.3.4.1 *Dynamic light scattering (DLS)*

The diameter of the nanomaterials in solution was measured using Malvern Zeta sizer Nano ZS (Malvern Instruments, Worcestershire, UK). This instrument is equipped with a helium-neon laser (λ= 633 nm) and measures the back scatter from a suspension at an angle of 173°. It is capable of measuring particles in the size range 0.6 nm – 6 μm.

5.3.4.2 *Optical microscopy of particle exposed cells*

Cell monolayers were exposed to SWCNT samples or crocidolite asbestos as described for cell viability assays. Micrographs were obtained using a light microscope (Olympus IX70).

5.3.5 UV-vis-NIR spectroscopy

The method was adopted from Priya and Byrne (2008). Stock solutions of 4000 μg/ml SWCNT in DPPC/PBS were prepared as described earlier [319]. This sample was then serially diluted using DPPC/PBS solution by a factor of 2, down to 1.95 μg/ml. Thus, the surfactant concentration was kept constant while that of the SWCNT was serially diluted. For SWCNT samples suspended in culture medium, a stock concentration of 500 μg/ml SWCNT was prepared in DPPC/PBS, A549 or NHBE culture medium. These stock concentrations were diluted 1:10 in A549 or NHBE medium to obtain concentrations of 50 μg/ml, followed by serial dilutions by a factor of 2 down to 0.195 μg/ml using the corresponding medium. The absorbance at a wavelength of 633 nm was measured using a UV-vis-NIR spectrometer (Perkin-Elmer Lambda 900). This wavelength was chosen to be within the region of SWCNT absorbance while avoiding interference from components of the cell culture medium [255, 319].

5.3.5.1 *Carboxy-DCFDA assay*

The carboxy-DCFDA assay was carried out as per manufacturer's instructions. Stock solutions of 10 mM carboxy-H_2DCFDA (Invitrogen, C-400) were prepared in DMSO and stored in the dark at -20°C. From this, a second stock solution of 1 mM was prepared in PBS immediately prior to use. A549 and NHBE cells were seeded at a density of $3x10^4$ cell/well in 24 well plates and incubated at 37 °C for 24 h for cells to adhere. Following 24 h, culture medium was discarded and cells were washed with 1 ml PBS followed by addition of 500 µl of fresh culture medium. For 1 h exposures, 5 µl of carboxy- H_2DCFDA (1 mM) were added into each well and cells were incubated for 15 min at 37 °C. Afterwards, 50 µl of test particle solution (500 µg/ml) were added to the cells (1:10 dilution). For 4 h exposures, cells were first exposed to test particles by adding 50 µl of test particle solution (500 µg/ml) to each well. Following 3 h incubation, 5 µl of carboxy- H_2DCFDA (1 mM) were added and cells were incubated for another 60 minutes. Therefore, cells were exposed to final particle concentrations of 50 µg/ml (13.16 µg/cm^2). The respective cell culture media with or without 10% DPPC/PBS supplement were used as the solvent control. Hydrogen peroxide (H_2O_2) at a concentration of 500 µM was used as positive control stimulus.

In parallel, cells were pre-treated with 25 mM of N-acetyl-l-cysteine (NAC) solution prepared in RPMI medium for 30 min before addition of carboxy-H_2DCFDA or particle exposure. By preparing a 1:10 dilution of NAC (250 mM stock concentration) in cell culture medium, addition of NAC did not significant change in pH of the culture medium.

At the end of the exposure period, cell supernatants were discarded, cells washed with PBS and harvested using Trypsin/EDTA followed by suspension in PBS/FBS (10%). Cells were transferred into FACS tubes and immediately analysed using flow cytometry and 10,000 cells were analysed per replicate [Becton Dickinson FACSCantoTM].

5.3.5.2 *Statistical analysis*

All experiments were carried out in duplicate containing two replicates, each. Statistical analysis was carried out as described in Chapter 4, 4.3.8.

5.4 Results

5.4.1 Particle dispersion

In this study, test particles were suspended in cell culture medium or DPPC/PBS solution. Concentrations of DPPC were chosen in order to assure complete particle coverage and mimic the degree of conditioning that would occur upon lung deposition. Due to the large surface area of SWCNT, 2.5 mg/ml of DPPC in PBS was calculated to be appropriate (based on W. Wallace, personal communication). Asbestos, despite having a smaller surface area, was suspended in the same concentration of DPPC in order to allow direct toxicity comparisons. Due to the complexity of biological media, full characterisation of SWCNT is challenging and often not feasible. In the present study, Raman spectroscopy, DLS, and optical microscopy were carried out in order to assess the physical characteristics of SWCNT upon dispersion in DPPC and cell culture medium.

As described in Chapter 3, although single SWCNT are only a few nanometres in diameter, they grow in bundles and are hard to separate so that they typically form micron-sized agglomerates which have a greater aerodynamic diameter and a smaller surface area compared to individually dispersed tubes [255]. As can be seen in Figure 5.2, optical microscopy confirmed the presence of SWCNT agglomerates of various sizes with diameters of micrometer range distributed on top of exposed cells. In both cell culture medium and DPPC, SWCNT were present as agglomerates, leading to cells being exposed to bundles of SWCNT rather than individual fibre shaped tubes, as seen in previous studies (Chapter 3 and 4). However, when comparing Figure 5.2 a and Figure 5.2 b, it could also show that the

relative agglomeration of SWCNT clearly differed between SWCNT dispersed in A549 medium (Figure 5.2 a) and DPPC followed by addition to A549 medium (Figure 5.2 b).

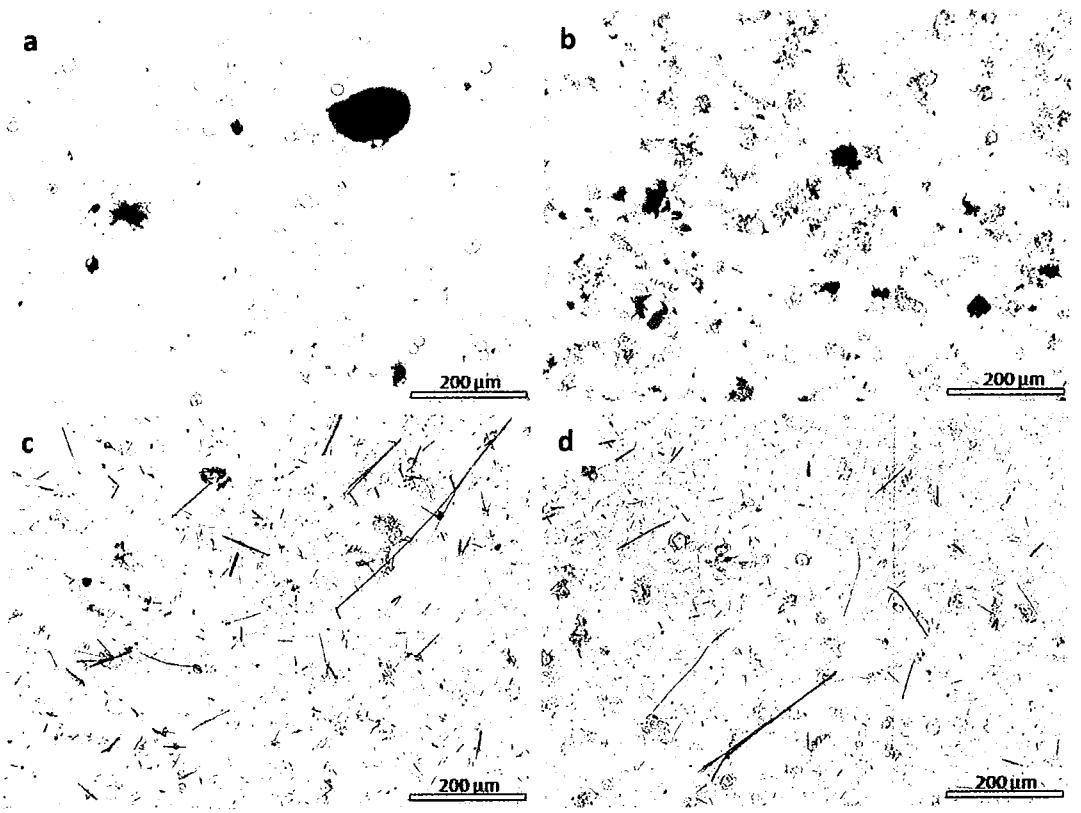

Figure 5.2: A549 cells exposed to 12.5 µg/ml of HiPco® SWCNT (a; b) or crocidolite asbestos (c; d) dispersed in A549 culture medium (a; c) or DPPC followed by addition to A549 culture medium (b; d).

Dispersion in A549 medium resulted in the least uniform dispersion leading to the formation of large, condensed agglomerates of SWCNT. In contrast, both DPPC and NHBE medium dispersion led to a more uniform SWCNT dispersion, resulting in greater exposure of cells to SWCNT as shown in Figure 5.3. Improved dispersion due to the use of DPPC was also reported for P90 carbon black particles [320].

Dynamic light scattering (DLS) measurements confirmed that all SWCNT samples were highly poly-disperse and tended to precipitate. However, this was also the reason why this method was not applicable for further analysis of the SWCNT samples used. Crocidolite asbestos dispersion appeared to be independent of DPPC.

In order to improve physical characterisation, UV-vis absorption analysis was carried out to analyse SWCNT suspensions as described by Priya and Byrne (2008). A linear and constant increase in absorbance was observed with increasing SWCNT concentrations for all dispersant vehicles used (Figure 5.3). This indicates that within the concentration range of SWCNT employed in this study, SWCNT were present as bundles and there was no evidence of a transition to dispersed isolated tubes at low concentrations, as is observed in water/sodium dodecyl benzene sulfonate (SDBS) suspensions at 0.07mg/ml. This effect was independent of the type of suspension vehicle used. Using UV-vis absorption spectroscopy, the same absorbance values were observed for SWCNT suspensions following DPPC or NHBE medium dispersion (Figure 5.3). However, dispersion with A549 culture medium in the absence of DPPC resulted in significantly lower absorbance, indicating higher amounts of SWCNT being suspended by DPPC or NHBE medium compared to A549 medium. Improved dispersion of SWCNT would ultimately modify their toxicological behaviour as well as their aerodynamic and therefore deposition characteristics [321]. In contrast to SWCNT, the dispersion of asbestos was independent of the type of dispersion medium (Figure 5.2 c, d) and it was easily dispersed leading to single fibres.

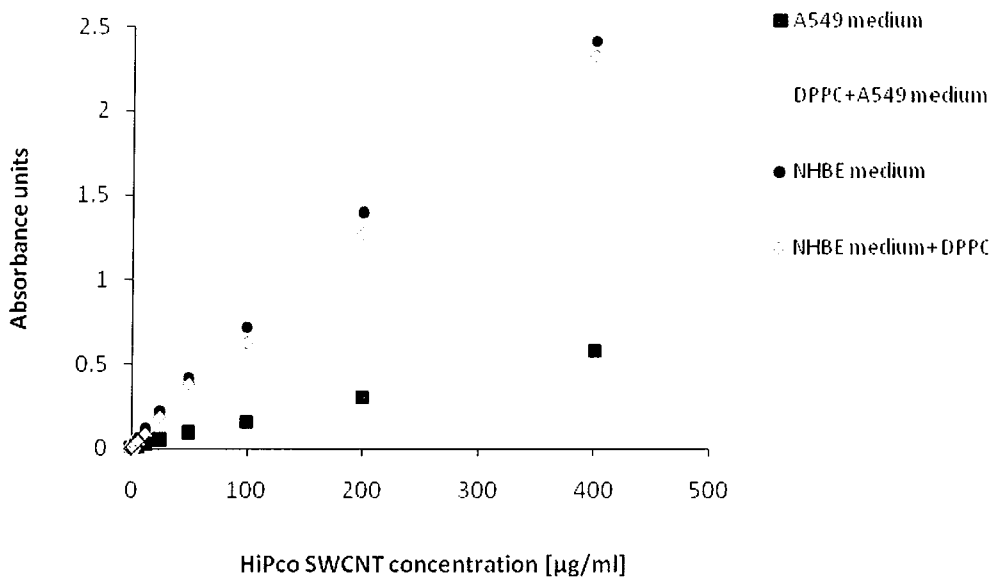

Figure 5.3: Absorbance values of SWCNT dispersed in A549 medium (■), DPPC followed by addition to A549 medium (△), NHBE medium (●), DPPC followed by addition to NHBE medium (◇).

The fact that DPPC may aid in the dispersion of SWCNT agrees with a study by Sager *et al.* (2007) who reported that DPPC in combination with BSA produces a satisfactory dispersion of carbon nanomaterials [241]. In a recent study by Porter *et al.* (2008), authors also employed DPPC as a non-toxic dispersant for MWCNT [240]. Dispersion using DPPC may lead to adsorption of surfactant components onto the particles. This could result in the conditioning of particle surfaces which may affect their expression of cytotoxicity or genotoxicity [69]. This was seen for DEP and also silica particles conditioned by DPPC [69, 322, 323]. A recent study by Foucaud *et al.* (2007) demonstrated that the oxidative potential of P90 carbon black can be modified by dispersion in medium containing DPPC and BSA. Dispersion in DPPC resulted in greater oxidative potential of particles as compared to particles suspended in physiological saline [320]. On the other hand, coating

with lung surfactant might mask their oxidative potential leading to decreased reactivity and attenuated toxicity [324]. Therefore, the next step of this study was to investigate the effects of SWCNT exposure on the ROS formation within lung epithelial cells and examine whether DPPC dispersion modulates cell responses.

5.4.2 Intracellular ROS formation

The results of this study showed that exposure of NHBE cells to cell culture medium dispersed carbon nanomaterials or asbestos for 1 h did not induce the formation of ROS. Only following the addition of H_2O_2 to the cell cultures, significant increases in ROS could be measured (Figure 5.4). However, when the particles were dispersed in DPPC solution, a significant increase in ROS was detected following HiPco® SWCNT, ArcD SWCNT, P90 carbon black and asbestos exposures whereby P90 carbon black was found to be the most active of the particles tested (Figure 5.4). Compared to cell responses to H_2O_2 (500 µM), ROS levels determined for nanomaterials and asbestos were low to moderate. DPPC dispersion increased the ROS forming ability of particles compared to dispersion in DPPC free medium by a factor of 1.5, 2.2, 3.8 and 1.4 for HiPco® SWCNT, ArcD SWCNT, P90 carbon black and asbestos, respectively (Figure 5.5).

As soon as NHBE cells were pre-treated with the antioxidant NAC, ROS formation was inhibited at all times (Figure 5.6). Neither the particles nor H_2O_2 exposure were able to induce ROS in NAC pre-treated cells. In addition, NAC decreased cellular ROS levels below those of untreated cells.

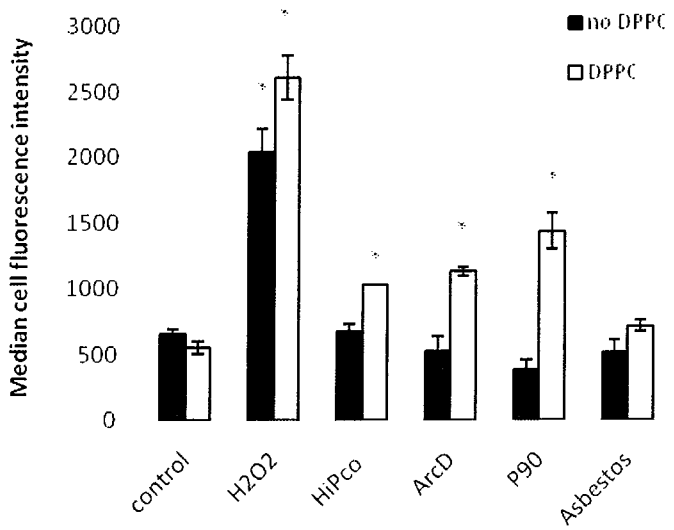

Figure 5.4: ROS formation in NHBE cells following 1 hour exposure to carbon nanomaterials and asbestos dispersed in NHBE culture medium (black) and DPPC (grey).

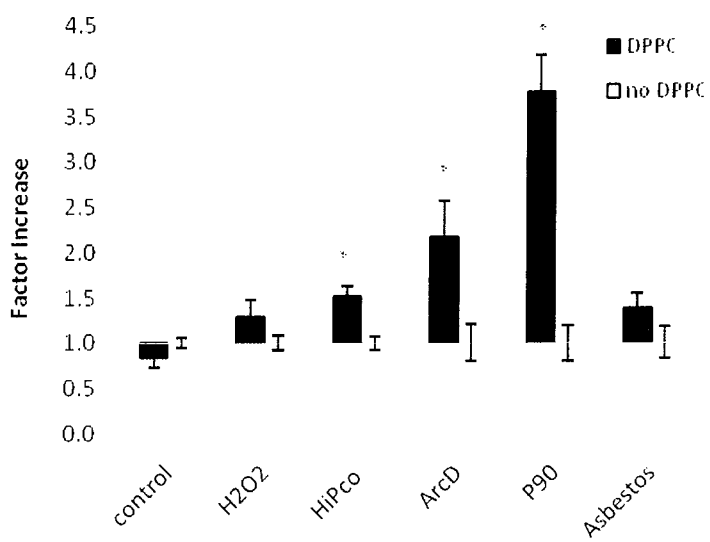

Figure 5.5: Comparison of ROS formation in NHBE cells in the presence (black) and absence (white) of DPPC dispersion.

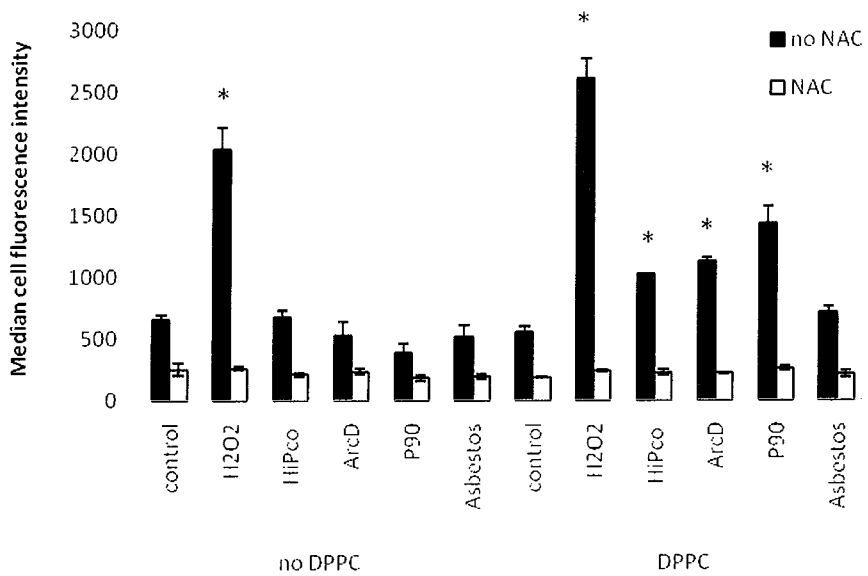

Figure 5.6: ROS formation in NHBE cells following exposure to 50 μg/ml carbon nanomaterials and asbestos dispersed in NHBE medium with (grey) and without (black) NAC pre-treatment.

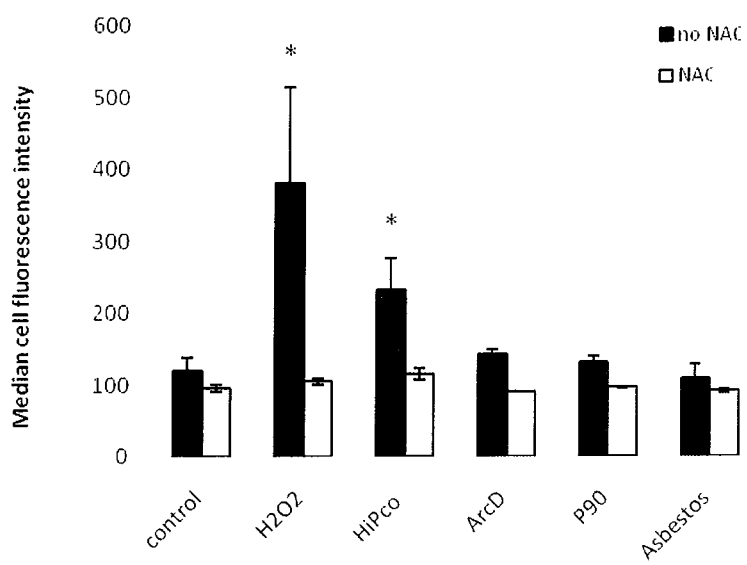

Figure 5.7: ROS formation in A549 cells following exposure to 50 μg/ml carbon nanomaterials dispersed in RPMI medium with (grey) and without (black) pre-treatment with NAC solution for 30 minutes.

Incubation with NAC before particle exposure inhibited ROS formation also in A549 cells (Figure 5.8). In the absence of NAC, HiPco® and ArcD SWCNT dispersed in FBS-free culture medium did result in slight intracellular ROS generation in this cell line with increases by factors of 1.9 and 1.1, respectively. When FBS was added as a cell culture medium supplement, no ROS response could be detected in A549 cells for any of the particles tested (Figure 5.9).

Again, ROS formation was increased upon exposure to particle dispersions in DPPC (Figure 5.9). However, the difference was less pronounced than that demonstrated for NHBE cells. The highest increase was detected for P90 carbon black which resulted in an increase by 90 % compared to culture medium (without FBS supplement) dispersed particles (Figure 5.9). The increases for HiPco® and ArcD SWCNT were not statistically significant Cell responses following 4 h exposures were comparable with the effects seen following 1 h.

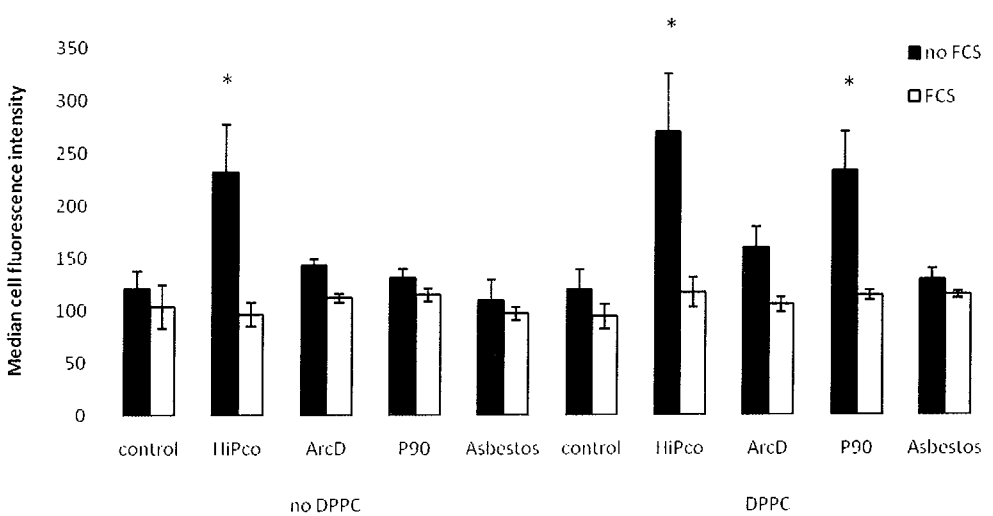

Figure 5.8: ROS formation in A549 cells following exposure to 50 µg/ml carbon nanomaterials and asbestos dispersed in RPMI medium with (grey) and without (black) FBS supplement.

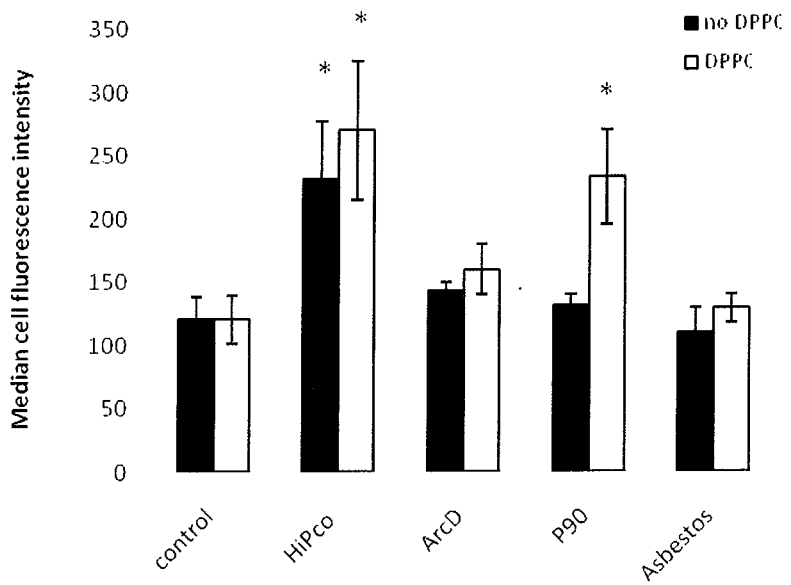

Figure 5.9: ROS formation in A549 cells following exposure to 50 μg/ml carbon nanomaterials dispersed in RPMI medium (black) or DPPC (grey).

5.5 Discussion

Oxidative stress has been identified as one of the best-developed paradigms to explain nanomaterial toxicity from a mechanistic point of view [71]. It is also believed to be the main mechanism by which air pollution particles cause adverse effects in exposed tissues including epithelial cells and macrophages [24, 325]. This study investigated the potential of two types of SWCNT, carbon black and asbestos to induce intracellular ROS in epithelial cells following short-term exposure. In addition, particles were dispersed in different types of dispersion media in order to assess the role of the biological environment on particle toxicity.

In standard cell growth media, none of the particles tested were able to significantly increase ROS in NHBE cells (Figure 5.4). In contrast, A549 cells significantly responded to HiPco® SWCNT exposure, but not to any other particle (Figure 5.7) even though it was observed that A549 directly interact with asbestos fibres following exposure as shown in Figure 5.10. The differences in cell responses might be explained by the use of different culture media. Whereas NHBE cells were exposed to particles suspended in specialized medium supplemented with a variety of growth factors and other additives, A549 cells were exposed to particles suspended in protein-free RPMI medium without the use of any supplements besides L-glutamine. Similar to FBS, the supplements present in NHBE medium might attenuate particle reactivity leading to decreased reactivity and toxicity as seen in Chapter 3, 3.4.2.1 [324]. ROS levels of A549 cells also returned to control levels as soon as particles were suspended in RPMI medium supplemented with FBS (Figure 5.8). Therefore, the presence of additional protein seemed to have a protective effect, rendering the particles un-reactive and

supporting the proposal that the protein corona formed around particles greatly influences particle toxicity [326].

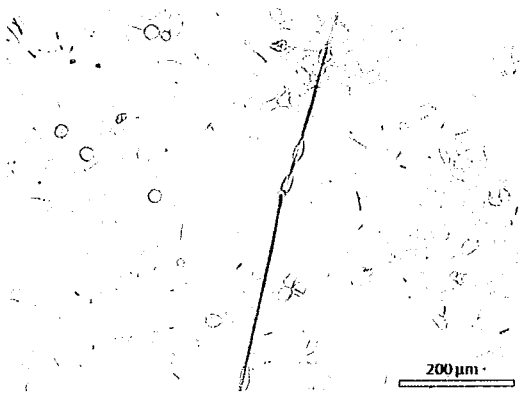

Figure 5.10: A549 cells interacting with asbestos fibres following exposure of A549 cell monolayer to 50 ug/ml of crocidolite asbestos. Scale bar indicates 200 µm.

Upon inhalation, particles may come into contact with lung surfactant which lines the alveoli and respiratory bronchioles in the deep lung [60]. In 3.4.4.4 it was shown that exposure of A549 cells to HiPco® SWCNT results in increased numbers of lamellar bodies, indicating an increase in surfactant production. Therefore, the use of phospholipids as dispersing agents may be of great relevance for particle toxicity studies. In the presence of DPPC, the potential of carbon nanomaterials, namely SWCNT and carbon black, to induce intracellular ROS was significantly increased (Figure 5.5 and Figure 5.9). The most pronounced effect could be seen for P90 carbon black exposure which resulted in increases of ROS by factors of 3.8 and 1.8 in NHBE and A549 cells, respectively. This agrees with studies by Foucaud *et al.* (2007) who also reported increased ROS production in monocytic cells following exposure to P90 carbon black suspended in DPPC compared to

suspensions in culture medium only [320]. There was no statistically significant increase in asbestos toxicity.

The increases in ROS in the presence of DPPC may be explained by improved dispersion of SWCNT and P90 carbon black particles. Interaction with DPPC may lead to hydrophilic coating of the particles, permitting dispersion in aqueous media, leading to greater surface areas available for reactions and therefore an increase in the registered toxic response as more cells would come into contact with particles. Therefore, it is likely that an increased number of cells will be exposed to SWCNT upon DPPC dispersion and nanotube-cell interactions may be increased. Improved dispersion due to lung surfactant coating was also reported to be the reason for increased genotoxicity of DEP [69]. As asbestos was well dispersed in culture medium only, the use of DPPC did not alter its reactivity.

Reactive oxygen species can also be generated due to mitochondrial damage following cellular uptake of particles [327, 328]. Decreased particle agglomerate size as seen for P90 carbon black [320] and HiPco® SWCNT upon DPPC dispersion may result in increased cell uptake and therefore ROS production. However, uptake of SWCNT dispersed in culture medium into A549 cells could not be confirmed using TEM (3.4.4.4) and as described in 3.4.1, HiPco® SWCNT remain bundled following DPPC dispersion. Alternatively, dispersion using DPPC may lead to increased bioavailability of transition metal residues and other impurities present in SWCNT samples, as described in Chapter 2, 2.3.4.3 that can promote Fenton and Haber-Weiss reactions leading to increased ROS formation. However, although HiPco® SWCNT contain significantly larger amounts of metal impurities, no correlation between the cellular response and metal content was observed.

Furthermore, it has been shown that catalyst residues are usually entrapped within SWCNT, completely surrounded by carbon structures and may therefore not influence particle toxicity [227]. The particulate matter content of chemicals has been correlated with their capability to induce oxidative stress in bronchial epithelial cells [22]. This organic particulate matter may synergize with transition metals in ROS generation [329]. ArcD produced SWCNT contain greater residues of amorphous carbon which may lead to increased toxicity compared to HiPco® SWCNT in the presence of DPPC (Figure 5.5). In terms of factor increase, ArcD SWCNT have a significantly larger effect than HiPco® SWCNT on the NHBE cells indicating that the amorphous carbon residues contribute significantly within the better dispersed samples. However, this is not seen to be the case for the A549 cells.

In addition, DPPC can alter the surface chemistry of the particles and ultimately influence their toxicity [55, 69, 330]. Alternatively, phospholipids might be modified by free radicals [55]. This may explain the increase in intracellular ROS following H_2O_2 exposure in the presence of DPPC as the degree of dispersion or sample contaminants would not be a factor here.

Furthermore, as a surfactant, DPPC forms micellar structures through their interaction with the particles. Therefore, it could be hypothesised that while "unstructured" DPPC may not affect cell responses, changes in the arrangement of hydrophilic and hydrophobic regions of DPPC molecules due to the presence of particles may render it more toxic. In the case of silica toxicity, DPPC has been used as protective agent, inhibiting toxicity by particle coating [55, 277, 331, 332]. However, it did not have a protective effect on chrysotile asbestos toxicity [277].

Cells of primary origin, such as NHBE cells, are generally regarded as being more sensitive than carcinoma cell lines as represented by A549 cells [333, 334]. This may explain why NHBE cells reacted more sensitively to DPPC dispersion than A549 cells. The fact that A549 cells are surfactant producing alveolar type II cells may also play a role.

5.6 Conclusion

This study illustrates that *in vitro* exposure of lung epithelial cells to carbon nanomaterials results in only moderate or low oxidative stress under the exposure conditions employed. However, ROS production as a result of carbon nanomaterial exposure was seen to be always higher compared to asbestos exposure. Cell responses seem to strongly depend on the vehicle used for particle dispersion. Whereas interaction with DPPC appears to alter the particles making them more reactive, leading to higher ROS formation within the cells, the presence of FBS seem to protect the cells from any oxidative insult. These findings may be of interest for occupational health risk assessment but also biomedical applications of the particles tested.

It has to be kept in mind that the carboxy-DCFDA assay is limited regarding the types of ROS it can detect. Therefore, in order to obtain a full picture of oxidative stress within exposed cells, further assays would need to be carried out including further endpoints such as production of superoxide, lipid peroxidation products or catalase dependent hydrogen peroxides.

Given that there is an increase in intracellular ROS in the presence DPPC dispersed SWCNT, it would be of interest whether these particles are also able to deplete antioxidants leading to a tier 2 response which would be characterised by an increase in inflammatory mediator release as described in Chapter 2, 2.2.4.3, Figure 2.3. This will be explored in the following chapter.

Chapter 6

Effects of SWCNT on inflammatory mediator response

This chapter is based on the following publication:

SWCNT suppress inflammatory mediator responses in human lung epithelium *in vitro*

Eva Herzog, Hugh J. Byrne, Alan Casey, Maria Davoren, Anke-Gabriele Lenz, Konrad L. Maier, Albert Duschl, Gertie Janneke Oostingh

Toxicology and Applied Pharmacology, accepted on 29th October 2008

doi:10.1016/j.taap.2008.10.015

6.1 Chapter summary

This study was carried out in order to evaluate the inflammatory response of immortalised and primary human lung epithelial cells (A549 and NHBE) to SWCNT. Special focus was placed on the mediating role of lung surfactant on particle toxicity. The toxicity of SWCNT dispersed in cell culture medium was compared to that of nanotubes dispersed in DPPC. Exposure was carried out for 6 to 48 h with the latter time-point showing the most significant responses. Moreover, exposure was performed in the presence of the pro-inflammatory stimulus TNF-α in order to mimic exposure of immunologically stimulated cells as would occur during infection or in the presence of chronic inflammation. Therefore, evaluating the effects of SWCNT exposure on LPS- or TNF-α induced cells may give an indication as to whether there are cellular states that are more susceptible to SWCNT toxicity compared to normal, healthy cell conditions and whether the presence of an infection or chronic inflammation may give rise to increased particle toxicity.

Endpoints evaluated included cell viability, proliferation and the analysis of inflammatory mediators such as IL-8, IL-6, TNF-α and MCP-1. Crocidolite asbestos was included as a well characterised, toxic fibre control. The results of this study showed that HiPco® SWCNT samples suppress inflammatory responses of A549 and NHBE cells. This was also true for TNF-α stimulated cells. The use of DPPC improved the degree of SWCNT dispersion in A549 medium and in turn, led to increased particle toxicity. However, it was not seen to modify NHBE cell responses.

6.2 Introduction

As SWCNT were seen to elicit an oxidative stress response in both A549 and NHBE cells, this study aimed to investigate whether particle exposure may also affect inflammatory mediator release. Lung epithelium plays a key role in the modulation of inflammatory processes by releasing inflammatory cytokines such as MCP-1, IL-8, IL-6 and TNF-α [15, 16] which were therefore included as endpoints for this study.

As SWCNT have been shown to interact with proteins (Chapter 4, 4.4.1.5) it is essential to investigate whether such interactions are taking place between SWCNT and the studied proteins including IL-8, IL-6, TNF-α and MCP-1. Adsorption of these proteins onto SWCNT surfaces may have consequences for SWCNT toxicity itself and could also lead to false positive results within protein analysis.

In addition to the inflammatory mediator response, cell viability measurements were carried out with the aim of confirming the absence of cytotoxicity within the SWCNT concentration range tested and in order to assess the influence of DPPC dispersion of SWCNT on this endpoint.

Inflammatory mediator responses were measured following cell exposures to HiPco® SWCNT as this SWCNT type appeared to be most effective in inducing intracellular ROS (Chapter 5, 5.4.2). As crocidolite asbestos exposure was reported to affect cell signalling cascades including inflammatory responses as described in Chapter 2, 2.3.4.2 and illustrated in Figure 2.8, it was again included as control particle.

It is believed that responses to nanomaterial exposure of individuals with pre-existing diseases may induce exacerbation of respiratory effects due to inflammation and oxidative stress [145, 335-337] and it has been proposed that bacterial products such as LPS associated with particles may have stimulatory effects on the cytokine production of macrophages [338]. There are also reports of diesel particles having suppressive or synergistic effects on LPS- or TNF-α-induced cytokine production [339-341]. Therefore, TNF- α and LPS-stimulated cells were used as a model for the presence of chronic inflammation as seen for conditions such as cancer [342, 343], respiratory diseases (e. g. asthma, chronic obstructive pulmonary disease (COPD)) [344, 345] and cardiovascular diseases [346]. Therefore, it may aid in the elucidation of particle effects on a more susceptible population.

6.3 Materials and Methods

6.3.1 Cell Culture

A549 and NHBE cells were cultured as described in Chapter 5, 5.3.1.1 and 5.3.1.2, respectively. The A549 reporter-gene cell lines, stably transfected with the promoter-region for IL-8 (A549-IL8), IL-6 (A549-IL6) or TNF-α (A549-TNFα) were obtained from the Department of Molecular Biology, University of Salzburg, Austria. These reporter-gene cells were cultured as previously described by Oostingh *et al.* (2008) using RPMI 1640 supplemented with L-glutamine, penicillin/ streptomycin, and 10% FBS [347]. All cell culture reagents were obtained from PAA Laboratories (Pasching, Austria). A549 cells maintaining a chromosomal integration of a luciferase reporter construct regulated by multiple copies of the NF-κB response elementwere purchased from Panomics (Fremont, USA) and used as described by the distributor.

6.3.2 Test Particles

HiPco® SWCNT and standard reference crocidolite asbestos (UICC) as described in 3.3.1 and 5.3.2 were used as test particles and dispersed and characterised as described in Chapter 5, 5.3.3 and 5.3.4.

From the stock concentrations of 500 µg/ml, working concentrations of 0.195 µg/ml to 50 µg/ml (0.06 µg/cm2 to 15.625 µg/cm^2) were prepared in A549 or NHBE medium by serial dilutions on a 96-multi-well plate. Therefore, despite the use of different multi-well culture dishes compared to ROS analysis, the concentrations were comparable even on the basis of mass per surface area.

For DPPC exposures, dilutions were carried out using the corresponding cell culture medium supplemented with 10% DPPC/PBS so that the DPPC concentration was kept constant at 0.25 mg/ml over the concentration range studied.

6.3.3 Cell exposures

For cell viability, luciferase and protein release assays, cells were seeded in tissue culture treated 96-well plates at a density of $1x10^4$, $5x10^3$, or $2.5x10^3$ cells/well and exposed for 6, 24 and 48 h, respectively. Following seeding, cells were incubated for 24 h to adhere and obtain their normal morphology. Cells were then exposed to SWCNT samples or crocidolite asbestos dispersed in culture medium or DPPC/PBS. Culture medium only or culture medium containing 0.25 mg/ml DPPC/PBS served as negative control media, respectively.

In addition, all exposures were carried out on cells stimulated with recombinant TNF-α (rh-TNF-α; Immunotools) at concentrations ranging between 1 to 150 ng/ml or LPS derived from *Pseudomonas aeruginosa* (LPS-PA) at concentrations of 25 and 50 μg/ml. A rh-TNF-α concentration of 10 ng/ml resulted in optimal cytokine induction of cells and was used as a positive control stimulus.

An overview of all experiments carried out within the course of this study is presented in Table D.1 in Appendix D, including promoter activation and cell viability measurements for the 4 different variants of transfected A549 cell lines (A549, A549-IL-8, A549-IL6, A549-TNF-α, A549-NF-κB), further cell viability

measurements for NHBE and untransfected A549 cells, IL-8, IL-6 and MCP-1 protein release by A549-IL8 cells and IL-8 and IL-6 release by NHBE cells. In all cases, 48 h exposures resulted in more pronounced cell responses compared to 6 or 24 h. Therefore, only results for the 48 h endpoint are illustrated within this chapter. However, a direct comparison between exposure time points illustrated in Appendix D, Figure D.1 to D.10 on the basis of A549-IL8 and NHBE cell viability, A549-IL8 promoter activation and IL-8 release by A549-IL8 and NHBE cells which was identified as representative for all remaining cell responses observed.

6.3.4 Cell viability assay

Cell viability was determined using the resazurin based Cell Titer-Blue® assay (Promega, Madison, USA) according to manufacturer's instructions. Following cell exposure, 20 µl of Cell Titer-Blue® solution were added onto each well and plates incubated for 1.5 h at 37 °C. Fluorescence was then measured at 560 nm emission and 590 nm excitation using a microplate reader (Tecan Infinite® 200, Grödig, Austria).

6.3.5 Luciferase reporter gene assay

Luciferase reporter gene assays were carried out under the same conditions as the cell viability assays. Following cell exposures, the luciferase assay was performed as described by Oostingh *et al.* (2008) [347].

Stable A549 cell clones were cultured in the presence of G418 (0.5 μg/ml final concentration) and were plated out on day one in tissue culture treated 96-well plates at a density of $5x10^3$ cells/ well and left overnight to adhere and obtain their normal morphology (day 2). The different cell lines were treated on day 2 with different rhTNF-α concentrations (1 ng/ml – 150 μg/ml) or left untreated. In addition, rhTNF-α induced cells or those left untreated were incubated with serially diluted amounts of test particles. Following exposure, cell supernatants were removed and 50 μl passive lysis buffer (Promega, Madison, USA) were added to each well according to manufacturer's instructions. After a 10 minute incubation time, the lysed cells (total of 40 μl) were transferred into white 96-well microtiter plates which provide maximum reflection and minimum auto-fluorescence and auto-luminescence. Alternatively, 96-well plates containing lysis buffer were stored for several days at -20 °C in the dark and subsequently processed. The luciferase signal was recorded using a luminometer (Tecan Infinite® 200, Grödig, Austria) following addition of 40 μl freshly prepared luciferin substrate to the lysate. Luciferin substrate was stored at -20 °C in the dark and was prepared as described in Table 6.1.

6

6.3.6 Real-time RT-PCR

For relative quantification of IL-8 gene expression, cells were seeded at a density of $5x10^5$ cells into 12 well plates and were allowed to adhere overnight. Cells were then exposed under submerse conditions to 500 μl of SWCNT suspensions of final concentrations of 0, 1, 10 and 50 μg/ml (0, 0.13 and 6.57 $\mu g/cm^2$) for 1, 6 or 24 h.

Particle load per surface area was therefore lower for mRNA analysis compared to ROS measurements or promoter activation and protein release studies.

Following exposure, A549 cells were lysed using 1% β-mercapto-ethanol in RNeasy lysate (RLT) buffer (Qiagen) and cell solutions were transferred into QIAShredder spintubes (Qiagen). For ribonucleic acid (RNA) isolation and DNA removal, RNeasy Mini Kit (Qiagen) was used according to manufacturer's instructions. DNA was generated using the first-strand cDNA synthesis kit (Amersham, Biosciences) and $pd(N)_6$ as primer.

Quantitative real-time PCR was performed using the Taqman-system and SybrGreen. The SYBR Green dye binds specifically to the minor groove of double-stranded DNA. Fluorescence intensity is measured after each amplification cycle. During PCR, a doubling of template molecules occurs only during the log-linear phase in each cycle. Following every amplification, melting curves have been constructed in order to ensure that primer dimers did not contribute to the fluorescence intensity of the specific PCR product.

Amplification of the housekeeping gene α-enolase served as internal control. Primer sequences used are shown in Table 6.2. The identification of a suitable houskeeping gene together with optimisation of gene efficiencies were carried out by the Clinical Cooperation Group "Inflammatory Lung Diseases" of the Institute of Inhalation Biology at the Helmholtz Zentrum München, German Research Centre for Environmental Health, Gauting, Germany prior to these studies. Gene expression data was normalized using the ratio between the expression of the gene of interest and α-enolase.

Table 6.1: Protocol for luciferin substrate

Luciferin substrate buffer x5 (500 ml)				
Constituent	Company	Product code	Amount	Storage temperature
Tricine	Sigma	T5816	8.96 g/L	RT
Magnesium Carbonate Pentahydrate	Sigma	227668	1.299 g	RT
Magnesium Sulfate	Sigma	246972	0.803 g	RT
EDTA	Serva	11278	0.093 g	RT
Luciferin substrate (150 ml)				
Constituent	Company	Product code	Amount	Storage temperature
DTT	Roche	708992	0.78 g	4°
D-Luciferin sodium salt	Sigma	L9504	0.010 g	-20°
Coenzym A lithium salt	Sigma	C3019	0.03146 g	-20°
ATP	Sigma	02055	0.04434 g	4°
LUC-buffer x5			30ml	RT
H2O			Up to 150 ml mark	RT

6

Table 6.2: Primers were used for mRNA analysis using real-time RT-PCR

Gene	**Primer**	**Base sequence**
Interleukin-8	5'-primer:	5'-ATG ACT TCC AAG CTG GCC GTG GCT-3'
	3'-primer:	5'-TCT CAG CCC TCT TCA AAA ACT TCT C-3'
Cyclooxygenase-2	5'-primer:	5'-GCT TTT TAC CTTTGA CAC CC-3'
	3'-primer:	5' -CTG CTC AAC ACC GGA ATT TT-3'
α-Enolase	5'- primer:	5'-GTT AGC AAG AAA CTG AAC GTC ACA-3'
	3'-primer:	5'-TGA AGG ACT TGT ACA GGT CAG-3'

6.3.7 Enzyme linked immunosorbent assays (ELISA)

Enzyme linked immunosorbent assays (ELISA) were performed to determine whether alterations in promoter activation also correspond to changes in protein secretion. In addition, this method was used to compare the effects on A549 and NHBE cells. ELISAs were performed for the cytokines IL-8, IL-6, TNF-α (Immunotools) and MCP-1 (BenderMed Systems) following particle exposures for 24 or 48 h. Cells were exposed as described for the luciferase assay.

Following coating the 96-well NUNC Maxi-Sorp plates with 50 µl 4 µg/ml capture antibody made up in coating buffer (Table 6.3) overnight, the wells were washed three times with washing buffer (Table 6.4). Fifty microlitre of serially diluted IL-8 standard or 5 times diluted cell culture supernatant in blocking buffer (Table 6.4) were added to the wells and incubated for 2 h at room temperature (RT). Thereafter, the wells were washed again, 50 µl of 2 µg/ml detection antibody in blocking buffer were added to each well and they were incubated for 2 hrs at RT. The wells were washed and 50 µl of 200-times diluted Streptavidin-Horseradish peroxidise (HRP) (Sigma, Wien, Austria) were added to each well. Plates were incubated for 30 minutes at RT and washed again. The signal was developed using 3,3',5,5'-Tetramethylbenzidin (TMB, Sigma, Wien, Austria) and the reaction was stopped using 2 M H_2SO_4. The optical density was analysed on a microplate reader (Tecan Infinite® 200, Grödig, Austria) at 450nm. For validation purposes, a standard curve was constructed for every experiment.

6.3.8 Statistical analysis

Statistical analysis was carried out as described in Chapter 4, 4.3.8.

Table 6.3: ELISA antibodies and supernatant dilutions

Protein	Coating and detection AB	Highest Standard concentration	Supernatant dilution
IL-8	4 µl/ml BD Biosciences (Schwechat, Austria)	10 µg/ml	1:5
IL-6	3 µl/ml BD Biosciences (Schwechat, Austria)	1 ng/ml	1:2
TNF-α	10 µl/ml	10 µg/ml	1:1
MCP-1	4 µl/ml	1 ng/ml	1:2

Table 6.4: Protocol for ELISA buffers

Buffer	Constituents
Coating buffer	0.1 M Na_2CO_3 Adjust to pH 9.5
10x PBS (1 litre)	80g NaCl 2g KCl 14.4g Na_2HPO_4 2.4g KH_2PO_4 Adjust to pH 7.4 using HCl
Washing buffer	10% 10x PBS 0.5% Tween 20 in H_2O
Blocking buffer	1% BSA in washing buffer

6.4 Results and Discussion

6.4.1 Dispersion of HiPco® SWCNT and crocidolite asbestos

As described in Chapter 5, 5.4.1, test particles were suspended in cell culture medium or DPPC/PBS solution and both dispersion methods resulted in a certain degree of agglomeration, leading to cells being exposed to bundles of SWCNT rather than individual fibre shaped tubes. However, the use of DPPC improved HiPco® SWCNT dispersion in A549 culture medium.

6.4.2 Interaction of SWCNT with test systems

As SWCNT have previously been shown to interact with colorimetric indicator dyes such as resazurin as used in the Alamar Blue™ and also Cell Titer-Blue® assays (Chapter 3, 3.4.3), SWCNT were tested for interactions with the unconverted as well as the converted form of the Cell Titer-Blue® dye. A maximum decrease fluorescence of 10% was observed (Figure 6.1) which agrees with previous studies showing only small interactions within the SWCNT concentrations used for this study (3.4.3). In addition, no significant interactions were observed between HiPco® SWCNT and the luciferase signal used as endpoint in the reporter-gene assays (Figure 6.2). Cells were exposed to HiPco® SWCNT for 30 min only before performing the luciferase assay. Within this time period, particles are not able to manifest cellular effects as it is not enough time for protein translation to take place. However, it does allow potential interactions between HiPco® SWCNT and luciferase to take place.

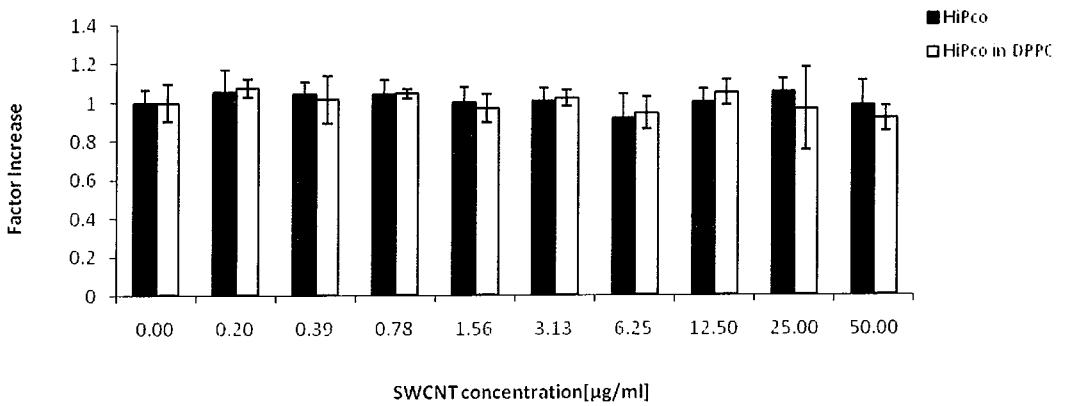

Figure 6.1: Decreases in converted Cell Titer-Blue® fluorescence following incubation with HiPco® SWCNT

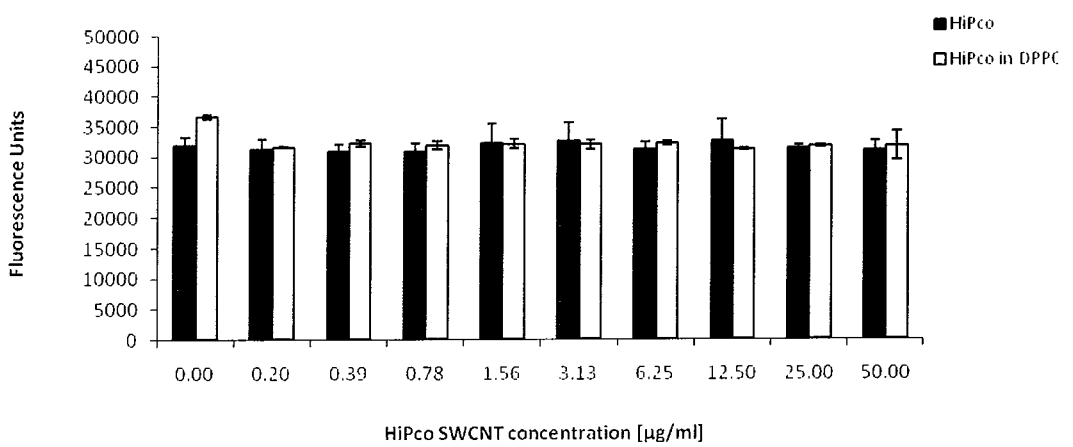

Figure 6.2: Decreases in luciferase signal following incubation with HiPco® SWCNT

Carbon nanomaterials have also been reported to be able to adsorb proteins including cytokines which would therefore not be available for detection using ELISA systems, leading to false results [30, 54, 225, 230, 255, 257]. Therefore, protein standards used for ELISA were incubated with HiPco® SWCNT at 37°C as would occur during cell exposures. No significant decreases in protein concentrations and therefore no interactions were observed for IL-8, IL-6 or MCP-1 proteins independent of DPPC dispersion at the particle concentrations employed in this study. However, it was noted that incubation of culture medium dispersed SWCNT with TNF-α protein standard did result in a 20% decrease in protein concentration (Figure 6.3) suggesting TNF-α protein adsorption by SWCNT.

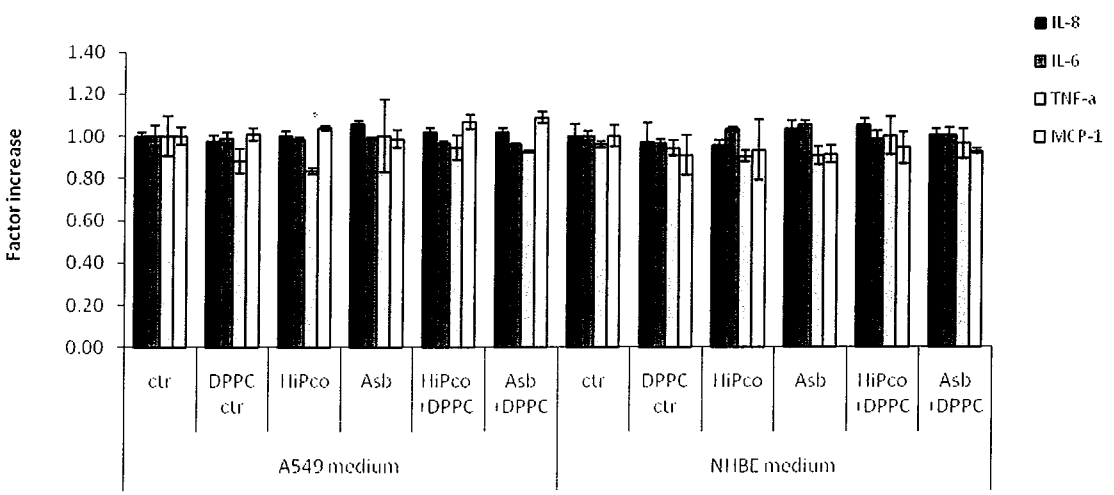

Figure 6.3: Decreases in IL-8, IL-6, TNF-α and MCP-1 protein concentration following incubation with HiPco® SWCNT (50 μg/ml).

6.4.3 Effects of HiPco® SWCNT and asbestos exposure on viability of lung epithelial cells

To assess whether any effects on inflammatory mediator releases were due to decreased cell viability, the resazurin-based Cell Titer-Blue® assay was carried out in parallel with all assays. Exposure of A549-IL8 and NHBE cells to culture medium dispersed SWCNT for up to 48 h at the concentration range tested did not result in any reduction of cell viability (Figure 6.4; Figure 6.5). The same was true for exposure over 6 or 24 h (Appendix D, Figures D.1 and D.3). In contrast, a dose-dependent increase in Cell Titer-Blue® fluorescence over control cells was observed for some exposure conditions which would indicate increased cell viability (Figure 6.4a; Figure 6.5a). This agrees with the effects described in Chapter 3 and Chapter 4, showing no cytotoxicity of A549 cells at concentrations up to and including 50 μg/ml HiPco® SWCNT. Cells stimulated with rhTNF-α showed the same effects (Figure 6.4a and Figure 6.5b). Therefore, any effects on inflammatory mediator response upon SWCNT exposure would not be due to loss of cell viability. However, significant cytotoxic effects were seen for A549-IL8 cells exposed to DPPC dispersed SWCNT. NHBE cells did not show a loss in viability under any exposure condition (Figure 6.5a).

Exposure of A549-IL8 or NHBE cells to asbestos for 48 h resulted in some loss of cell viability of up to 20%. No differences between culture medium and DPPC dispersion was observed for non-stimulated cells (Figure 6.4b, Figure 6.5b).

Cell viability observed for A549 cells transfected with the IL-6 promoter construct (A549-IL6) correlated well with A549-IL8 cell responses showing a slightly more

sensitive response. In contrast, A549-TNFα cells appeared significantly more sensitive, particularly to DPPC exposure. Therefore, transfection with the TNF-α promoter construct and clonal expansion might have resulted in significant changes on the gene level so that this cell line was not able to represent A549 cells anymore. Therefore, this cell line was not included in any further assessments.

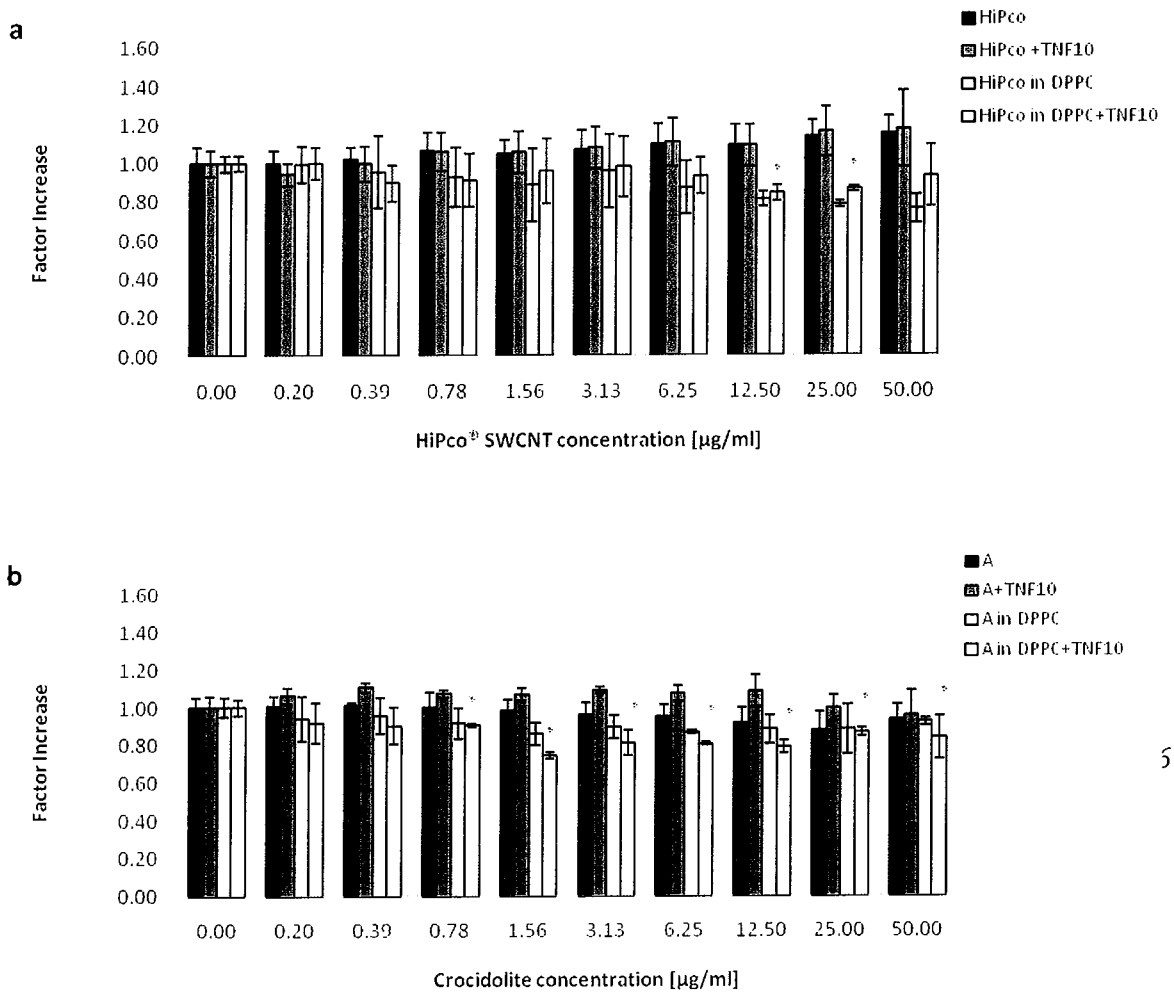

Figure 6.4: Cell viability of A549-IL8 cells following 48 h exposure to (a) HiPco® SWCNT and (b) crocidolite asbestos dispersed in A549 medium or DPPC in the presence or absence of stimulation with 10 ng/ml rh-TNF-α as measured using the Cell Titer-Blue® assay. * Denotes a significant difference from the control ($p \leq 0.05$).

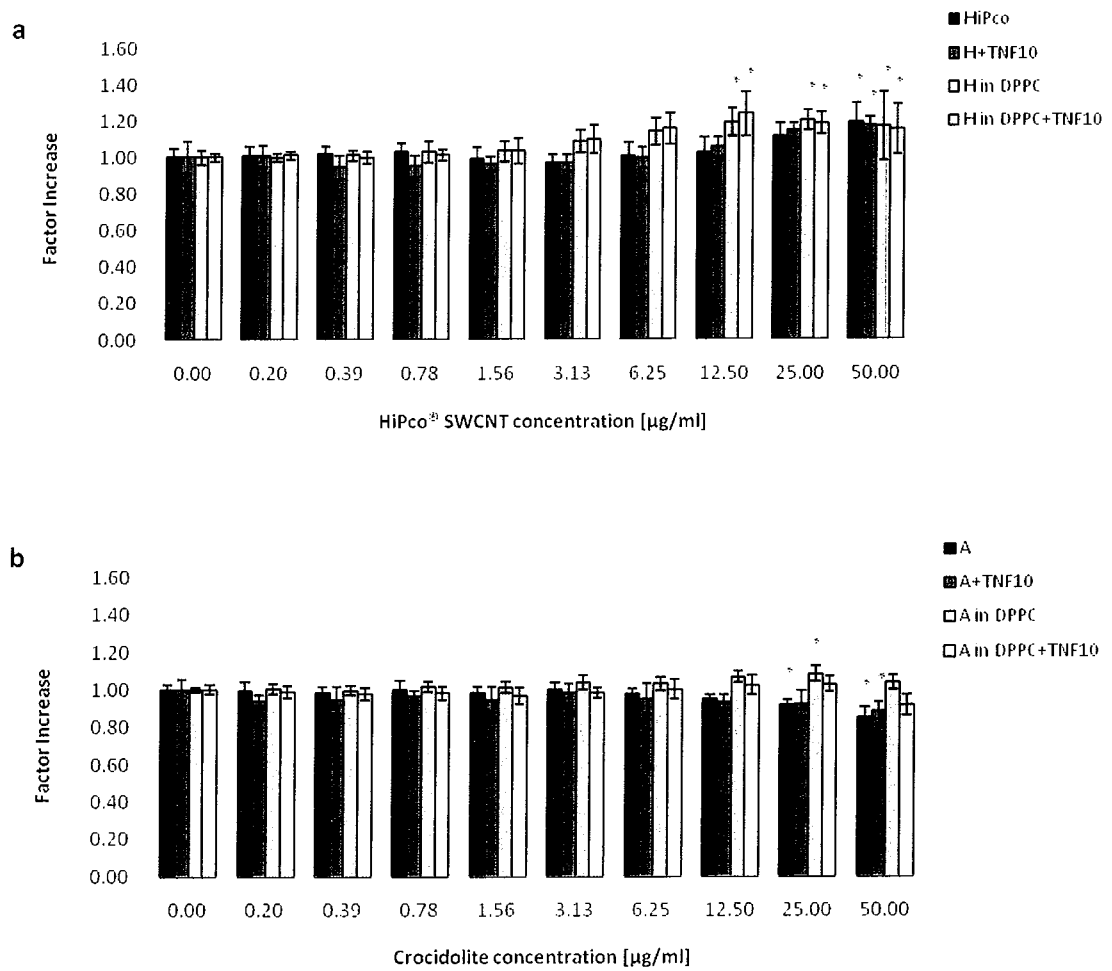

Figure 6.5: Cell viability of NHBE cells following 48 h exposure to (a) HiPco® SWCNT or (b) crocidolite asbestos dispersed in NHBE medium or DPPC in the presence or absence of stimulation with 10 ng/ml rh-TNF-α as measured using the Cell Titer-Blue® assay. * Denotes a significant difference from the control ($p \leq 0.05$).

The activation of A549-NF-κB cells was assessed following 6 h exposure. Following this exposure period, no significant decrease in cell viability was observed under any exposure condition.

6.4.4 Effects of positive control stimuli

Human recombinant TNF-α was used as positive control stimulus for A549 and NHBE cells. As can be seen in Figure 6.6, A549-IL8 cells were stimulated using rhTNF-α concentrations of 1, 10, 100 and 150 ng/ml leading to increases in IL-8 promoter activation by a factor ranging between 6.6 and 20. As 10 ng/ml rhTNF-α did result in medium promoter activation (Figure 6.6), it was selected as the concentration for further stimulations. Following further 24 h stimulation with 10 ng/ml rhTNF-α, promoter activation was reduced down to a factor of around 8 (Figure 6.7). Therefore stimulation was more pronounced following 24 compared to 48 h incubations with rhTNF- α. At the same time, there was no reduction in cell viability for any of the cell lines tested as shown for A549-IL8 in Appendix D, Figure D.4. The effects of rhTNF-α stimulation on A549 cells transfected with the IL-6 and the TNF-α promoter construct are shown in Figure 6.8. As demonstrated, 10 ng/ml rhTNF-α was able to stimulate promoter activation in all three cell lines. Highest stimulations were observed for A549-IL8 cells followed by A549-IL6 and A549-TNFα.

Exposure to rh-TNFα also induced the release of inflammatory proteins by A549 and NHBE cells (Figure 6.9; Figure 6.10). A concentration of 10 ng/ml rh-TNF-α resulted in medium stimulation of IL-8 protein release (Figure 6.9) as was seen for promoter activation of A549-IL8 cells (Figure 6.6). However, in contrast to the effects on promoter activation, protein release was higher following 48 h exposures compared to 24 h exposures (Figure 6.10). Again, IL-8 was the endpoint stimulated most by rhTNF-α.

The use of LPS-PA was significantly less effective in stimulating promoter activation of A549 cells. Increases in IL-8 promoter activation by a factor of only 1.3, 1.7 and 2.2 were measured following 6, 24 and 48 h exposures, respectively (Figure 6.11a). Increases by a factor of only 1.1 to 1.3 were observed for IL-8 protein release (Figure 6.11b).

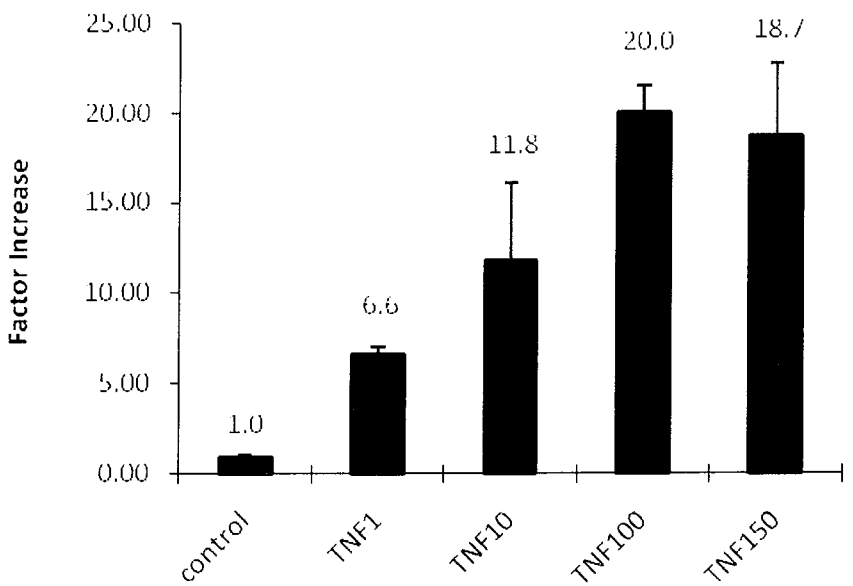

6

Figure 6.6: Effects of rh-TNF-α [ng/ml] on IL-8 promoter activation following 24 h exposure of A549-IL8 cells.

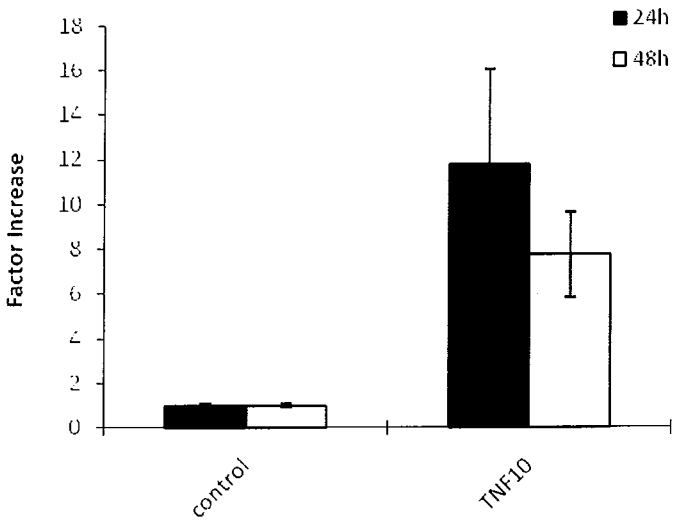

Figure 6.7: IL-8 promoter activation following 24 and 48 h exposure of A549-IL8 cells to 10 ng/ml rh-TNF-α.

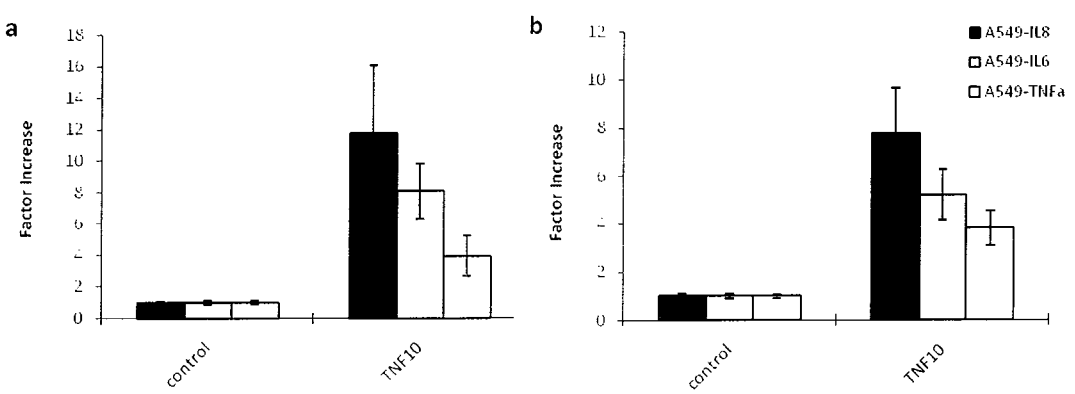

Figure 6.8: Effects of rh-TNF-α stimulation on promoter activation of A549-IL8, A549-IL6 and A549-TNFα cells following (a) 24 and (b) 48 h exposures.

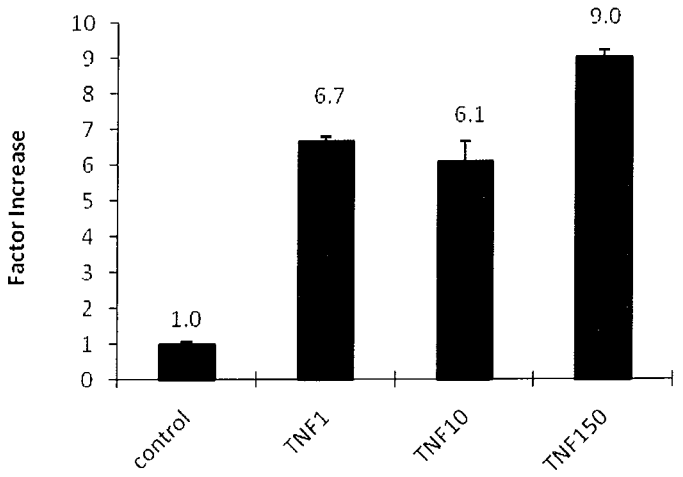

Figure 6.9: **Effects of rh-TNF-α [ng/ml]on IL-8 protein release following 24 h exposure of A549-IL8 cells.**

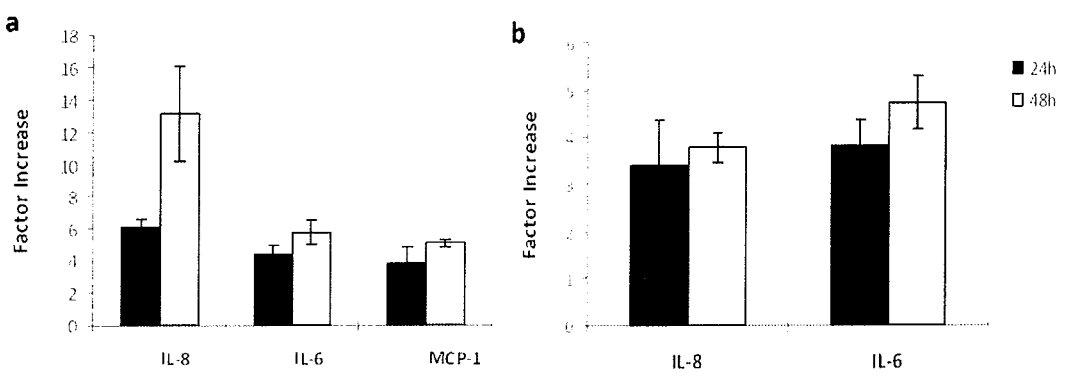

Figure 6.10: Factor increase in IL-8, IL-6 and MCP-1 protein release by (a) A549 and (b) NHBE cells following 24h and 48h exposure to 10 ng/ml rh-TNF-α.

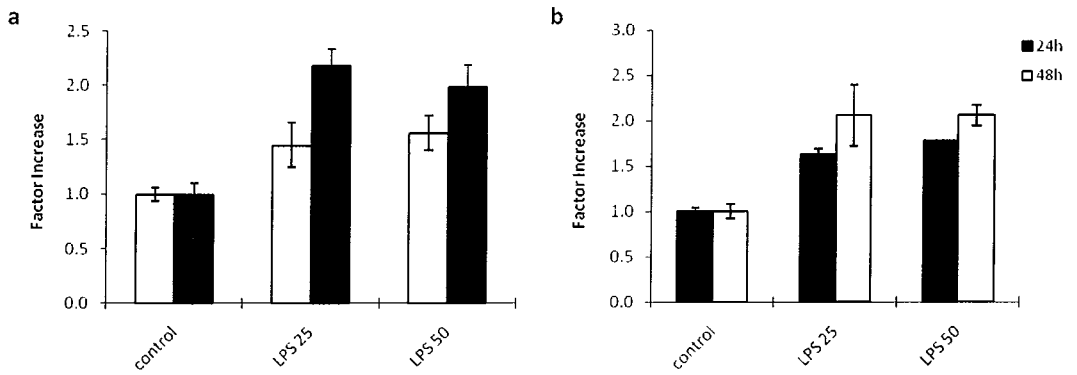

Figure 6.11: (a) IL-8 promoter activation and (b) IL-8 protein release by A549-IL8 cells following 24 and 48 h exposure to LPS-PA at concentration of 25 μg/ml (LPS25) and 50 μg/ml (LPS50).

6.4.5 Effects of HiPco® SWCNT exposure on selected inflammatory mediators

One of the main objectives of this study was to address the question of whether SWCNT exposure has the potential of modulating the immunological response of lung epithelial cells. The release of inflammatory mediators upon particle exposure, as described in Chapter 2, 2.2.4.2, has been frequently used to discriminate between pathogenic and non-pathogenic particles [348]. In order to analyse immunological responses caused by particle exposure, stable transfected A549 cells containing the promoter regions for the cytokines IL-8 or IL-6 were used as a screening tool.

6.4.5.1 *Effects of HiPco® SWCNT exposure on A549 promoter activation*

Using A549-IL8 reporter gene cells, it was observed that 48 h exposure of cells to HiPco® SWCNT resulted in a dose- and time-dependent reduction in IL-8 promoter activation as measured by decreased luciferase activity reaching levels of only 64% compared to control cells with significant decreases starting at 12.5 μg/ml (Figure 6.12a). This effect was time-dependent and was most pronounced following 48 h compared to 6 and 24 h (Appendix D, Figure D.5).

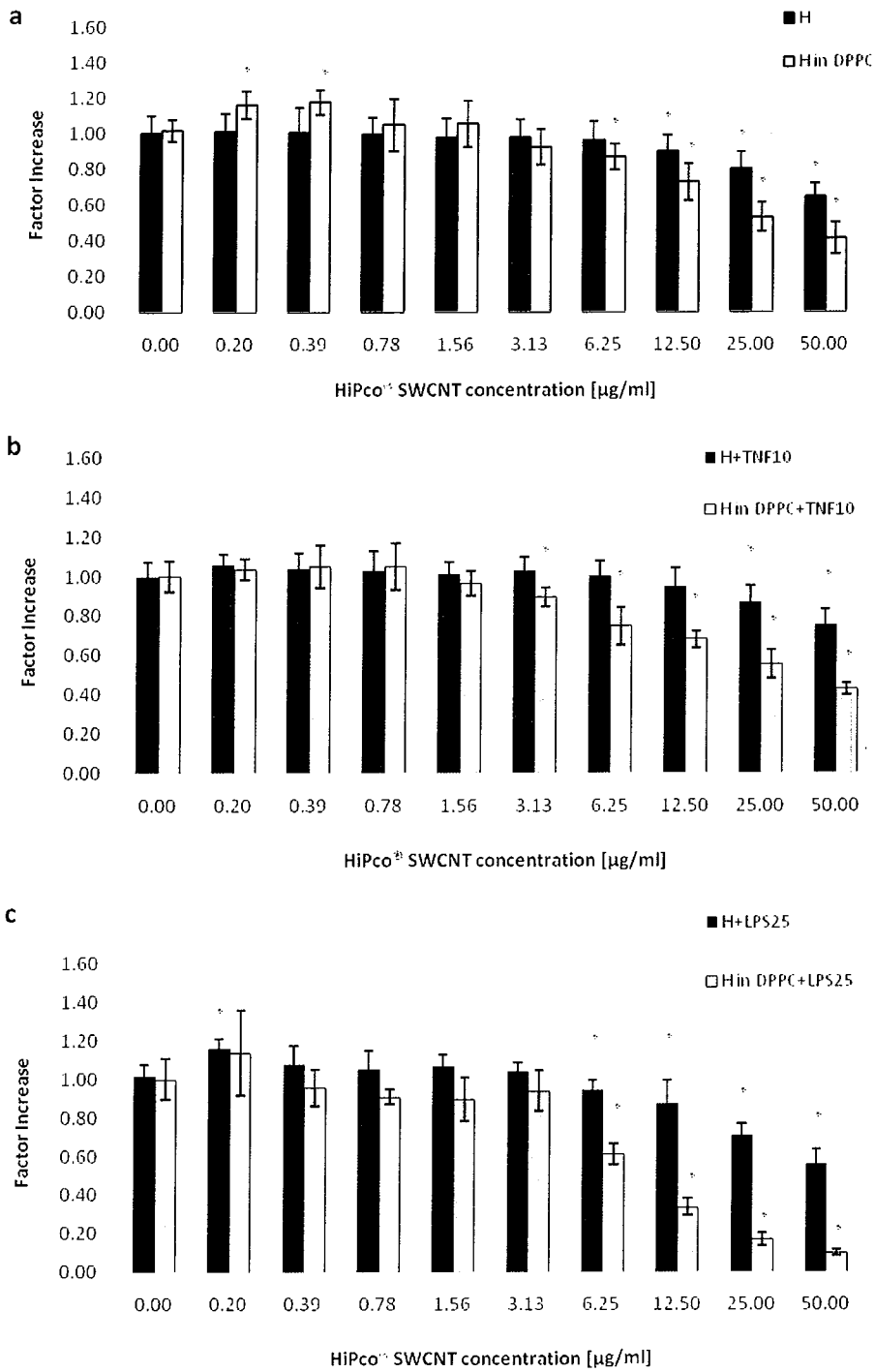

Figure 6.12: IL-8 Promoter activation of A549-IL8 reporter gene cells following 48 h exposure to HiPco® SWCNT with or without DPPC dispersion as measured by luciferase assay. (a). no stimulation, (b). stimulation with rh-TNF-a, (c). stimulation with LPS-PA. * Denotes a significant difference from the control ($p \leq 0.05$).

In addition to the IL-8 promoter, effects on the IL-6 promoter and NF-κB activity were investigated using IL-6 and NF-κB reporter-gene systems. As seen for IL-8, IL-6 promoter activity was decreased following HiPco® SWCNT exposure in a dose- and time-dependent manner with 48 h exposures resulting in the most pronounced effects.

Activity of the NFκB transcription factor was assessed following 6 h exposure as recommended by Oostingh *et al.* (2008) [347]. No effects were observed for HiPco® SWCNT exposure.

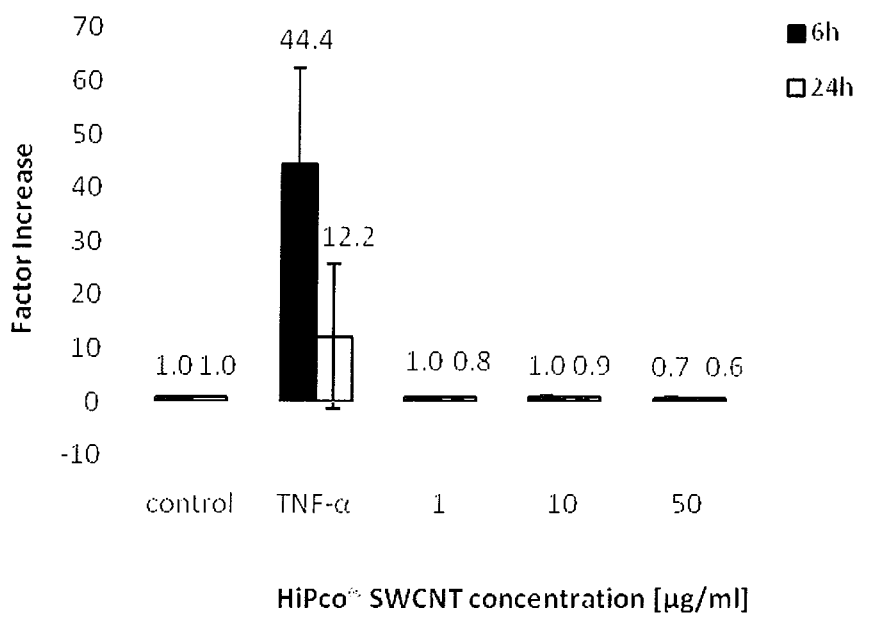

Figure 6.13: Factor increase in IL-8 mRNA expression following 6 and 24 h exposure to HiPco® SWCNT as measured using real-time RT-PCR.

6.4.5.2 *Effects of HiPco® SWCNT exposure on gene expression*

Real time RT-PCR was used to confirm the effects observed and it was shown that not only was the IL-8 promoter activation inhibited by SWCNT exposure but also IL-8 mRNA in A549 cells decreased following 6 and 24 h exposures (Figure 6.13). In contrast, rhTNF-α exposure led to increases of up to 45 and 16 fold for 6 and 24 h, respectively. This confirms that the luciferase reporter-gene cell-system used in this study is an adequate test method and as it represents a more suitable system for screening purposes, it was preferred to mRNA analysis for further investigations within the context of this study.

6.4.5.3 *Effects of HiPco® SWCNT exposure on protein release*

In parallel to promoter activation of the IL-8 and IL-6 gene, IL-8 and IL-6 protein release was measured using ELISA. Since transfection was most effective and cell performance seemed to be best for A549-IL8 cells compared to A549-IL6 and A549-TNF-α cells, A549-IL8 cells were used for protein analysis. As seen using reporter-gene systems, IL-8 decreased time- and dose-dependently following HiPco® SWCNT exposure (Appendix D, Figure D.6a). Following 48 h exposure, decreases of up to 40% were observed (Figure 6.14a). On the one hand, this confirms the effects seen using reporter gene assays and furthermore, it shows that the particles were also effective on the level of protein production of the cells.

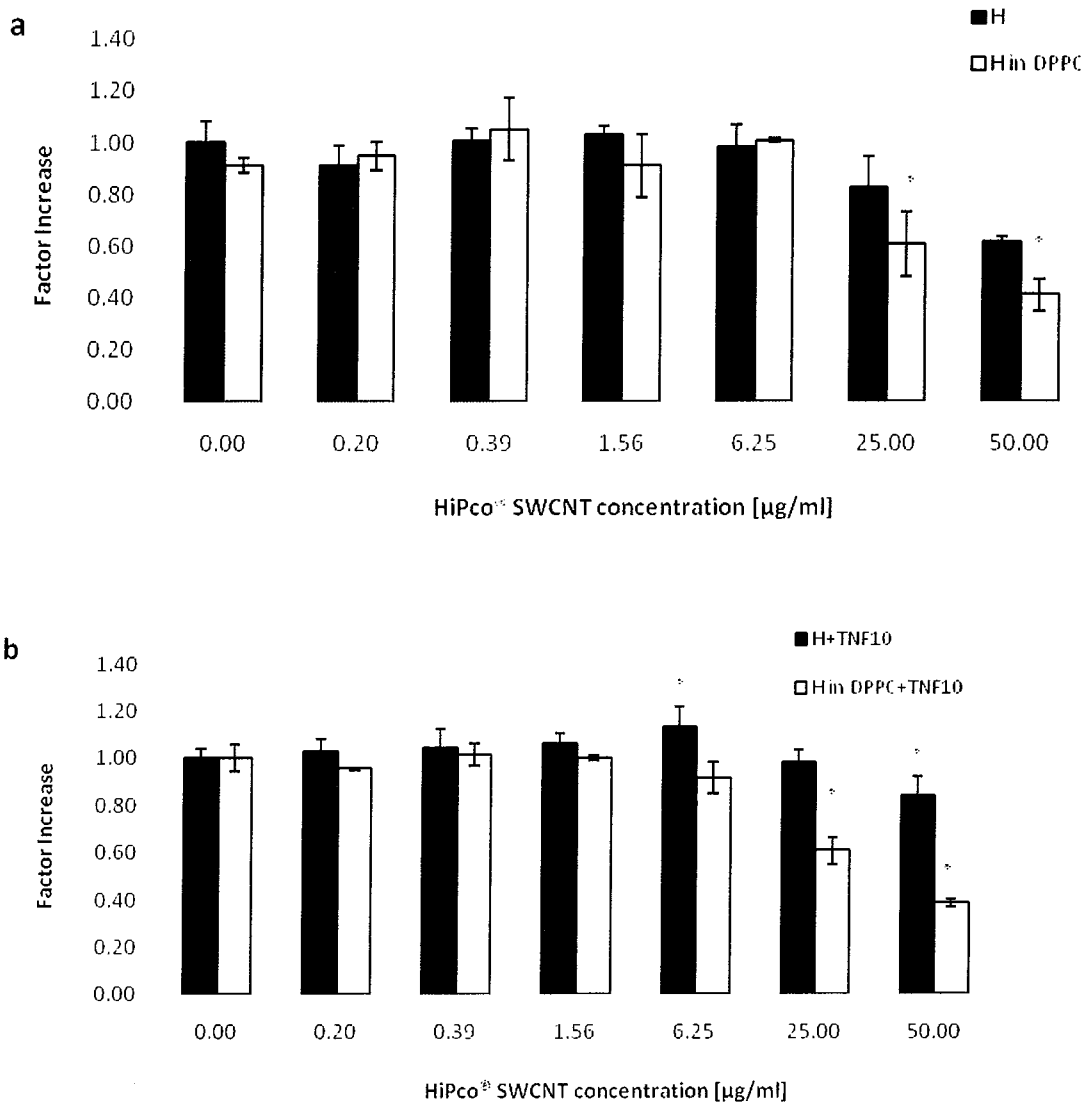

Figure 6.14: IL-8 protein release following 48 h exposure to HiPco® SWCNT dispersed in culture medium or DPPC of (a) unstimulated A549 cells and (b) cells stimulated with rh-TNF-α (b) as measured using ELISA. * Denotes a significant difference from the control ($p \leq 0.05$).

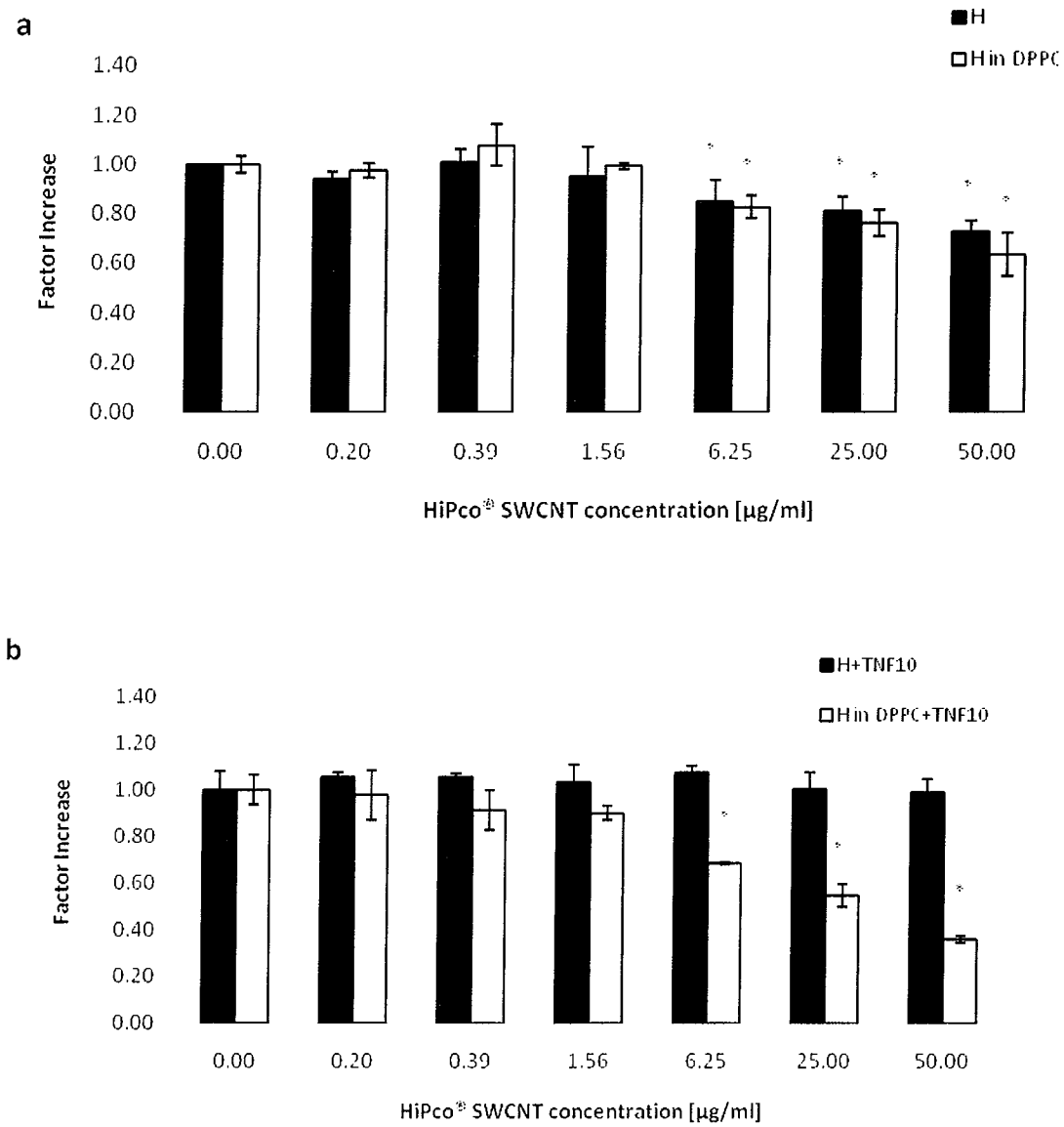

Figure 6.15: IL-6 protein release following 48 h exposure to HiPco® SWCNT dispersed in culture medium or DPPC of (a) unstimulated A549 cells and (b) cells stimulated with rh-TNF-α as measured using ELISA. * Denotes a significant difference from the control ($p \leq 0.05$).

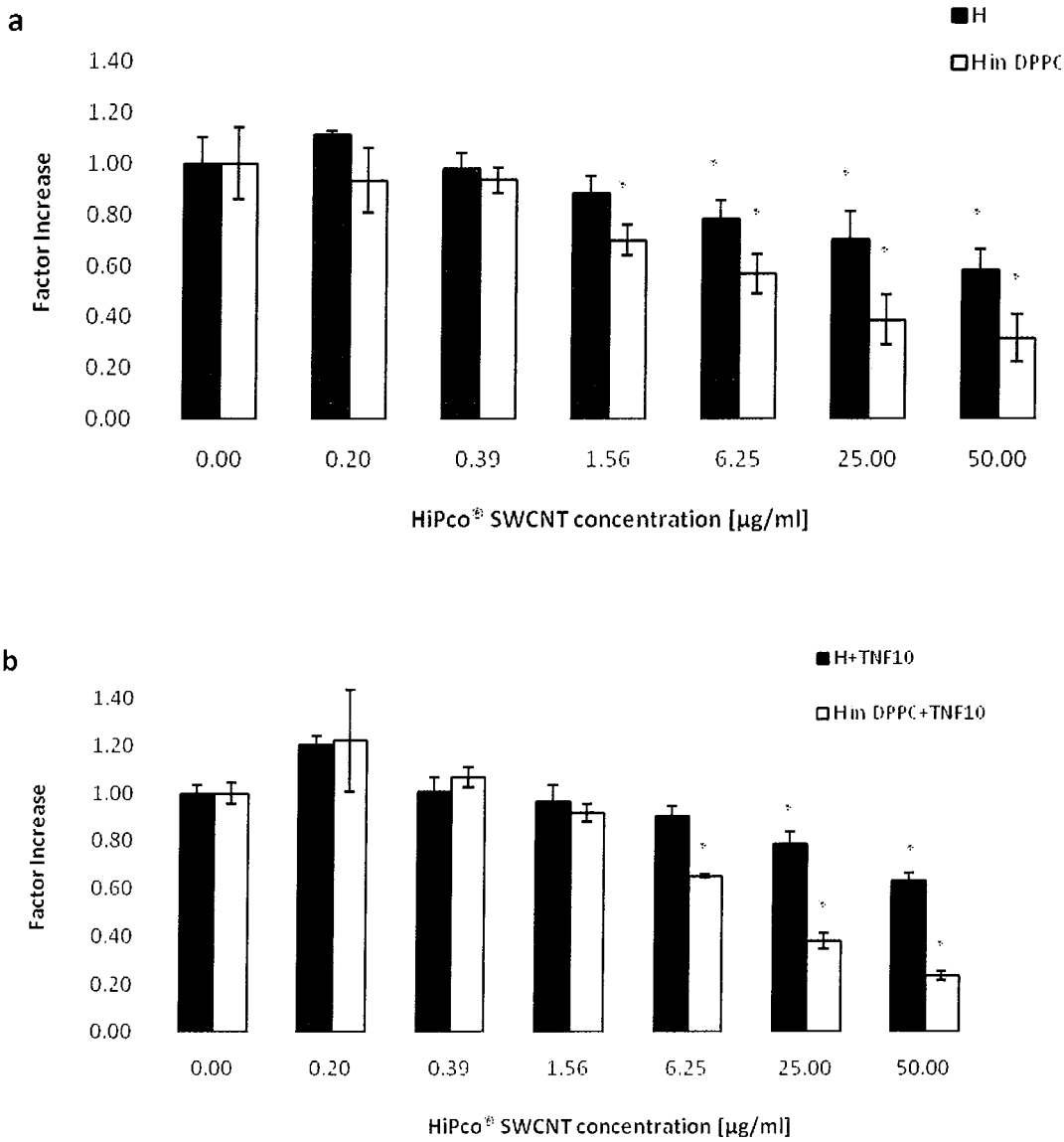

Figure 6.16: MCP-1 protein release following 48 h exposure to HiPco® SWCNT dispersed in culture medium or DPPC of (a) unstimulated A549 cells and (b) cells stimulated with rh-TNF-α as measured using ELISA. * Denotes a significant difference from the control ($p \leq 0.05$).

The release of IL-6 also decreased in a dose- and time dependent manner. Following 48 h, decreases in IL-6 protein release of 27% were observed following exposure to culture medium dispersed nanotubes in the absence of rh-TNF-α stimulation (Figure 6.15a).

Levels of TNF-α protein release in A549 cells remained below detection limits of the test system and were therefore not determined with the ELISA system used. Instead, MCP-1 was included as a further endpoint and results for A549 cells are shown in Figure 6.16. The release of this protein appeared to be more sensitive when compared to IL-8 and IL-6 and following 48 h exposure as MCP-1 levels were reduced by more than 40% (Figure 6.16a). Overall, these reductions in protein release observed agree with studies by Witzmann and Monteiro-Riviere (2006) who also reported downregulation of proteins following exposure of human keratinocytes to MWCNT [224].

6.4.5.4 *Effects of HiPco® SWCNT on protein release of NHBE cells*

In parallel to exposures carried out on A549 cells, the normal bronchial epithelial cell line NHBE was used to assess the effects of particle exposure on primary cells as this may be considered a more relevant model to mimic human exposure. Just like A549 cells, NHBE cells decreased IL-8 and IL-6 release when exposed to increasing concentrations of HiPco® SWCNT and effects were more pronounced following 48 h compared to 24 h (Appendix D, Figure D.8).

When NHBE cells were exposed to SWCNT, IL-8 and IL-6 were reduced by 22% and 36%, respectively, following 48 h exposure (Figure 6.17a and Figure 6.18a). Levels of TNF-α and MCP-1 protein remained below detection limits and could therefore not be analysed. Overall, the responses of A549 and NHBE cells to culture medium dispersed SWCNT did not differ significantly.

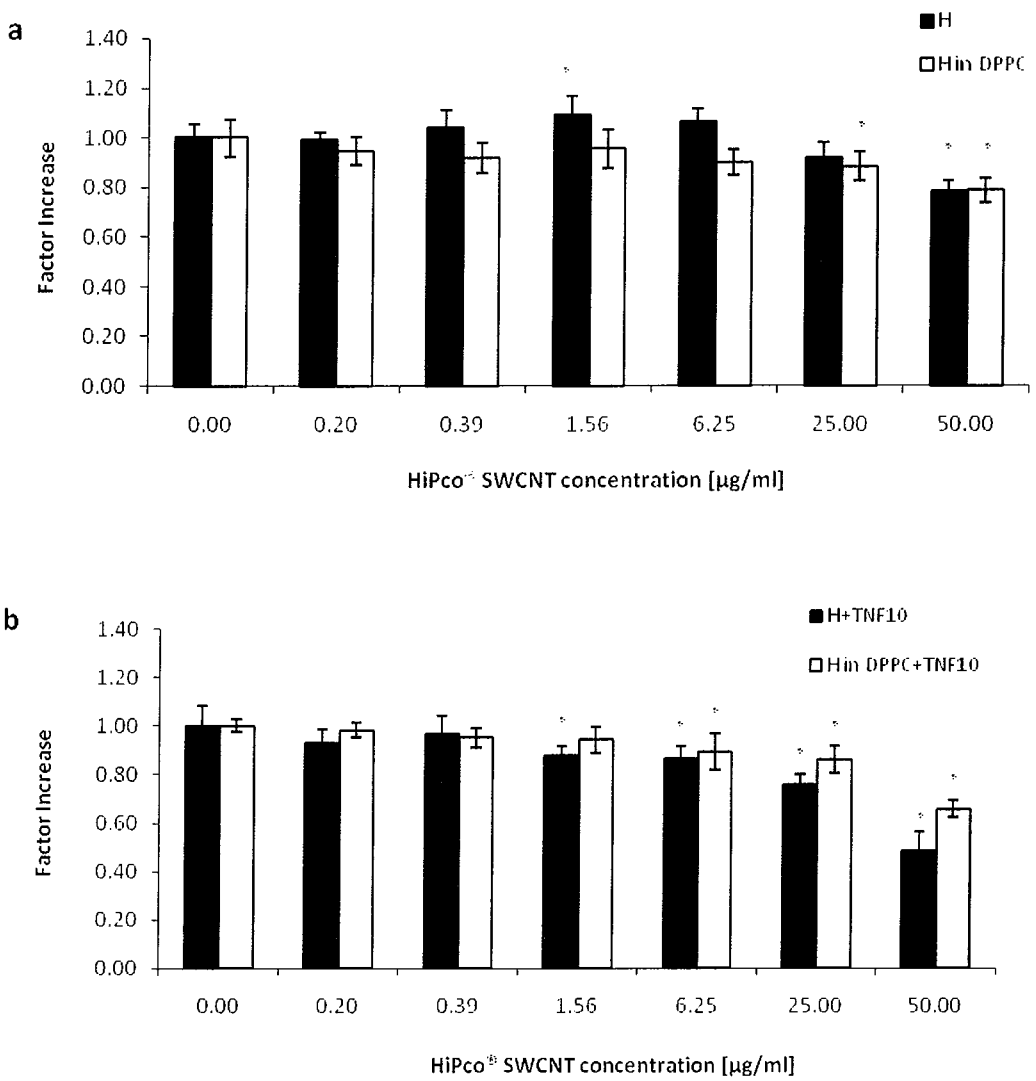

Figure 6.17: IL-8 protein release following 48 h exposure to HiPco® SWCNT dispersed in culture medium or DPPC by (a) un-stimulated NHBE cells or (b) cells stimulated by rh-TNF-α as measured by ELISA. * Denotes a significant difference from the control ($p \leq 0.05$).

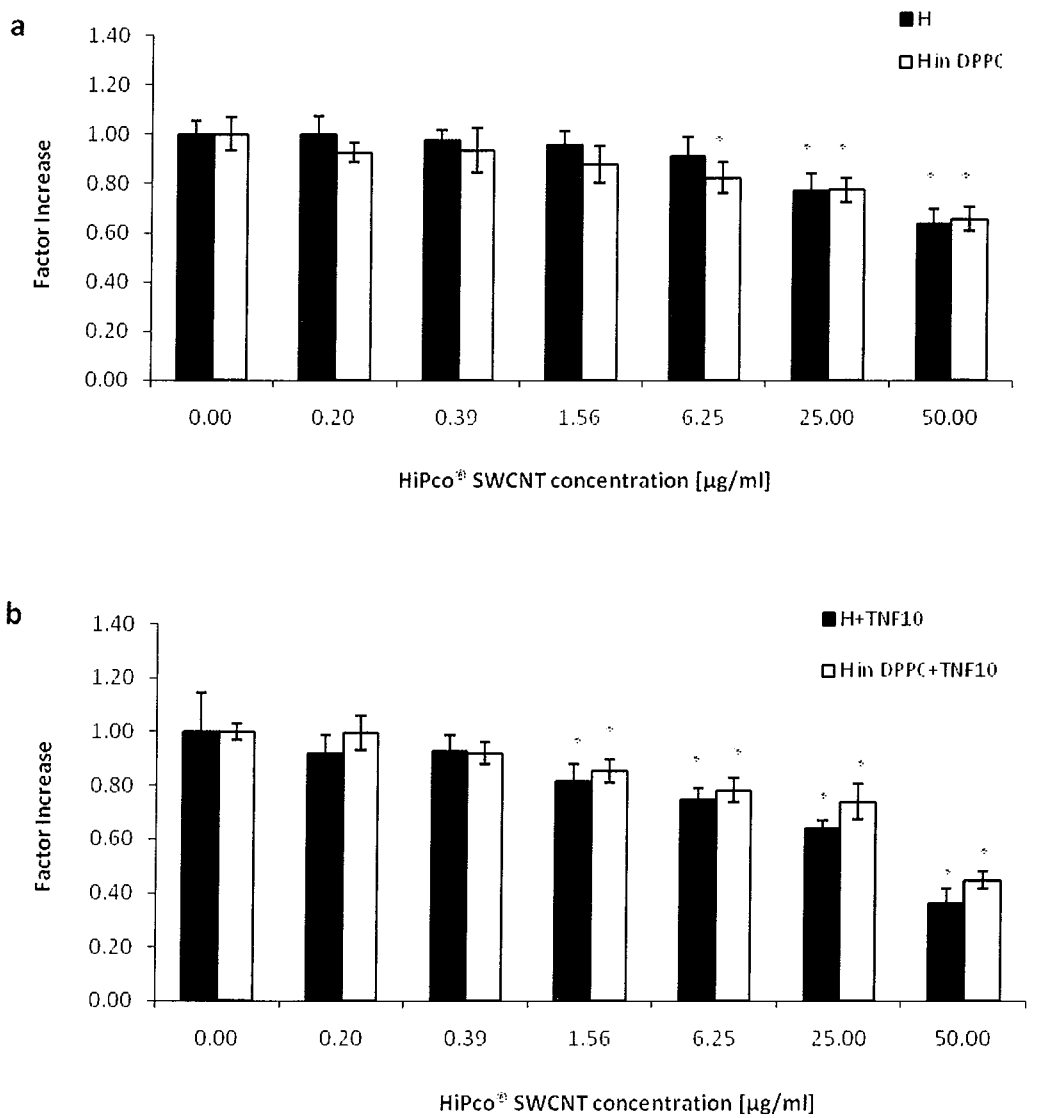

Figure 6.18: IL-6 protein release following 48 h exposure to HiPco® SWCNT dispersed in culture medium or DPPC by (a) un-stimulated NHBE cells or (b) cells stimulated by rh-TNF-α as measured by ELISA. * Denotes a significant difference from the control ($p \leq 0.05$).

No reductions in cell viability were found following exposure to cell culture medium dispersed SWCNT (Figure 6.4; Figure 6.5). Furthermore, there were no significant interactions between SWCNT and the test systems employed within the concentration range tested. This demonstrates that under the conditions employed, culture medium dispersed HiPco® SWCNT exposure results in the suppression of inflammatory mediator response of A549 and NHBE cells which would indicate that epithelial cells do not elicit an inflammatory alarm response upon SWCNT exposure. Suppression of inflammatory mediator responses by SWCNT would agree with studies by Shvedova *et al.* (2008) who observed increased bacterial infectivity *in vivo* and decreased bacterial uptake and clearance *in vitro* in mice exposed to SWCNT followed by induction of a pulmonary infection [181]. It also further confirms that the particles are not significantly contaminated with LPS which would otherwise lead to inflammatory activation.

6.4.6 Effects of crocidolite asbestos exposure on selected inflammatory mediators

Asbestos exposure has been linked to asbestosis, lung cancer and malignant mesothelioma of the pleura [349]. In a recent study by Poland *et al.* (2008) it was shown that long multi-walled carbon nanotubes (MWCNT) can result in asbestos-like pathogenic behaviour including inflammation and granuloma formation following direct exposure of the mesothelial lining of the body cavity of mice [201]. Similar to asbestos, SWCNT can have a large aspect ratio, consisting of long, thin fibres with aerodynamic characteristics that allow them to be inhaled deeply into

the lungs. Therefore, the second question to be addressed within this study was whether the response seen following SWCNT exposure resembles that of asbestos.

Reporter-gene cell assays and ELISA revealed comparable data. Illustrated are data from protein analysis as this endpoint seemed to result in lower data variability. Data of IL-8 promoter activation are illustrated in Appendix D, Figure D.6. As seen following SWCNT exposure, effects on promoter activation and protein release were augmented following 48 h compared to shorter exposure periods (Appendix D, Figure D.6 and Figure D.8). Therefore, 48 h results on protein release are shown.

When A549 cells were exposed to asbestos, decreases could only be measured for MCP-1 protein release which was inhibited by up to 40% (Figure 6.21a). The same decrease in MCP-1 was seen following SWCNT treatment. In contrast to the effects of SWCNT, IL-8 and IL-6 protein levels slightly increased following culture medium dispersed asbestos exposure (Figure 6.19a and Figure 6.20a). In NHBE cells, small decreases of up to 11% were seen for IL-8 and no effect was seen for IL-6 (Figure 6.22a and Figure 6.23a)

Due to the reductions in cell viability observed following asbestos exposures, it was concluded that crocidolite asbestos has no significant effects on IL-8 or IL-6 responses of NHBE cells in this study. However, it stimulated cytokine responses of A549 cells and significantly decreased their MCP-1 release (Figure 19a to Figure 21a). Other studies evaluating the effects of crocidolite asbestos on A549 and NHBE cells reported much stronger increases of IL-6 and IL-8 than observed here which might be due to differences in exposure conditions or asbestos origin [350-352].

6.4.7 Effects of particle exposure on rh-TNF-α stimulated cells

The next question of interest was whether the effects of particle exposure differ between cells in a healthy and a diseased state. As described in 6.2, it is reported that nanomaterial exposure of individuals with pre-existing diseases may exacerbate some respiratory effects due to inflammation and oxidative stress [145, 337, 353]. Therefore, evaluating the effects of SWCNT exposure on rh-TNF-α- or LPS-induced epithelial cells may give further indications of whether the presence of an infection may give rise to increased SWCNT toxicity compared to normal, unstimulated cells or whether the presence of SWCNT can modulate inflammatory responses during infections. It has also been proposed that bacterial products such as LPS associated with particles may have stimulatory effects on the cytokine production of macrophages and maybe also epithelial cells [338, 340]. While epithelial cells respond only slightly to LPS when compared to macrophages, they do express TLR receptors and have been shown to release IL-8 in response to treatment with different kinds of LPS with LPS from *Pseudomonas aeruginosa* (LPS-PA) being most effective [354].

6

As shown previously, rh-TNF-α concentration of 10 ng/ml was identified as the most suitable as it results in a medium stimulation of cells allowing decreases as well as further increases of cytokine production, as shown in Figure 6.6. In addition, it could serve as positive control for the induction of IL-8 and IL-6.

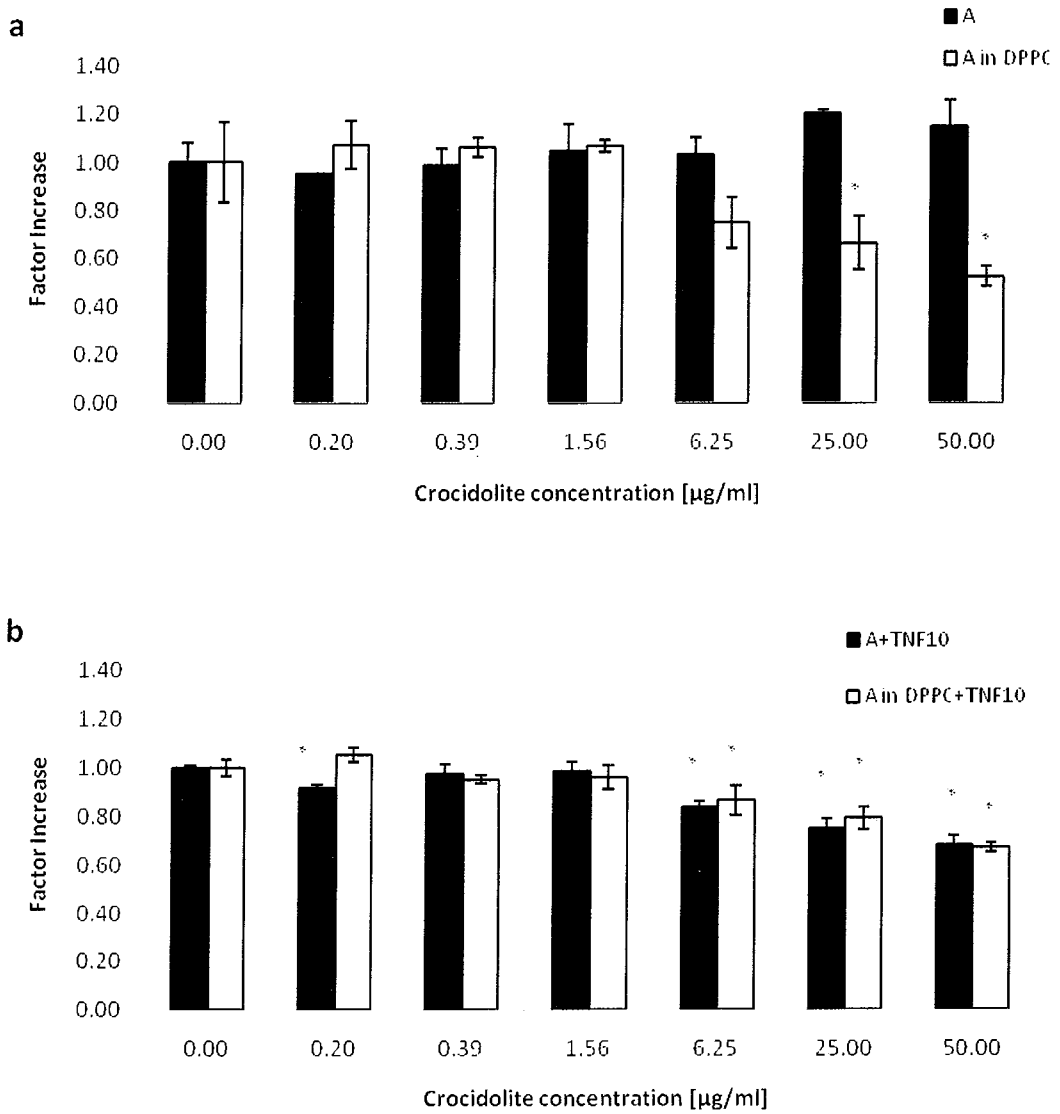

Figure 6.19: IL-8 protein release following 48 h exposure to crocidolite asbestos dispersed in culture medium or DPPC of (a) unstimulated A549 cells and (b) cells stimulated with rh-TNF-α as measured using ELISA. * Denotes a significant difference from the control ($p \leq 0.05$).

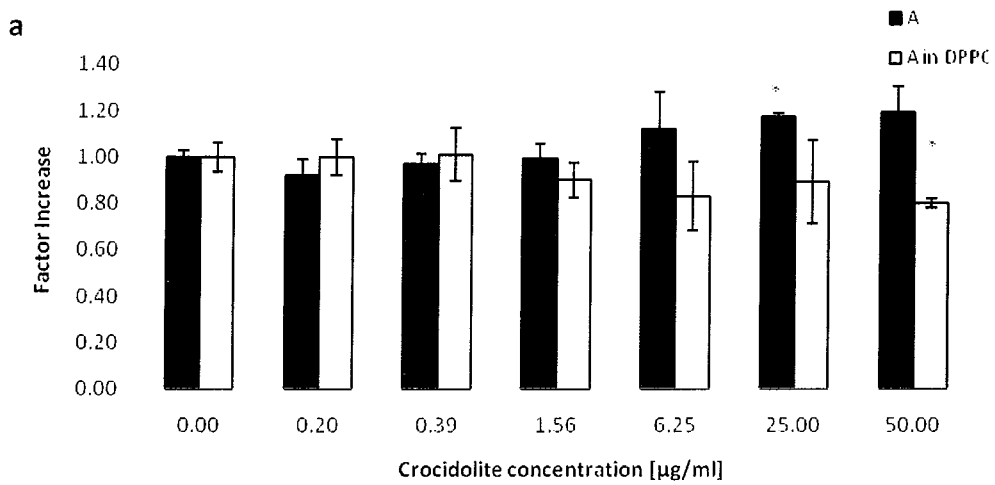

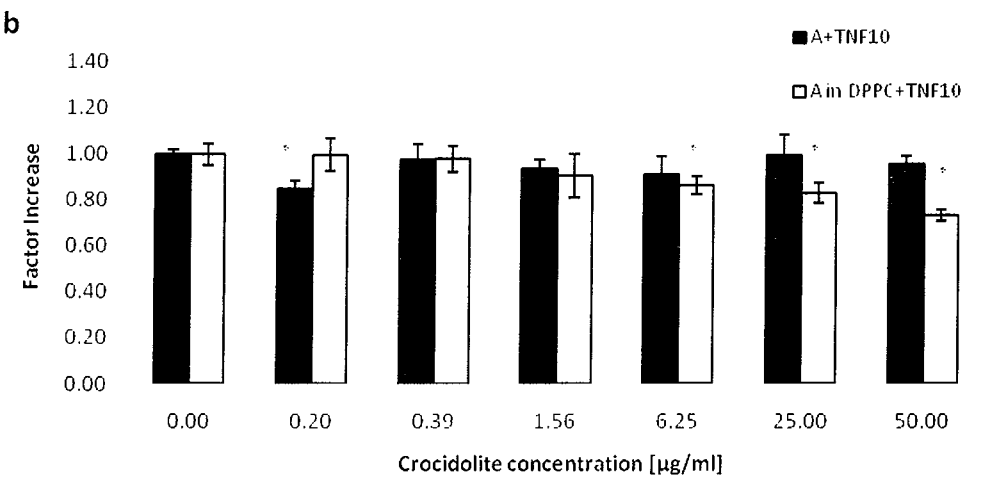

6

Figure 6.20: IL-6 protein release following 48 h exposure to crocidolite asbestos dispersed in culture medium or DPPC of (a) unstimulated A549 cells and (b) cells stimulated with rh-TNF-α as measured using ELISA. * Denotes a significant difference from the control ($p \leq 0.05$).

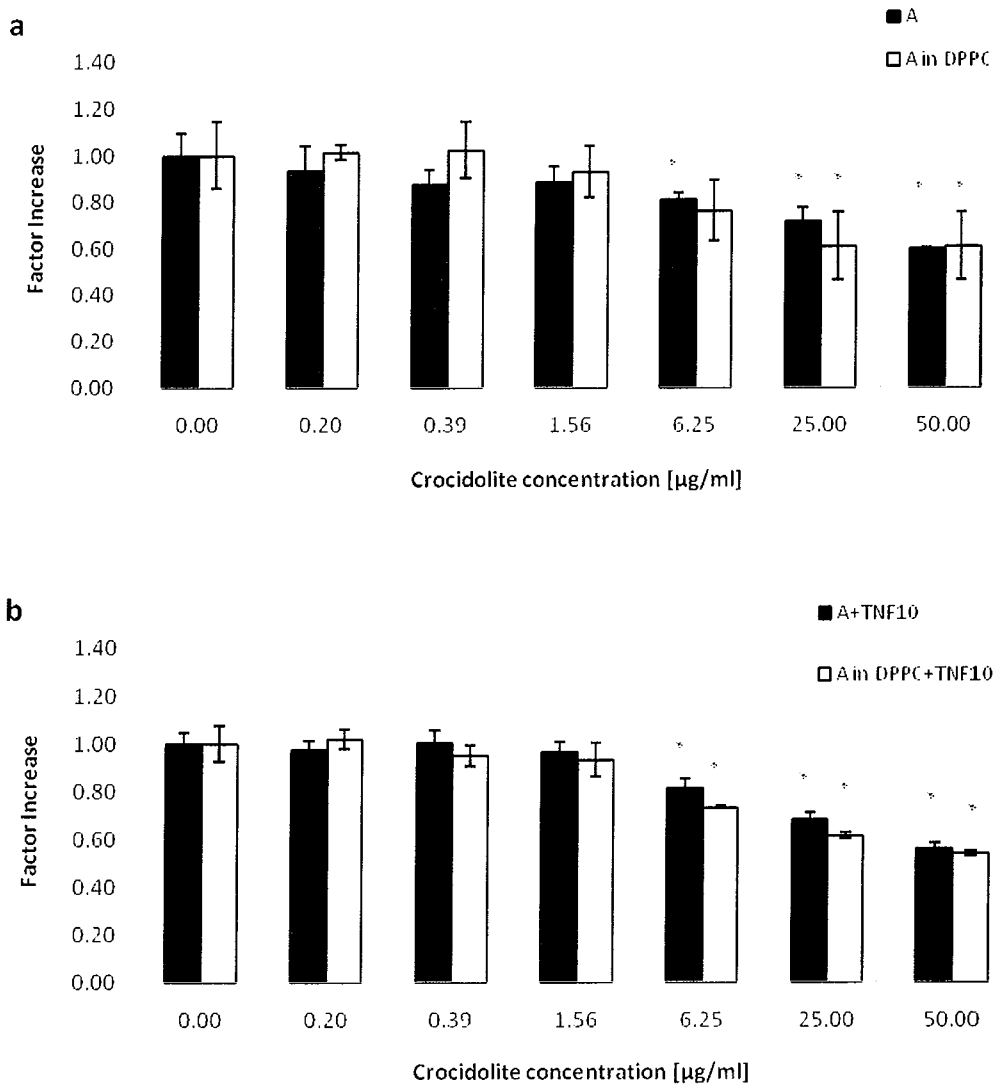

Figure 6.21: MCP-1 protein release following 48 h exposure to crocidolite asbestos dispersed in culture medium or DPPC of (a) unstimulated A549 cells and (b) cells stimulated with rh-TNF-α as measured using ELISA. * Denotes a significant difference from the control ($p \leq 0.05$).

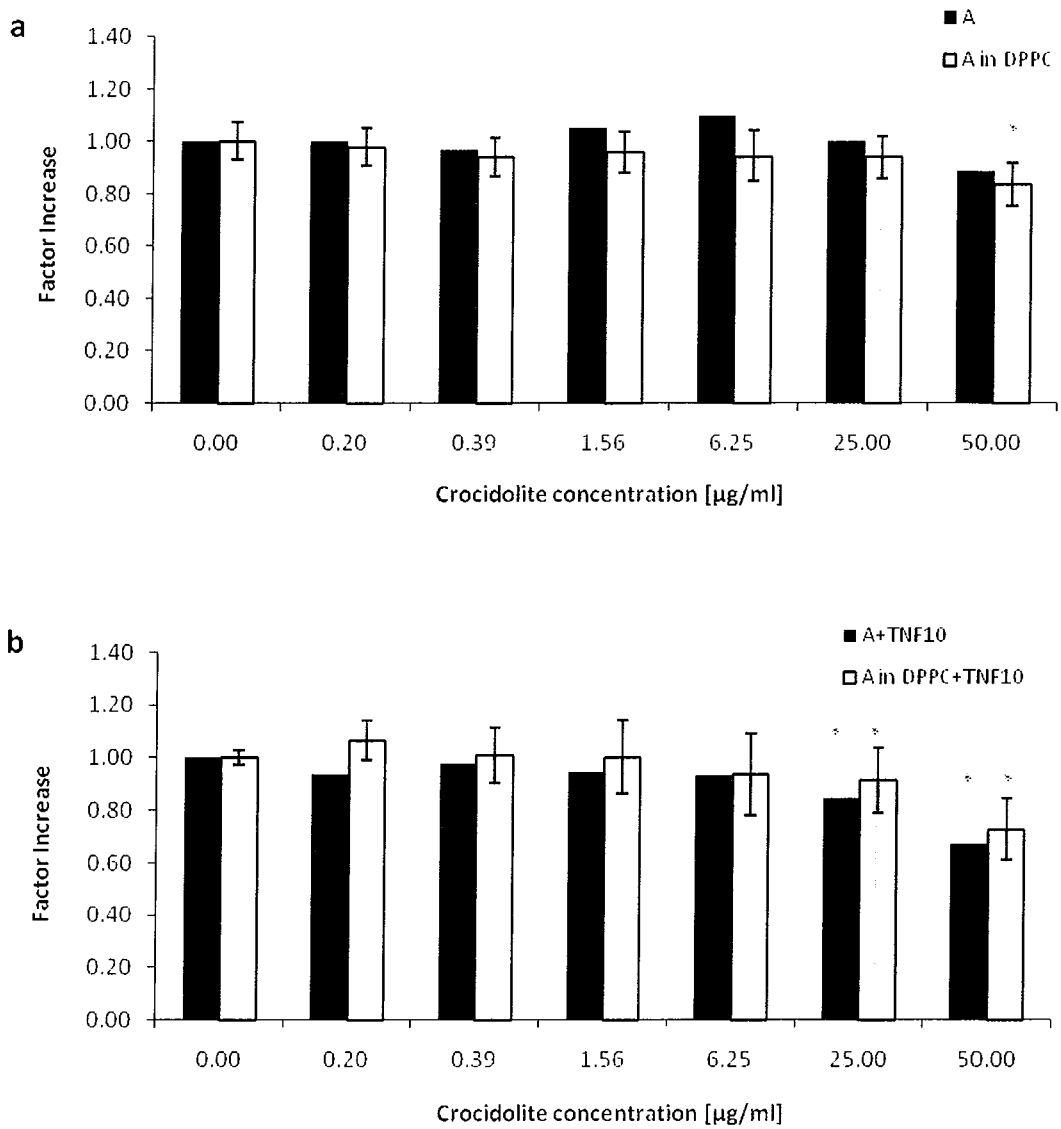

Figure 6.22: IL-8 protein release following 48 h exposure to crocidolite asbestos dispersed in culture medium or DPPC by (a) un-stimulated NHBE cells or (b) cells stimulated by rh-TNF-α as measured by ELISA. * Denotes a significant difference from the control ($p \leq 0.05$).

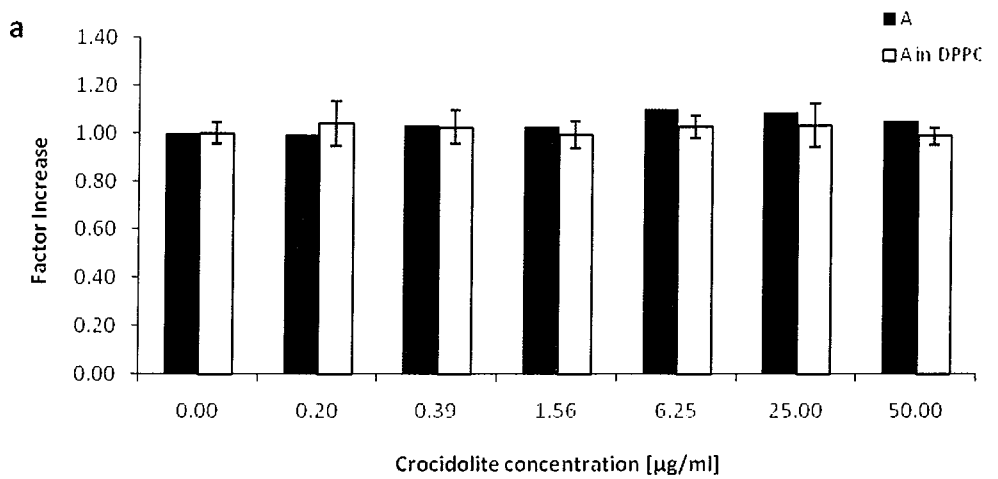

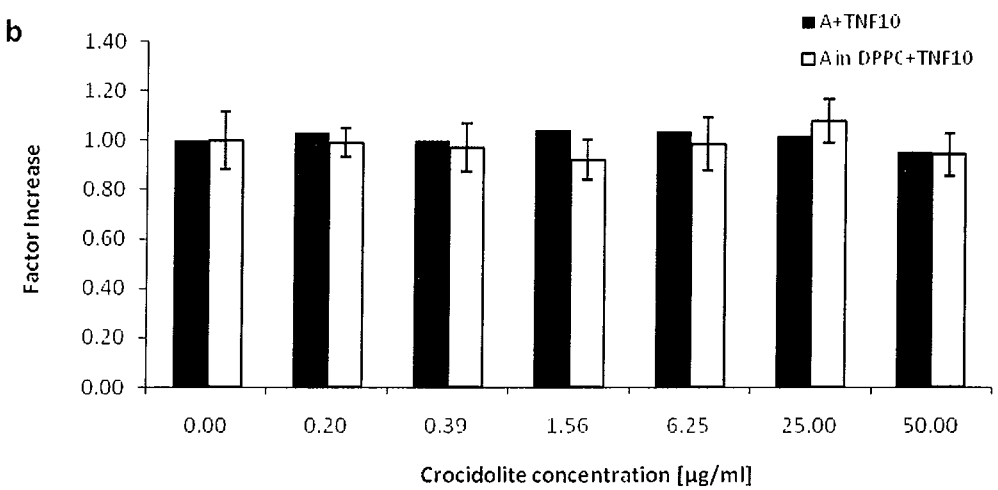

6

Figure 6.23: IL-6 protein release following 48 h exposure to crocidolite asbestos dispersed in culture medium or DPPC by (a) un-stimulated NHBE cells or (b) cells stimulated by rh-TNF-α as measured by ELISA. * Denotes a significant difference from the control ($p \leq 0.05$).

Whereas stimulation with rh-TNF-α resulted in an increase in IL-8 promoter activation of A549 cells by an average factor of 8 (800%) compared to non-stimulated control cells following 48 h (Figure 6.7) and protein release of IL-8 and IL-6 was increased by 13 and 6 fold, respectively (Figure 6.10), SWCNT exposure did not result in any further increase in the stimulation induced by rh-TNF-α (Figure 6.14 to Figure 6.15). The same was shown for NHBE cells (Figure 6.17 and Figure 6.18). Cell viability following SWCNT exposure was independent of TNF-α stimulation (Figure 6.4a and Figure 6.5a). In contrast, compared to stimulated control cells, the presence of SWCNT decreased IL-8 promoter activation of A549 cells by more than 20% following 48 h, similar to the effects seen for un-stimulated cells (Figure 6.12b). The decrease in IL-8 and IL-6 protein release seen in unstimulated cells upon SWCNT exposure was significantly inhibited by the presence of rh-TNF-α stimulation leading to reduction of only 16% for IL-8 and no significant reductions in IL-6 (Figure 6.14b and Figure 6.15b) compared to 40% and 27% for non-stimulated cells, respectively. Therefore, co-stimulation with rh-TNF-α appeared to decrease the suppressive effects of SWCNT on IL-6 and IL-8. MCP-1 protein response was independent of rh-TNFα stimulation (Figure 6.16).

The decreases in mediator responses seen in TNF-α stimulated cells upon addition of SWCNT may also be explained by the adsorbing properties of these particles. As seen in Figure 6.3, SWCNT have been shown to reduce TNF-α levels in culture medium by up to 20%. Therefore, decreased inflammatory mediator responses with increasing concentrations of SWCNT may also be due to decreased levels of TNF-α available for the cells due to binding of TNF-α onto SWCNT. This may also explain observations by Hamilton *et al.* (2006) who reported decreased TNF-α

production by alveolar macrophages in the presence of CNT *ex vivo* [214]. In general, the decreases in inflammatory mediator responses seen for SWCNT exposures even in the presence of inflammatory stimulation are consistent with rodent studies by Shvedova *et al.* (2008) reporting enhanced pulmonary infectivity following SWCNT exposure [181].

Following asbestos exposure, rh-TNF-α stimulated cells decreased their IL-8 and IL-6 protein release compared to un-stimulated cells (Figure 6.19b and Figure 6.20b). Again, no modulating effect of rh-TNF-α stimulation was seen for the effects of SWCNT or asbestos exposure on MCP-1 release or viability of A549 cells (Figure 6.21b; Figure 6.4). NHBE responded differently to A549 cells and appeared to be significantly more responsive to rh-TNF-α treatment. While non-stimulated NHBE cells showed reductions of 22% and 36% upon SWCNT treatment for IL-8 and IL-6 (Figure 6.17a; Figure 6.18a), the cytokine levels of stimulated cells exposed to SWCNT decreased by 51% and 64%, respectively (Figure 6.17b; Figure 6.18b). This difference may be explained by the differences in cell type with NHBE cells being normal primary epithelial cells of bronchial origin and A549 cells being a carcinoma cell line originating from alveolar epithelium.

SWCNT exposure of A549 cells stimulated with LPS-PA showed significantly higher decreases in cytokine responses (Figure 6.12c) but also high levels of cytotoxicity, particulary in the presence of DPPC (Appendix D, Figure D.1e,f and Figure D.5e,f). A LPS-PA concentration as high as 25 μg/ml was needed in order to achieve significant cytokine induction in A549 cells, leading to increases of IL-8 promoter activation and protein release by an average of 2.2 fold following 48 h exposure, so

that it was assumed not to be a realistic exposure scenario and LPS stimulation was not included in any of the further studies.

Taken together, rh-TNF-α treated cells did show responses different to that of non-stimulated ones. However, neither SWCNT nor asbestos particles were able to further increase inflammatory mediator responses of stimulated cells.

6.4.8 The effects of DPPC dispersion on SWCNT and asbestos toxicity

The final objective of this study was to determine whether DPPC dispersion influences the toxicity of SWCNT and asbestos. Exposure of cells to medium containing DPPC did not alter cell responses compared to cells exposed to culture medium only as shown in Figure 6.24 and Figure 6.25. However, as can be seen in Figure 6.12a and Figure 6.14a to Figure 6.16a, DPPC dispersion of SWCNT did result in increased suppression of IL-8, IL-6 and MCP-1 in A549 cells compared to culture medium dispersed nanotubes. This effect was even more pronounced when cells were stimulated with rh-TNF-α or LPS (Figure 6.12b, c and Figure 6.14b to Figure 6.16b). Therefore, it seems that during an ongoing inflammatory reaction, these cells might be more vulnerable to the effects of SWCNT in DPPC.

As shown in Figure 6.19 and Figure 6.20, DPPC dispersion also modulated the effects of asbestos on un-stimulated A549 cells, leading to decreases in IL-8 and IL-6 of up to 50 and 20%, respectively whereas increases of approximately 20% were observed in the absence of DPPC for both endpoints. Furthermore, dispersion in DPPC led to decreases in IL-6 protein of rh-TNF-α stimulated cells by up to 23%

which was not apparent in the absence of DPPC (Figure 6.20b). The MCP-1 release by A549 cells to asbestos appeared to be independent of DPPC (Figure 6.21), as were the effects of particle exposure on NHBE cells (Figure 6.17, Figure 6.18, Figure 6.22 and Figure 6.23). Cell viability of non-stimulated A549 cells post asbestos exposure was independent of DPPC dispersion (Figure 6.4b). Only the viability of cells stimulated with TNF-α decreased following dispersion in DPPC. The same was true for the viability of NHBE cells (Figure 6.5).

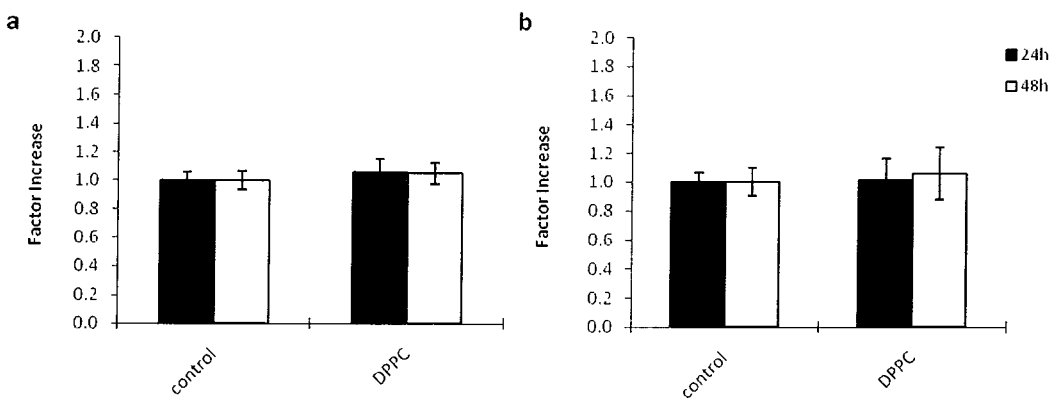

Figure 6.24: Effects of cell exposure to culture medium supplemented with 0.25 μg/ml DPPC on (a) cell viability and (b) promoter activation of A549-IL-8 cells following 24 and 48 h exposure.

6

As shown in Chapter 5, Figure 5.2 and Figure 5.3, DPPC improved SWCNT dispersion, resulting in more cells being exposed to SWCNT which may have resulted in increased loss of cell viability and therefore inflammatory response. It was thus hypothesised that the type of dispersion vehicle used for studying SWCNT *in vitro* greatly influences their cellular effects. In previous studies it was demonstrated that improved dispersion of carbon black nanoparticles can lead to increased *in vivo* inflammation and damage compared to poorly dispersed

nanomaterials [355]. Therefore, improved dispersion of SWCNT may explain the increases in particle toxicity observed in this study.

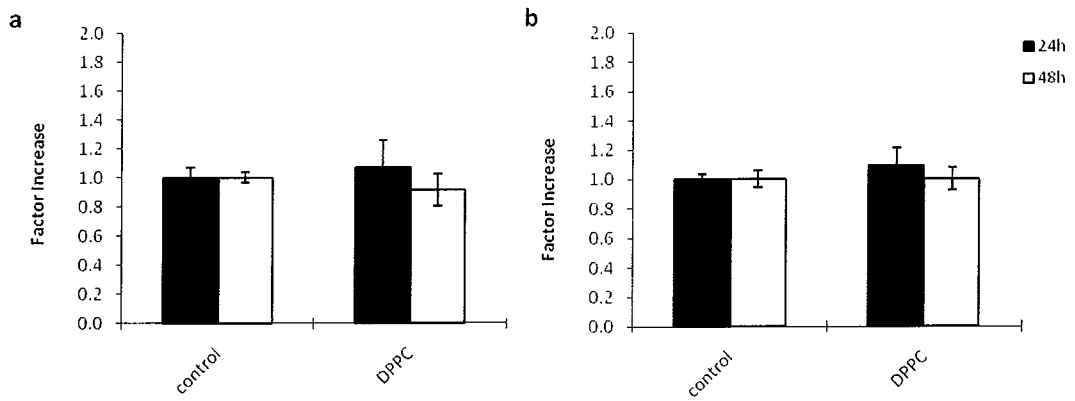

Figure 6.25: Effects of cell exposure to culture medium supplemented with 0.25 µg/ml DPPC on (a) cell viability and (b) IL-8 protein release of NHBE cells following 24 and 48 h exposure.

The degree of SWCNT dispersion was the same for NHBE medium with or without DPPC (Chapter 5, Figure 5.3). This can explain the fact that NHBE cell responses were not modified by the presence of DPPC. No significant influence of DPPC on asbestos dispersion or cytotoxicity was observed. Therefore, it remains unknown why DPPC dispersion can also modify the inflammatory response of A549 cells to asbestos fibres.

As a surfactant, DPPC forms micellar structures through their interaction with the particles. Therefore, it could be hypothesised that while "unstructured" DPPC may not affect cell responses, changes in the arrangement of hydrophilic and hydrophobic regions of DPPC molecules due to the presence of particles may render it more toxic to A549 cells as described in Chapter 5, 5.5. DPPC dispersion may also lead to changes in particle surface chemistry [69, 330] and particle

coating by DPPC may modify or increase particle uptake by cells leading to particles coming into contact with different cellular compartments/targets which could change toxic responses. In contrast to bronchial epithelial cells such as NHBE cells, A549 cells represent alveolar type II cells that are able to produce lung surfactant. In addition, they possess surface receptors that recognize and internalize surfactant for recycling which may lead to increased interaction and uptake of DPPC coated particles by A549 cells compared to NHBE cells. This may also explain the changes in cell responses seen following asbestos exposure, which seemed to be independent of the degree of particle dispersion. As DPPC dispersion significantly modulated cellular responses in terms of intracellular ROS formation (Chapter 5) and inflammatory mediator responses following SWCNT, P90 carbon black and asbestos exposure, the use of DPPC as dispersant vehicle may be of great importance and relevance for future *in vitro* studies investigating the effects of particle exposure on lung target cells.

6.4.9 Normal A549 vs. A549-IL-8

The sensitivity of transfected A549 cells, normal, untransfected A549 cells and NHBE cells was compared based on their IL-8 protein responses following 48 h exposure to HiPco® SWCNT and crocidolite asbestos as illustrated in Figure 6.26. The A549-IL8 cell line was chosen, as this cell line was used for all protein analysis performed previously.

When comparing the two cell lines, no significant difference was observed for concentration between 0.195 and 6.25 μg/ml. At the two highest concentrations

used in this study, normal A549 cells seemed to be less sensitive showing lower reductions compared to the transfected cell line (Figure 6.26a). This can be explained by the procedure that was used to generate A549-IL8 cells, where only cells that contained the reporter-gene construct of choice were allowed to expand. This cell population differs slightly in sensitivity. However, cell responses to crocidolite asbestos exposure were identical with both cell lines slightly increasing IL-8 release (Figure 6.26b). In contrast, NHBE cells appeared slightly more sensitive to asbestos exposure compared to A549 cell lines but showed the same response as A549-IL8 cells to SWCNT exposure (Figure 6.26).

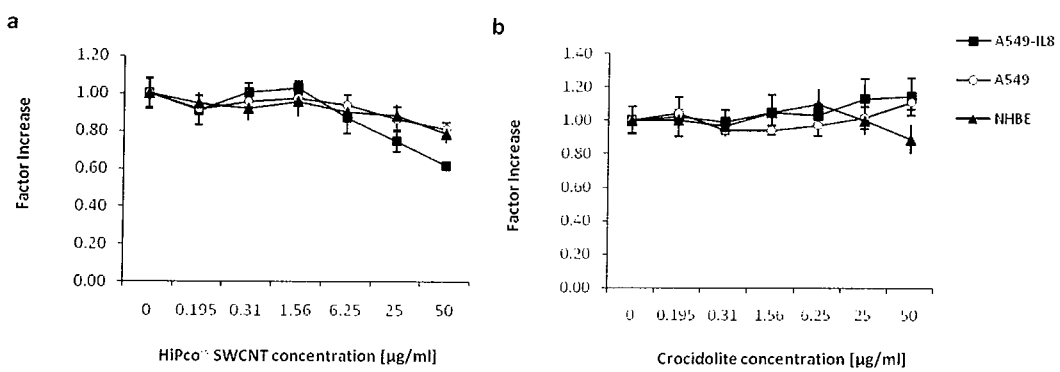

Figure 6.26: Correlation between NHBE, A549-IL8 and normal A549 cells based on IL-8 release following 48 h exposure to (a) HiPco® SWCNT and (b) crocidolite asbestos.

6.5 Conclusion

To conclude, this study showed that exposure to HiPco® SWCNT samples can lead to the suppression of a variety of inflammatory mediators including IL-8, IL-6 and MCP-1 *in vitro*. This was true for human type II alveolar epithelial cells (A549) as well as primary normal human bronchial cells (NHBE). This confirms results described in Chapter 5 where no ROS could be detected within cells following exposure to particles dispersed in FBS supplemented culture medium. Interestingly, however, even though intracellular ROS could be detected following exposure to DPPC dispersed SWCNT, as shown in Chapter 5, an inflammatory response was still absent which may indicate low levels of oxidative stress as represented by tier 1 of the hierarchical oxidative stress model as described in Chapter 2, 2.2.4.3 and Figure 2.3.

Comparing the two cell types employed in this study, NHBE and A549 cells appeared to respond similarly to the presence of medium dispersed SWCNT. However, NHBE cells stimulated by rh-TNF-α seemed to be significantly more sensitive to SWCNT exposure. Stimulation with rh-TNF-α was used as a model for diseased epithelium and it was demonstrated that cell responses selectively differed from that of un-stimulated cells.

No definite conclusion can be drawn as to whether HiPco® SWCNT samples have the potential of reacting in an asbestos-like manner. Only asbestos was able to slightly increase IL-8 and IL-6 responses. In contrast, both particle types were able to selectively decrease IL-8, IL-6 and MCP-1 and changed their reactivity following DPPC dispersion. However, suppression of IL-8 was generally greater following

HiPco® SWCNT exposure compared to asbestos. Therefore, HiPco® SWCNT exposures showed similarities but also differences to crocidolite asbestos so that risk assessment needs further comparative studies.

Dispersion of particles in DPPC helped to mimic pulmonary exposure more closely. Effective dispersion of nanomaterials and the use of biologically relevant media are important for accuracy in toxicity assays. However, further physical and chemical characterisation of the interactions between DPPC and particles such as SWCNT are needed for better understanding of the mechanisms taking place as it is unclear whether dispersion in DPPC increases particle toxicity or the presence of particle increases DPPC toxicity.

Overall, suppression of an immunological response may have negative consequences as the normal status quo of the immune system has changed and may render the immune system less reactive towards infections. Furthermore, activation of an immune response is needed in case of oxidative stress triggered by these particles and cell signalling by lung epithelial cells is of utmost importance in order to attract phagocytic cells such as monocytes and macrophages, which represent the first line of defence against invading particles and are needed for tissue clearance, to the site of particle deposition. Due to the fundamental role of phagocytic cells within particle toxicity, monocyte derived macrophages were included as an additional cell model within the study described in the following chapter.

Chapter 7

Effects of SWCNT on macrophages

7.1 Chapter summary

This study investigated whether SWCNT exposure may have the potential of affecting lipid and inflammatory mediator release of monocyte derived macrophages (MdM) by including gene expression of COX-2, intracellular PGE_2 formation, IL-8 gene expression and protein release of IL-6, TNF-α and MCP-1. Results indicate that exposure of MdM to SWCNT did not affect intracellular PGE_2 formation or IL-8 or COX-2 gene expression. However, response of macrophages seemed to be strongly influenced by the blood donor with the consequence that no overall significant effects of SWCNT exposure could be determined. Co-stimulation of particle exposed macrophages with LPS led to synergistic effects on IL-8 and COX-2 mRNA expression. However, this effect could not be confirmed for IL-8 protein release.

Lipid mediator response was also investigated using A549 cells. As previously seen for IL-8 expression (Chapter 6), SWCNT exposure reduced COX-2 expression. No significant changes in PGE_2 formation were seen for A549 or MdM cells with the exception of ArcD SWCNT exposed A549 cells which showed slightly increased PGE_2 levels.

7

7.2 Introduction

Following the observation of effects of SWCNT exposure on inflammatory responses of epithelial cells, the aims of this *in vitro* study were to determine whether SWCNT exposure can also modulate inflammatory mediator release of macrophages. As described in Chapter 1, 1.2.1, not only epithelial cells but also macrophages represent a principal target of particle exposure [22] [23] [24] [338]. Therefore, monocyte derived macrophages (MdM) which can serve as a model for alveolar macrophages were chosen as test model. As can be seen from Figure 7.1 and Figure 7.2, following exposure, these MdM attempt to engulf and internalize the particles present in their environment. This was true for asbestos fibres but also HiPco® and ArcD SWCNT indicating that MdM do directly interact with particles potentially leading to effects on cell signalling as described previously (Chapter 2, 2.2.4.3) [151, 156, 356, 357]. Furthermore, frustrated phagocytosis, as seen for asbestos fibres in Figure 7.1 may lead to oxidative stress and initiate signalling cascades as described in Chapter 2, 2.3.4.2.

Including MdM in addition to previously employed A549 lung epithelial cells would aid in creating a more complete picture of the pulmonary response to SWCNT. Above all, as MdM were shown to directly interact with the particles, they were chosen as a further cell model for this study.

Ultrafine particles have long been identified as an inhalation hazard and have been associated with adverse cardio-respiratory effects [358-360] so that the data existing on ultrafine particle toxicity is an important resource. Therefore, endpoints investigated in this study following MdM exposure were based on

mechanisms previously identified for ultrafine particle toxicity as described in Chapter 2, 2.2.4.3 including effects on inflammatory and lipid mediator responses. As described by Beck-Speier *et al.* (2005), following exposure of alveolar macrophages to ultrafine carbon particles, PGE_2 release seemed to be the most sensitive response being independent of particles' oxidative potential [39]. Therefore, PGE_2 production was chosen as an endpoint in order to evaluate whether SWCNT have also the potential to affect lipid mediator responses of exposed cells *in vitro*. The expression of COX-2, a key enzyme of prostaglandin synthesis, is one of the limiting steps in the pathway of PGE_2 formation and was included as further endpoint.

In addition, evaluation of the cytokines and chemokines IL-8, IL-6, TNF-α and MCP-1 were included in this study in order to further evaluate the inflammatory responses of exposed cells. As described in Chapter 6, co-exposure of cells to SWCNT and LPS or TNF-α may give valuable information whether the presence of an immuno-stimulant or a pre-existing disease may affect SWCNT toxicity.

7

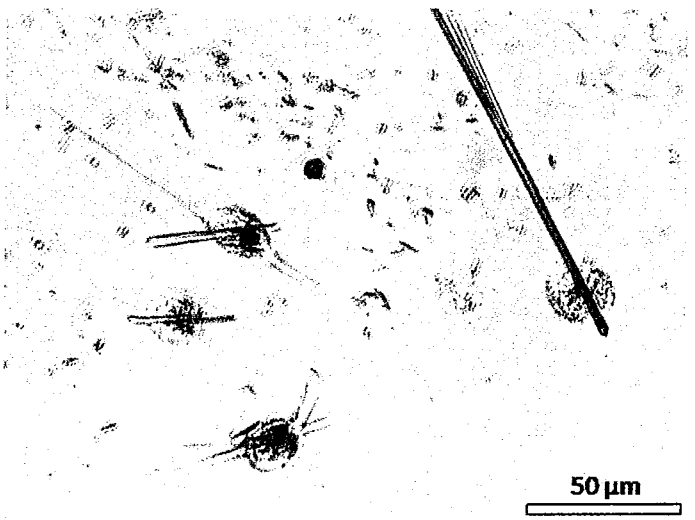

Figure 7.1: MdM exposed to 50 µg/ml of crocidolite asbestos.

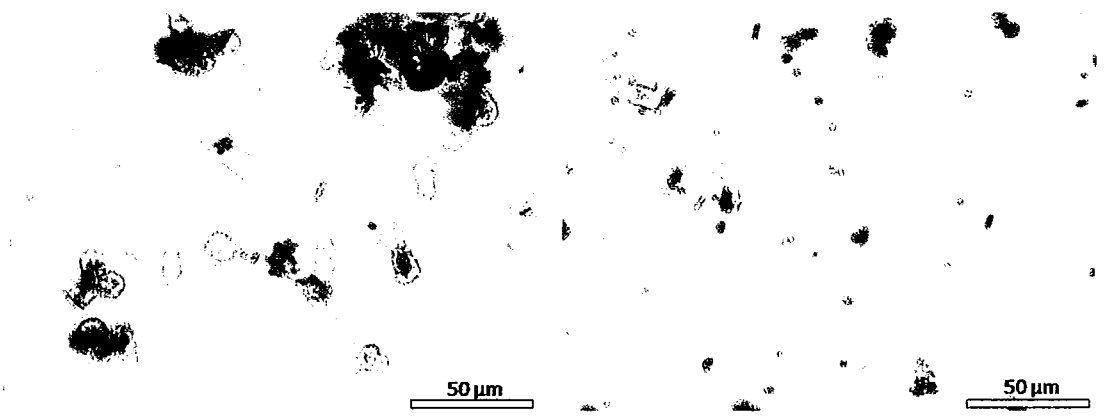

Figure 7.2: MdM cells following exposure to 50 µg/ml of (a) HiPco® SWCNT and (b) ArcD SWCNT.

7.3 Materials and Methods

7.3.1 A549 cell culture

A549 cells were cultured as described in Chapter 5.

7.3.2 Monocyte derived macrophages (MdM)culture

Peripheral blood mononuclear cells (PBMC) were isolated from heparinised (10 U/ml) blood from 5 healthy human volunteers or from buffy coats of 8 different donors by density gradient centrifugation. Blood was diluted (1:2) with phosphate buffered saline (PBS) and 25 ml was layered over 13 ml of Lymphoprep™ (Fresenius Kabi Norge AS, Oslo, Norway) and centrifuged for 30 min at 450g. Lymphocytes/monocytes were then removed and cultured in 6 well-plates using LPS-free RPMI cell culture medium supplemented with 10% FBS. After 1.5 h incubation, non-adherent cells were removed by several washings with PBS and 100 ng/ml macrophage-colony stimulating factor (M-CSF; Immunotools) were added to allow cells to develop into macrophages. After 5 days incubation, MdM were harvested by cell scraping, $1x10^6$ cells/ml were seeded into low attachment 24-well plates (Costar, 3473) and exposed to SWCNT at final concentrations of 0, 1, 10 and 50 µg/ml. Lower exposure concentrations were chosen for this study in order to avoid particle cytotoxicity. The absence of significant loss in cell viability following exposure was verified using Trypan Blue staining as described in Chapter 3, 3.3.5.4.

7.3.3 Preparation of SWCNT-suspension

Due to the high sensitivity of macrophages to LPS, HiPco® and ArcD produced SWCNT were tested for LPS contamination using the Lymulus amobocyte lysate assay (LAL) which showed a negative response.

Stock concentrations of SWCNT were prepared in cell culture medium as described in Chapter 5, 5.3.3.1.

7.3.4 Intracellular PGE_2 measurement

Intracellular PGE_2 was measured following incubation of A549 and MdM with SWCNT for 1 or 6 h. Therefore, cells were washed with PBS followed by ultrasonication in Hepes buffer, pH 7.4, using an ultrasonic tip (3x15 seconds). Afterwards, aliquots of cell suspensions were stored for protein analysis. The remaining homogenates were immediately deproteinised by adding an 8-fold volume of 90% methanol solution containing 0.5 mM EDTA (Sigma) and 1 mM 4-hydroxy-2,2,6,6-tetramethylpiperidine-1-oxyl (Fluka, Taufkirchen, Germany). Methanol suspensions were stored at -80°C for 24 h followed by centrifugation at 14,000 g for 20 min at 4°C in order to remove proteins. Aliquots of the obtained supernatants were dried in a vacuum centrifuge and used for determination of PGE_2 using a PGE_2 enzyme immunosorbant assay (EIA) kit according to manufacturer's instructions (Cayman, Arbor, MI). In parallel, protein content was determined using the Bio-Rad assay (Bio-Rad, Munich, Germany).

7.3.5 Real-time reverse transcriptase (RT) polymerase chain reaction (PCR)

7.3.5.1 *A549 cells*

For gene expression analysis, cells were seeded in 12 well plates (Costar, Germany) and exposed to SWCNT with a final concentration of 0, 1, 10 and 50 μg/ml for 6 or 24 h as described in Chapter 6, 6.3.6. Following exposure, real-time RT-PCR for relative quantification of COX-2 mRNA expression was carried out as described in Chapter 6 6.3.6 using the primers illustrated in Table 6.2 and the housekeeping gene α-enolase internal control.

7.3.5.2 *MdM cells*

Gene expression analysis was carried out following exposure of MdM for 2 and 6 hour incubation to SWCNT. For PCR, $2x10^4$ cells were lysed in 200 μl TRI®-Reagent (Sigma). To assist the precipitation, tRNA was added to each sample. Following isolation, the RNA was reverse-transcribed using oligo(dT) as primer. The LightCycler® system (Roche Diagnostics, Mannheim, Germany) was used for quantitative PCR following manufacturer's instructions. The LightCycler®–FastStart DNA Master SYBR Green I kit (Roche Diagnostics, Mannheim, Germany) was used for cDNA amplification. Gene expression analysis was then carried out as described in in Chapter 6, 6.3.6 using α-enolase as the housekeeping gene. Primer sequences are illustrated in Chapter 6, Table 6.2.

7.3.6 Intracellular TNF-α protein staining

Immunofluorescence staining was used to quantify intracellular TNF-α protein in MdM cells. Following maturation of monocytic cells to MdM, cells were harvested using cell scrapers and collected in 50 ml tubes. After centrifugation at 400g for 7 minutes, cell pellets were resuspended in PBS and again centrifuged at 400g for 7 minutes in order to wash the cells. Cells were then resuspended in LPS-free culture medium, cell numbers were determined and $1x10^6$ cells were seeded per well using 24-well low attachment multiplates (Costar, 3473). In order to close cellular pores, 10 µg/ml Befeldin A solution (Sigma, B-7651) were added. Cells were then exposed to particle solutions for 5 h. Following exposure, cells were transferred into 1.5 ml Eppendorf tubes and centrifuged at 400g for 5 minutes. Cell pellets were resuspended in PBS/2%FBS solution. On ice, cell surfaces were then stained by adding 2.5 µl (1:20) cluster of differentiation (CD)-14-FITC (Beckman Coulter) and were incubated for 20 minutes at room temperature. Cells were again centrifuged at 400g for 5 min and washed with 500 µl PBS. On ice, 200 µl of BD Cytofix/Cytoperm™ (BD Biosciences Pharmingen) were added and cells were incubated in the dark. After washing the cells with PBS/2%FBS, the pellet was divided into two and again washed with PBS. Pellet number one served as negative control and was incubated on ice following addition of 35 µl BD Perm/Wash™ buffer(BD Biosciences Pharmingen), 0.4 µl rhTNF-α (10 times molar excess) and 2 µl anit-TNFα- phycoerythrin (PE). The second pellet was incubated with 35 µl BD Perm/Wash™ buffer and 2 µl anti-TNF-α-PE only. After 20 min, cells were washed and resuspended in 750 µl PBS/2%FBS. Cell fluorescence was then determined using flow cytometry (BD FACSCanto™).

7.3.7 Enzyme linked immunosorbant assays (ELISA)

In order to assess effects of particle exposure on protein release, ELISAs were performed for the cytokines IL-8, IL-6, TNF-α (Immunotools) and MCP-1 (BenderMed Systems) following particle exposures for 6 and 24 h as described in Chapter 6, Table 6.3 and Table 6.4.

7.4 Results

Monocytes were isolated from PBMC by plastic adherence. This was followed by the addition of M-CSF to improve maturation of monocytes to macrophages. As can be seen in Figure 7.3, following a 5 day incubation in the presence of M-CSF at 37°C, cells displayed typical morphological features of macrophages including increased size compared to monocytes, pseudopodia (PP) and filopodia (FP) as shown in Figure 7.3 c and Figure 7.3 d, respectively.

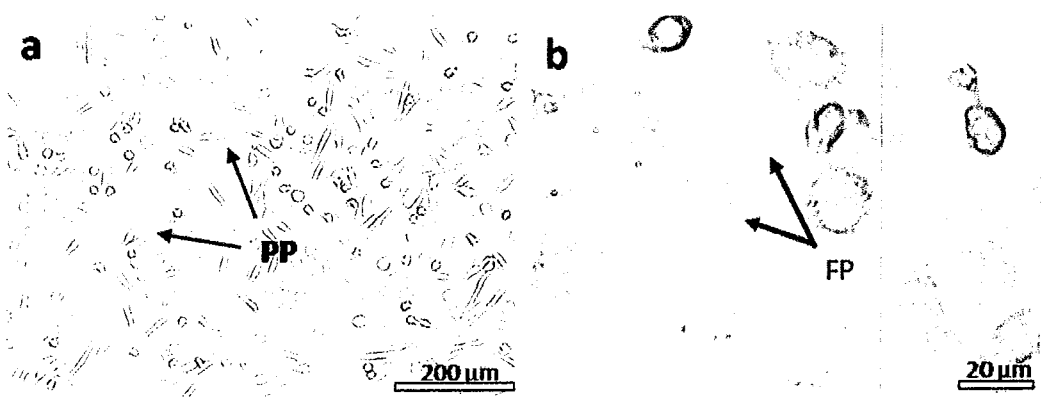

Figure 7.3: MdM cells on day 5 after monocyte isolation and incubation with M-CSF.

7

Human monocytes and therefore MdM can be identified by the expression of CD14 receptors on their surfaces which is also involved in LPS-induced cytokine production [25, 361]. Furthermore, around 15% of monocytes in healthy humans also express CD16 surface receptors [362]. Therefore, in parallel to intracellular TNF-α stainingcells were immunofluorescently stained using anti-CD-14-PE antibodies, in order to further identify and characterise MdM andcells were found

to express CD-14 surface antibodies so that it was concluded that MdM isolation and maturation was successful.

As was shown in Figure 7.2, following exposure, the majority of SWCNT agglomerates seemed to adhere to macrophage surfaces as previously seen for A549 cells. Some nanotubes even appeared to be taken up by the macrophages as indicated by black stained cellular bodies. Similar observations have also been made by other authors [213, 216, 363].

7.4.1.1 *Effects on COX-2, IL-8 and TNFα mRNA expression*

For gene expression analysis, MdM derived from fresh blood samples of 5 different donors were pre-incubated with particles at concentrations of 10 and 50 μg/ml. After 1 h, cells were stimulated with LPS for an additional 2 or 5 h period or left unstimulated for the same period of time. Cells exposed to LPS only served as a positive control. Following exposure, the expression of IL-8, COX-2 and TNF-α mRNA levels was determined using real-time monitoring of cDNA. Relative gene expression data was normalized by dividing the expression of IL-8, COX-2 or TNF-α by the expression of the housekeeping gene α-enolase.

Increases in gene expression of macrophages differed greatly depending on blood donor. As can be seen in Appendix E, following stimulation with LPS, the expression of IL-8 mRNA was upregulated between 2 and 13 fold (Figure E.1; Figure E.2), COX-2 mRNA 25 to 202 fold (Figure E.3; Figure E.4) and TNF-α mRNA was increased up to 85 fold (Figure E.5). Intracellular TNF-α protein was increased

by up to a factor of 101 (Figure E.6). Protein release of IL-8 was upregulated between 2 and 10 fold (Figure E.7), IL-6 release by a factor between 6 and 194 (Figure E.8) and TNF-α protein release by 25 to 221 fold (Figure E.9).

Exposure of MdM to suspended SWCNT alone did not significantly increase the expression of IL-8 (Figure E.1 and Figure E.2), COX-2 (Figure E.3 and Figure E.4) or TNFα (Figure E.5). The cells of 3 out of 5 blood donors showed upregulation in IL-8 (Figure E.1a, c, e) whereas mRNA of the remaining 2 donor cells selectively decreased following SWCNT treatment (Figure E.1b, d). This was the same for both types of carbon nanotubes tested (Figure E.1 and Figure E.2). The expression of COX-2 mRNA showed slightly different patterns but as seen for IL-8 expression, no consistent response could be observed (Figure E.3 and Figure E.4). Cells from only one donor showed strong increases in COX-2 gene expression following HiPco® SWCNT exposure (Figure E.3e). In contrast only slight increases or even downregulation could be seen for others (Figure E.3a–d).

Cell responses following ArcD SWCNT treatment appeared more consistent with very small increases in COX-2 expression (Figure E.4). The same was true for TNF-α mRNA (Figure E.5). However, stimulation of SWCNT pre-treated cells with LPS resulted in a clearly enhanced expression of all three endpoints tested (Figure 7.5 and Figure 7.6) indicating synergistic effects between SWCNT and LPS treatment.

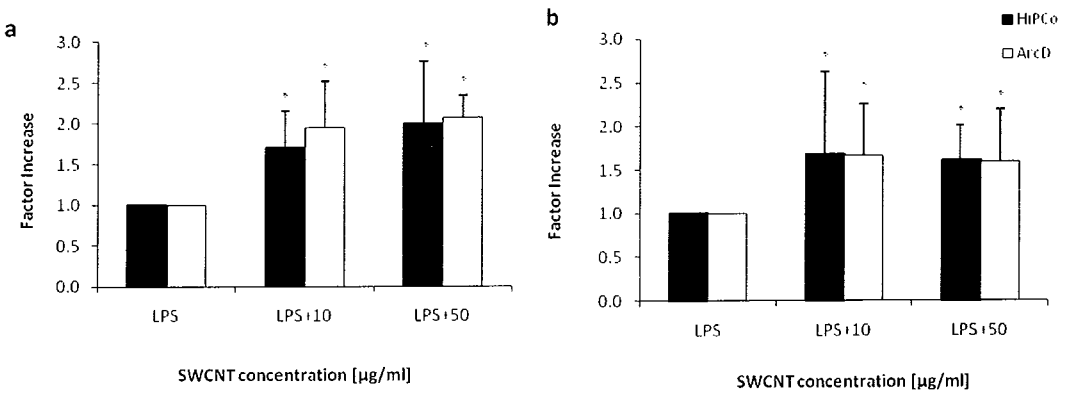

Figure 7.4: Co-stimulatory effects between LPS (100 ng/ml) and SWCNT at concentrations of 10 µg/ml and 50 µg/ml on (a) IL-8 and (b) COX-2 mRNA expression of MdM cells. * Denotes a significant difference from the control ($p \leq 0.05$).

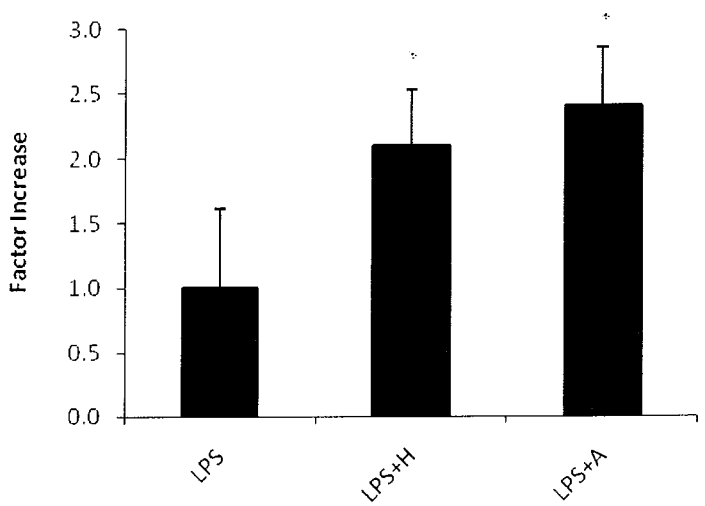

Figure 7.5: Co-stimulatory effects between LPS (100 ng/ml) and SWCNT at concentrations of 10 µg/ml and 50 µg/ml on TNF-α mRNA expression of MdM cells. * Denotes a significant difference from the control ($p \leq 0.05$).

7.4.1.2 *Effects on IL-8, IL-6, MCP-1 and TNF-α protein release*

In order to investigate whether effects on mRNA consequently affected protein translation and release, protein analysis was carried out using the same exposure conditions. In contrast to gene expression analysis, protein release was measured following exposure of MdM derived from 8 different buffy coats. This had the advantage of increased sample supply. Conversely, blood samples were stored overnight (under controlled storage conditions) before being available for processing. In addition, in contrast to fresh blood samples, the disease state of buffy coat donors was unknown. Treatment of buffy coat MdM with 100 ng/ml LPS did result in increases in IL-8, IL-6 and TNF-α protein release by all donors (Appendix E, Figure E.7 to E21). Interleukin-8 release was increased by factors ranging between 2.5 and 11 depending on donor (Figure E.7a-h). Increase in IL-6 release ranged from 6.4 to 230 fold (Figure E.8a-h) and TNF-α protein release from 10 to 240 fold (Figure E.9a-h). The formation of MCP-1 was not stimulated by LPS treatment (Figure E.10). This already indicates the great variability in responses seen for cells derived from different donors which was also seen following exposure to SWCNT. Whereas protein release of some donors could be upregulated by SWCNT treatment, cells derived from other donors did not respond to SWCNT or even decreased their protein release. This was true for IL-8, IL-6 and TNF-α (Figures E.7 to E.9). The release of MCP-1 remained either unaffected or decreased upon SWCNT treatment (Figure E.10). The same inconsistency was seen for co-stimulations of cells with SWCNT and LPS. In contrast to mRNA expression, protein release was not increased in a synergistic manner. Decreases of LPS in the

presence of SWCNT were observed for several samples. Therefore, co-stimulatory effects of SWCNT and LPS could not be confirmed on the protein level.

Using MdM derived from fresh blood samples, intracellular TNF-α protein was quantified using immunofluorescence staining. As seen for IL-8 and COX-2, again effects on mRNA could not be confirmed on the protein level (Figure 7.7). Cell treatment with SWCNT did not significantly affect TNF-α protein translation and showed no co-stimulatory effects with LPS.

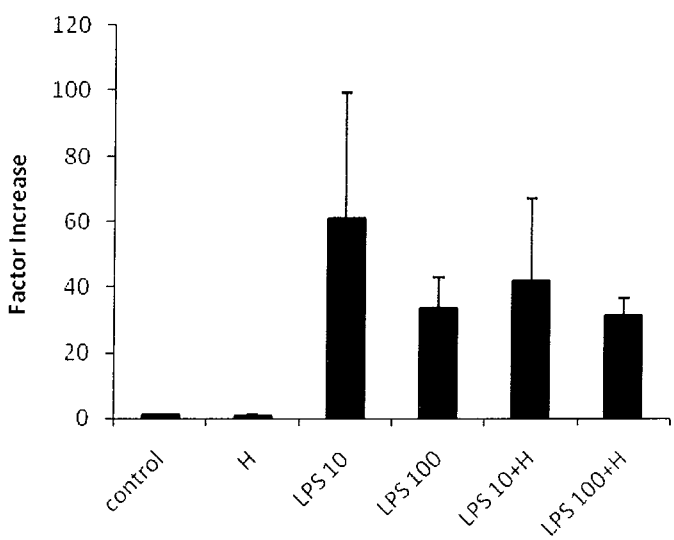

7

Figure 7.6: Intracellular TNF-α protein following exposure of MdM cells (n=3) to HiPco® SWCNT (50 μg/ml) with and without co-stimulation with LPS (10 ng/ml and 100 ng/ml) as measured by flow cytometry.

7.4.2 Effects on intracellular PGE2 formation

Downstream of COX-2, intracellular PGE_2 protein levels were determined by employing an enzyme immuno assay (EIA). Investigating PGE_2 production following SWCNT exposure, only slight and statistically insignificant alterations were seen when MdM were exposed for 6 h (Figure 7.8). Lipopolysaccharide served as positive control stimulus and resulted in an approximately 2-fold increase in PGE_2. Sequential exposure of MdM cells to SWCNT and LPS did not result in significant effects (Figure 7.9).

7.4.2.1 *Effects on COX-2 expression and intracellular PGE_2* formation of A549 cells

Cell responses in terms of COX-2 expression and PGE_2 have not been investigated within the course of this study, so far. Therefore, for comparison purposes, these endpoints were also assessed following exposure of A549 to SWCNT.

In order to evaluate the gene expression of COX-2, A549 cells were exposed to SWCNT at concentrations of 1, 10 and 50 µg/ml for 6 or 24 h. Tumour necrosis factor α (TNF-α) was used positive control stimuli for epithelial cells. Stimulation with TNF-α resulted in a maximum upregulation of COX expression of up to 200% compared to unstimulated control cells (Figure 7.10).

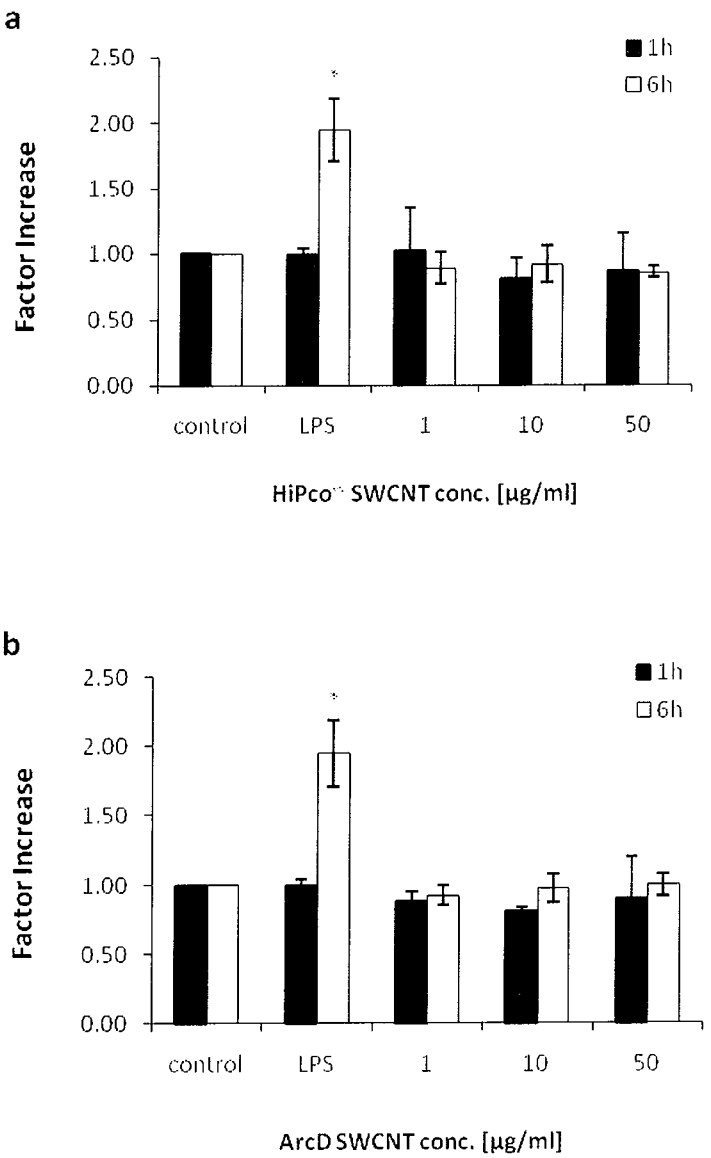

Figure 7.7: Factor increase in intracellular PGE_2 production per mg of total protein in MdM cells following 1h and 6h exposure to (a) HiPco® and (b) ArcD SWCNT.

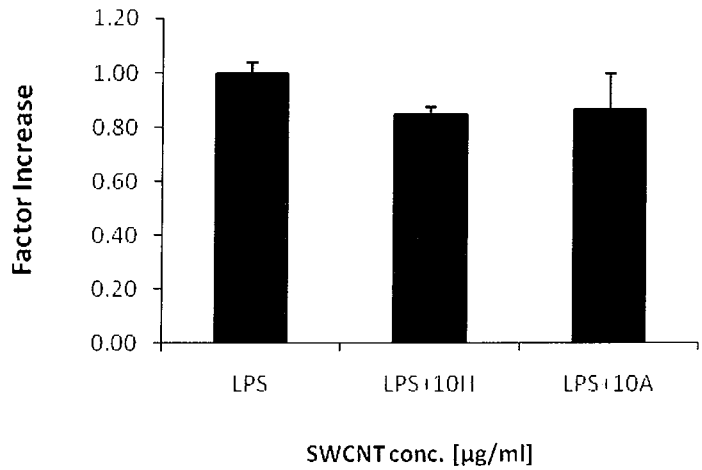

Figure 7.8: Factor increase in PGE_2 production per mg of total protein in MdM cells following 6h exposure to HiPco® (H) and ArcD (A) SWCNT followed by 1 h exposure to LPS.

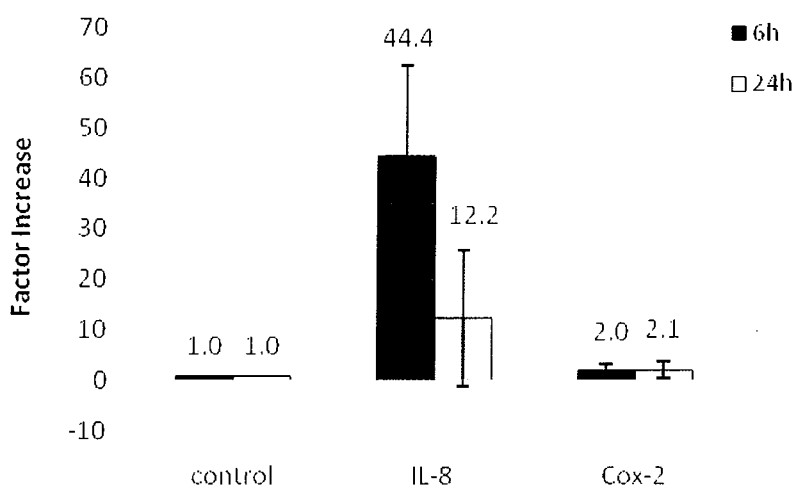

Figure 7.9: Effects of rhTNF-α stimulation on IL-8 and COX-2 mRNA expression of A549 cells following 6h and 24h.

When exposed to SWCNT, A549 cells did not show any increases in gene expression of COX-2, as illustrated in Figure 7.11. In contrast, decreases of mRNA expression were observed. Exposure to HiPco® SWCNT at a concentration of 50 μg/ml lead to decreases in COX-2 expression by up to 40% (Figure 7.11a). Arc discharge produced SWCNT were even more potent and decreases of up to 60% were observed at concentrations as low as 1 μg/ml (Figure 7.11b). Data variation, however, was too high to see any dose- or time-dependence of SWCNT effects.

As seen for MdM, exposure of A549 cells to the highest concentration of HiPco® SWCNT for 6 h slightly decreased the production of PGE_2 by 10% (Figure 7.12a). In contrast, ArcD SWCNT exposure resulted in increased PGE_2 production instead of suppression. This was however only significant following 1 hour exposure to 50 μg/ml (Figure 7.12b). No other exposure condition resulted in any significant effects. Hence, as seen for MdM exposures, the reductions observed for mRNA expression of particularly COX-2 do not appear to have consequences on PGE_2 formation.

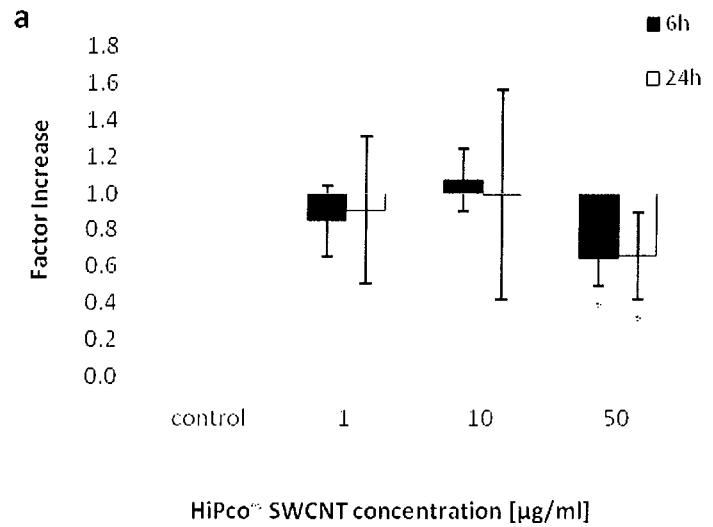

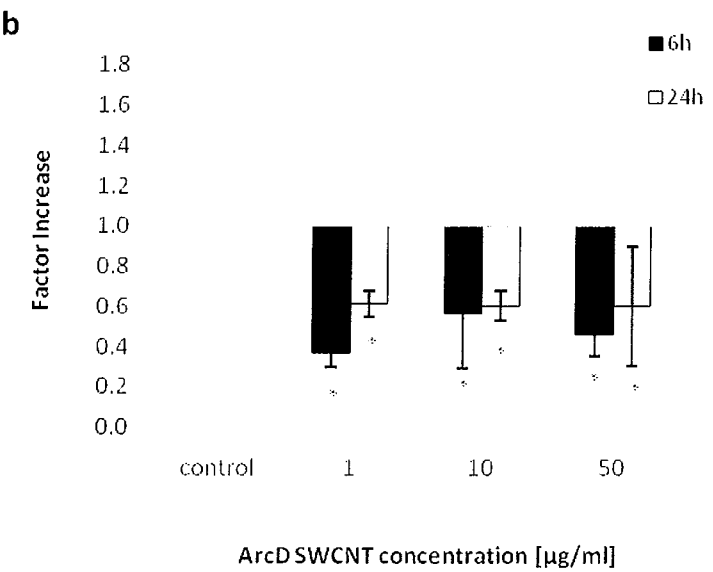

7

Figure 7.10: Changes in COX-2 mRNA expression following exposure of A549 cells to (a) HiPco® SWCNT and (b) ArcD SWCNT for 6h and 24h.

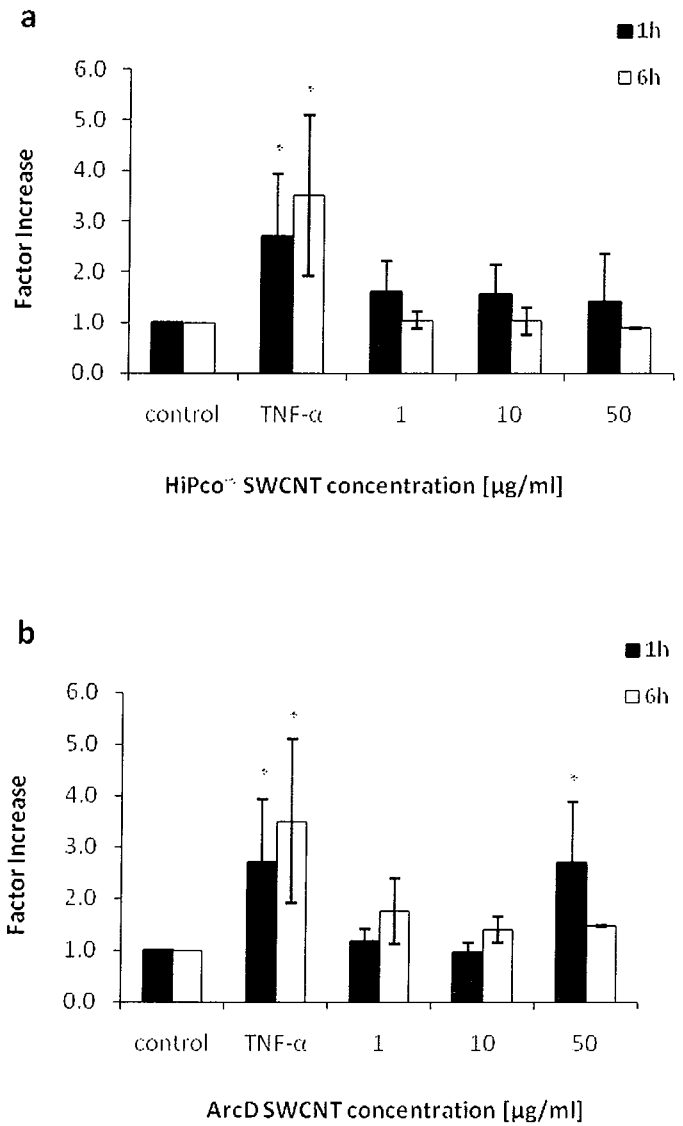

7

Figure 7.11: Factor increase in intracellular PGE_2 production per mg of total protein in A549 cells following 1h and 6h exposure to (a) HiPco® and (b) ArcD SWCNT.

7.5 Discussion

This study was carried out in order to investigate whether SWCNT can affect the molecular cell response of macrophages including lipid and inflammatory mediator release in order to obtain a more complete picture of SWCNT toxicity. Of particular interest was the question whether a bacterial stimulus can influence the inflammatory response of lung target cells to inhaled nanomaterials.

Alveolar macrophages are thought to be one of the primary target cells of nanomaterial toxicity as they represent the first defence mechanism against inhaled particles on the lung surfaces [364] [23] [24]. However, cells may become overloaded, phagocytic ability impaired and consequently clearance from the lung reduced. It has been shown that if macrophages attempt to phagocytose long fibres such as asbestos, and potentially also carbon nanotubes, the process of phagocytosis is frustrated and reactive oxygen species become released [151, 156, 356, 357]. This may be the initiating factor in the pathogenesis of lung disease after pulmonary exposure to fibres [357, 365]. In response to ultrafine particle exposure, agglomerates of ultrafine carbon particles have been shown to be taken up predominantly in phagolysosomes by alveolar macrophages [366] and cells respond by producing pro- and anti-inflammatory mediators, including metabolites of arachidonic acid [39]. Furthermore, macrophages demonstrated increased sensitivity, with regard to their ability to migrate towards a chemoattractant, impaired phagocytic ability and cytokine release following nanomaterial exposure [151, 367, 368].

7

Mononuclear cells in the circulation have the capacity for phagocytosis and propensity to differentiate to macrophages, migrate to the lung in response to injury [25] [26] and respond to endotoxins by IL-6 and IL-8 production in a manner similar to alveolar macrophages [27-29]. In this study, monocyte derived macrophages (MdM) were chosen as a test model as these cells can easily be obtained and differentiated. Human monocytes and therefore MdM can be identified by the expression of CD-14 receptors on their surfaces which is also involved in LPS-induced cytokine production [25, 361].

The mechanism of the effects of particles on alveolar macrophages as proposed by Beck-Speier *et al.* (2005) includes uptake of particle by cells and particle interference with cell membranes, leading to cell signalling cascades that initiate the formation of arachidonic acid which can in turn serve as a substrate for COX-2 and 5-LO leading to leukotriene and prostaglandin synthesis as described in Chapter 2 2.2.4.3 and illustrated in Figure 2.5 [39]. The formation of intracellular PGE_2 was identified as the most sensitive endpoint and was therefore investigated together with COX-2 gene expression.

In this study, SWCNT alone did not have any effect on intracellular PGE_2 concentrations or gene expression of macrophages. The same was true for A549 cells with the exception of ArcD SWCNT at concentrations of 50 μg/ml, which increased PGE2 formation by a factor of 2. As seen for IL-8 expression, COX-2 mRNA was down-regulated in A549 cells following SWCNT exposure.

Sequential exposure of MdM to SWCNT and LPS resulted in significant upregulation of COX-2, IL-8 and TNF-α transcripts compared to the effects of

SWCNT or LPS treatment alone. This may suggest a co-stimulatory effect of SWCNT on IL-8, COX-2 and TNF-α induction by toll-like receptor (TLR)-4 ligands such as LPS. Moreover, the absence of a direct effect of SWCNT on COX-2 induction indicates the absence of significant contamination by LPS and also shows that SWCNT *per se* do not stimulate via TLR-4. Hofer *et al.* (2004) reported similar findings following exposure of MdM and diesel particles. However, the co-stimulatory effect of diesel particles and LPS was less than that observed between SWCNT and LPS in this study [340]. Consequences of these synergistic effects would include general disturbance of the immune response which might render organisms susceptible to pathogens or increase their immune response. Increased frequency of infection or chronic inflammatory diseases may be the result.

However, no co-stimulatory effect could be observed on PGE_2 production in MdM cells and the effects seen on gene expression could not be confirmed on the level of protein production. In contrast, Hofer *et al.* (2004) reported increases in COX-2 protein as well as PGE_2 following co-stimulation of monocytic cell line MM6 to DEP and LPS [340]. Dutta *et al.* (2007) reported decreased COX-2 induction by LPS in the presence of SWCNT and Becker *et al.* (2005b) showed suppressed LPS-induced TNF-α and IL-8 release following exposure of alveolar macrophages to PM but not following carbon black treatment [212, 338].

Unfortunately, no definitive conclusion can be drawn on the effects of SWCNT exposure only on macrophages for any of the endpoints tested (gene expression of IL-8, COX-2 and TNF-α, intracellular TNF-α and PGE_2 or protein release of IL-8, IL-6, TNF-α and MCP-1). Great inter-individual variations were observed between responses of cells derived from different donors including cells responding to

SWCNT treatment by upregulation and downregulation of mRNA and proteins. Great variability of data obtained using blood cultures has also been previously reported by Howe *et al.* (2005). Authors observed an intra-variability of 7% and an inter-variability of around 20% [369]. In order to investigate this aspect in more detail, studies would need to be repeated including a larger number of cell donors which would allow carrying out improved statistical analysis. Furthermore, experiments would need to be repeated using blood from the same donors in order to determine intra-variability of the data obtained.

The fact that SWCNT on their own did not cause any upregulation of the cytokine expression indicates that no LPS contamination of particles was present. However, IL-8, IL-6 and TNF-α protein release were selectively increased following nanotube treatment.

The discrepancies observed between gene expression and protein release may also be due to differences in macrophage origin. Whereas mRNA and intracellular protein analysis was carried out on MdM derived from fresh blood samples, protein release studies were performed on MdM isolated from buffy coats. The storage and processing of blood samples before monocyte isolation as performed for buffy coat samples might have influenced cell performance. Therefore, it would be of advantage to carry out gene expression and protein analysis on the same set of cells.

7.6 Conclusion

Overall, SWCNT exposure did not have any effect on COX-2, IL-8 or TNF-α gene expression of MdM. Prostaglandin E_2 levels were only slightly affected following exposure to SWCNT. This was true for MdM and A549 cells. However, synergistic effects between SWCNT and LPS were observed on the gene expression of macrophages. In the presence of SWCNT, the response of MdM to LPS was increased in a synergistic manner compared to their response to LPS treatment in the absence of SWCNT. These effects appeared to be specific to mRNA transcription as they could not be confirmed on the level of protein formation and release. Great data variability and inconsistency of results was observed for protein data making interpretation difficult. This may point towards a role of macrophage origin for cell responses (fresh blood vs. buffy coat derived MdM) or the existence of responders and non-responders within the population. Including a higher number of cell donors and combined analysis of mRNA and proteins might help to resolve this issue. Due to the high data variability, the question whether DPPC dispersion may influence MdM responses was not investigated. However, as seen for epithelial cells (Chapter 6), inflammatory responses appeared to be affected by SWCNT exposure.

7

Chapter 8

Conclusions on the toxicity assessment of SWCNT

8.1 Challenges associated with the *in vitro* toxicity assessment of SWCNT

8.1.1 The field of nanotoxicology

"Nanotechnology is an area which has highly promising prospects for turning fundamental research into successful innovations, not only to boost the competitiveness of our industry but also to create new products that will make positive changes in the lives of our citizens, be it in medicine, environment, electronics or any other field." (European Commissioner for Science & Research, Janez Potočnik). The new field of nanotechnology not only brings about new innovations, it also leads to novel requirements in terms of risk assessment. Nanomaterials with their outstanding chemical and physical properties that make them so attractive for industrial and medical applications may also lead to unforeseen adverse effects upon environmental and human exposure. Furthermore, new types of xenobiotics may also require novel, alternative or improved approaches in terms of toxicity assessment.

Humans have always been exposed to different types of nanomaterials arising from natural sources, such as atmospheric photochemistry, volcanic activity and forest fires. Since the Industrial Revolution in Europe at the end of the 19th century, air pollution has become of global concern and combustion-derived particles such as diesel soot [370], welding fume [371], carbon black [368] and coal fly-ash [153] have been identified as health hazards [149]. Consequently, all

the knowledge drawn from studies on ultrafine particles can help in the understanding of nanomaterial toxicity.

8.1.2 Carbon nanotubes

Single-walled carbon nanotubes (SWNCT) are nanomaterials that are likely to be exploited commercially. Consequently production volumes may continue to rise so that SWCNT have been included into a set of reference materials and their safety testing has been recommended by the OECD [372]. Therefore, SWCNT toxicity assessment as carried out in this study could be of great value to nanomaterial risk assessment and nanotoxicology in general.

Carbon nanotubes are the type of nanomaterial that probably presents the greatest challenges to toxicity assessment. They are not only of nanoscaled diameter, but also of fibre shape, giving rise to concern due to the similarity to asbestos fibres which are known for their detrimental health effects [151, 156, 356, 357]. In addition, this form complicates physical characterisation of nanotube samples as particle size analysis is commonly based on the assumption of spherical geometry (e. g. DLS). The measurement and interpretation of optical spectra obtained during carbon nanotube characterisation is often difficult so that accurate sample characterisation remains a serious obstacle to SWCNT research [126], particle characterisation is of utmost importance for interstudy comparisons and the development of common mechanisms of nanomaterial toxicity.

Carbon nanotubes exist in many structural forms and thus varying electronic properties. For example each batch of SWCNT produced by the HiPco® method may contain around 50 different nanotube species with characteristic diameters and chiralities [126]. As illustrated in Figure 8.1, armchair SWCNT are metallic particles whereas zigzag and intermediate forms may be either semiconducting or semi-metallic depending on their structure [126]. Moreover, SWCNT can not only be produced by the HiPco® but also by electric ArcD or other methods as described in Chapter 2, 2.3.1. This in turn determines the type of contaminants present in raw SWCNT samples, including catalysts such as iron, nickel or yttrium and carbon soot. Different degrees of refinement lead to further variations in contaminant concentrations. Additionally, CNT can exist in various lengths, diameters and shapes ranging from small, rigid tubes to long and curly ones containing various structural defects. Every single type of SWCNT may have a unique toxicological profile. Consequently it is a great challenge to assess the toxicity of SWCNT in all their peculiarities making a defined set of relevant endpoints combined with high-throughput screening tools inevitable.

Their highly adsorptive nature creates further challenges. Single walled carbon nanotubes tend to aggregate in bundles that are bound by van der Waals attractions. The resulting tube-tube pertubations prevent detailed spectral analysis of particle samples due to broadening and blurring of optical spectra. Together with their insolubility in biological media, it frequently results in highly polydispersed samples, which makes characterisation difficult and toxicity testing of singly dispersed raw nanotube samples impracticable. In addition, it leads to adsorption of a variety of organic molecules onto carbon nanotube surfaces

(4.4.1.5). This may have consequences on their intrinsic toxicity leading to indirect effects as described in Chapter 4, 4.4.1.5. Absorbance and fluorescence quenching or protein adsorption may give rise to interactions with commonly used toxicity test systems leading to false measurements and the risk of data misinterpretation. As a result, screening for potential interactions as carried out within the studies described in Chapters 3, 4 and 6 (3.4.3; 4.4.1.5; 6.4.2) and taking them into account is essential when working with carbon nanotube and other carbon based nanomaterials (3.4.3; 4.4.1.5; 6.4.2). Furthermore, identification and development of alternative test methods may be required (Chapter 4).

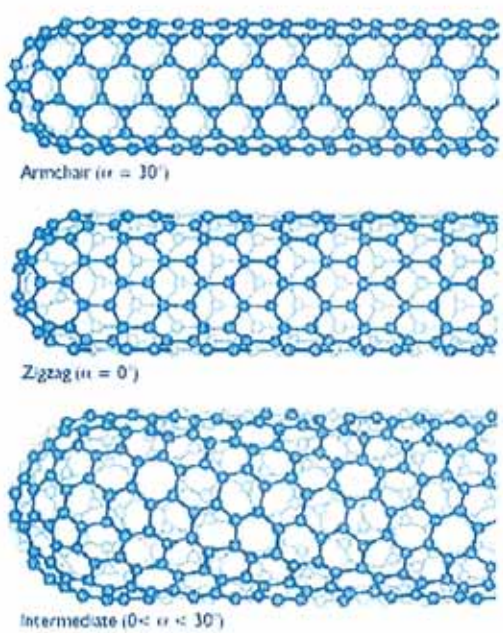

8

Figure 8.1: Different structures of SWCNT depending on their chirality (wrapping angle) including "armchair", "zigzag" and intermediate structures [126].

Sorting of SWCNT by their different structures and therefore physical properties remains an enormous challenge to their commercial applications [126]. This in turn may question the real risk associated with SWCNT. If SWCNT will not be produced and used on a large scale, risk will be limited. Unfortunately to date, there is very limited data available on the real environmental and human nanomaterial exposure levels which would be essential for risk assessment. Hazard is defined as the potential to cause harm but risk on the other hand is the likelihood of harm. Even though it is presumed that SWCNT pose a hazard to human and environmental health [44, 182, 183, 201, 202, 373], it is still unknown whether they also pose a risk. *"Dosis sola venenum facit."* (Paracelsus), so that more data is needed in order to determine wether exposure to SWCNT may reach levels high enough to induce adverse health effects. Only if carbon nanotubes become airborne in large quantities and are consequently inhaled, they have the potential to interact with human tissue. Nevertheless, they are in production at present so that the immediate need exists for toxicity testing and risk assessment. During manufacture, human exposure would most likely be of an occupational type so that this study focused on the effects of raw SWCNT dust samples rather than the intrinsic toxicity of isolated nanotubes. Consequently, samples were only processed minimally without attempting to refine, functionalise or homogeneously disperse them. As the lungs represent one of the main target tissues of occupational exposure, exposures were primarily carried out on pulmonary epithelial cells. One of the best paradigms of nanomaterial toxicity is represented by the hierarchical oxidative stress model as described in Chapter 2, 2.2.4.3. Therefore, endpoints investigated within the course of this study included

cytotoxicity and cell proliferation, oxidative stress, lipid and inflammatory mediator responses of exposed cells.

8.2 Conclusions on SWCNT toxicity derived from the present study

8.2.1 Overall findings on the toxicity of SWCNT

Throughout this study, attention was paid to choose the most relevant dispersion vehicle for pulmonary toxicity assessment and considering its influence on SWCNT reactivity. Although individual SWCNT are only a few nanometres in diameter, they are grown in bundles and remain as such in aqueous media and when suspended in cell culture medium [255]. Due to their highly adsorptive nature, it is most likely that during human exposure, particles such as CNT would come into contact with a variety of different molecules leading to coating by various components present within a biological system [54, 214, 230]. For that reason, it was decided to use FBS as a media supplement since it seemed to be the most relevant exposure scenario. Raman and fluorescence emission analysis indicated that FBS can aid the dispersion of SWCNT but there was no apparent debundling or reduction in agglomeration state over the concentration range studied [255].

Upon inhalation, particles deposited on lung tissue will come into contact with lung lining fluid which is made up of lung surfactant. The main component of this lung surfactant, DPPC, dispersed in physiological saline has been recognised as simple model of lung lining fluid [69, 240]. The use of DPPC as nanomaterial dispersant

was therefore considered to increase biological relevance of exposure set-ups and was included as additional dispersion vehicle within this study. Although the use of DPPC further improved SWCNT dispersion, nanotubes still remained highly agglomerated (Chapter 5, 5.4.1). Of course, the degree of dispersion ultimately determines the way in which particles are presented to exposed tissue which has severe consequences for their toxicity as bundles of SWCNT expose a smaller reactive surface area compared to the same mass of SWCNT present in single entities. Increased sample size also reduces the likelihood of cellular internalization. No evidence of cellular uptake was also seen in this study following TEM analysis (3.4.4.4).

Investigations of the *in vitro* cytotoxicity of HiPco® SWCNT on human lung carcinoma cells (A549), as described in Chapter 3, revealed only low acute toxicity. High concentrations of SWCNT (>100 µg/ml) were needed in order to reduce cell viability following exposure for 24 h. This effect was confirmed on the basis of overall cell metabolism (AB assay), lysosomal viability (NR assay), mitochondrial activity (MTT and WST-1 assays) and cellular protein content (CB assay). Serum supplements had only very slight effects on the cytotoxicities of SWCNT (Chapter 3, 3.4.2.1) but DPPC dispersion could increase particle toxicity (Chapter 6, 6.4.8).

The existence of interactions between SWCNT and the toxicity indicators employed was identified and characterised using spectroscopical studies, further validating the absence of acute cytotoxicity since fluorescence and absorbance quenching by the nanotubes due to adsorption of indicator dye molecules onto SWCNT surfaces contributed to the toxicity determined using indicator dyes. However, prolonged exposure of cells to SWCNT did lead to increased cell toxicity

8

indicating that SWCNT can affect cell performance over time. Yet, SWCNT-dye interaction prevented exact quantification of data. In order to overcome this problem, more qualitative toxicity assessment was carried out including cell staining and microscopy (Chapter 3, 3.4.4). Following short-term exposure over 24 h, Trypan Blue staining confirmed the findings obtained using fluorescence/absorbance based assays (Chapter 3, 3.4.4.1) and PI staining revealed cell necrosis in proximity to SWCNT agglomerates attached to the cell monolayer (Chapter 3, 3.4.4.2). No intracellular localization of SWCNT was seen in A549 as analysed using TEM. However, increased numbers of surfactant storing lamellar bodies were observed in exposed cells (Chapter 3, 3.4.4.4). Following extended exposure periods of 96 h, immunostaining revealed cytoskeletal changes characterised by disruption in actin and tubulin filament organisation including accumulation of actin and tubulin around SWCNT particles (Chapter 3, 3.4.4.3).

The clonogenic assay was employed as an alternative to dye based toxicity assessment in order to improve quantification of SWCNT exposure effects (Chapter 4). Furthermore, it allowed the assessment of a more chronic exposure to the particles. Using this assay, it was shown that the toxicity differs between HiPco® and ArcD produced SWCNT with HiPco® SWCNT samples being more reactive. Both types of SWCNT elicited a stronger cytotoxic response than carbon black nanoparticles. Furthermore, it was possible to distinguish between effects on cell viability and cell proliferation by including colony size as an additional endpoint in the clonogenic assay. All three particle types tested were highly effective in inhibiting cell proliferation.

The effects seen for SWCNT cytotoxicity were not specific to pulmonary cell models but were also seen for dermal cells, represented by the normal human keratinocyte cell line HaCaT which was included as a second cell model for comparison purposes.

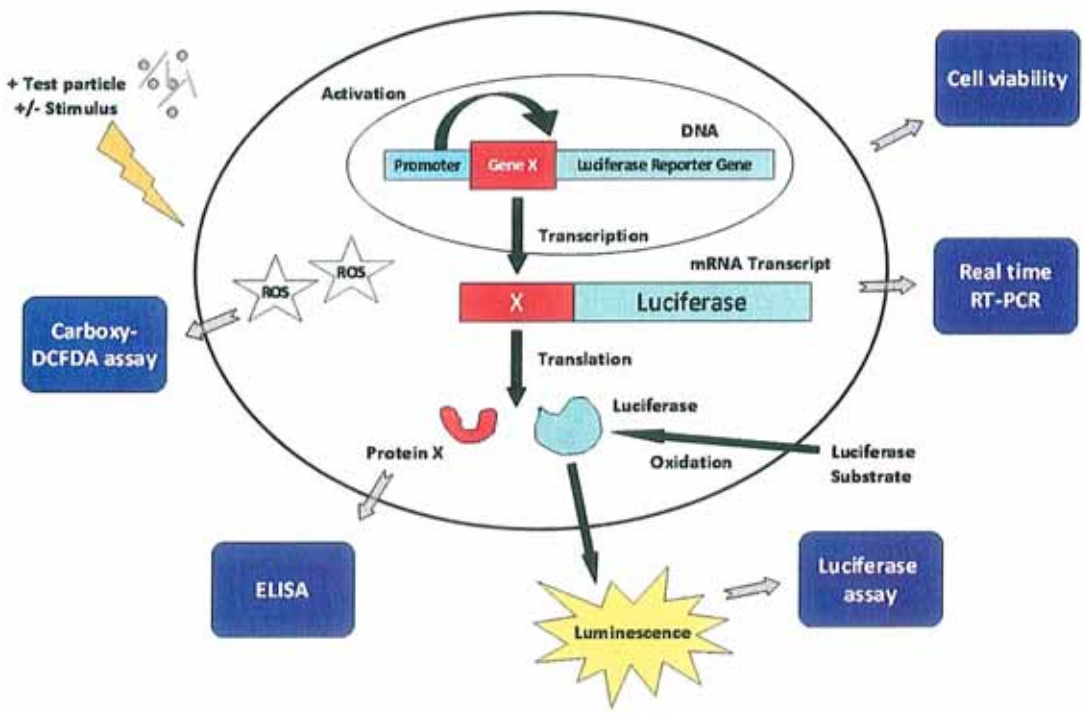

Figure 8.2: Study design for the evaluation of SWCNT toxicity on the sub-cellular level.

It was shown that SWCNT not only interact with colorimetric indicator dyes, but also components of cell culture medium including FBS [54, 255, 257]. Therefore, the potential of SWCNT to induce indirect effects by adsorbing essential nutrients was investigated. It could be demonstrated that cell viability as well as clonogenic survival was impaired following long-term exposure to SWCNT depleted culture medium (Chapter 4, 4.4.1.5.2). Therefore, the toxicity of SWCNT is not only attributed to its direct effects on exposed cells but also indirect effects on their biological environment.

As illustrated in Figure 8.2, a combination of cell viability assays, promoter activation, gene expression, protein and ROS analysis was employed to further investigate the mechanisms of SWCNT toxicity and their effects on the sub-cellular level, including the release of lipid and inflammatory mediators.

In the presence of FBS, HiPco® SWCNT exposure never induced an inflammatory response in exposed cells. This was characterised by suppression of IL-8 gene expression as well as IL-8, IL-6 and MCP-1 protein release (Chapter 6, 6.4.5). The same effect was seen upon exposure of cells that had already been induced by treatment with the immunological stimulant TNF-α and was true for both the carcinoma cell line A549 and the primary human bronchial epithelial cells (NHBE). Dispersion in DPPC solution even augmented the suppressive effects observed.

It was also observed that the presence of SWCNT lead to decreases in TNF-α concentrations in samples of culture medium spiked with known amounts of rhTNF-α in the absence of cells. Therefore, indirect effect due TNF-α adsorption may contribute to the decreases in inflammatory responses seen following SWCNT exposure (Chapter 6, 6.4.2).

Both HiPco® and ArcD produced SWCNT did not seem to increase but instead were found to decrease COX-2 gene expression of lung epithelial cells as seen for IL-8 expression. However, only ArcD SWCNT slightly increased the synthesis of the lipid mediator PGE_2. Therefore, COX-2 downregulation does not seem to be directly related to PGE_2 formation and its consequences remain unknown (Chapter 7). It also remains unknown whether SWCNT exposure may affect other arachidonic acid metabolites such as leukotrienes or isoprostanes.

Overall, these results would indicate that SWCNT do not elicit an inflammatory response in exposed epithelial tissue and therefore no tier 2 oxidative stress response at concentrations up to 50 μg/ml. However, suppression of immunological responses may change the status quo of the immune system rendering it less reactive towards infections. In case of oxidative stress, as seen following cell exposures to DPPC dispersed SWCNT (Chapter 5, 5.4.2), activation of an immune response is needed and cell signalling by lung epithelial cells is of great importance to attract phagocytic cells which represent the first line of defence against invading particles and are needed for tissue clearance, to the site of particle deposition [23].

No definite conclusion could be drawn as to whether HiPco® SWCNT samples have the potential of reacting in an asbestos-like manner. The likelihood of fibres to be pathogenic is believed to depend on three aspects. They have to be thin enough to gain access to the lung but need to be of a length too long to be removed by macrophages (>15 μm). In addition they have to be biopersistent and therefore insoluble in biological environments leading to a build up in exposed tissue [44]. Carbon nanotubes would theoretically and potentially fulfil all three requirements, having a nanosize diameter and being up to several microns long (at least in the absence of agglomeration). They are very stiff and insoluble in aqueous media. Consequently there is reasonable concern about their safety. Within this study, only asbestos was able to slightly increase IL-8 and IL-6 responses. In contrast, both particle types were able to selectively decrease IL-8, IL-6 and MCP-1 and changed their reactivity following DPPC dispersion (Chapter 6, 6.4.8). However, suppression of IL-8 was generally greater (Chapter 6, 6.4.5) and ROS production

always higher (Chapter 5, 5.4.2) following HiPco® SWCNT exposure compared to asbestos exposure. Therefore, HiPco® SWCNT exposures showed similarities but also differences to crocidolite asbestos so that risk assessment needs further comparative studies including additional endpoints.

The principle targets of pulmonary SWCNT exposure are not only lung epithelial cells but also macrophages which clear the alveolar region from deposited material [22, 23]. Responses by the macrophages to inhaled foreign material are essential for appropriate immune responses but impaired function is believed to play a key role in the pathogenesis of some lung disease, e. g. through frustrated phagocytosis [24, 106, 151, 158, 356, 357, 365]. When macrophages encounter ultrafine particles, they have been shown to release a variety of cytokines, affect the arachidonic acid pathway and show decreased phagocytic ability [39, 338, 367, 374]. Using these cells as an additional cell model to previously employed A549 lung epithelial cells would allow a more complete picture of the pulmonary toxicity of SWCNT to be obtained. Therefore, monocyte derived macrophages (MdM) were chosen as a further test model (Chapter 7). As for studies on lung epithelium, endpoints investigated included cytotoxicity, gene expression COX-2, intracellular PGE_2, IL-8 expression and protein release, IL-6, TNF-α and MCP-1 release.

Great variability was seen for all responses of MdM following SWCNT treatment which indicates that particle effects were strongly influenced by cellular origin with the consequence that no significant effects of SWCNT exposure could be determined during this study. However, on the level of gene expression, it could be shown that co-stimulation of macrophages with SWCNT and LPS resulted in synergistic effects in terms of IL-8, COX-2 and TNF-α expression. In the presence of

SWCNT exposure, treatment with LPS led to significant increases in cell stimulation compared to the treatment with LPS only. This in turn may lead to an overstimulation of the immune system in case of co-existence of both bacterial infections and SWCNT inhalation. However, in this study the co-stimulatory effect of SWCNT and LPS could not be confirmed on the basis of protein release (Chapter 7, 7.4.1.2). Unfortunately, gene expression was only analysed using macrophages derived from fresh blood whereas protein analysis was mainly performed on buffy coat derived cells. Cell origin may therefore account for the discrepancies observed and combined mRNA and protein analysis would need to be carried out. However, overall, there are indications that some donors do elicit inflammatory responses upon SWCNT exposure but further investigations including larger numbers of cell donors would be needed to assess whether responders and non-responders exist within the population. As soon as these issues have been resolved, the influence of DPPC dispersion on MdM responses would be of interest. Furthermore, exposure of macrophages and lung epithelial cells was carried out separately, whereas co-culture of epithelial cells, macrophages and possibly also dendritic cells would represent a more realistic exposure scenario allowing cell signalling and interaction between cell types [375-377].

8

8.2.2 Final recommendations

Over the course of this study it was observed that exposure to SWCNT not only affected cell viability and proliferation (Chapter 3 and 4) but also cell signalling (Chapters 6 and 7). With regard to particle exposure, the interplay between cell

types is of utmost importance so that, co-culture studies may represent a next step in the toxicity assessment of nanotubes and nanomaterials in general to increase biological relevance.

Throughout this study, interaction between SWCNT and biological systems was observed including binding of culture medium components and decrease of TNF-α concentrations due to SWCNT exposure, leading to indirect toxicity. Furthermore, interaction with serum proteins and DPPC influenced the direct toxicity and oxidative potential of SWCNT. Similar interactive effects of CNT material were also reported by other authors including adsorption of various amino acids and vitamins from cell culture medium leading to decreased cell viability, as reported by Guo *et al.* (2008) [230], binding of lung surfactant proteins, as investigated by Salvador-Morales *et al.* (2007), potentially leading to lung infection and emphysema [12], or interactions of MWCNT with the MARCO receptor leading to rupture of macrophage membranes as described by Hirano *et al.* (2008) [215]. This highlights the great relevance and importance of particle environment and dispersion medium for CNT toxicity. Due to their highly adsorptive properties, this is possibly even more relevant for carbon based nanomaterials than other types of nanosized materials. As a result, the analysis of the so-called "protein corona" of nanomaterials may be a key-indicator of their biological effects [326, 378]. Together with gene expression and protein analysis, this would need to be carried out on a large-scale, high-throughput basis due to the vast number of different types of SWCNT and even larger numbers of nanomaterials requiring toxicity assessment.

References

[1] Royal Society and Royal Academy of Engineering. Nanoscience and nanotechnologies: opportunities and uncertainties. *Royal Society Publications, London;* 2004. www.royalsoc.ac.uk/policy (accessed 03.12.2005).

[2] Iijima, S. Helical Microtubules of Graphitic Carbon. *Nature* **354:**56-58; 1991.

[3] Ding, L.; Stilwell, J.; Zhang, T.; Elboudwarej, O.; Jiang, H.; Selegue, J. P.; Cooke, P. A.; Gray, J. W.; Chen, F. F. Molecular characterization of the cytotoxic mechanism of multiwall carbon nanotubes and nano-onions on human skin fibroblast. *Nano Letters* **5:**2448-2464; 2005.

[4] Dreher, K. L. Health and Environmental Impact of Nanotechnology: Toxicological assessment of manufactured nanoparticles. *Toxicological Sciences* **77:**3-5; 2004.

[5] Bottini, M.; Bruckner, S.; Nika, K.; Bottini, N.; Bellucci, S.; Magrini, A.; Bergamaschi, A.; Mustelin, T. Multi-walled carbon nanotubes induce T lymphocyte apoptosis. *Toxicology Letters* **160:**121-126; 2006.

[6] Thess, A.; Lee, R.; Nikolaev, P.; Dai, H.; Petit, P.; Robert, J.; Xu, C.; Lee, Y. H.; Kim, S. G.; Rinzler, A. G.; Colbert, D. T.; Scuseria, G. E.; Tomanek, D.; Fisher, J. E.; Smalley, R. E. Crystalline ropes of metallic carbon nanotubes. *Science* **273:**483-487; 1996.

[7] Hedderman, T. G.; Keogh, S. M.; Chambers, G.; Byrne, H. J. Solubilization of SWNTs with organic dye molecules. *Journal of Physical Chemistry B* **108:**18860-18865; 2004.

[8] Valentini, L.; Armentano, I.; Ricco, L.; Alongi, J.; Pennelli, G.; Mariani, A.; Russo, S.; Kenny, J. M. Selective interaction of single-walled carbon nanotubes with conducting dendrimer. *Diamond and Related Materials* **15:**95-99; 2006.

[9] Casey, A.; Farrell, G. F.; McNamara, M.; Byrne, H. J.; Chambers, G. Interaction of carbon nanotubes with sugar complexes. *Synthetic Metals* **153:**357-360; 2005.

[10] Chambers, G.; Carroll, C.; Farrell, G. F.; Dalton, A. B.; McNamara, M.; Panhuis, M. I. H.; Byrne, H. J. Characterization of the interaction of gamma cyclodextrin with single-walled carbon nanotubes. *Nano Letters* **3:**843-846; 2003.

[11] Moulton, S. E.; Minett, A. I.; Murphy, R.; Ryan, K. P.; McCarthy, D.; Coleman, J. N.; Blau, W. J.; Wallace, G. G. Biomolecules as selective dispersants for carbon nanotubes. *Carbon* **43:**1879-1884; 2005.

[12] Salvador-Morales, C.; Townsend, P.; Flahaut, E.; Vénien-Bryan, C.; Vlandas, A.; Green, M. L. H.; Sim, R. B. Binding of pulmonary surfactant proteins to carbon nanotubes; potential for damage to lung immune defence mechanisms. *Carbon* **45:**607-617; 2007.

[13] Driscoll, K. E.; Guthrie, G. D. Editorial. Comprehensive toxicology - toxicology of the respiratory system. **8:**373-391; 1997.

[14] Takizawa, H. Airway epithelial cells as regulators of airway inflammation (Review). *International Journal of Molecular Medicine* **1:**367-378; 1998.

[15] Barlow, P. G.; Clouter-Baker, A.; Donaldson, K.; Maccallum, J.; Stone, V. Carbon black nanoparticles induce type II epithelial cells to release chemotaxins for alveolar macrophages. *Particle and Fibre Toxicology* **2:**11; 2005.

[16] O'Brien, A. D.; Standiford, T. J.; Christensen, P. J.; Wilcoxen, S. E.; Paine, R. Chemotaxis of alveolar macrophages in response to signals derived from alveolar epithelial cells. *Journal of Laboratory and Clinical Medicine* **131:**417-424; 1998.

[17] Timblin, C. R.; Shukla, A.; Berlanger, I.; BeruBe, K. A.; Churg, A.; Mossman, B. T. Ultrafine airborne particles cause increases in protooncogene expression and proliferation in alveolar epithelial cells. *Toxicology and Applied Pharmacology* **179:**98-104; 2002.

[18] Hawgood, S.; Clements, J. A. Pulmonary Surfactant and Its Apoproteins. *Journal of Clinical Investigation* **86:**1-6; 1990.

[19] Donaldson, K.; Borm, P. J.; Oberdörster, G.; Pinkerton, K. E.; Stone, V.; Tran, C. L. Concordance between *in vitro* and *in vivo* dosimetry in the proinflammatory effects of low-toxicity, low-solubility particles: the key role of the proximal alveolar region. *Inhalation Toxicology* **20:**53-62; 2008.

[20] Bhaskaran, M.; Kolliputi, N.; Wang, Y.; Gou, D. M.; Chintagari, N. R.; Liu, L. Trans-differentiation of alveolar epithelial type II cells to type I cells involves autocrine signaling by transforming growth factor beta 1 through the Smad pathway. *Journal of Biological Chemistry* **282:**3968-3976; 2007.

[21] Oberdörster, G.; Maynard, A.; Donaldson, K.; Castranova, V.; Fitzpatrick, J.; Ausman, K.; Carter, J.; Karn, B.; Kreyling, W.; Lai, D.; Olin, S.; Monteiro-Riviere, N.; Warheit, D.; Yang, H. Principles for characterizing the potential human health effects from exposure to nanomaterials: elements of a screening strategy. *Particle and Fibre Toxicology* **2**:8; 2005.

[22] Li, N.; Sioutas, C.; Cho, A.; Schmitz, D.; Misra, C.; Sempf, J.; Wang, M.; Oberley, T.; Froines, J.; Nel, A. Ultrafine particulate pollutants induce oxidative stress and mitochondrial damage. *Environmental health perspectives* **111**:455-460; 2003.

[23] Castranova, V.; Bowman, L.; Reasor, M. J.; Lewis, T.; Tucker, J.; Miles, P. R. The Response of Rat Alveolar Macrophages to Chronic Inhalation of Coal-Dust and/or Diesel Exhaust. *Environmental research* **36**:405-419; 1985.

[24] Driscoll, K. E.; Carter, J. M.; Hassenbein, D. G.; Howard, B. Cytokines and particle-induced inflammatory cell recruitment. *Environmental health perspectives* **105 Suppl 5**:1159-1164; 1997.

[25] Randolph, G. J.; Jakubizick, C.; Qu, C. Antigen presentation by monocytes and monocyte-derived cells. *Current opinion in Immunology* **20**:1-9; 2007.

[26] Andreesen, R.; Brugger, W.; Scheibenbogen, C.; Kreutz, M.; Leser, H. G.; Rehm, A.; Lohr, G. W. Surface phenotype analysis of human monocyte to macrophage maturation. *Journal of Leukocyte Biology* **47**:490-497; 1990.

R

[27] Kotloff, R. M.; Little, J.; Elias, J. A. Human alveolar macrophage and blood monocyte interleukin-6 production. *American journal of respiratory cell and molecular biology* **3:**497-505; 1990.

[28] Monn, C.; Becker, S. Cytotoxicity and induction of proinflammatory cytokines from human monocytes exposed to fine (PM2.5) and coarse particles (PM10-2.5) in outdoor and indoor air. *Toxicology and Applied Pharmacology* **155:**245-252; 1999.

[29] Sandiford, T. J.; Kunkel, S. L.; Rolfe, M. W.; Evanoff, H. L.; Allen, R. M.; Strieter, R. M. Regulation of human alveolar macrophage- and blood monocyte-derived interleukin-8 by prostaglandin E2 and dexamethasone. *Journal of Respiratory Cell and Molecular Biology* **6:**75-81; 1992.

[30] Monteiro-Riviere, N. A.; Inman, A. O. Challenges for assessing carbon nanomaterial toxicity to the skin. *Carbon* **44**:1070 – 1078; 2006.

[31] Shvedova, A. A.; Castranova, V.; Kisin, E. R.; Schwegler-Berry, D.; Murray, A. R.; Gandelsman, V. Z.; Maynard, A.; Baron, P. Exposure to carbon nanotube material: assessment of nanotube cytotoxicity using human keratinocyte cells. *Journal of Toxicology and Environmental Health A* **66:**1909-1926; 2003.

R

[32] Van de Sandt, J.; Roguet, R.; Cohen, C.; Esdaile, D.; Ponec, M.; Corsini, E.; Barker, C.; Fusenig, N.; Liebsch, M.; Benford, D.; dem Brugerolle de Fusenig, A.; Fartasch, M. The use of human keratinocytes and human skin models for predicting skin irritation. The Report and Recommendations of ECVAM Workshop 38. *ECVAM Workshop*: ATLA; 1999: 723-743.

[33] Chiang, I. W.; Brinson, B. E.; Smalley, R. E.; Margrave, J. L.; Hauge, R. H. Purification and characterization of single-wall carbon nanotubes. *Journal of Physical Chemistry B* **105:**1157-1161; 2001.

[34] Nikolaev, P.; Bronikowski, M. J.; Bradely, R. K.; Rohmund, F.; Colbert, D. T.; Smith, K. A.; Smalley, R. E. Gas-phase catalytic growth of single walled carbon nanotubes from carbon monoxide. *Chemical Physics Letters* **313:**91-97; 1999.

[35] Yudasaka, M.; Kataura, H.; Ichihashi, T.; Qin, L. C.; Kar, S.; Iijima, S. Diameter enlargement of HiPco single-wall carbon nanotubes by heat treatment. *Nano Letters* **1:**487-489; 2001.

[36] Iijima, S.; Ichihashi, T. Single shell nanotubes of 1-nm diamter. *Nature* **363:**603-605; 1993.

[37] Baan, R. A. Carcinogenic hazards from inhaled carbon black, titanium dioxide, and talc not containing asbestos or asbestiform fibers: Recent evaluations by an IARC Monographs working group. *Inhalation Toxicology* **19:**213-228; 2007.

[38] Barlow, P. G.; Donaldson, K.; MacCallum, J.; Clouter, A.; Stone, V. Serum exposed to nanoparticle carbon black displays increased potential to induce macrophage migration. *Toxicology Letters* **155:**397-401; 2005.

[39] Beck-Speier, I.; Dayal, N.; Karg, E.; Maier, K. L.; Schumann, G.; Schulz, H.; Semmler, M.; Takenaka, S.; Stettmaier, K.; Bors, W.; Ghio, A.; Samet, J. M.; Heyder, J. Oxidative stress and lipid mediators induced in alveolar macrophages by ultrafine particles. *Free Radical Biology and Medicine* **38:**1080-1092; 2005.

[40] Wilson, M. R.; Lightbody, J. H.; Donaldson, K.; Sales, J.; Stone, V. Interactions between ultrafine particles and transition metals *in vivo* and *in vitro*. *Toxicology and Applied Pharmacology* **184:**172-179; 2002.

[41] Creutzenberg, O.; Hansen, T.; Ernst, H.; Muhle, H.; Oberdörster, G.; Hamilton, R. Toxicity of a quartz with occluded surfaces in a 90-day intratracheal instillation study in rats. *Inhalation Toxicology* **20:**995-1008; 2008.

[42] Duffin, R.; Tran, L.; Brown, D.; Stone, V.; Donaldson, K. Proinflammogenic effects of low-toxicity and metal nanoparticles *in vivo* and *in vitro*: Highlighting the role of particle surface area and surface reactivity. *Inhalation Toxicology* **19:**849-856; 2007.

[43] Warheit, D. B.; Webb, T. R.; Reed, K. L. Pulmonary toxicity screening studies in male rats with M5 respirable fibers and particulates. *Inhalation Toxicology* **19:**951-963; 2007.

[44] Donaldson, K.; Aitken, R.; Tran, L.; Stone, V.; Duffin, R.; Forrest, G.; Alexander, A. Carbon nanotubes: a review of their properties in relation to pulmonary toxicology and workplace safety. *Toxicological Sciences* **92:**5-22; 2006.

[45] Albin, M.; Pooley, F. D.; Stromberg, U.; Attewell, R.; Mitha, R.; Johansson, L.; Welinder, H. Retention patterns of asbestos fibers in lung-tissue among asbestos-cement workers. *Occupational and Environmental Medicine* **51:**205-211; 1994.

[46] Heintz, N. H.; Janssen, Y. M.; Mossman, B. T. Persistent Induction of C-Fos and C-Jun expression by asbestos. *Proceedings of the National Academy of Sciences of the United States of America* **90:**3299-3303; 1993.

[47] Mossman, B. T. Assessment of the pathogenic potential of asbestiform vs. nanoasbestiform particulates (cleavage fragments) in *in vitro* (cell or organ culture) models and bioassays. *Regulatory Toxicology and Pharmacology* **52:**200-203; 2008.

[48] Jia, G.; Wang, H.; Yan, L.; Wang, X.; Pei, R.; Yan, T.; Zhao, Y.; Guo, X. Cytotoxicity of carbon nanomaterials: single-wall nanotube, multi-wall nanotube, and fullerene. *Environmental Science and Technology* **39:**1378-1383; 2005.

R

[49] Kagan, V. E.; Tyurina, Y. Y.; Tyurin, V. A.; Konduru, N. V.; Potapovich, A. I.; Osipov, A. N.; Kisin, E. R.; Schwegler-Berry, D.; Mercer, R.; Castranova, V.; Shvedova, A. A. Direct and indirect effects of single walled carbon nanotubes on RAW 264.7 macrophages: role of iron. *Toxicology Letters* **165:**88-100; 2006.

[50] Monteiro-Riviere, N. A.; Nemanich, R. J.; Inman, A. O.; Wang, Y. Y.; Riviere, J. E. Multi-walled carbon nanotube interactions with human epidermal keratinocytes. *Toxicology Letters* **155:**377-384; 2005.

[51] Pulskamp, K.; Wörle-Knirsch, J. M.; Hennrich, F.; Kern, K.; Krug, H. Human lung-epithelial cells show biphasic oxidative burst after single-walled carbon nanotube contact. *Carbon* **45:**2241-2249; 2007.

[52] Tian, F.; Cui, D.; Schwarz, H.; Estrada, G. G.; Kobayashi, H. Cytotoxicity of single-wall carbon nanotubes on human fibroblasts. *Toxicology In Vitro* **20:**1202-1212; 2006.

[53] Oberdörster, G. Significance of particle parameters in the evaluation of exposure-dose-response relationships of inhaled particles. *Inhalation Toxicology* **8:**73-89; 1996.

[54] Casey, A.; Herzog, E.; Lyng, F. M.; Byrne, H. J.; Chambers, G.; Davoren, M. Single walled carbon nanotubes induce indirect cytotoxicity by mediumdepletion in A549 lungcells. *Toxicology Letters* **179(2):**78-85; 2008.

[55] Hamilton, R. F., Jr.; Thakur, S. A.; Holian, A. Silica binding and toxicity in alveolar macrophages. *Free Radical Biology and Medicine* **44:**1246-1258; 2008.

[56] Davoren, M.; Herzog, E.; Casey, A.; Cottineau, B.; Chambers, G.; Byrne, H. J.; Lyng, F. M. *In vitro* toxicity evaluation of single walled carbon nanotubes on human A549 lung cells. *Toxicology In Vitro* **21:**438-448; 2007.

[57] Lucca, E.; Angeretti, N.; Forloni, G. Influence of cell culture conditions on the protective effect of antioxidants against B-amyloid toxicity: studies with lazaroids. *Brain Research* **764:**293-298; 1997.

[58] Ribéreau-Gayon, G.; Jung, M.-L.; Beck, J.-P.; Anton, R. Effect of fetal calf serum on the cytotoxic activity of mistletoe (*Viscum album*L.) lectins in cell culture. *Phototherapy Research* **9:**336-339; 2006.

[59] Hook, G. E. R. Does Pulmonary surfactant aid in defence of the lungs. *Environmental Health Perspectives* **101:**98-98; 1993.

[60] Schürch, S.; Lee, M.; Gehr, P. Pulmonary surfactant - Surface-properties and function of alveolar and airway surfactant. *Pure and Applied Chemistry* **64:**1745-1750; 1992.

[61] Dobbs, L. G.; Wright, J. R.; Hawgood, S.; Gonzalez, R.; Venstrom, K.; Nellenbogen, J. Pulmonary surfactant and its components inhibit secretion of phosphatidylcholine from cultured rat alveolar type II cells. *Proceedings of the Acadamey of Natural Sciences USA* **84:**1010-1014; 1987.

[62] King, R. J. Pulmonary surfactant. *Journal of Applied Physiology* **53:**1-8; 1982.

[63] Scarpelli, E. M. Lung surfactant: dynamic properties, metabolic pathways, and possible significance in the pathogenesis of the respiratory distress syndrome. *Bulletin of the New York Academy of Medicine* **44:**431-445; 1968.

[64] Gajdosikova, A.; Gajdosik, A.; Koneracka, M.; Zavisova, V.; Stvrtina, S.; Krchnarova, V.; Kopcansky, P.; Tomasovicova, N.; Stolc, S.; Timko, M. Acute toxicity of magnetic nanoparticles in mice. *Neuroendocrinology Letters* **27 Suppl 2:**96-99; 2006.

[65] Griese, M. Pulmonary surfactant in health and human lung diseases: state of the art. *European Respiratory Journal* **13:**1455-1476; 1999.

[66] Griese, M.; Beck, J. The interaction of phosphatidylcholine with alveolar type II pneumocytes is dependent on its physical state. *Experimental Lung Research* **25:**577-594; 1999.

[67] Schürch, S.; Gehr, P.; Hof, V. I.; Geiser, M.; Green, F. Surfactant displaces particles toward the epithelium in airways and alveoli. *Respiration Physiology* **80:**17-32; 1990.

[68] Post, M.; Vangolde, L. M. G. Metabolic and developmental aspects of the pulmonary surfactant system. *Biochimica Et Biophysica Acta* **947:**249-286; 1988.

R

[69] Wallace, W.; Keane, M.; Murray, D.; Chisholm, W.; Maynard, A.; Ong, T.-m. Phospholipid lung surfactant and nanoparticle surface toxicity: Lessons from diesel soots and silicate dusts. *Nanotechnology and Occupational Health* **9:** 23-38; 2007.

[70] Wallace, W. E.; Keane, M. J.; Hill, C. A.; Xu, J.; Ong, T. M. Mutagenicity of diesel exhaust particles and oil shale particles dispersed in lecithin surfactant. *Journal of Toxicology and Environmental Health* **21:**163-171; 1987.

[71] Nel, A.; Xia, T.; Li, N. Toxic potential of materials at the nanolevel. *Science* **311:**622-627; 2006.

[72] Halliwell, B.; Gutteridge, J. M. C. *Free radicals in biology and medicine.* Oxford: Oxford University Press; 1999.

[73] Meyer, M.; Kuusi, O. Nanotechnology: Generalization in an interdisciplinary field of science and technology. *International Journal for Philosophy of Chemistry* 10:153-168; 2002.

[74] Feynman, R. There's plenty of room at the bottom. In: Talk on December 26, annual meeting of the American Physical Society at the Californian Institute of Technology. Also published in "Miniaturisation" Horace D Gilbert, Reinhold Publishing Corporation, NY 10003., ed.; 1959.

[75] Drexler, E. *Engines of creation.* Anchor Press/Doubleday, New York; 1986.

[76] Research and Markets. The World Nanotechnology Market (2006); 2006. http://www.researchandmarkets.com/reportinfo.asp?report_id=344515 (accessed 13.11.2008)

[77] Research and Markets. Markets Nanotechnology - World R&D Report 2008 - Research in Nanoscience and Nanotechnology; 2008. http://www.researchandmarkets.com/reportinfo.asp?cat_id=0&report_id=661761&q=nanotechnology&p=1 (accessed 13.11.2008).

[78] Maynard, A. Spoonful of caution with nano hype. Interview by Naomi Lubick. *Environmental Science and Technology* **41:**2661-2665; 2007.

[79] CORDIS. Third International Dialogue on Responsible Research and Development of Nanotechnology. In: Tomellini, R.; Giordani, J., eds. Brussels: European Union; 2008.

[80] SCENIHR. The scientific aspects of the existing and proposed definitions relating to products of nanoscience and nanotechnologies. Brussels: European Commission; 2007.

[81] Kleeman, M. J.; Schauer, J. J.; Cass, G. R. Size and composition distribution of fine particulate matter emitted from motor vehicles. *Environmental Science and Technology* **34:**1132-1142; 2000.

[82] Satoh, N.; Nakashima, T.; Kamikura, K.; Yamamoto, K. Quantum size effect in TiO2 nanoparticles prepared by finely controlled metal assembly on dendrimer templates. *Nature Nanotechnology* **3:**106-111; 2008.

[83] Wardak, A.; Gorman, M. E.; Swami, N.; Deshpande, S. Identification of risks in the life cycle of nanotechnology-based products. *Journal of Industrial Ecology* **12:**435-448; 2008.

[84] Kataura, H.; Kumazawa, Y.; Maniwa, Y.; Umezu, I.; Suzuki, S.; Ohtsuka, Y.; Achiba, Y. Optical properties of single-wall carbon nanotubes. *Synthetic Metals* **103:**2555-2558; 1999.

[85] Saito, R.; Dresselhaus, G.; Dresselhaus, M. S. *Physical properties of carbon nanotubes.* London: Imperal College Press; 1999.

[86] Bai, C. L.; Wang, C.; Xie, X. S.; Wolynes, P. G. Single molecule physics and chemistry. *Proceedings of the National Academy of Sciences of the United States of America* **96:**11075-11076; 1999.

[87] Borm, P. J.; Robbins, D.; Haubold, S.; Kuhlbusch, T.; Fissan, H.; Donaldson, K.; Schins, R.; Stone, V.; Kreyling, W.; Lademann, J.; Krutmann, J.; Warheit, D.; Oberdorster, E. The potential risks of nanomaterials: a review carried out for ECETOC. *Particle and Fibre Toxicology* **3:11**; 2006.

[88] Dowling, A. P. Development of nano technologies. *Nanotoday* **7(12), Suppl 1:**p. 30-35; 2004.

[89] Owen, R.; Depledge, M. Nanotechnology and the environment: Risks and rewards. *Marine Pollution Bulletin* **50:**609-612; 2005.

[90] Lei, H. L. Nanoparticles deliver drug to atherosclerotic plaques. b5media; 2006. http://www.aheartylife.com/2006/07/28/nanoparticles-deliver-drug-to-atherosclerotic-plaques/ (accessed 27.10.2008)

[91] Smart, S. K.; Cassady, A. I.; Lu, G. Q.; Martin, D. J. The biocompatibility of carbon nanotubes. *Carbon* **44:**1034-1047; 2006.

[92] Oberdörster, G.; Maynard, A.; Donaldson, K.; Castranova, V.; Fitzpatrick, J.; Ausman, K.; Carter, J.; Karn, B.; Kreyling, W.; Lai, D.; Olin, S.; Monteiro-Riviere, N.; Warheit, D.; Yang, H. Principles for characterizing the potential human health effects from exposure to nanomaterials: elements of a screening strategy. *Particle and Fibre Toxicology* **2**:8; 2005.

[93] Borm, P. J. A.; Kreyling, W. Toxicological hazards of inhaled nanoparticles - Potential implications for drug delivery. *Journal of Nanoscience and Nanotechnology* **4**:521-531; 2004.

[94] Oberdörster, G.; Oberdörster, E.; Oberdörster, J. Nanotoxicology: an emerging discipline evolving from studies of ultrafine particles. *Environmental Health Perspectives* **113**:823-839; 2005.

[95] Muller J.; Huaux F.; Lison D. Respiratory Toxicity of multiwalled carbon nanotubes: How worried should we be? *Carbon* **44**:1048-1056; 2006.

[96] Lansdown, A. B. G. Zinc and titanium oxides: promising UV-absorbers but what influences do they have on the intact skin? *International Journal of Cosmetic Science* **19**:167-172; 1997.

[97] Zhang, Z.; Kleinstreuer, C.; Donohue, J. F.; Kim, C. S. Comparison of micro- and nano-size particle depositions in a human upper airway model. *Journal of Aerosol Science* **36**:211-233; 2005.

R

[98] Brezova, V.; Dvoranova, D.; Rapta, P.; Stasko, A. Photoinduced electron transfer between C-70 fullerene and 3,3 ',5,5 '-tetramethylbenzidine studied by electron paramagnetic resonance. *Spectrochimica Acta Part a-Molecular and Biomolecular Spectroscopy* **56**:2729-2739; 2000.

[99] Yamakoshi, Y.; Umezawa, N.; Ryu, A.; Arakane, K.; Miyata, N.; Goda, Y.; Masumizu, T.; Nagano, T. Active oxygen species generated from photoexcited fullerene (C-60) as potential medicines: O-2(-center dot) versus O-1(2). *Journal of the American Chemical Society* **125**:12803-12809; 2003.

[100] Hoet, P. H.; Bruske-Hohlfeld, I.; Salata, O. V. Nanoparticles - known and unknown health risks. *Journal of Nanobiotechnology* **2**:12; 2004.

[101] Oberdörster, G.; Ferin, J.; Lehnert, B. E. Correlation between particle size, in vivo particle persistence, and lung injury. *Environmental Health Perspectives* **102 Suppl 5**:173-179; 1994.

[102] Donaldson, K.; Tran, C. L. Inflammation caused by particles and fibers. *Inhalation Toxicology* **14**:5-27; 2002.

[103] Tran, C. L.; Buchanan, D.; Cullen, R. T.; Searl, A.; Jones, A. D.; Donaldson, K. Inhalation of poorly soluble particles. II. Influence of particle surface area on inflammation and clearance. *Inhalation Toxicology* **12**:1113-1126; 2000.

R

[104] Long, H.; Shi, T.; Borm, P. J.; Maatta, J.; Husgafvel-Pursiainen, K.; Savolainen, K.; Krombach, F. ROS-mediated TNF-alpha and MIP-2 gene expression in alveolar macrophages exposed to pine dust. *Particle and Fibre Toxicology* **1**:3; 2004.

[105] Sayes, C. M.; Gobin, A. M.; Ausman, K. D.; Mendez, J.; West, J. L.; Colvin, V. L. Nano-C60 cytotoxicity is due to lipid peroxidation. *Biomaterials* **26:**7587-7595; 2005.

[106] Shukla, A.; Gulumian, M.; Hei, T. K.; Kamp, D.; Rahman, Q.; Mossman, B. T. Multiple roles of oxidants in the pathogenesis of asbestos-induced diseases *Free Radical Biology and Medicine* **34:**1117-1129; 2003.

[107] Vallyathan, V.; Shi, X. The role of oxygen free radicals in occupational and environmental lung diseases. *Environmental Health Perspectives* **105 Suppl 1:**165-177; 1997.

[108] Chung, K. F. Cytokines as targets in chronic obstructive pulmonary disease. *Current Drug Targets* **7**:675-681; 2006.

[109] Schins, R. P.; Borm, P. J. Mechanisms and mediators in coal dust induced toxicity: a review. *The Annals of Occupational Hygiene* **43:**7-33; 1999.

[110] Tangirala, R. K.; Murao, K.; Quehenberger, O. Regulation of expression of the human monocyte chemotactic protein-1 receptor (hCCR2) by cytokines. *The Journal of Biological Chemistry* **272**:8050-8056; 1997.

R

[111] Schins, R. P.; Knaapen, A. M.; Cakmak, G. D.; Shi, T.; Weishaupt, C.; Borm, P. J. Oxidant-induced DNA damage by quartz in alveolar epithelial cells. *Mutation Research* **517**:77-86; 2002.

[112] Muller, J.; Huaux, F.; Lison, D. Respiratory Toxicity of multiwalled carbon nanotubes: How worried should we be? *Carbon* **44**:1048-1056; 2006.

[113] Muller, J.; Huaux, F.; Moreau, N.; Misson, P.; Heilier, J.-F.; Delos, M.; M., A.; Fonseca, A.; Nagy, J. B.; Lison, D. Respiratory toxicity of multiwalled carbon nanotubes. *Toxicology and Applied Pharmacology*:221-231; 2005.

[114] Bayram, H.; Devalia, J. L.; Sapsford, R. J.; Ohtoshi, T.; Miyabara, Y.; Sagai, M.; Davies, R. J. The effects of diesel exhaust particles on cell function and release of inflammatory mediators from human bronchial epithelial cells *in vitro*. *American Journal of Respiratory Cell and Molecular Biology* **18**:441-448; 1998.

[115] Finkelman, F. D.; Yang, M. Y.; Orekhova, T.; Clyne, E.; Bernstein, J.; Whitekus, M.; Diaz-Sanchez, D.; Morris, S. C. Diesel exhaust particles suppress *in vivo* IFN-gamma production by inhibiting cytokine effects on wand NKT cells. *Journal of Immunology* **172**:3808-3813; 2004.

[116] Xiao, G. G.; Wang, M. Y.; Li, N.; Loo, J. A.; Nel, A. E. Use of proteomics to demonstrate a hierarchical oxidative stress response to diesel exhaust particle chemicals in a macrophage cell line. *Journal of Biological Chemistry* **278**:50781-50790; 2003.

[117] Takizawa, H.; Abe, S.; Okazaki, H.; Kohyama, T.; Sugawara, I.; Saito, Y.; Ohtoshi, T.; Kawasaki, S.; Desaki, M.; Nakahara, K.; Yamamoto, K.; Matsushima, K.; Tanaka, M.; Sagai, M.; Kudoh, S. Diesel exhaust particles upregulate eotaxin gene expression in human bronchial epithelial cells via nuclear factor-kappa B-dependent pathway. *American Journal of Physiology-Lung Cellular and Molecular Physiology* **284:**L1055-L1062; 2003.

[118] Krishna, M. T.; Chauhan, A. J.; Frew, A. J.; Holgate, S. T. Toxicological mechanisms underlying oxidant pollutant-induced airway injury. *Review Environmental Health* **13:**59-71; 1998.

[119] Nel, A.; Diaz-Sanchez, D.; Li, N. The role of particulate pollutants in pulmonary inflammation and asthma: evidence for the involvement of organic chemicals and oxidative stress. *Current Opinion on Pulmonary Medicine* **7:**20-26; 2001.

[120] Kudo, I.; Murakami, M. Phospholipase A(2) enzymes. *Prostaglandins and other Lipid Mediators* **68-9:**3-58; 2002.

[121] Kudo, I.; Murakami, M. Divresity and functions of phospholipase A(2)s as a initiator of the arachidonic acid metabolism. *Japanese Journal of Pharmacology* **88:**55p-55p; 2002.

[122] Roberts, L. J.; Morrow, J. D. Measurement of F-2-isoprostanes as an index of oxidative stress *in vivo*. *Free Radical Biology and Medicine* **28:**505-513; 2000.

R

[123] Knudsen, P. J.; Dinarello, C. A.; Strom, T. B. Prostaglandins posttranscriptionally inhibit monocyte expression of interleukin-1 activity by increasing intracellular cyclic adenosine-monophosphate. *Journal of Immunology* **137:**3189-3194; 1986.

[124] Kunkel, S. L.; Spengler, M.; May, M. A.; Spengler, R.; Larrick, J.; Remick, D. Prostaglandin-E2 regulates macrophage-derived tumor necrosis factor gene-expression. *Journal of Biological Chemistry* **263:**5380-5384; 1988.

[125] Mohr, C.; Davis, G. S.; Graebner, C.; Hemenway, D. R.; Gemsa, D. Enhanced release of prostaglandin-E(2) from macrophages of rats with silicosis. *American Journal of Respiratory Cell and Molecular Biology* **6:**390-396; 1992.

[126] Weisman, R. B. Simplifying carbon nanotube identification. *The Industrial Physicist*; 2004.

[127] Cientifica. Nanotubes Report 2004. *Cientifica*; 2004.

[128] Evans, J. Manufacturing the carbon nanotube market. *RSC Advancing the Chemical Sciences*; 2007.

[129] Hsu, W. K.; Terrones, M.; Hare, J. P.; Terrones, H.; Kroto, H. W.; Walton, D. R. M. Electrolytic formation of carbon nanostructures. *Chemical Physics Letters* **262:**161-166; 1996.

[130] Journet, C.; Maser, W. K.; Bernier, P.; Loiseau, A.; delaChapelle, M. L.; Lefrant, S.; Deniard, P.; Lee, R.; Fischer, J. E. Large-scale production of single-walled carbon nanotubes by the electric-arc technique. *Nature* **388:**756-758; 1997.

[131] Puretzky, A. A.; Geohegan, D. B.; Fan, X.; Pennycook, S. J. Dynamics of single-wall carbon nanotube synthesis by laser vaporization. *Applied Physics A-Materials Science & Processing* **70:**153-160; 2000.

[132] Scott, C. D.; Arepalli, S.; Nikolaev, P.; Smalley, R. E. Growth mechanism for single-wall carbon nanotubes in a laser-ablation process. *Applied Physics A-Materials Science & Processing* **72:**573-580; 2001.

[133] Kroto, H. W.; Heath, J. R.; Obrien, S. C.; Curl, R. F.; Smalley, R. E. C-60 - Buckminsterfullerene. *Nature* **318:**162-163; 1985.

[134] Walters, D. A.; Ericson, L. M.; Casavant, M. J.; Liu, J.; Colbert, D. T.; Smith, K. A.; Smalley, R. E. Elastic strain of freely suspended single-wall carbon nanotube ropes. *Applied Physics Letters* **74:**3803-3805; 1999.

[135] Yu, X. F.; Mu, T.; Huang, H. Z.; Liu, Z. F.; Wu, N. Z. The study of the attachment of a single-walled carbon nanotube to a self-assembled monolayer using X-ray photoelectron spectroscopy. *Surface Science* **461:**199-207; 2000.

[136] Kagan, V. E.; Bayir, H.; Shvedova, A. A. Nanomedicine and nanotoxicology: two sides of the same coin. *Nanomedicine: Nanotechnology, Biology, and Medicine* **1:**313-316; 2005.

[137] Fiorito, S.; Serafino, A.; Andreola, F.; Togna, A.; Togna, G. Toxicity and biocompatibility of carbon nanoparticles. *Journal of Nanoscience and Nanotechnology* **6:**591-599; 2006.

R

[138] Kam, N. W. S.; O'Connell, M.; Wisdom, J. A.; Dai, H. J. Carbon nanotubes as multifunctional biological transporters and near-infrared agents for selective cancer cell destruction. *Proceedings of the National Academy of Sciences of the United States of America* **102:**11600-11605; 2005.

[139] Maynard, A. D.; Baron, P. A.; Foley, M.; Shvedova, A. A.; Kisin, E. R.; Castranova, V. Exposure to carbon nanotube material: aerosol release during the handling of unrefined single-walled carbon nanotube material. *Journal of Toxicology and Environmental Health A* **67:**87-107; 2004.

[140] Lin, T.; Bajpai, V.; Ji, T.; Dai, L. M. Chemistry of carbon nanotubes. *Australian Journal of Chemistry* **56:**635-651; 2003.

[141] Ye, J. P.; Shi, X. L.; Jones, W.; Rojanasakul, Y.; Cheng, N. L.; Schwegler-Berry, D.; Baron, P.; Deye, G. J.; Li, C. H.; Castranova, V. Critical role of glass fiber length in TNF-alpha production and transcription factor activation in macrophages. *American Journal of Physiology-Lung Cellular and Molecular Physiology* **276:**L426-L434; 1999.

[142] Mossman, B. T.; Borm, P. J.; Castranova, V.; Costa, D. L.; K., D.; Kleeberger, S. R. Mechanisms of action of inhaled fibres, particles and nanoparticles in lung and cardiovascular diseases. *Particle and Fibre Toxicology* **4**; 2007.

[143] Dockery, D. W.; Cunningham, J.; Damokosh, A. I.; Neas, L. M.; Spengler, J. D.; Koutrakis, P.; Ware, J. H.; Raizenne, M.; Speizer, F. E. Health effects of acid aerosols on North American children: Respiratory symptoms. *Environmental Health Perspectives* **104:**500-505; 1996.

[144] Samet, J. M.; Dominici, F.; Curriero, F. C.; Coursac, I.; Zeger, S. L. Fine particulate air pollution and mortality in 20 US Cities, 1987-1994. *New England Journal of Medicine* **343:**1742-1749; 2000.

[145] Seaton, A.; Macnee, W.; Donaldson, K.; Godden, D. Particulate Air-Pollution and Acute Health-Effects. *Lancet* **345:**176-178; 1995.

[146] Turnball, A. B.; Harrison, R. M. Major Component Contributions to PM10 Composition in the UK Atmosphere. *Atmospheric Environment* **34**; 2000.

[147] Borm, P. J. A. Particle toxicology: From coal mining to nanotechnology. *Inhalation Toxicology* **14:**311-324; 2002.

[148] Simkhovich, B. Z.; Kleinman, M. T.; Kloner, R. A. Air pollution and cardiovascular injury epidemiology, toxicology, and mechanisms. *Journal of the American College of Cardiology* **52:**719-726; 2008.

[149] Donaldson, K.; Tran, L.; Jimenez, L. A.; Duffin, R.; Newby, D. E.; Mills, N.; MacNee, W.; Stone, V. Combustion-derived nanoparticles: a review of their toxicology following inhalation exposure. *Particle and Fibre Toxicology* **2:**10; 2005.

[150] Brown, D. M.; Donaldson, K.; Stone, V. Effects of PM10 in human peripheral blood monocytes and J774 macrophages. *Respiratory Research* **5:**29; 2004.

R

[151] Brown, D. M.; Kinloch, I. A.; Bangert, U.; H., W. A.; Walter, D. M.; Walker, G. S.; Scotchford, C. A.; Donaldson, K.; Stone, V. An *in vitro* study of the potential of carbon nanotubes and nanofibres to induce inflammatory mediators and frustrated phagocytosis. *Carbon* **45:**1743-1756; 2007.

[152] Brown, D. M.; Stone, V.; Findlay, P.; MacNee, W.; Donaldson, K. Increased inflammation and intracellular calcium caused by ultrafine carbon black is independent of transition metals or other soluble components. *Occupational and Environmental Medicine* **57:**685-691; 2000.

[153] Gilmour, P. S.; Ziesenis, A.; Morrison, E. R.; Vickers, M. A.; Drost, E. M.; Ford, I.; Karg, E.; Mossa, C.; Schroeppel, A.; Ferron, G. A.; Heyder, J.; Greaves, M.; MacNee, W.; Donaldson, K. Pulmonary and systemic effects of short-term inhalation exposure to ultrafine carbon black particles. *Toxicology and Applied Pharmacology* **195:**35-44; 2004.

[154] Stone, V.; Shaw, J.; Brown, D. M.; MacNee, W.; Faux, S. P.; Donaldson, K. The role of oxidative stress in the prolonged inhibitory effect of ultrafine carbon black on epithelial cell function. *Toxicology in Vitro* **12:**649-+; 1998.

[155] Stone, V.; Tuinman, M.; Vamvakopoulos, J. E.; Shaw, J.; Brown, D.; Petterson, S.; Faux, S. P.; Borm, P.; MacNee, W.; Michaelangeli, F.; Donaldson, K. Increased calcium influx in a monocytic cell line on exposure to ultrafine carbon black. *European Respiratory Journal* **15:**297-303; 2000.

[156] Shukla, A.; Ramos-Nino, M.; Mossman, B. Cell signaling and transcription factor activation by asbestos in lung injury and disease. *The International Journal of Biochemistry & Cell Biology* **35:**1198-1209; 2003.

[157] Bernstein, D. M.; Chevalier, J.; Smith, P. Comparison of calidria chrysotile asbestos to pure tremolite: Final results of the inhalation biopersistence and histopathology examination following short-term exposure. *Inhalation Toxicology* **17:**427-449; 2005.

[158] Goodglick, L. A.; Kane, A. B. Cytotoxicity of long and short crocidolite asbestos fibers *in vitro* and *in vivo*. *Cancer Research* **50:**5153-5163; 1990.

[159] Kane, A. B. Epidemiology and pathology of asbestos-related diseases. *Reviews in Mineralogy* **28:**347-359; 1993.

[160] Kane, A. B. Asbestos bodies: Clues to the mechanism of asbestos toxicity? *Human Pathology* **34:**735-736; 2003.

[161] Kane, A. B.; Hurt, R. H. Nanotoxicology: the asbestos analogy revisited. *Nature Nanotechnology* **3:**378-379; 2008.

[162] Ding, M.; Dong, Z. G.; Chen, F.; Pack, D.; Ma, W. Y.; Ye, J. P.; Shi, X. L.; Castranova, V.; Vallyathan, V. Asbestos induces activator protein-1 transactivation in transgenic mice. *Cancer Research* **59:**1884-1889; 1999.

R

[163] Dehonor, M.; Masenelli-Varlot, K.; Gonzalez-Montiel, A.; Gauthier, C.; Cavaille, J. Y.; Terrones, M. Grafting of polystyrene on nitrogen-doped multi-walled carbon nanotubes. *Journal of Nanoscience and Nanotechnology* **7:**3450-3457; 2007.

[164] Driscoll, H. E.; Carter, J. M.; Howard, B. W.; Hassenbein, D.; Janssen, Y. M.; Mossman, B. T. Crocidolite activates NF-kappa B and MIP-2 gene expression in rat alveolar epithelial cells: role of mitochondrial-derived oxidants. *Environmental Health Perspectives* **106:**1171-1174; 1998.

[165] Gilmour, P. S.; Brown, D. M.; Beswick, P. H. Free radical activity of industrial fibres: role of iron in oxidative stress and activation of transcription factors. *Environmental Health Perspectives* **105:**1313-1317; 1997.

[166] Manning, C. B.; Vallyathan, V.; Mossman, B. T. Diseases caused by asbestos: mechanisms of injury and disease development. *International Immunopharmacology* **2:**191-200; 2002.

[167] Murr, L. E.; Garza, K. M.; Soto, K. F.; Carrasco, A.; Powell, T. G.; Ramirez, D. A.; Guerrero, P. A.; Lopez, D. A.; Venzor, J., 3rd. Cytotoxicity assessment of some carbon nanotubes and related carbon nanoparticle aggregates and the implications for anthropogenic carbon nanotube aggregates in the environment. *International Journal of Environmental Research and Public Health* **2:**31-42; 2005.

[168] Donaldson, K.; Brown, G. M.; Brown, D. M.; Bolton, R. E.; Davis, J. M. G. Inflammation generating potential of long and short fiber amosite asbestos samples. *British Journal of Industrial Medicine* **46:**271-276; 1989.

[169] Soto, K.; Garza, K. M.; Murr, L. E. Cytotoxic effects of aggregated nanomaterials. *Acta Biomaterialia* **3:**351-358; 2007.

[170] Zheng, M.; Diner, B. A. Solution redox chemistry of carbon nanotubes. *Journal of the American Chemical Society* **126:**15490-15494; 2004.

[171] Donaldson, K.; Brown, D.; Clouter, A.; Duffin, R.; MacNee, W.; Renwick, L.; Tran, L.; Stone, V. The pulmonary toxicology of ultrafine particles. *Journal of Aerosol Medicine – Deposition clearance and effects in the lung* **15:**213-220; 2002.

[172] Chou, C. C.; Hsiao, H. Y.; Hong, Q. S.; Chen, C. H.; Peng, Y. W.; Chen, H. W.; Yang, P. C. Single-walled carbon nanotubes can induce pulmonary injury in mouse model. *Nano Letters* **8:**437-445; 2008.

[173] Grubek-Jaworska, H.; Nejman, P.; Czuminska, K.; Przybylowski, T.; Huczko, A.; Lange, H.; Bystrzejewski, M.; Baranowski, P.; Chazan, R. Preliminary results on the pathogenic effects of intratracheal exposure to one-dimensional nanocarbons. *Carbon* **44:**1057-1063; 2006.

[174] Huczko, A.; Lange, H.; Bystrzejewski, M.; Baranowski, P.; Grubek-Jaworska, H.; Nejman, P.; Przybylowski, T.; Czuminska, K.; Glapinski, J.; Walton, D. R. M.; Kroto, H. W. Pulmonary toxicity of 1-D nanocarbon materials. *Fulleren Nanotube Carbon Nanostructures* **13**; 2005.

[175] Huczko, A.; Lange, H.; Calko, E.; Grubek-Jaworska, H.; Droszcz, P. Physiological testing of carbon nanotubes: are they asbestos-like? *Fullerene Science and Technology* **9**; 2001.

[176] Lam, C. W.; James, J. T.; McCluskey, R.; Hunter, R. L. Pulmonary toxicity of single-wall carbon nanotubes in mice 7 and 90 days after intratracheal instillation. *Toxicological Sciences* **77:**126-134; 2004.

[177] Muller, J.; Decordier, I.; Hoet, P. H.; Lombaert, N.; Thomassen, L.; Huaux, F.; Lison, D.; Kirsch-Volders, M. Clastogenic and aneugenic effects of multi-wall carbon nanotubes in epithelial cells. *Carcinogenesis* **29:**427-433; 2008.

[178] Muller, J.; Huaux, F.; Fonseca, A.; Nagy, J. B.; Moreau, N.; Delos, M.; Raymundo-Pinero, E.; Beguin, F.; Kirsch-Volders, M.; Fenoglio, I.; Fubini, B.; Lison, D. Structural defects play a major role in the acute lung toxicity of multiwall carbon nanotubes: toxicological aspects. *Chemical Research in Toxicology* **21:**1698-1705; 2008.

[179] Warheit, D. B.; Laurence, B. R.; Reed, K. L.; Roach, D. H.; Reynolds, G. A.; Webb, T. R. Comparative pulmonary toxicity assessment of single-wall carbon nanotubes in rats. *Toxicological Sciences* **77:**117-125; 2004.

[180] Han, S. G.; Andrews, R.; Gairola, C. G.; Bhalla, D. K. Acute pulmonary effects of combined exposure to carbon nanotubes and ozone in mice. *Inhalation Toxicology* **20:**391-398; 2008.

[181] Shvedova, A. A.; Fabisiak, J. P.; Kisin, E. R.; Murray, A. R.; Roberts, J. R.; Tyurina, Y. Y.; Antonini, J. M.; Feng, W. H.; Kommineni, C.; Reynolds, J.; Barchowsky, A.; Castranova, V.; Kagan, V. E. Sequential exposure to carbon nanotubes and bacteria enhances pulmonary inflammation and infectivity. *American Journal of Respiratory Cell and Molecular Biology* **38:**579-590; 2008.

[182] Sadeghi, A. M.; Dorkoosh, F. A.; Avadi, M. R.; Weinhold, M.; Bayat, A.; Delie, F.; Gurny, R.; Larijani, B.; Rafiee-Tehrani, M.; Junginger, H. E. Permeation enhancer effect of chitosan and chitosan derivatives: comparison of formulations as soluble polymers and nanoparticulate systems on insulin absorption in Caco-2 cells. *European Journal of Pharmaceutics and Biopharmaceutics* **70:**270-278; 2008.

[183] Shvedova, A. A.; Kisin, E. R.; Mercer, R.; Murray, A. R.; Johnson, V. J.; Potapovich, A. I.; Tyurina, Y. Y.; Gorelik, O.; Arepalli, S.; Schwegler-Berry, D.; Hubbs, A. F.; Antonini, J.; Evans, D. E.; Ku, B. K.; Ramsey, D.; Maynard, A.; Kagan, V. E.; Castranova, V.; Baron, P. Unusual inflammatory and fibrogenic pulmonary responses to single-walled carbon nanotubes in mice. *American Journal of Physiology and Lung Cell Molecular Physiology* **289:**L698-708; 2005.

R

[184] Shvedova, A. A.; Kisin, E. R.; Murray, A. R.; Gorelik, O.; Arepalli, S.; Castranova, V.; Young, S. H.; Gao, F.; Tyurina, Y. Y.; Oury, T. D.; Kagan, V. E. Vitamin E deficiency enhances pulmonary inflammatory response and oxidative stress induced by single-walled carbon nanotubes in C57BL/6 mice. *Toxicology and Applied Pharmacology* **221:**339-348; 2007.

[185] Shvedova, A. A.; Kisin, E. R.; Murray, A. R.; Kommineni, C.; Castranova, V.; Fadeel, B.; Kagan, V. E. Increased accumulation of neutrophils and decreased fibrosis in the lung of NADPH oxidase-deficient C57BL/6 mice exposed to carbon nanotubes. *Toxicology and Applied Pharmacology* **231:**235-240; 2008.

[186] Li, Z.; Hulderman, T.; Salmen, R.; Chapman, R.; Leonard, S. S.; Young, S. H.; Shvedova, A.; Luster, M. I.; Simeonova, P. P. Cardiovascular effects of pulmonary exposure to single-wall carbon nanotubes. *Environmental Health Perspectives* **115:**377-382; 2007.

[187] Mangum, J. B.; Turpin, E. A.; Antao-Menezes, A.; Cesta, M. F.; Bermudez, E.; Bonner, J. C. Single-walled carbon nanotube (SWCNT)-induced interstitial fibrosis in the lungs of rats is associated with increased levels of PDGF mRNA and the formation of unique intercellular carbon structures that bridge alveolar macrophages in situ. *Particle and Fibre Toxicology* **3:**15; 2006.

[188] Mitchell, L. A.; Gao, J.; Wal, R. V.; Gigliotti, A.; Burchiel, S. W.; McDonald, J. D. Pulmonary and systemic immune response to inhaled multiwalled carbon nanotubes. *Toxicological Sciences* **100:**203-214; 2007.

[189] Huczko, A.; Lange, H. Carbon nanotubes: experimental evidence for a null risk of skin irritation and allergy. *Fullerene Science and Technology* **9**; 2001.

[190] Nikula, K. J.; Vallyathan, V.; Green, F. H. Y.; Hahn, F. F. Influence of exposure concentration or dose on the distribution of particulate material in rat and human lungs. *Environmental Health Perspectives* **109:**311-318; 2001.

[191] Yokoyama, A.; Sato, Y.; Nodasaka, Y.; Yamamoto, S.; Kawasaki, T.; Shindoh, M.; Kohgo, T.; Akasaka, T.; Uo, M.; Watari, F.; Tohji, K. Biological behavior of hat-stacked carbon nanofibers in the subcutaneous tissue in rats. *Nano Letters* **5:**157–161; 2005.

[192] Koyama, S.; Endo, M.; Kim, Y.-A.; Hayashi, T.; Yanagisawa, T.; Osaka, K.; Koyama, H.; Haniu, H.; Kuroiwa, N. Role of systemic T-cells and histopathological aspects after subcutaneous implantation of various carbon nanotubes in mice. *Carbon* **44:**1079-1092; 2006.

[193] Liu, Z.; Davis, C.; Cai, W.; He, L.; Chen, X.; Dai, H. Circulation and long-term fate of functionalized, biocompatible single-walled carbon nanotubes in mice probed by Raman spectroscopy. *Proceedings of the National Academy of Science of the United States of America* **105:**1410-1415; 2008.

[194] Singh, R.; Pantarotto, D.; Lacerda, L.; Pastorin, G.; Klumpp, C.; Prato, M.; Bianco, A.; Kostarelos, K. Tissue biodistribution and blood clearance rates of intravenously administered carbon nanotube radiotracers. *Proceedings of the National Academy of Science of the United States of America* **103:**3357-3362; 2006.

[195] Schipper, M. L.; Nakayama-Ratchford, N.; Davis, C. R.; Kam, N. W.; Chu, P.; Liu, Z.; Sun, X.; Dai, H.; Gambhir, S. S. A pilot toxicology study of single-walled carbon nanotubes in a small sample of mice. *Nature Nanotechnology* **3:**216-221; 2008.

[196] Cherukuri, P.; Gannon, C. J.; Leeuw, T. K.; Schmidt, H. K.; Smalley, R. E.; Curley, S. A.; Weisman, R. B. Mammalian pharmacokinetics of carbon nanotubes using intrinsic near-infrared fluorescence. *Proceedings of the National Academy of Science of the United States of America* **103:**18882-18886; 2006.

[197] Yang, S. T.; Wang, X.; Jia, G.; Gu, Y.; Wang, T.; Nie, H.; Ge, C.; Wang, H.; Liu, Y. Long-term accumulation and low toxicity of single-walled carbon nanotubes in intravenously exposed mice. *Toxicology Letters* **181:**182-189; 2008.

[198] Deng, X.; Jia, G.; Wang, H.; Sun, H.; Wang, X.; Yang, S.; Wang, T.; Liu, Y. Translocation and fate of multi-walled carbon nanotubes *in vivo*. *Carbon* **45:**1419-1424; 2007.

[199] Radomski, A.; Jurasz, P.; Alonso-Escolano, D.; Drews, M.; Morandi, M.; Malinski, T.; Radomski, M. W. Nanoparticle-induced platelet aggregation and vascular thrombosis. *British Journal of Pharmacology* **146:**882-893; 2005.

[200] Bardi, G.; Tognini, P.; Ciofani, G.; Raffa, V.; Costa, M.; Pizzorusso, T. Pluronic-coated carbon nanotubes do not induce degeneration of cortical neurons *in vivo* and *in vitro*. *Nanomedicine* **(in press);** 2008.

[201] Poland, C. A.; Duffin, R.; Kinloch, I.; Maynard, A.; Wallace, W. A.; Seaton, A.; Stone, V.; Brown, S.; Macnee, W.; Donaldson, K. Carbon nanotubes introduced into the abdominal cavity of mice show asbestos-like pathogenicity in a pilot study. *Nature Nanotechnology* **3:**423-428; 2008.

[202] Takagi, A.; Hirose, A.; Nishimura, T.; Fukumori, N.; Ogata, A.; Ohashi, N.; Kitajima, S.; Kanno, J. Induction of mesothelioma in p53+/- mouse by intraperitoneal application of multi-wall carbon nanotube. *Toxicological Sciences* **33:**105-116; 2008.

[203] Keshava, N.; Murray, A. R.; Gorelik, O.; Arepalli, S.; Gendelsman, V. Z.; Castranova, V.; Shvedova, A. A. Transcriptional regulation in response to carbon nanotubes in human bronchial epithelial cells as detected by microarray analysis. *Toxicologist* **78:**145; 2004.

[204] Magrez, A.; Kasas, S.; Salicio, V.; Pasquier, N.; Seo, J. W.; Celio, M.; Catsicas, S.; Schwaller, B.; Forro, L. Cellular toxicity of carbon-based nanomaterials. *Nano Letters* **6:**1121-1125; 2006.

[205] Manna, S. K.; Sarkar, S.; Barr, J.; Wise, K.; Barrera, E. V.; Jejelowo, O.; Rice-Ficht, A. C.; Ramesh, G. T. Single-walled carbon nanotube induces oxidative stress and activates nuclear transcription factor-kappaB in human keratinocytes. *Nano Letters* **5:**1676-1684; 2005.

[206] Pulskamp, K.; Diabate, S.; Krug, H. F. Carbon nanotubes show no sign of acute toxicity but induce intracellular reactive oxygen species in dependence on contaminants. *Toxicology Letters* **168:**58-74; 2007.

[207] Rotoli, B. M.; Bussolati, O.; Bianchi, M. G.; Barilli, A.; Balasubramanian, C.; Bellucci, S.; Bergamaschi, E. Non-functionalized multi-walled carbon nanotubes alter the paracellular permeability of human airway epithelial cells. *Toxicology Letters* **178:**95-102; 2008.

[208] Sharma, C. S.; Sarkar, S.; Periyakaruppan, A.; Barr, J.; Wise, K.; Thomas, R.; Wilson, B. L.; Ramesh, G. T. Single-walled carbon nanotubes induces oxidative stress in rat lung epithelial cells. *Journal of Nanoscience and Nanotechnology* **7:**2466-2472; 2007.

[209] Simon-Deckers, A.; Gouget, B.; Mayne-L'hermite, M.; Herlin-Boime, N.; Reynaud, C.; Carriere, M. *In vitro* investigation of oxide nanoparticle and carbon nanotube toxicity and intracellular accumulation in A549 human pneumocytes. *Toxicology* **253**:137-146; 2008.

[210] Wörle-Knirsch, J. M.; Pulskamp, K.; Krug, H. F. Oops they did it again! Carbon nanotubes hoax scientists in viability assays. *Nano Letters* **6:**1261-1268; 2006.

[211] Yacobi, N. R.; Phuleria, H. C.; Demaio, L.; Liang, C. H.; Peng, C. A.; Sioutas, C.; Borok, Z.; Kim, K. J.; Crandall, E. D. Nanoparticle effects on rat alveolar epithelial cell monolayer barrier properties. *Toxicology In Vitro* **21:**1373-1381; 2007.

R

[212] Dutta, D.; Sundaram, S. K.; Teeguarden, J. G.; Riley, B. J.; Fifield, L. S.; Jacobs, J. M.; Addleman, S. R.; Kaysen, G. A.; Moudgil, B. M.; Weber, T. J. Adsorbed proteins influence the biological activity and molecular targeting of nanomaterials. *Toxicological Sciences* **100:**303-315; 2007.

[213] Fiorito, S.; Serafino, A.; Andreola, F.; Bernier, P. Effects of fullerenes and single-wall carbon nanotubes on murine and human macrophages. *Carbon* **44:**1100-1105; 2006.

[214] Hamilton, R. F., Jr.; Buford, M. C.; Wood, M. B.; Arnone, B.; Morandi, M.; Holian, A. Engineered carbon nanoparticles alter macrophage immune function and initiate airway hyper-responsiveness in the BALB/c mouse model. *Nanotoxicology* **1:**104-117; 2006.

[215] Hirano, S.; Kanno, S.; Furuyama, A. Multi-walled carbon nanotubes injure the plasma membrane of macrophages. *Toxicology and Applied Pharmacology* **232:**244-251; 2008.

[216] Porter, A. E.; Gass, M.; Muller, K.; Skepper, J. N.; Midgley, P. A.; Welland, M. Direct imaging of single-walled carbon nanotubes in cells. *Nature Nanotechnology* **2:**713-717; 2007.

[217] Salvador-Morales, C.; Flahaut, E.; Sim, E.; Sloan, J.; H. Green, M. L.; Sim, R. B. Complement activation and protein adsorption by carbon nanotubes. *Molecular Immunology* **43:**193-201; 2006.

[218] Tamura, K.; Takashi, N.; Akasaka, T.; Roska, I. D.; Uo, M.; Totsuka, Y.; Watari, F. Effects of micro/nano particle size on cell function and morphology. *Key Engineering Materials* **16:**919-922; 2004.

[219] Chlopek, J.; Czajkowska, B.; Szaraniec, E.; Frackowiak, E.; Szostak, K.; Bèguin, F. *In vitro* studies of carbon nanotube biocompatibility. *Carbon* **44:**1106-1111; 2006.

[220] Lobo, A. O.; Antunes, E. F.; Palma, M. B. S.; Pacheco-Soares, C.; Trava-Airoldi, V. J.; Corat, E. J. Biocompatibility of multi-walled carbon nanotubes grown on titanium and silicon surfaces. *Materials Science and Engineering* **28:**532-538; 2008.

[221] Sayes, C. M.; Liang, F.; Hudson, J. L.; Mendez, J.; Guo, W.; Beach, J. M.; Moore, V. C.; Doyle, C. D.; West, J. L.; Billups, W. E.; Ausman, K. D.; Colvin, V. L. Functionalization density dependence of single-walled carbon nanotubes cytotoxicity *in vitro*. *Toxicology Letters* **161:**135-142; 2006.

[222] Grabinski, C. M.; Hussain, M. D.; Lafdi, K.; Braydich-Stolle, L.; Schlager, J. Effect of particle dimension on biocompatibility of carbon nanomaterials. *Carbon* **45:**2828-2835; 2007.

[223] Monteiro-Riviere, N. A.; Inman, A. O.; Wang, Y. Y.; Nemanich, R. J. Surfactant effects on carbon nanotube interactions with human keratinocytes. *Nanomedicine* **1:**293-299; 2005.

[224] Witzmann, F. A.; Monteiro-Riviere, N. A. Multi-walled carbon nanotube exposure alters protein expression in human keratinocytes. *Nanomedicine* **2:**158-168; 2006.

[225] Zhang, L. W.; Zeng, L.; Barron, A. R.; Monteiro-Riviere, N. A. Biological interactions of functionalized single-wall carbon nanotubes in human epidermal keratinocytes. *International Journal of Toxicology* **26:**103-113; 2007.

[226] Pacurari, M.; Yin, X. J.; Zhao, J.; Ding, M.; Leonard, S. S.; Schwegler-Berry, D.; Ducatman, B. S.; Sbarra, D.; Hoover, M. D.; Castranova, V.; Vallyathan, V. Raw single-wall carbon nanotubes induce oxidative stress and activate MAPKs, AP-1, NF-kappaB, and Akt in normal and malignant human mesothelial cells. *Environmental Health Perspectives* **116:**1211-1217; 2008.

[227] Wick, P.; Manser, P.; Limbach, L. K.; Dettlaff-Weglikowska, U.; Krumeich, F.; Roth, S.; Stark, W. J.; Bruinink, A. The degree and kind of agglomeration affect carbon nanotube cytotoxicity. *Toxicology Letters* **168:**121-131; 2007.

[228] Cui, D.; Tian, F.; Ozkan, C. S.; Wang, M.; Gao, H. Effect of single wall carbon nanotubes on human HEK293 cells. *Toxicology Letters* **155:**73-85; 2005.

[229] Flahaut, E.; Durrieu, M. C.; Remy-Zolghadri, M.; Bareille, R.; Baquey, C. Investigation of the cytotoxicity of CCVD carbon nanotubes towards human umbilical vein endothelial cells. *Carbon* **44:**1093-1099; 2006.

[230] Guo, L.; Von Dem Bussche, A.; Buechner, M.; Yan, A.; Kane, A. B.; Hurt, R. H. Adsorption of essential micronutrients by carbon nanotubes and the implications for nanotoxicity testing. *Small* **4:**721-727; 2008.

[231] Raja, P. M.; Connolley, J.; Ganesan, G. P.; Ci, L.; Ajayan, P. M.; Nalamasu, O.; Thompson, D. M. Impact of carbon nanotube exposure, dosage and aggregation on smooth muscle cells. *Toxicology Letters* **169:**51-63; 2007.

[232] Mattson, M. P.; Haddon, R. C.; Rao, A. M. Molecular functionalization of carbon nanotubes and use as substrates for neuronal growth. *Journal of Molecular Neuroscience* **14:**175-182; 2000.

[233] Hussain, S. M.; Hess, K. L.; Gearhart, J. M.; Geiss, K. T.; Schlager, J. J. *In vitro* toxicity of nanoparticles in BRL 3A rat liver cells. *Toxicology in Vitro* **19:**975-983; 2005.

[234] Liu, X.; Gurel, V.; Morris, D.; Murray, D. W.; Zhitkovich, A.; Kane, A. B.; Hurt, R. H. Bioavailability of nickel in single-wall carbon nanotubes. *Advanced Materials* **19:**2790-2796; 2007.

[235] Fenoglio, I.; Tomatis, M.; Lison, D.; Muller, J.; Fonseca, A.; Nagy, J. B.; Fubini, B. Reactivity of carbon nanotubes: Free radical generation or scavenging activity? *Free Radical Biology and Medicine* **40:**1227-1233; 2006.

[236] O'Connell, M. J.; Bachilo, S. M.; Huffman, C. B.; Moore, V. C.; Strano, M. S.; Haroz, E. H.; Rialon, K. L.; Boul, P. J.; Noon, W. H.; Kittrell, C.; Ma, J.; Hauge, R. H.; Weisman, R. B.; Smalley, R. E. Band gap fluorescence from individual single-walled carbon nanotubes. *Science* **297:**593-596; 2002.

[237] Hesterberg, T. W.; Chase, G.; Axten, C.; Miller, W. C.; Musselman, R. P.; Kamstrup, O.; Hadley, J.; Morscheidt, C.; Bernstein, D. M.; Thevenaz, P. Biopersistence of synthetic vitreous fibers and amosite asbestos in the rat lung following inhalation. *Toxicology and Applied Pharmacology* **151:**262-275; 1998.

[238] Searl, A.; Buchanan, D.; Cullen, R. T.; Jones, A. D.; Miller, B. G.; Soutar, C. A. Biopersistence and durability of nine mineral fibre types in rat lungs over 12 months. *Annals of Occupational Hygiene* **43:**143-153; 1999.

[239] Schürch, S.; Bachofen, H.; Goerke, J.; Green, F. Surface properties of rat pulmonary surfactant studied with the captive bubble method: adsorption, hysteresis, stability. *Biochimica et Biophysica Acta* **1103:**127-136; 1992.

[240] Porter, D.; Sriram, K.; Wolfarth, M.; Jefferson, A.; Schwegler-Berry, D.; Andrew, M. E.; Castranova, V. A biocompatible medium for nanoparticle dispersion. *Nanotoxicology* **2:**144-154; 2008.

[241] Sager, T. M.; Porter, D. W.; Robinson, V. A.; Lindsley, W. G.; Schwegler-Berry, D. E.; Castranova, V. Improved method to disperse nanoparticles for *in vitro* and *in vivo*investigation of toxicity. *Nanotoxicology* **1:**118-129; 2007.

[242] Sarkar, S.; Sharma, C.; Yog, R.; Periakaruppan, A.; Jejelowo, O.; Thomas, R.; Barrera, E. V.; Rice-Ficht, A. C.; Wilson, B. L.; Ramesh, G. T. Analysis of stress responsive genes induced by single-walled carbon nanotubes in BJ Foreskin cells. *Journal of Nanoscience and Nanotechnology* **7:**584-592; 2007.

[243] Kalbacova M.; Dunschl, L.; Kataura, H.; Hempel, U. The study of the interaction of human mesenchymal stem cells and monocytes/macrophages with single-walled carbon nanotube films. *Physica status solidi. B. Basic research* **243**:3514-3518; 2006.

[244] Jacobsen, N. R.; Pojana, G.; White, P.; Moller, P.; Cohn, C. A.; Korsholm, K. S.; Vogel, U.; Marcomini, A.; Loft, S.; Wallin, H. Genotoxicity, cytotoxicity, and reactive oxygen species induced by single-walled carbon nanotubes and C(60) fullerenes in the FE1-Mutatrade markMouse lung epithelial cells. *Environmental and Molecular Mutagenesis* **49:**476-487; 2008.

[245] Kisin, E. R.; Murray, A. R.; Keane, M. J.; Shi, X. C.; Schwegler-Berry, D.; Gorelik, O.; Arepalli, S.; Castranova, V.; Wallace, W. E.; Kagan, V. E.; Shvedova, A. A. Single-walled carbon nanotubes: geno- and cytotoxic effects in lung fibroblast V79 cells. *Journal of Toxicology and Environmental Health A* **70:**2071-2079; 2007.

[246] Yang, H.; Liu, C.; Yang, D.; Zhang, H.; Xi, Z. Comparative study of cytotoxicity, oxidative stress and genotoxicity induced by four typical nanomaterials: the role of particle size, shape and composition. *Journal of Applied Toxicology* **29**:69-78; 2008.

[247] Zhu, L.; Chang, D. W.; Dai, L.; Hong, Y. DNA damage induced by multiwalled carbon nanotubes in mouse embryonic stem cells. *Nano Letters* **7:**3592-3597; 2007.

[248] Dumortier, H.; Lacotte, S.; Pastorin, G.; Marega, R.; Wu, W.; Bonifazi, D.; Briand, J. P.; Prato, M.; Muller, S.; Bianco, A. Functionalized carbon nanotubes are non-cytotoxic and preserve the functionality of primary immune cells. *Nano Letters* **6:**1522-1528; 2006.

[249] Szendi, K.; Varga, C. Lack of genotoxicity of carbon nanotubes in a pilot study. *Anticancer Research* **28:**349-352; 2008.

[250] Kostarelos, K.; Lacerda, L.; Pastorin, G.; Wu, W.; Wieckowski, S.; Luangsivilay, J.; Godefroy, S.; Pantarotto, D.; Briand, J. P.; Muller, S.; Prato, M.; Bianco, A. Cellular uptake of functionalized carbon nanotubes is independent of functional group and cell type. *Nature Nanotechnology* **2:**108-113; 2007.

[251] Kawamoto, H.; Uchida, T.; Kojima, K.; Tachibana, M. Raman study of DNA-wrapped single-wall carbon nanotube hybrids under various humidity conditions. *Chemical Physics Letters* **431:**118-120; 2006.

[252] Yu, X.; Chattopadhyay, D.; Galeska, I.; Papadimitrakopoulos, F.; Rusling, J. F. Peroxidase activity of enzymes bound to the ends of single-wall carbon nanotube forest electrodes. *Electrochemistry Communications* **5:**408-411; 2003.

R

[253] Gregan, E.; Keogh, S. M.; Hedderman, T. G.; Chambers, G.; Byrne, H. J. Stokes/anti-Stokes Raman spectroscopy of high-pressure carbon oxide (HiPco) single-walled carbon nanotubes. *Opto-Ireland 2002: Optics and Photonics Technologies and Applications*. Galway, Ireland: SPIE; 2003: 1149-1157.

[254] Hedderman, T. G. Solubilisation, purification and processing of single walled carbon nanotubes using organic molecules. *PhD Thesis, School of Physics*. Dublin: Dublin Institute of Technology; 2006.

[255] Casey, A.; Davoren, M.; Herzog, E.; Lyng, F. M.; Byrne, H. J.; Chambers, G. Probing the interaction of single walled carbon nanotubes within cell culture medium as a precursor to toxicity testing. *Carbon* **45:**34-40; 2007.

[256] Liebsch, H. M.; Spielmann, H. Balb/c 3T3 cytotoxicity test. In: O'Hare, S.; Atterwill, C. K., eds. *Methods in Molecular Biology, In Vitro Toxicity Testing Protocols*: Humana Press Inc. N.J.; 1995: 177-187.

[257] Casey, A.; Herzog, E.; Davoren, M.; Lyng, F. M.; Byrne, H. J.; Chambers, G. Spectroscopic analysis confirms the interactions between single walled carbon nanotubes and various deyes commonly used to assess cytotoxicity. *Carbon* **45(7):**1425-1432; 2007.

[258] Dresselhaus, M. S.; Dresselhaus, G.; Jorio, A.; Souza, A. G.; Saito, R. Raman spectroscopy on isolated single wall carbon nanotubes. *Carbon* **40:**2043-2061; 2002.

[259] Curran, S. A.; Ajayan, P. M.; Blau, W. J.; Carroll, D. L.; Coleman, J. N.; Dalton, A. B. A composite from poly(m-phenylenevinylene-co-2,5-dioctoxy-p-phenylenevinylene) and carbon nanotubes: a novel material for molecular optoelectronics. *Advanced Materials* **10:**1091-1093; 1998.

[260] Hadjiev, V. G.; Iliev, M. N.; Arepalli, S.; Nikolaev, P.; Files, B. S. Raman scattering test of single-wall carbon nanotube composites. *Applied Physics Letters* **78:**3193-3195; 2001.

[261] Keogh, S. M.; Hedderman, T. G.; Gregan, E.; Farrell, G.; Chambers, G.; Byrne, H. J. Spectroscopic analysis of single-walled carbon nanotubes and semiconjugated polymer composites. *Journal of Physical Chemistry B* **108:**6233-6241; 2004.

[262] Wise, K. E.; Park, C.; Siochi, E. J.; Harrison, J. S. Stable dispersion of single wall carbon nanotubes in polyimide: the role of non-covalent interactions. *Chemical Physics Letters* **391:**207-211; 2004.

[263] Kukovecz, A.; Kramberger, C.; Georgakilas, V.; Prato, M.; Kuzmany, H. A detailed Raman study on thin single-wall carbon nanotubes prepared by the HiPCO process. *European Physical Journal B* **28:**223-230; 2002.

[264] Kukovecz, A.; Smolik, M.; Bokova, S.; Kataura, H.; Achiba, Y.; Kuzmany, H. Determination of the diameter distribution of single-wall carbon nanotubes from the Raman G-band using an artificial neural network. *Journal of Nanoscience and Nanotechnology* **5:**204-208; 2005.

[265] Yu, Z. H.; Brus, L. Rayleigh and Raman scattering from individual carbon nanotube bundles. *Journal of Physical Chemistry B* **105:**1123-1134; 2001.

[266] O'Brien, J.; Wilson, I.; Orton, T.; Pognan, F. Investigation of the Alamar Blue (resazurin) fluorescent dye for the assessment of mammalian cell cytotoxicity. *European Journal of Biochemistry* **267:**5421-5426; 2000.

[267] Bradford, M. M. Rapid and sensitive method for quantitation of microgram quantities of protein utilizing principle of protein-dye binding. *Analytical Biochemistry* **72:**248-254; 1976.

[268] Matejovicova, M.; Mubagwa, K.; Flameng, W. Effect of vanadate on protein determination by the coomassie brilliant blue microassay procedure. *Analytical Biochemistry* **245:**252-254; 1997.

[269] Mosmann, T. Rapid colorimetric assay for cellular growth and survival: Application to proliferation and cytotoxicity assays. *Journal of Immunological Methods* **65:**55-63; 1983.

[270] Supino, R. MTT assays. In: O'Hare, S.; Atterwill, C. K., eds. *Methods in Molecular Biology. In Vitro Toxicity Testing Protocols*: Humana Press Inc. N.J.; 1998: 137-149.

[271] Ranke, J.; Molter, K.; Stock, F.; Bottin-Weber, U.; Poczobutt, J.; Hoffmann, J.; Ondruschka, B.; Filser, J.; Jastorff, B. Biological effects of imidazolium ionic liquids with varying chain lengths in acute *Vibrio fischeri* and WST-1 cell viability assays. *Ecotoxicology and Environmental Safety* **58:**396-404; 2004.

[272] Tan, A. S.; Berridge, M. V. Superoxide produced by activated neutrophils efficiently reduces the tetrazolium salt, WST-1 to produce a soluable formazan: a simple colorimetric assay for measuring respiratory burst actiation and for sceening anti-inflammatory agents. *Journal of Immunological Methods* **238:**59-68; 2000.

[273] Borenfreund, E.; Babich, H.; Martinalguacil, N. Comparisons of 2 *in vitro* Cytotoxicity assays - the Neutral Red (Nr) and tetrazolium Mtt tests. *Toxicology in Vitro* **2:**1-6; 1988.

[274] Brus, I.; Glass, G. B. Estimation of cytotoxic injury to gastric parietal cells by trypan blue exclusion test followed by hematoxylin-eosin counterstaining of fixed smears. *Stain Technology* **48:**127-132; 1973.

[275] Gulden, M.; Seibert, H. Impact of bioavailability on the correlation between *in vitro* cytotoxic and *in vivo* acute fish toxic concentrations of chemicals. *Aquatic Toxicology* **72:**327-337; 2005.

[276] Emerson, R. J.; Davis, G. S. Effect of alveolar lining material-coated silica on rat alveolar macrophages. *Environmental Health Perspectives* **51:**81-84; 1983.

[277] Schimmelpfeng, J.; Drosselmeyer, E.; Hofheinz, V.; Seidel, A. Influence of surfactant components and exposure geometry on the effects of quartz and asbestos on alveolar macrophages. *Environmental Health Perspectives* **97:**225-231; 1992.

[278] Antonini, J. M.; Reasor, M. J. Effect of short-term exogenous pulmonary surfactant treatment on acute lung damage associated with the intratracheal instillation of silica. *Journal of Toxicology and Environmental Health* **43**:85-101; 1994.

[279] Antonini, J. M.; Mccloud, C. M.; Reasor, M. J. Acute silica toxicity - Attenuation by amiodarone-induced pulmonary phospholipidosis. *Environmental Health Perspectives* **102**:372-378; 1994.

[280] Hurt, R. H.; Monthioux, M.; Kane, A. Toxicology of carbon nanomaterials: Status, trends, and perspectives on the special issue. *Carbon* **44**:1028-1033; 2006.

[281] Achterrath, U.; Blumcke, S. Electron-histochemical investigations on Clara cells and type II pneumocytes of normal rat lungs. *Lung* **152**:123-129; 2005.

[282] van Lambalgen, R.; Lelieveld, P. The PIT method: an automated *in vitro* technique for drug toxicity testing. *Investigational New Drugs* **5**:161-165; 1987.

[283] Lieber, M.; Smith, B.; Szakal, A.; Nelsonrees, W.; Todaro, G. Continuous tumor-cell line from a human lung carcinoma with properties of type-II alveolar epithelial cells. *International Journal of Cancer* **17**:62-70; 1976.

[284] Askin, F. B.; Kuhn, C. Cellular origin of pulmonary surfactant. *Laboratory Investigation* **25**:260-&; 1971.

[285] Whitsett, J. A.; Weaver, T. E. Hydrophobic surfactant proteins in lung function and disease. *New England Journal of Medicine* **347:**2141-2148; 2002.

[286] Nicholas, T. E. Pulmonary surfactant: no mere paint on the alveolar wall. *Respirology* **1:**247-257; 1996.

[287] Hook, G. E. R. Alveolar Proteinosis and phospholipidoses of the lungs. *Toxicologic Pathology* **19:**482-513; 1991.

[288] Stearns, R. C.; Paulauskis, J. D.; Godleski, J. J. Endocytosis of ultrafine particles by A549 cells. *American Journal of Respiratory Cell and Molecular Biology* **24:**108-115; 2001.

[289] Wirtz, H. R. W.; Dobbs, L. G. Calcium mobilization and exocytosis after one mechanical stretch of lung epithelial-cells. *Science* **250:**1266-1269; 1990.

[290] Maynard, A. D.; Aitken, R. J.; Butz, T.; Colvin, V.; Donaldson, K.; Oberdörster, G.; Philbert, M. A.; Ryan, J.; Seaton, A.; Stone, V.; Tinkle, S. S.; Tran, L.; Walker, N. J.; Warheit, D. B. Safe handling of nanotechnology. *Nature* **444:**267-269; 2006.

[291] Puck, T. T.; Markus, P. I. Action of X-rays on mammalian cells. *Journal of Experimental Medicine* **103:**653-666; 1956.

[292] Brown, J. M.; Attardi, L. D. Opinion - The role of apoptosis in cancer development and treatment response. *Nature Reviews Cancer* **5:**231-237; 2005.

[293] Maguire, P.; Mothersill, C.; Seymour, C.; Lyng, F. M. Medium from irradiated cells induces dose-dependent mitochondrial changes and BCL2 responses in unirradiated human keratinocytes. *Radiation Research* **163:**384-390; 2005.

[294] O'Reilly, J. P.; Mothersill, C. Comparative effects of UV A and UV B on clonogenic survival and delayed cell death in skin cell lines from humans and fish. *International Journal of Radiation Biology* **72:**111-119; 1997.

[295] Franken, N. A.; Rodermond, H. M.; Stap, J.; Haveman, J.; van Bree, C. Clonogenic assay of cells *in vitro*. *Nature Protocols* **1:**2315-2319; 2006.

[296] Glaviano, A.; Nayak, V.; Cabuy, E.; Baird, D. M.; Yin, Z.; Newson, R.; Ladon, D.; Rubio, M. A.; Slijepcevic, P.; Lyng, F.; Mothersill, C.; Case, C. P. Effects of hTERT on metal ion-induced genomic instability. *Oncogene* **25:**3424-3435; 2006.

[297] Boukamp, P.; Petrussevska, R. T.; Breitkreutz, D.; Hornung, J.; Markham, A.; Fusenig, N. E. Normal keratinization in a spontaneously immortalized aneuploid human keratinocyte cell-line. *Journal of Cell Biology* **106:**761-771; 1988.

[298] Spadinger, I.; Marples, B.; Matthews, J.; Skov, K. Can colony size be used to detect low-dose effects. *Radiation Research* **138:**S21-S24; 1994.

[299] Jarvinen, K.; Pietarinen-Runtti, P.; Linnainmaa, K.; Raivio, K. O.; Krejsa, C. M.; Kavanagh, T.; Kinnula, V. L. Antioxidant defense mechanisms of human mesothelioma and lung adenocarcinoma cells. *American Journal of Physiology-Lung Cellular and Molecular Physiology* **278:**L696-L702; 2000.

[300] Russo, A.; Degraff, W.; Friedman, N.; Mitchell, J. B. Selective modulation of glutathione levels in human normal versus tumor-cells and subsequent differential response to chemotherapy drugs. *Cancer Research* **46:**2845-2848; 1986.

[301] Donaldson, K.; Brown, D. M.; Mitchell, C.; Dineva, M.; Beswick, P. H.; Gilmour, P.; MacNee, W. Free radical activity of PM10: Iron-mediated generation of hydroxyl radicals. *Environmental Health Perspectives* **105:**1285-1289; 1997.

[302] Horáková, K.; Sovcikova, A.; Seemannova, Z.; Syrova, D.; Busanyova, K.; Drobna, Z.; Ferencik, M. Detection of drug-induced, superoxide-mediated cell damage and its prevention by antioxidants. *Free Radical Biology and Medicine* **30:**650-664; 2001.

[303] Perez, R. P.; Perez, K. M.; Handel, L. M.; Hamilton, T. C. *In vitro* interactions between platinum analogs in human ovarian-carcinoma cell-lines. *Cancer Chemotherapy and Pharmacology* **29:**430-434; 1992.

[304] Hedderman, T. G.; Keogh, S. M.; Chambers, G.; Byrne, H. J. In-depth study into the interaction of single walled carbon nanotubes with anthracene and p-terphenyl. *Journal of Physical Chemistry B* **110:**3895-3901; 2006.

[305] Ozturk, S.; Kaseko, G.; Mahaworasilpa, T.; Coster, H. G. Adaptation of cell lines to serum-free culture medium. *Hybridoma and Hybridomics* **22:**267-272; 2003.

[306] Zenin, V. V.; Nikolsky, N. N.; Skopicheva, V. I.; Sorokin, A. B. Dependence of the 3t6 cell-proliferation on the serum content. *Tsitologiya* **24:**947-953; 1982.

[307] Lima, P. D. L.; Vasconcellos, M. C.; Montenegro, R. A.; Sombra, C. M. L.; Bahia, M. O.; Costa-Lotufo, L. V.; Pessoa, C. O.; Moraes, M. O.; Burbano, R. R. Genotoxic and cytotoxic effects of iron sulfate in cultured human lymphocytes treated in different phases of cell cycle. *Toxicology in Vitro* **22:**723-729; 2008.

[308] Posadaz, A.; Sanchez, E.; Gutierrez, M. I.; Calderon, M.; Bertolotti, S.; Biasutti, M. A.; Garcia, N. A. Riboflavin and rose bengal sensitised photooxidation of sulfathiazole and succinylsulfathiazole - Kinetic study and microbiological implications. *Dyes and Pigments* **45:**219-228; 2000.

[309] Zirak, P.; Penzkofer, A.; Schiereis, T.; Hegemann, P.; Jung, A.; Schlichting, I. Absorption and fluorescence spectroscopic characterization of BLUF domain of AppA from Rhodobacter sphaeroides. *Chemical Physics* **315:**142-154; 2005.

[310] Carter, J. D.; Ghio, A. J.; Samet, J. M.; Devlin, R. B. Cytokine production by human airway epithelial cells after exposure to an air pollution particle is metal-dependent. *Toxicology and Applied Pharmacology* **146:**180-188; 1997.

[311] LeBel, C. P.; Ischiropoulos, H.; Bondy, S. C. Evaluation of the Probe 2',7'-Dichlorofluorescin as an indicator of reactive oxygen species formation and oxidative stress. *Chemical Research in Toxicology* **5:**227-231; 1992.

[312] Molecular Probes. Reactive Oxygen Species (ROS) Detection Reagents. Manuals and Product Inserts. *Molecular Probes, Invitrogen;* 2006. http://probes.invitrogen.com/media/pis/mp36103.pdf (accessed 13.11.2008)

[313] Molecular Probes. Image-iT ™ LIVE Green Reactive Oxygen Species Detection Kit (I36007). Product Information, *Molecular Probes, Invitrogen;* 2004. http://probes.invitrogen.com/media/pis/mp36007.pdf (accessed 13.11.2008)

[314] Becker, S.; Mundandhara, S.; Madden, M. Regulation of cytokine production in alveolar macrophage and airway epithelial cells in response to particulate air pollution: Further mechanistic understanding. *Toxicology and Applied Pharmacology* **197:**140-140; 2004.

[315] Mossman, B. T.; Churg, A. Mechanisms in the pathogenesis of asbestosis and silicosis. *American Journal of Respiratory and Critical Care Medicine* **157:**1666-1680; 1998.

[316] Bowes, D. R.; Farrow, C. M. Major and trace element compositions of the UICC standard asbestos samples. *American Journal of Industrial Medicine* **32:**592-594; 1997.

[317] Lang, D. S.; Schocker, H.; Hockertz, S. Effects of crocidolite asbestos on human bronchoepithelial-dependent fibroblast stimulation in coculture: the role of IL-6 and GM-CSF. *Toxicology* **159:**81-98; 2001.

[318] Ono-Ogasawara, M.; Kohyama, N. Evaluation of surface roughness of fibrous minerals by comparison of BET surface area and calculated one. *Annals of Occupational Hygiene* **43:**505-511; 1999.

[319] Priya, B. R.; Byrne, H. J. Investigation of sodium dodecyl benzene sulfonate assisted dispersion and debundling of single-wall carbon nanotubes. *Journal of Physical Chemistry C* **112:**332-337; 2008.

[320] Foucaud, L.; Wilson, M. R.; Brown, D. M.; Stone, V. Measurement of reactive species production by nanoparticles prepared in biologically relevant media. *Toxicology Letters* **174:**1-9; 2007.

[321] Donaldson, K.; Stone, V.; Clouter, A.; Renwick, L.; MacNee, W. Ultrafine particles. *Occupational and Environmental Medicine* **58:**211-+; 2001.

[322] Keane, M. J.; Xing, S. G.; Harrison, J. C.; Ong, T.; Wallace, W. E. Genotoxicity of Diesel-exhaust particles dispersed in simulated pulmonary surfactant. *Mutation Research* **260:**233-238; 1991.

[323] Murray, D.; Harrison, J.; Wallace, W. A 13C CP/MAS and 31P NMR study of the interactions of dipalmitoylphosphatidyl choline with respirable silica and kaolin. *Journal of Colloid and Interface Science* **288:**166-170; 2005.

[324] Gao, N.; Keane, M. J.; Ong, T.; Ye, J.; Miller, W. E.; Wallace, W. E. Effects of phospholipid surfactant on apoptosis induction by respirable quartz and kaolin in NR8383 rat pulmonary macrophages. *Toxicology and Applied Pharmacology* **175:**217-225; 2001.

[325] Li, N.; Wang, M.; Oberley, T. D.; Sempf, J. M.; Nel, A. E. Comparison of the pro-oxidative and proinflammatory effects of organic diesel exhaust particle chemicals in bronchial epithelial cells and macrophages. *Journal of Immunology* **169:**4531-4541; 2002.

[326] Lynch, I.; Dawson, K. A. Protein-nanoparticle interactions. *Nanotoday* **3:**40-47; 2008.

[327] Xia, T.; Korge, P.; Weiss, J. N.; Li, N.; Venkatesen, M. I.; Sioutas, C.; Nel, A. Quinones and aromatic chemical compounds in particulate matter induce mitochondrial dysfunction: implications for ultrafine particle toxicity. *Environmental Health Perspectives* **112:**1347-1358; 2004.

[328] Xia, T.; Kovochich, M.; Brant, J.; Hotze, M.; Sempf, J.; Oberley, T.; Sioutas, C.; Yeh, J. I.; Wiesner, M. R.; Nel, A. E. Comparison of the abilities of ambient and manufactured nanoparticles to induce cellular toxicity according to an oxidative stress paradigm. *Nano Letters* **6:**1794-1807; 2006.

[329] Kodavanti, U. P.; Schladweiler, M. C.; Ledbetter, A. D.; Hauser, R.; Christiani, D. C.; Samet, J. M.; McGee, J.; Richards, J. H.; Costa, D. L. Pulmonary and systemic effects of zinc-containing emission particles in three rat strains: multiple exposure scenarios. *Toxicological Sciences* **70:**73-85; 2002.

[330] Buford, M. C.; Hamilton, R. F., Jr.; Holian, A. A comparison of dispersing media for various engineered carbon nanoparticles. *Particle and Fibre Toxicology* **4:**6; 2007.

[331] Patzold, S.; Schmidt, A.; Seidel, A. Loss of cathepsin B activity in alveolar macrophages after *in vitro* quartz phagocytosis. *Journal of Toxicology and Environmental Health* **40:**547-554; 1993.

[332] Wallace, W. E.; Keane, M. J.; Mike, P. S.; Hill, C. A.; Vallyathan, V.; Regad, E. D. Contrasting respirable quartz and kaolin retention of lecithin surfactant and expression of membranolytic activity following phospholipase A2 digestion. *Journal of Toxicology and Environmental Health* **37:**391-409; 1992.

[333] Kode, A.; Yang, S. R.; Rahman, I. Differential effects of cigarette smoke on oxidative stress and proinflammatory cytokine release in primary human airway epithelial cells and in a variety of transformed alveolar epithelial cells. *Respiratory Research* **7:**132; 2006.

[334] Oostingh, G. J.; Schlickum, S.; Friedl, P.; Schon, M. P. Impaired induction of adhesion molecule expression in immortalized endothelial cells leads to functional defects in dynamic interactions with lymphocytes. *The Journal of Investigative Dermatology* **127:**2253-2258; 2007.

[335] Oberdörster, G. Airborne pollutants and acute health effects. *Lancet* **345:**799-800; 1995.

[336] Oberdörster, G.; Gelein, R. M.; Ferin, J.; Weiss, B. Association of particulate air pollution and acute mortality: involvement of ultrafine particles? *Inhalation Toxicology* **7:**111-124; 1995.

[337] Utell, M. J.; Frampton, M. W. Acute health effects of ambient air pollution: The ultrafine particle hypothesis. *Journal of Aerosol Medicine-Deposition Clearance and Effects in the Lung* **13:**355-359; 2000.

[338] Becker, S.; Dailey, L.; Soukup, J. M.; Silbajoris, R.; Devlin, R. B. TLR-2 is involved in airway epithelial cell response to air pollution particles. *Toxicology and Applied Pharmacology* **203:**45-52; 2005.

[339] Amakawa, K.; Terashima, T.; Matsuzaki, T.; Matsumaru, A.; Sagai, M.; Yamaguchi, K. Suppressive effects of diesel exhaust particles on cytokine release from human and murine alveolar macrophages. *Experimental Lung Research* **29:**149-164; 2003.

[340] Hofer, T. P. J.; Bitterle, E.; Beck-Speier, I.; Maier, K. L.; Frankenberger, M.; Heyder, J.; Ziegler-Heitbrock, L. Diesel exhaust particles increase LPS-stimulated COX-2 expression and PGE(2) production in human monocytes. *Journal of Leukocyte Biology* **75:**856-864; 2004.

[341] Yang, H. M.; Antonini, J. M.; Barger, M. W.; Butterworth, L.; Roberts, J. R.; Ma, J. K. H.; Castranova, V.; Ma, J. Y. C. Diesel exhaust particles suppress macrophage function and slow the pulmonary clearance of Listeria monocytogenes in rats. *Environmental Health Perspectives* **109:**515-521; 2001.

[342] Beutler, B.; Cerami, A. The common mediator of shock, cachexia, and tumor necrosis. *Advances in Immunology* **42**:213-231; 1988.

[343] Mannel, D. N.; Ruschoff, J.; Orosz, P. The role of TNF in tumour growth and metastasis. *Research in Immunology* **144**:364-369; 1993.

[344] Chung, K. F. Cytokines in chronic obstructive pulmonary disease. *The European Respiratory Journal* **34**:50s-59s; 2001.

[345] Puthothu, B.; Bierbaum, S.; Kopp, M. V.; Forster, J.; Heinze, J.; Weckmann, M.; Krueger, M.; Heinzmann, A. Association of TNF-alpha with severe respiratory syncytial virus infection and bronchial asthma. *Pediatric Allergy Immunology: Official publication of the European Society of Pediatric Allergy and Immunology*; 2008.

[346] Zhang, H.; Park, Y.; Wu, J.; Chen, X.; Lee, S.; Yang, J.; Dellsperger, K. C.; Zhang, C. Role of TNF-alpha in vascular dysfunction. *Clinical Sciences* **116:**219-230; 2009.

[347] Oostingh, G. J.; Schmittner, M.; Ehart, A. K.; Tischler, U.; Duschl, A. A high-throughput screening method based on stably transformed human cells was used to determine the immunotoxic effects of fluoranthene and other PAHs. *Toxicology in Vitro* **22:**1301-1310; 2008.

[348] Ovrevik, J.; Hetland, R. B.; Schins, R. P.; Myran, T.; Schwarze, P. E. Iron release and ROS generation from mineral particles are not related to cytokine release or apoptosis in exposed A549 cells. *Toxicology Letters* **165:**31-38; 2006.

[349] LaDou, J. The asbestos cancer epidemic. *Environmental Health Perspectives* **112**:285-290; 2004.

[350] Luster, M. I.; Simeonova, P. P. asbestos induces inflammatory cytokines in the lung through redox sensitive transcription factors. *Toxicology Letters* **102**:271-275; 1998.

[351] Simeonova, P.; Flood, L.; Luster, M. Molecular regulation of IL-6 by asbestos. *Journal of Leukocyte Biology*:45-45; 1997.

[352] Simeonova, P. P.; Luster, M. I. Asbestos induction of nuclear transcription factors and interleukin 8 gene regulation. *American Journal of Respiratory Cell and Molecular Biology* **15**:787-795; 1996.

[353] Ferin, J.; Oberdörster, G.; Penney, D. P. Pulmonary retention of ultrafine particles in rats. *American Journal of Respiratory Cell and Molecular Biology* **6**:535-542; 1992.

[354] Hansen, L. A.; Poulsen, O. M.; Wurtz, H. Endotoxin potency in the A549 lung epithelial cell bioassay and the limulus amebocyte lysate assay. *Journal of Immunological Methods* **226**:49-58; 1999.

[355] Shvedova, A. A.; Sager, T.; Murray, A. R.; Kisin, E.; Porter, D. W.; Leonard, S. S.; Schwegler-Berry, D.; Robinson, V. A.; Castranova, V. Critical issues in the evaluation of possible adverse pulmonary effects resulting from airborne nanoparticles. In: Monteiro-Riviere, N. A.; Tran, C. L., eds. *Nanotoxicology: Characterization, Dosing and Health Effects*. New York, London: Informa Healthcare; 2007: 225-236.

[356] Goodglick, L. A.; Kane, A. B. Role of reactive oxygen metabolites in crocidolite asbestos toxicity to mouse macrophages. *Cancer Research* **46:**5558-5566; 1986.

[357] Vallyathan, V.; Mega, J. F.; Shi, X. L.; Dalal, N. S. Enhanced generation of free-radicals from phagocytes induced by mineral dusts. *American Journal of Respiratory Cell and Molecular Biology* **6:**404-413; 1992.

[358] Dockery, D. W.; Pope, C. A., 3rd. Acute respiratory effects of particulate air pollution. *Annual Review of Public Health* **15:**107-132; 1994.

[359] Hoek, G.; Dockery, D. W.; Pope, A.; Neas, L.; Roemer, W.; Brunekreef, B. Association between PM10 and decrements in peak expiratory flow rates in children: reanalysis of data from five panel studies. *European Respiratory Journal* **11:**1307-1311; 1998.

[360] Pope, C. A., 3rd; Thun, M. J.; Namboodiri, M. M.; Dockery, D. W.; Evans, J. S.; Speizer, F. E.; Heath, C. W., Jr. Particulate air pollution as a predictor of mortality in a prospective study of U.S. adults. *American Journal of Respiratory and Critical Care Medicine* **151:**669-674; 1995.

[361] Dentener, M. A.; Bazil, V.; Vonasmuth, E. J. U.; Ceska, M.; Buurman, W. A. Involvement of Cd14 in lipopolysaccharide-induced tumor-necrosis-factor-alpha, Il-6 and Il-8 release by human monocytes and alveolar macrophages. *Journal of Immunology* **150:**2885-2891; 1993.

[362] Passlick, B.; Flieger, D.; Zieglerheitbrock, H. W. L. Identification and characterization of a novel monocyte subpopulation in human peripheral-blood. *Blood* **74:**2527-2534; 1989.

[363] Cherukuri, P.; Bachilo, S. M.; Litovsky, S. H.; Weisman, R. B. Near-infrared fluorescence microscopy of single-walled carbon nanotubes in phagocytic cells. *Journal of the American Chemoca; Society* **126:** 15638-15639; 2004.

[364] Thiele, L.; Rothen-Rutishauser, B.; Jilek, S.; Wunderli-Allenspach, H.; Merkle, H. P.; Walter, E. Evaluation of particle uptake in human blood monocyte-derived cells *in vitro*. Does phagocytosis activity of dendritic cells measure up with macrophages? *Journal of Controlled Release* **76:**59-71; 2001.

[365] Kamp, D. W.; Graceffa, P.; Pryor, W. A.; Weitzman, S. A. The Role of Free-Radicals in asbestos-induced diseases. *Free Radical Biology and Medicine* **12:**293-315; 1992.

[366] Beck-Speier, I.; Dayal, N.; Karg, E.; Maier, K. L.; Roth, C.; Ziesenis, A.; Heyder, J. Agglomerates of ultrafine particles of elemental carbon and TiO2 induce generation of lipid mediators in alveolar macrophages. *Environmental Health Perspectives* **109 Suppl 4:**613-618; 2001.

[367] Becker, S.; Soukup, J. M.; Sioutas, C.; Cassee, F. R. Response of human alveolar macrophages to ultrafine, fine, and coarse urban air pollution particles. *Experimental Lung Research* **29:**29-44; 2003.

[368] Renwick, L. C.; Brown, D.; Clouter, A.; Donaldson, K. Increased inflammation and altered macrophage chemotactic responses caused by two ultrafine particle types. *Occupational and Environmental Medicine* **61:**442-447; 2004.

[369] Howe, O. L.; Daly, P. A.; Seymour, C.; Ormiston, W.; Nolan, C.; Mothersill, C. Elevated G2 chromosomal radiosensitivity in Irish breast cancer patients: a comparison with other studies. *International Journal of Radiation Biology* **81:**373-378; 2005.

[370] Dybdahl, M.; Risom, L.; Bornholdt, J.; Autrup, H.; Loft, S.; Wallin, H. Inflammatory and genotoxic effects of diesel particles *in vitro* and *in vivo*. *Mutation Research-Genetic Toxicology and Environmental Mutagenesis* **562:**119-131; 2004.

[371] McNeilly, J. D.; Heal, M. R.; Beverland, I. J.; Howe, A.; Gibson, M. D.; Hibbs, L. R.; MacNee, W.; Donaldson, K. Soluble transition metals cause the pro-inflammatory effects of welding fumes *in vitro*. *Toxicology and Applied Pharmacology* **196:**95-107; 2004.

[372] OECD. Working party on manufactured nanomaterials: List of manufactured nanomaterials and list of endpoints for phase one of the OECD testing programme. In: OECD, ed. *OECD Environment, Health and Safety Publications Series on the Safety of Manufactured Nanomaterials*. Paris: OECD; 2008.

R

[373] Shvedova, A. A.; Kisin, E. R.; Murray, A. R.; Gorelik, O.; Arepalli, S.; Castranova, V.; Young, S.-H.; Gao, F.; Tyurina, Y. Y.; Oury, T. D.; Kagan, V. E. Vitamin E deficiency enhances pulmonary inflammatory response and oxidative stress induced by single-walled carbon nanotubes in C57BL/6 mice. *Toxicology and Applied Pharmacology* **221:**339-348; 2007.

[374] Becker, S.; Soukup, J. M. Coarse (PM2.5-10), fine (PM2.5), and ultrafine air pollution particles induce/increase immune costimulatory receptors on human blood-derived monocytes but not on alveolar macrophages. *Journal of Toxicology and Environmental Health- A* **66:**847-859; 2003.

[375] Heneweer, M.; Muusse, M.; Dingemans, M.; de Jong, P. C.; van den Berg, M.; Sanderson, J. T. Co-culture of primary human mammary fibroblasts and MCF-7 cells as an *in vitro* breast cancer model. *Toxicological Sciences* **83:**257-263; 2005.

[376] Liu, S. H.; Chu, I. M.; Pan, I. H. Effects of hydroxybenzyl alcohols on melanogenesis in melanocyte-keratinocyte co-culture and monolayer culture of melanocytes. *Journal of Enzyme Inhibition and Medicinal Chemistry* **23:**526-534; 2008.

[377] Rothen-Rutishauser, B. M.; Kiama, S. G.; Gehr, P. A three-dimensional cellular model of the human respiratory tract to study the interaction with particles. *American Journal of Respiratory Cell and Molecular Biology* **32:**281-289; 2005.

[378] Lynch, I.; Cedervall, T.; Lundqvist, M.; Cabaleiro-Lago, C.; Linse, S.; Dawson, K. A. The nanoparticle-protein complex as a biological entity; a complex fluids and surface science challenge for the 21st century. *Advances in Colloid and Interface Science* **134-135:**167-174; 2007.

[379] Pisanic, T. R., 2nd; Blackwell, J. D.; Shubayev, V. I.; Finones, R. R.; Jin, S. Nanotoxicity of iron oxide nanoparticle internalization in growing neurons. *Biomaterials* **28**:2572-2581; 2007.

[380] Blaise C., Gagne F., Ferard J. F., Eullaffroy P. Ecotoxicity of selected nano-materials to aquatic organisms. *Environmental Toxicology* **23(5):** 591-598; 2008.

[381] Cañas J. E., Long M., Nations S., Vadan R., Dai L., Luo M., Ambikapathi R., Lee E. H., Olszyk D. Effects of functionalized and non-functionalized single-walled carbon nanotubes on root elongation of select crop species. *Environmental Toxicology and Chemistry* **(in press);** 2008.

[382] Cheng J., Flahaut E., Cheng S. H. Effect of carbon nanotubes on developing zebrafish (*Danio rerio*) embryos. *Environmental Toxicology and Chemistry* **26(4):** 708-716; 2007.

[383] Ghafari P., St-Denis C. H., Power M. E., Jin X., Tsou V., Mandal H. S., Bols N. C., Tang X. S. Impact of carbon nanotubes on the ingestion and digestion of bacteria by ciliated protozoa. *Nature Nanotechnology* **3(6):** 347-351; 2008.

[384] Herzog E., Casey A., Lyng F. M., Chambers G., Byrne H. J., Davoren M. A new approach to the toxicity testing of carbon-based nanomaterials--the clonogenic assay. *Toxicology Letters* **174(1-3):** 49-60; 2007.

[385] Herzog E., Byrne H. J., Casey A., Davoren M., Lenz A. G., Maier K. L., Duschl A., Oostingh G. J. SWCNT suppress inflammatory mediator responses in human lung epithelium *in vitro*. *Toxicology and Applied Pharmacology* **(in press);** 2008.

[386] Kang S., Mauter M. S., Elimelech M. Physicochemical determinants of multiwalled carbon nanotube bacterial cytotoxicity. *Environmental Science and Technology* **42(19):** 7528-7534; 2008.

[387] Karlsson H. L., Cronholm P., Gustafsson J., Moller L. Copper oxide nanoparticles are highly toxic: A comparison between metal oxide nanoparticles and carbon nanotubes. *Chemical Research in Toxicology* **21(9):** 1726-1732; 2008.

[388] Liu J., Hopfinger A. J. Identification of possible sources of nanotoxicity from carbon nanotubes inserted into membrane bilayers using membrane interaction quantitative structure--activity relationship analysis. *Chemical Research in Toxicology* **21(2):** 459-466; 2008.

R

[389] Mouchet F., Landois P., Sarremejean E., Bernard G., Puech P., Pinelli E., Flahaut E., Gauthier L. Characterisation and *in vivo* ecotoxicity evaluation of double-wall carbon nanotubes in larvae of the amphibian *Xenopus laevis*. *Aquatic toxicology* **87(2):** 127-137; 2008.

[390] Oberdörster E., Zhu S., Blickley T. M., McClellan-Green P., Haasch M. L. Ecotoxicology of carbon-based engineered nanoparticles: Effects of fullerene (C60) on aquatic organisms. *Carbon* **44(6):** 1112-1120; 2006

[391] Sato Y., Yokoyama A., Shibata K., Akimoto Y., Ogino S., Nodasaka Y., Kohogo T., Tamura K., Akasaka T., Uo M., Motomiya K., Jeyadevan B., Ishiguro M., Hatakeyama R., Watari F., Tohji K. Influence of length on cytotoxicity of multi-walled carbon nanotubes against human acute monocytic leukemia cell line THP-1 *in vitro* and subcutaneous tissue of rats *in vivo*. *Molecular Biosystems* **1(2):** 176-182; 2005.

[392] Scott-Fordsmand J. J., Krogh P. H., Schaefer M., Johansen A. The toxicity testing of double-walled nanotubes-contaminated food to *Eisenia veneta* earthworms. *Ecotoxicology and Environmental Safety* **(in press);** 2008

[393] Templeton R. C., Ferguson P. L., Washburn K. M., Scrivens W. A., Chandler G. T. Life-cycle effects of single-walled carbon nanotubes (SWNTs) on an estuarine meiobenthic copepod. *Environmental Science and Technology* **40(23):** 7387-7393; 2006

[394] Rouse, J. H. Polymer-assisted dispersion of single-walled carbon nanotubes in alcohols and applicability toward carbon nanotube/sol-gel composite formation. *Langmuir* **21:**1055-1061; 2005.

[395] Hyung, H.; Fortner, J. D.; Hughes, J. B.; Kim, J. H. Natural organic matter stabilizes carbon nanotubes in the aqueous phase. *Environmental Science and Technology* **41:**179-184; 2007.

[396] Bianco, A.; Kostarelos, K.; Prato, M. Applications of carbon nanotubes in drug delivery. *Current opinion in chemical biology* **9:**674-679; 2005.

[397] Singh, R.; Pantarotto, D.; Lacerda, L.; Pastorin, G.; Klumpp, C.; Prato, M.; Bianco, A.; Kostarelos, K. Tissue biodistribution and blood clearance rates of intravenously administered carbon nanotube radiotracers. *Proceedings of the National Academy of Science of the United States of America* **103:**3357-3362; 2006.

R

Appendix A

Publications and presentations

A 1. Publications

E. Herzog, H. J. Byrne, M. Davoren, A. Casey, M. Schmittner, A. Duschl, G. J. Oostingh. Oxidative stress response of human lung epithelial cells upon carbon nanoparticle exposure depends on the dispersion media. *Toxicology and Applied Pharmacology,* **submitted** October 2008

E. Herzog, H. J. Byrne, A. Casey, M. Davoren, A.-G. Lenz, K. L. Maier, A. Duschl, G. J. Oostingh. SWCNT suppress inflammatory mediator responses in human lung epithelium *in vitro*. *Toxicology and Applied Pharmacology,* accepted on 29th October 2008, **doi:10.1016/j.taap.2008.10.015**

A. Casey, **E.Herzog**, F.M. Lyng, H.J. Byrne, G. Chambers, M. Davoren. Single-walled carbon nanotubes induce indirect cytotoxictiy by medium depletion in A549 lung cells. *Toxicology Letters* **179(2):**78-84; 2008

P. Knief, C. Clarke, **E. Herzog**, M. Davoren, F.M. Lyng, A.D. Meade, H.J. Byrne. Raman spectroscopy – a platform for the rapid measurement of carbon nanotube-induced cytotoxicity. *The Analyst,* **submitted** December 2008

E. Herzog, A. Casey, F.M. Lyng, G. Chambers, H.J. Byrne, M. Davoren. A new approach to the toxicity testing of carbon nanomaterials – the clonogenic assay. *Toxicology Letters* **174(1-3)**:49-60; 2007

A. Casey, **E. Herzog**, M. Davoren, H.J. Byrne, G. Chambers. Spectroscopic analysis confirms the interactions between single walled carbon nanotubes and various dyes commonly used to assess cytotoxicity. *Carbon* **45(7)**:1425-1432; 2007

M. Davoren, **E. Herzog**, A. Casey, B. Cottineau, G. Chambers, H. J. Byrne, F. Lyng. *In vitro* toxicity evaluation of single walled carbon nanotubes on human A549 lung cells. *Toxicology in vitro* **21(3)**:438-448; 2007

Casey, M. Davoren, **E. Herzog**, F.M. Lyng, H.J. Byrne, G. Chambers. Probing the interaction of single walled carbon nanotubes within cell culture medium: A precursor to toxicity testing. *Carbon* **45(1)**:34-40; 2007

A 2. Oral presentations

E.Herzog, H.J. Byrne, M. Davoren, A. Casey, A. Duschl, G.J. Oosthing. **Single-walled carbon nanotubes vs. asbestos – the role of lung surfactant dispersion.** *Nanotox2008, Switzerland (September 2008)*

E.Herzog, H.J. Byrne, M. Davoren, A. Casey, A. Duschl, G.J. Oosthing. **The effects of lung surfactant dispersion on the inflammatory mediator response of lung epithelium following exposure to single-walled carbon nanotubes and crocidolite asbestos.** *9th International Conference on Particles – Risks and Opportunities, South Africa (September 2008)*

E. Herzog, A. Casey, F.M. Lyng, G. Chambers, M. Davoren, H.J. Byrne. **The application of the clonogenic assay to the toxicity testing of carbon nanomaterials.** *Nanotoxicity, Paris, France (June 2007)*

E.Herzog, A. Casey, H.J. Byrne, F.M. Lyng, G. Chambers, M. Davoren. **Problems associated with the cytotoxicity testing of single walled carbon nanotubes.** *Invitox 2006, Belgium (October 2006)*

A 3. Poster presentations

E.Herzog, H.J. Byrne, M. Davoren, A. Casey, A. Duschl, G.J. Oosthing. **Single-walled carbon nanotubes vs. asbestos – the role of lung surfactant dispersion.** *Irish Society of Toxicology (IST) meeting, Ireland (October 2008)*

E.Herzog, T. Pfaller, A. Casey, H.J. Byrne, M. Davoren, A. Duschl, G.J. Oosthing. **Challenges associate witht the toxicity testing of nanoparticles**. *Nanotox2008, Switzerland (September 2008)*

E. Herzog, A. Casey, F.M. Lyng, M. Davoren, H.J. Byrne. **Single-walled carbon nanotubes – direct vs. indirect effects**. *ESF-EMBO Symposium, Sant Feliu, Spain (November 2007)*

E. Herzog, A. Casey, F.M. Lyng, M. Davoren, H.J. Byrne. **Single-walled carbon nanotubes – direct vs. indirect effects**. *IST annual meeting, Dublin, Ireland (November 2007)*

E. Herzog, A. Casey, F.M. Lyng, H.J. Byrne, M. Davoren. **A new approach to the toxicity testing of carbon nanomaterials.** *Nanotoxicology 2007, Venice, Italy (April 2007)*

A

E. Herzog, A. Casey, F.M. Lyng, H.J. Byrne, M. Davoren. **A new approach to the toxicity testing of carbon nanomaterials.** *IST annual meeting, Dublin, Ireland (November 2007)*

Appendix B

Awards, workshops, conferences and training

B 1. Awards received

FEI Young Scientist Award to attend the TEM UCA Summer Workshop on Nanoparticle Research, Cadiz University, Puerto Real, Spain, 18.09.2006 – 29.09.2006

Boehringer Ingelheim Fonds Travel Grant to visit the Institute of Inhalation Biology, Helmholtz Zentrum München, Environmental Research Centre for Environmental Health, Munich, Germany

ESF Award to attend the ESF-EMBO symposium conference on "Probing interactions between nanoparticles/biomaterials and biological systems – alternative approaches to bio- and nano-safety", Sant Feliu de Guixols, Spain, 3 - 8 November 2007

Irish Society of Toxicoloty (IST) Travel Award to attend the 2nd International Conference on Nanotoxicology, Zürich, Switzerland

Award for one of the five best abstracts submitted to the 2nd International Conference on Nanotoxicology, Zürich, Switzerland

B 2. Workshops, conferences and training attended

Invitox 2006 – 14th International Workshop on *In vitro* Toxicology

Ostend, Belgium

TEM UCA Summer Workshop on Nanoparticle Research

Cadiz University, Puerto Real, Spain, 18 – 29 September 2006

Ultramicrotome Training by Dr David Cottell, UCD

15 – 19 October 2006

Zeiss Cell Observer System Training

30 November 2006

NanoToxicity 2007 – Managing the risk governance

Paris, France, 26 – 28 June 2007

Nano Toxicology 2007 Conference

San Servolo, Venice, Italy, 19 – 21 April 2007

International Symposium on "The Dosimetry of Incidental and Manufactured Nanoparticles" (GSF-Focus Network Aerosols and Health), Commemorating the 60th Birthday of Wolfgang G. Kreyling

Helmholtz Zentrum, Neuherberg, Germany, 22 June 2007

Joint Conference on Nanotechnology - Implications for human health, the environment and food safety

Dublin, Ireland 2 September 2007

ESF-EMBO Symposium Conference on "Probing interactions between nanoparticles/biomaterials and biological systems – alternative approaches to bio- and nano-safety"

Sant Feliu de Guixols, Spain, 3 - 8 November 2007

Research Training

Institute of Inhalation Biology, Helmholtz Zentrum München, Environmental Research Centre for Environmental Health.

Munich, Germany, July 2007 - October 2007

Research Training

Department of Molecular Biology, University of Salzburg

Salzburg, Austria, October 2007 – April 2008

NanoImpact Workshop on "Standardization and reference materials"

University College Dublin (UCD), Dublin, Ireland, June 2008

9th International Conference on Particles – Risks and Opportunities

Cape Town, South Africa, September 2008

Nanotoxicology - 2nd International Conference on Nanotoxicology

Zürich, Switzerland, 7 - 10 September 2008

Annual meeting of the Irish Society (IST) 2008 on "Food Supplements:

Toxicological concerns in context"

Cork, Ireland, 16 October 2008

Appendix C

Supplementary material for Chapter 2

Table C.1: Summary of toxicity studies performed on CNT

CNT type	*In vitro/in vivo*	Model	Dispersion vehicle and method	Endpoints investigated	Findings and Conclusions	*Ref*
MWCNT (coated with pluronic F127)	*In vivo*	Mouse	Pluronic F127	Injection into mouse cerebral cortex	No degeneration of neurons surrounding the site of injection MWCNT do not induce apoptosis of cortical neurons and avoids F-127 induced apoptosis	[200]
SWCNT	*In vivo*	Bacteria Microalgae Microinvertebrates Fish	Aqueous suspension	Ecotoxicity Sediment toxicity	SWCNT were able to increase reference sediment toxicity and its elutriate toxicity	[380]
MWCNT (pristine and oxidized)	*In vitro*	Human T-cells	Dispersion in distilled water	Cytotoxicity	Oxidized MWCNT are highly more toxic than pristine MWCNT and induce significant loss in cell viability through apoptosis at doses of 400 μg/ml	[5]
CNT (varying Fe contents and surface areas) Carbon nanofibres	*In vitro*	Human monocytic cell line (THP-1) Human monocytes	Dispersion in culture medium using short-term sonication	Cytotoxicity Inflammation Oxidative stress Phagocytosis	Cellular responses varied with fibre morphology and state of aggregation Long, straight and well-dispersed particles were most reactive All nanotubes tested reduced phagocytic ability and led to frustrated phagocytosis	[151]
SWCNT	*In vivo*	Crop (cabbage, carrot,		Ecotoxicity	Increased effects of SWCNT on root length compared to f-	[381]

CNT type	*In vitro/in vivo*	Model	Dispersion vehicle and method	Endpoints investigated	Findings and Conclusions	*Ref*
f-SWCNT		cucmber, lettuce, onion, tomatoe)		Particle uptake Interaction with root surface	SWCNT Inhibition of root elongation in tomatoe, enhance elongation in onion and cucumber following SWCNT exposure Inhibition of root elongation in lettuce by f-SWCNT Effects more pronounced after 24h compared to 48h Presence of nanotube sheets on root surfaces but no visible uptake	
HiPco® SWCNT	*In vitro*	Cell free system	Dispersion in culture medium using short-term sonication	Culture medium interactions	Interaction of SWCNT with components of cell culture medium including phenol red, FBS and riboflavin	[255]
HiPco® SWCNT	*In vitro*	Cell-free system	Dispersion in indicator dye solutions	Indicator dye interactions	Interaction between SWCNT and frequently used toxicity indicator dyes including resazurin, Neutral Red, MTT, WST-1 and Coomassie Blue Interactions result in changes in absorbance/emission spectra resulting leading to the risk of data misinterpretation	[257]
HiPco® SWCNT ArcD SWCNT	*In vitro*	Alveolar type II epithelium (A549)	Dispersion in culture medium using short-term sonication	Indirect cytotoxicity Cell proliferation	SWCNT cause indirect cytotixicyty due to nutrient adsorption and therefore medium depletion which in turn leads to decreases in cell proliferation	[54]
SWCNT	*In vivo*	Zebrafish (Danio rerio)	Aqueous suspensions	Aquatic toxicity Zebrafish	Delay in hatching between 52 – 72h postfertilization following exposure to SWCNT and DWCNT but was likely to be induced	[382]

CNT type	*In vitro/in vivo*	Model	Dispersion vehicle and method	Endpoints investigated	Findings and Conclusions	*Ref*
DWCNT				development	by catalyst residues No effect on embryonic development Microscaled SWCNT agglomerates formed which could not enter the chorion of fish embryos	
HiPco® SWCNT (raw)	*In vivo*	Rabbits (adult New Zealand, white)	Dispersion in 1% pluronic F108 surfactant followed by centrifugation	Intravenous injection 30 min – 24h exposure	Displacement of nanotube coating of synthetic surfactant molecules by blood proteins within seconds Half-life of nanotube blood concentration of 1.0 +/- 0.1h No adverse effects from low-level nanotube exposure Following 24h significant SWCNT concentrations could only be found in the liver	[196]
MWCNT (highly pure)	*In vitro*	Fibroblasts (HS-5) Osteoblasts (hFOB)	Dispersion in poly-sulfane	Cytotixicity Inflammation	High cell viability and only slight increase in collagen formation post MWCNT exposure No IL-6 release No ROS Good biocompatibility of MWCNT	[219]
SWCNT	*In vivo* *In vitro*	Mouse (ICR, 8 weeks old) macrophages		Intratracheal instillation Molecular effects	activation of alveolar macrophages chronic inflammatory responses severe pulmonary granuloma formation uptake of SWCNT by macrophages is able to activate	[172]

CNT type	*In vitro/in vivo*	Model	Dispersion vehicle and method	Endpoints investigated	Findings and Conclusions	*Ref*
					transcription factors including NF-κB and AP-1, leading to oxidative stress, release of proinflammatory cytokines, recruitment of leukocytes, induction of protective and antiapoptotic gene expression and activation of T cells resulting innate and adaptive immune response may explain the chronic pulmonary inflammation and granuloma formation seen in vivo	
SWCNT	*In vitro*	Human embryonic kidney cells (HEK293)	Suspension in 0.5% DMSO	Cell adhesion Protein secretion Cell viability and proliferation	Decreased cell adhesion and proliferation with increased dose and time of exposure Cell surface attachment of SWCNT Upregulation of genes involved in apoptosis including Rb, p16, p53 Downregulation of genes associated with the G1 phase of the cell cycle causing cell arrest and eventually cell death Secretion of proteins that wrap around SWCNT leading to isolation of SWCNT attached cells from main cell population	[228]
HiPco® SWCNT	*In vitro*	Human type II alveolar epithelium (A549)	Dispersion in culture medium using short-term sonication	Cytotoxicity Ultrastructural alterations 24h exposure	Low acute cytotoxicity with most EC_{50}'s > 800 μg/ml Increased number of lamellar bodies and decreased microvilli following treatment with high doses	[56]
MWCNT (14C-taurine	*In vivo*	Mouse (male KunMing)	Aqueous suspension	Intravenous injection	Following intravenous injections, MWCNT accumulated predominantly in the liver and retained there for a long time; Entrapment in Kupffer cells was observed but low acute liver	[198]

CNT type	*In vitro/in vivo*	Model	Dispersion vehicle and method	Endpoints investigated	Findings and Conclusions	*Ref*
labeled)				Intratracheal instillation Stomach intubation Biodistribution Translocation	toxicity; small amounts found in spleen and lung with gradual elimination Intratracheal instillation resulted in accumulation in the lung with gradual elimination Following stomach intubation, MWCNT were found in stomach, small and large intestine and feces; no translocation to the blood or adsorption by the intestinal tract was found;	
CVD MWCNT	*In vitro*	Human skin fibroblasts (HSF42)		Cytotoxicity Cell proliferation Gene expression Promoter analysis	Cell cycle arrest Increases in necrosis/apoptosis Disturbance of multiple cellular pathways Induction of genes involved in cellular transport, metabolism, cell cycle regulation and stress response Induction of genes indicative of strong immune and inflammatory responses	[3]
f-SWCNT	*In vitro*	Primary immune cells (isolated from mouse spleen)	Dispersion in water followed by culture medium	Cell uptake Cell viability 24h exposure	f-SWCNT can enter the cytoplasm of B lymphocytes, T-lymphocytes and macrophages of the spleen Un-soluble nanotubes were present as aggregates found in macrophages and affect their phagocytic ability No cytotoxicity	[248]
SWCNT	*In vitro*	Macrophages (RAW 264.7)	Dispersion in culture medium	Protein binding	Albumin was identified as the major fetal bovine or human serum/plasma protein adsorbed onto SWCNT	[212]

CNT type	*In vitro/in vivo*	Model	Dispersion vehicle and method	Endpoints investigated	Findings and Conclusions	*Ref*
f-SWCNT			using sonication or pluronic F127 surfactant	Inflammation	Inhibition of COX-2 induction by LPS in the presence of SWCNT; anti-inflammatory response was inhibited by scavenger receptor antagonist fucoidan which also reduced SWCNT uptake Surfactant coating inhibited albumin adsorption and anti-inflammatory properties Albumin-coated SWCNT reduced LPS-mediated COX-2 induction under serum-free conditions SWCNT did not reduced binding of LPS to macrophages	
SWCNT MWCNT (purified)	*In vitro*	Cell free system	Suspension in 5% SDS/PBS	Oxidative stress	No detection of free radicals Quenching of ROS by MWCNT	[235]
SWCNT (highly pure)	*In vitro*	Murine macrophages (J774) Human macrophages	Dispersion in culture medium by long-term sonication	Cytotoxicity Inflammation Phagocytosis	Low nitric oxide (NO) release Low cellular uptake Low cytotoxicity Contact of mammalian cells with pure SWCNT without catalyst metals and graphite contaminants is unlikely to result in any inflammatory response or impairment of phagocytosis	[213]
CVD CNT	*In vitro*	Human umbilical vein endothelial	Dispersion in culture medium followed by	Cytotoxicity	No cytotoxicity	[229]

CNT type	*In vitro/in vivo*	Model	Dispersion vehicle and method	Endpoints investigated	Findings and Conclusions	*Ref*
		cells (HUVEC)	centrifugation			
SWCNT	*In vivo*	Protozoan Tetrahymena thermophila		Ecotoxicity Particle uptake	Internalization possibly allowing bioaccumulation along the food chain Protocoa aggregation leading to decreased ability to ingest and digest prey bacteria species SWCNT may be used to improve the efficiency of wastewater treatment	[383]
MWCNT CVD SWCNT (iron catalyst)	*In vitro*	Mouse keratinocytes	Dispersion in cell culture medium using sonication	Cytotoxicity Oxidative stress MMP	Reductions in cell viability in a time-dependent manner up to 48h with full recovery of mitochondrial function at 72h MWCNT treatment caused 3-fold increase in ROS compared to SWCNT treatment following 24h High aspect ration carbon material toxicity is believed to depend on dimension and composition	[222]
MWCNT (various purities)	*In vivo*	Guinea pigs (male, three-colour)	Suspension in PBS + 1% Tween80	Intratracheal instillation to a single dose for 3 months Inflammation	Bronchial obliterans organizing pneumonia with focal non-specific desquamative interstitial pneumonia-like reaction No fibrosis or mild peribronchiolar fibrosis Infiltration of inflammatory cells and increased IL-8 concentration in BALF dependend on nanomaterial tested No changes in protein concentrations of BALF Indications that intratracheal instillation of MWCNT may induce pulmonary pathology	[173]

CNT type	*In vitro/in vivo*	Model	Dispersion vehicle and method	Endpoints investigated	Findings and Conclusions	*Ref*
SWCNT f-SWCNT	*In vitro*	Human hepatoma (HepG2)	Dispersion using sonication	Indirect cytotoxicity Protein adsorption	Dose-dependent adsorption and depletion of over 14 amino acids and vitamins from cell culture medium Reduced cell viability following culture in depleted media; restoring of viability due to addition of folate	[230]
SWCNT MWCNT (75% purity)	*In vitro* *Ex vivo*	Alveolar macrophages isolated from BALB/c mice and DO11.10+/+ transgenic mice	Dispersion in heat inactivated FBS using homogenizing and sonication	Cell viability Antigen-presentation Cytokine release Airway hyper-responsiveness Lung lavage cell differentials	Accumulation carbon nanoparticles in plasma membrane of cells Decreases in TNF-α production, increases in IL-1β and increases in IL-12 Increased alveolar macrophage function with regard to antigen-presentation Significantly exacerbated airway hyper-responsiveness Influx of macrophages into the lung	[214]
MWCNT	*In vivo*	Mouse (C57Bl)		Pharyngeal aspiration Interactions between MWCNT and Ozone (O3) exposure Cytotoxicity	Pronounced cellular response and increases in cytotoxicity/inflammatory markers in MWCNT exposed mice Increased total BALF cells, LDH, TNFα, IL-1β and mucin levels following O3/MWCNT exposure No additive or synergistic effect between CNT and ozone In contrast, some responses were attenuated following sequential exposure	[180]

CNT type	*In vitro/in vivo*	Model	Dispersion vehicle and method	Endpoints investigated	Findings and Conclusions	*Ref*
				Inflammation		
HiPco® SWCNT ArcD SWCNT	*In vitro*	Human alveolar type II epithelium (A549) Human keratinocytes (HaCaT) Human bronchial epithelial cells (BEAS-2B)	Dispersion in culture medium using short-term sonication	Clonal survival Cell proliferation	No effects on colony formation of A549 or HaCaT cells following 10 and 7 days exposures, respectively Significant effects on colony size and therefore cell proliferation starting at concentrations as low as 1.56 μg/ml	[384]
HiPco® SWCNT	*In vitro*	Human alveolar type II epithelium (A549) Primary human bronchial epithelium (NHBE)	Dispersion in culture medium or DPPC/PBS using short-term sonication	Cytotoxicity Inflammation	Downregulation of IL-8 Inhibition of promoter activation of IL-8 and IL-6 Suppression of inflammatory mediator release (IL-8, IL-6, MCP-1) Increased toxicity following DPPC dispersion	[385]
CVD MWCNT (highly purified)	*In vitro*	Mouse macrophage cell line (J774.1)	Suspension in 10% pluronic F68 surfactant (final concentration of 1% in culture medium)	Cytotoxicity Gene expression	Cytotoxicity of MWCNT higher than that of crocidolite asbestos Toxicity not affected by antioxidant or glutathione inhibitor treatment Cytotoxicity could not be explained by changes in gene	[215]

CNT type	*In vitro/in vivo*	Model	Dispersion vehicle and method	Endpoints investigated	Findings and Conclusions	*Ref*
					expression No activation of MAP kinases or apoptosis Association of MWCNT with plasma membrane of macrophages Disruption of membrane integrity Protein adsorption onto MWCNT, e.g. macrophage receptor with collagenous structure (MARCO) Indications that cytotoxic effects triggered by reactions with MARCO on plasma membrane leading to membrane rupture	
Soot with high CNT content	*In vivo*	Humans Albion rabbits	Water suspension	Patch test (dermal toxicity) Modified Draize rabbit eye test (cular instillation) 24-96 h exposures	No association of CNT with skin irritation or allergene risks. Dermatological trials have not shown signs of health hazard.	[189]
ArcD-CNT	*In vivo*	Guniea pigs (male dunkin	Suspension in saline with Tween	Intratracheal instillation	No induction of abnormalities in pulmonary function or measurable inflammation	[175]

CNT type	*In vitro/i n vivo*	Model	Dispersion vehicle and method	Endpoints investigated	Findings and Conclusions	*Ref*
(pristine)		Hartley)		4 weeks exposure to a single dose	Working with CNT is unlikely to be associated with any health risks	
CVD-MWCNT ArcD MWCNT	*In vivo*	Guinea pigs	Suspension in saline + SDS	Intratracheal instillation of single bolus dose 90 days exposure	Organizing pneumoitis with focal non specific desquamative interstitial pneumonia-like reaction Increase of lung resistance Pulmonary lesions Toxicity depends on time of exposure and material characteristics	[174]
SWCNT	*In vitro*	Mouse lung epithelial cells (FE1-Mutatrade markMouse)		Cytotoxiciyt Cell proliferation Mutagenicity	No cytotoxicity Decreased cell proliferation and larger fraction of cells in G1 phase No increase in strand break levels Significant increases in FPG sensitive sites/oxidized purines No effects on the mutant frequency in the cII gene SWCNT less genotoxic than carbon black or DEP	[244]
ArcD SWCNT (purified) CVD MWCNT	*In vitro*	Alveolar macrophages	Dispersion in culture medium using sonication	Cytotoxicity Phagocytosis Ultrastructural	Cytotoxicity in sequence order of SWCNT>MWCNT>SiO_2>C60 SWCNT most effective in impairing phagocytosis Swelling of endoplasmic reticulum, vacuolar changes and	[48]

CNT type	*In vitro/in vivo*	Model	Dispersion vehicle and method	Endpoints investigated	Findings and Conclusions	*Ref*
				alterations	phagosomes following SWCNT exposure	
HiPco® SWCNT (non-purified and purified)	*In vitro*	Macrophages (RAW 263.7)		Oxidative stress	Neither type of SWCNT was able to induce production of superoxide radicals or NO Higher detection of OH* after exposure to non-purified SWCNT Increased lipid peroxidation and GSH depletion following exposure to iron containing SWCNT Iron effects redox dependent macrophage responses	[49]
MWCNT (purified, unpurified, functionalised, annealed)	*In vivo*	Bacteria		Role of physical and chemical properties on MWCNT toxicity	Correlation between bacterial cytotoxicity and physicochemical properties that enhance MWCNT-cell contact Higher toxicity with uncapped, debundled, short and dispersed MWCNT	[386]
MWCNT	*In vitro*	Alveorlar type II epithelium (A549)		Cytotoxicity DNA damage Oxidative stress	Cytotoxicity and DNA damage at lowest dose tested MWCNT less toxic than CuO nanoparticles	[387]
SWCNT	*In vitro*	Human bronchial epithelial cells (BEAS-2B)		Oxidative stress Gene transcription	Following exposure to 60 – 240 µg/ml for 18h altered expression of 187 transcripts was observed including genes involved in metabolism (Cyp1B1, aspargine synthetase, NNMT), cell cycle control (p21, CD24, GAS1, PA26) and others (matric metalloproteinase, ferrodoxin reductase, cathepsin L2) SWCNT appear to alter a variety of genes including those	[203]

CNT type	*In vitro/in vivo*	Model	Dispersion vehicle and method	Endpoints investigated	Findings and Conclusions	*Ref*
					involved in oxidative stress	
SWCNT	*In vitro*	Lung fibroblasts (V79) Salmonella typhimurium (YG1024/YG1029)		Cytotoxicity Genotoxicity	Dose- and time-dependent cytotoxicity DNA strand breaks as seen using the Comet assay Some but not significant micronucleus induction No mutations in Salmonella typhimurium	[245]
f-SWCNT (pristine) f-MWCNT	*In vitro*	Mouse embryonic fibroblasts (3T3, 3T6) Chinese hamster ovary cells (CHO) Human alveolar type II epithelium (A549) Human cervical cancer cells (HeLa) Human embryonic kidney cells		Cell uptake	Uptake of f-CNT by a wide range of cells Ability of intracellular trafficking through different cellular barriers	[250]

CNT type	*In vitro/in vivo*	Model	Dispersion vehicle and method	Endpoints investigated	Findings and Conclusions	*Ref*
		(HEK293) Keratinocytes Human T-cell lymphoma (Jurkat) Mouse intestinal epithelila cells (MOD-K) Fungal cells (Cryptococcus neoformans) Yest (Saccharomyces cerevisiae) Bacteria (E. coli)				
CVD SWCNT (highly pure) CVD MWCNT (different diamters; purified)	*In vivo*	Mouse (BALB/c)	Suspension in physiological saline	Subcutaneous implantation for up to 3 months T-cell responses	No fatalities No large changes in weight of mice Only SWCNT activated major histocompatibility complex (MHC) class I pathway of antigen-antibody response system (higher CD4+/CD8+ value) following 1 week resulting in edematous reactions	[192]

CNT type	*In vitro/in vivo*	Model	Dispersion vehicle and method	Endpoints investigated	Findings and Conclusions	*Ref*
				Histopathology	After 2 weeks, activation of MHC class II pathway was seen for all samples Toxicological response of CNT was absolutely lower than that of asbestos	
HiPco® CNT ArcD CNT (raw and purified)	*In vivo*	Mice (male B6C3F1)	Dispersion in heat inactivated mouse serum	Intratracheal instillation 7 and 90 days exposure to single bolus dose	Induction of dose-dependent epithelioid granulomas Mortality observed with high dose Intrinsic toxicity and biopersistence observed	[176]
SWCNT	*In vivo*	Mouse (C57BL/6, HO-1 transgenic, ApoE(-/-) transgenic)	Suspension in PBS	Intrapharyngeal instillation Aortic mitochondrial alterations Oxidative stress 7, 28 and 60 days exposure to single dose 8 weeks exposure to repeated doses	Activation of HO-1 Aortic mitochondrial DNA damage accompanied by changes in mitochondrial glutathione and protein carbonyl levels in C57BL/6 mice Stimulated progression of atherosclerosis following repeated exposure of ApoE(-/-) mice but no modification of lipid profiles Acceleratied plaque formation when fed on atherogenic diet Increased plaque areas in the aortas and brachiocephalic arteries accompanied by increased mitochondrial DNA damage but not inflammation	[186]

CNT type	*In vitro/in vivo*	Model	Dispersion vehicle and method	Endpoints investigated	Findings and Conclusions	*Ref*
f-SWCNT (watersoluble)	*Ex vivo*	Mouse (6-week old BALB/c)	Suspension in saline solution	Intravenous injection Biodistribution Blood circulation behaviour Use of Raman spectroscopy for SWCNT detection in tissues	Raman spectroscopy can be used to detect CNT in animals for biodistribution studies Degree of functionalisation in important to the in vivo behaviours of nanotubes SWCNT detected in feces, kidney and bladder Majority of f-SWCNT detected in feces indicating biliary excretion; only small percentage excreted via renal pathway No obvious toxic effects based on necroscopy, histologogy and blood chemistry studies Potential of f-SWCNT for biomedical applications	[193]
CNT	*In vitro*	Cell free system	Insertion into dimyristophylphosphatidylcholine (DMPC)	Interaction between CNT and membrane bilayers	Alteration of DMPC bilayer molecule packing including the creation of open, unoccupied rings directly around the nanotube Increased rigidity of bilayer structure Solvated calcium ions preferentially transported through the inserted nanotubes as compared to hydrated sodium ions Increased diffusion of ethanol, caffeine and urea through membrane bilayer	[388]
CVD MWCNT	*In vitro*	Mouse fibroblasts (L929)	MWCNT films	Cytotoxicity Cell adhesion	No cytotoxicity Good cell adhesion on MWCNT films	[220]

CNT type	*In vitro/in vivo*	Model	Dispersion vehicle and method	Endpoints investigated	Findings and Conclusions	*Ref*
CVD MWCNT CNF (purified and functionalised	*In vitro*	Lung carcinoma cell lines (H596, H446, Calu-1)	Suspension in gelatine followed culture medium and sonication	Cytotoxicity Cell proliferation	More pronounced inhibition of cell proliferation and cell death with increasing aspect ration of test material and with the presence of chemically active functional groups Cytotoxicity within 24h H569 cells most sensitive Similar morphological alterations fro all materials including cell detachment, eosinophilia and pipnotic nuclei	[204]
CVD SWCNT (highly pure)	*In vivo*	Rats(female CDF (F344)/CrlBR)	Milling and suspension in 1% pluronic F-68 surfactant in PBS followed by sonication	Oropharyngeal aspiration Lung histopathology Cell proliferation Growth factor expression 1 and 21 days exposure	No overt inflammatory response Formation of small, focal interstitial fibrotic lesions within the alveolar region of the lung at 21 days Bridging of a small fraction of alveolar macrophages by unique intercellular carbon structures that extended into the cytoplasm of each macrophage; the same was observed in situ in lungs of exposed rats Increased cell proliferation only at sites of fibrotic lesion formation Increased expressionof platelet-derived growth factors (PDFG-A, PDFG-B, PDFG-C) at 1 day; no increased mRNA levels at 21 days post exposure	[187]
SWCNT	*In vitro*	Human alveolar type II epithelium (A549)		Cytotoxicity Oxidative stress	ROS seen following 72h exposure to concentrations of 1 – 10 µg/ml Dose-dependent decrease in cell viability from 0.5 µg/ml on	[205]

CNT type	*In vitro/in vivo*	Model	Dispersion vehicle and method	Endpoints investigated	Findings and Conclusions	*Ref*
		Lung cancer cell line (H1299) Human keratinocytes (HaCaT) Cervical cancer cell line (HeLa)			Activation of NF-κB at concentrations of 1 μg/ml Activated NF-κB protein complex binding to DNA and initiation of transcription	
CNT	*In vitro*	Embryonic rat brain neuron cells		Cell growth	Inhibition of cell growth	[232]
HiPco® SWCNT SWCNT (laser ablation)	*In vivo*	Human	Air	Aerosol inhalation (filter samples) Dermal exposure (cotton gloves) 30 min and 11-16h exposures	Concentrations from 0.7 – 53 μg/m3 found on filters (HiPco® material produced visible large clumps) Deposition on individual gloves from 0.2 – 6mg (visible contamination) Propensity of unprocessed SWCNT to form an aerosol during handling	[139]
MWCNT	*In vivo*	Mouse (C57BL/6 adult males)	Air	Whole body inhalation Histopathology Gene	Uptake of MWCNT by alveolar macrophages No inflammation or tissue damage No increase in white blood cell levels in BALF Nonmonotonic systemic immunosuppression after 14 days, not	[188]

CNT type	*In vitro/in vivo*	Model	Dispersion vehicle and method	Endpoints investigated	Findings and Conclusions	*Ref*
				expression	after 7 days, characterised by reduced T-cell-dependent antibody response to sheep erythrocytes and reduced T-cell proliferative ability in presence of mitogen Decreased natural killer cell function No change in gene expression in lung Increased IL-10 and NADPH oxidoreductase-1 mRNA levels in spleen	
CVD MWCNT (unmodified)	*In vitro*	Human epidermal keratinocytes (HEK)	Dispersion in culture medium using short-term sonication	Cytotoxicity Cytokine release Protein expression	Vacuoles within cytoplasm of MWCNT containing cells Decreased cell viability Time- and dose-dependent Increase in IL-8 release Localization and initiation of irritation response could not be shown Proteomic analysis suggested disregulation of intermediate filament expression, cell cycle inhibition, altered vesicular trafficking or exocytosis and downregulation of membrane scaffold protein CNT are believed to be potentially dermatotoxic	[50]
CVD MWCNT	*In vitro*	Human epidermal keratinocytes (HEK)	Suspension in culture medium + different dilutions of surfactants (Pluronic F127, L61, L92,	Surfactant effects	Cell viability proportional to surfactant concentration ranging from 27 – 98.5 % with Pluronic F127 and more than 90% for other surfactants Surfactant dispersed and reduced MWCNT aggregation in	[223]

CNT type	*In vitro/in vivo*	Model	Dispersion vehicle and method	Endpoints investigated	Findings and Conclusions	*Ref*
			Tween20, Tween60)		medium Increased IL-8 release following MWCNT exposure, independent of surfactant content	
CVD DWCNT	*In vivo*	Amphibian larvae (Xenopus laevis)	Suspension in water	Ecotoxicity Genotoxicity	No genotoxicity based on micronucleus assay Acute toxicity at all concentrations related to physical blockage of gills and/or digestive tract DWCNT detected inside the intestine	[389]
MWCNT (ground and unground)	*In vivo*	Rats (female Sprague Dawley)	Suspension in sterile 0.9% saline + 1% Tween80	Intratracheal instillation of single bolus dose 1 and 2 months exposure	Unground MWCNT accumulated in the airways Ground MWCNT were cleared more rapidly Both MWCNT induced inflammatory (more marked for ground MWCNT) and fibrotic reaction Both MWCNT caused pulmonary lesions at 2 months Biopersistence and intrinsic pulmonary toxicity	[113]
MWCNT(purified and ground)	*In vitro*	Peritoneal macrophages Alveolar macrophages		Cytotoxicity Inflammation	Intact MWCNT lower activity than ground MWCNT Ground MWCNT lead to LDH release and TNF-α upregulation Increased agglomeration in unground samples may result in decreased availability and decreased inflammatory potential	[177]
MWCNT	*In vivo*	Rat Human		Intratracheal instillation	Dose-dependent increase in micronuclei levels in type II pneumocytes in vivo	[177]

CNT type	*In vitro/in vivo*	Model	Dispersion vehicle and method	Endpoints investigated	Findings and Conclusions	*Ref*
	In vitro	epithelial cells (MCF-7)		Genotoxicity	Increased micronuclei levels in epithelial cells in vitro Centromere-positive and –negative micronuclei in MCF-7 cells Evidence of the potential of MWCNT to induce clastogenic as well as aneugenic effects	
MWCNT (progressively and selectively modified to display varying degrees of structural defects)	*In vivo* *In vitro*	Rat (Wistar) Rat lung epithelial cells		Intratracheal instillation Short- and long-term lung responses Role of structural defects on MWCNT toxicity genotoxicity	Acute pulmonary and toxicity and genotoxicity was reduced upon heating but restored upon grinding, indicating that the intrinsic toxicity of CNT is mainly mediated by the presence of defective sites in their carbon framework	[178]
HiPco® SWCNT MWCNT	*In vitro*	Murine macrophages	Suspensionin DMSO	Cytotoxicity Cytokine release	Threshold dose for cytotoxicity was 2.5 µg/ml Relative SWCNT toxicity same as asbestos at 5 µg/ml No stimulation of cytokine production (IL-10, IL-12) Cytotoxicities and related insults did not seem to be morphologically specific for murine macrophages	[167]
SWCNT	*In vivo*	Water fly (Daphnia		Fresh-water	Unsolubilized particles were floating on top of the water and	[390]

CNT type	*In vitro/in vivo*	Model	Dispersion vehicle and method	Endpoints investigated	Findings and Conclusions	*Ref*
		magna) Amphipod crustacean Hyalella azteca Fish (Japanese medaka) Marine copepods Juvenile large-mout bass		toxicity	were digested Significant increase in lipid peroxidation in fish brains after 48h exposure to 500 µg/ml but not after 1000 µg/ml Clarification of water within the fish tank suggesting an effect on microorganisms present	
SWCNT (raw)	*In vitro*	Normal human mesothelial cells Malignant human mesothelial cells	Dispersion in culture medium (0.1% FBS)	Cytotoxicity Oxidative stress Cell signalling	ROS generation Cell death Enhanced DNA damage H2AX phosphorylation Activation of PARP, AP-1, NF-κB, P38 and Act All effects occurred in a dose-dependent manner SWCNT can potentially cause adverse cellular responses in mesothelial cells through activation of cell signaling associated with oxidative stress	[226]
MWCNT (short,	*In vivo*	Mouse	Dispersion in 0.5% BSA/saline	Intraperitoneal	Long MWCNT resulted in asbestos-like pathogenic behaviour including inflammation (PMN and protein exudation) and	[201]

CNT type	*In vitro/in vivo*	Model	Dispersion vehicle and method	Endpoints investigated	Findings and Conclusions	*Ref*
long, curled)		(C57BL/6)	solution using sonication	injection 24h and 7 day exposure Asbestos-like behaviour	foreign body giant cells and granuloma formation on the peritoneal side of the diaphragm No effects on pleural side of the diaphragm No effects from sample that do not conatin long fibres	
HiPco® SWCNT	*In vitro*	Human monocyte derived macrophages (MdM)	Dispersion in tetrahydrofuran (THF) using sonication	Cytotoxicity Cell uptake	Translocation of SWCNT into cells Entering of cytoplasm and localization within the cell nucleus causing cellmortality in a dose-dependent manner	[216]
SWCNT (purified and un-purified)	*In vitro*	Human alveolar type II epithelium (A549)	Storage in 1% SDS, precipitation in acetone, resuspension in water and dispersion in culture medium using sonication	Cytotoxicity Oxidative stress	Decreased toxicity of purified SWCNT No acute cytotoxicity No HO-1 expression Un-purified SWCNT more effective in inducing oxidative stress than purified samples based on ROS, peroxynitrite and superoxide detection	[51]
CVD SWCNT (purified and un-purified) CVD MWCNT	*In vitro*	Human alveolar type II epithelium (A549) Rat alveolar macrophages	Acetone-precipitation, sedimentation, centrifugation and dispersion in culture medium	Cytotoxicity Inflammation Oxidative stress	CNT cross cell membranes of rat macrophages and might therefore influence cell physiology and function No acute cytotoxicity No inflammatory response	[206]

CNT type	*In vitro/in vivo*	Model	Dispersion vehicle and method	Endpoints investigated	Findings and Conclusions	*Ref*
		(NR8383)			Rising tendency of TNF-α release from LPS-primed cells due to CNT treatment Dose- and time-dependent increase in ROS and decrease in MMP with un-purified CNT; no effect following exposure to purified CNT Metal traces are believed to be responsible for the biological effects observed	
SWCNT MWCNT (purified, open)	*In vivo*	Rats (Wistar-Kyoto)	Suspension in 0.9% saline	Intravenous injections of single dose	Time and rate of carotid artery thrombosis development was accelerated Particle were able to activate platelets	[199]
HiPco® f-SWCNT (purified)	*In vitro*	Rat aortic smooth muscle cells (SMC)	Dispersion in osmosis-purfied water using filtration, sonication and centrifugation	Cell growth	Removal of aggregated material increased cell numbers in comparison to unfiltered samples below 100 μg/ml At 100 μg/ml, both filtered and unfiltered media exhibited a similar decrease in cell numbers SWCNT was more inhibitory in terms of cell growth than activated carbon material	[231]
CVD MWCNT (90% purity) CVD SWCNT (50% puritiy) ArcD CNT	*In vitro*	Human lung epithelial cells (Calu-3)	Dispersion in PBS followed by culture medium addition	Paracellular permeability	No cytotoxicity Large decrease in trans-epithelial electrical resistance (TEER) and increase in mannitol permeability following MWCNT treatment; smaller effects for SWCNT and no effects for ArcD CNT	[207]

CNT type	*In vitro/in vivo*	Model	Dispersion vehicle and method	Endpoints investigated	Findings and Conclusions	*Ref*
(MWCNT/SWCNT)					No further increase in TEER due to the addition of MWCNT during tight monolayer formation Prevention of TEER recovery due to MWCNT	
HiPco® SWCNT ArcD SWCNT (purified) CVD SWCNT (purified) CVD DWCNT (purified)	*In vitro*	Erythrocytes Plasma	Dispersion in 0.5% TritonX-100 or serum or plasma	Complement activation	All CNT samples could activate the complement system by the classical pathway HiPco® SWCNT more effective than DWCNT In contrast to DWCNT, alternative pathway consumption by SWCNT very low	[217]
CVD DWCNT (purified)	*In vitro*	Cell free system	n/a	Surfactant protein interactions	SP-A and SP-D selectively bind to DWCNT Binding was Ca2+ -ion dependent Binding was variable between CNT batches and therefore believed to be mediated by surface impurities or chemical modification Chronic exposure may result in sequestration of SP-D and SP-A which might lead to lung infection and emphysema	[12]
MWCNT (220 and 825 nm)	*In vivo*	Rat (male Wistar)	Clusters	Bilaterial implantation 1 and 4 weeks exposure to 2 bilateral	Granuloma formation Inflammation; inflammatory response around 220 nm MWCNT was lower than 835 nm MWCNT	[391]

CNT type	*In vitro/in vivo*	Model	Dispersion vehicle and method	Endpoints investigated	Findings and Conclusions	*Ref*
				implants	Macrophages could envelope smaller MWCNT more readily	
SWCNT	*In vitro*	Foreskin cells		Stress responses	Induction of oxidative stress Increase in stress responsive genes (HMOX1, HMOX2, Cyp1B1, ATM, CCNC, DNAJB4, GADD45A)	[242]
f-CNT (water-soluble)	*In vitro*	Human dermal fibroblasts (HDF)	Dispersion in 1% pluronic F108 surfactant	Cytotoxicity Cell interactions	Lower toxicity with increased sidewall functionalisation Decreased SWCNT fluorescence due to functionalisation In aqueous suspensions, SWCNT precipitate out and selectively deposit and interfere with cell membranes	[221]
f-SWCNT	*In vivo*	Mouse		Intravenous injection Acute and chronic toxicity	Survival, clinical and laboratory parameters reveal no evidence of toxicity over 4 months Histology and Raman spectroscopy demonstrate persistence of SWCNT in liver and spleen macrophages for 4 months without apparent toxicity	[195]
DWCNT	*In vivo*	Soil-dwelling earthworm (Eisenia veneta)	Mixed into dry food	Ecotoxicity	Reproduction (cocoon production) was the most sensitive endpoing and was affected at concentrations > 37 DWCNT/kg food No effects on hatchability, survival or mortality	[392]
SWCNT	*In vitro*	Lung epithelial cells		Oxidative stress	Increased ROS in a time- and dose-dependent manner Decreased glutathione content No involvement of mitochondria in SWCNT induced ROS	[208]

CNT type	*In vitro/in vivo*	Model	Dispersion vehicle and method	Endpoints investigated	Findings and Conclusions	*Ref*
					formation Decreased SOD levels following 24h Decreased ROS following treatment with antioxidants	
HiPco® SWCNT	*In vitro*	Human keratinocytes (HaCaT)	Dispersion in culture medium using short-term sonication	Cytotoxicity Oxidative stress	Loss in cell viability and morphological alterations Cytotoxicity might be due to catalytical effects of iron Accelerated oxidative stress including increased free radical and peroxide generation, depletion of glutathione levels, oxidation of SH-groups and depletionof total antioxidant reserve in vitamin E Oxidative stress might greatly be associated and enhance by the high levels of catalysts present in the SWCNT samples	[31]
HiPco® SWCNT (purified)	*In vivo*	Mouse (female C57BL/6)	Suspension in PBS	Pharyngeal aspiration 1,3,7,28 and 60 days exposure to single bolus dose	Rapid progressive fibrosis and granulomas Dose-dependent increase in expiratory time Increased pulmonary resistance Delivery and deposition of SWCNT in aggregates or dispersed structures Exposure to respirable SWCNT can be risk to develop lung lesionse	[183]

CNT type	*In vitro/in vivo*	Model	Dispersion vehicle and method	Endpoints investigated	Findings and Conclusions	*Ref*
HiPco® SWCNT (purified)	*In vivo*	Mouse (B57BL/6)	Suspension in PBS	Pharyngeal aspiration Role of vitamin E and diet on SWCNT toxicity	Vitamin E-deficient diet caused depletion in antioxidants (α-tocopherol, GSH, ascorbate) and accumulation of lipid peroxidation products SWCNT co-treatment resulted in greater decrease in antioxidant levels which were associated with higher sensitivity to SWCNT-induced acute inflammation and enhance pro-fibrotic responses Vitamin E and therefore diet may be of practical importance in optimizing protective strategies	[373]
HiPco® SWCNT (purified)	*In vivo*	Mouse (adult B57BL/6 and NADPH-oxidase-deficient gp91phox(-/-))	Suspension in PBS	Pharyngeal aspiration Role of NADPH-oxidase on SWCNT toxicity	NADPH oxidase-deficient mice responded with a marked accumulation of polymorphonuclear neutrophils (PMN) Elevated apoptosis of lung cells Production of pro-inflammatory cytokines (TNF-α, IL-6, MCP-1) Decreased production of anti-inflammatory and profibrotic cytokine (TGF-β) Reduction of collagen deposition NADPH-oxidase-derived ROS play a role in determining the course of pulmonary response to SWCNT	[185]
HiPco® SWCNT (purified)	*In vivo*	Mouse (C57BL/6)	Suspension in PBS	Pharyngeal aspiration Effects of sequential exposure to	Sequential exposure amplified lung inflammation and collagen formation SWCNT pre-exposure significantly decreased pulmonary clearance of LM-exposed mice which was associated with	[181]

CNT type	*In vitro/in vivo*	Model	Dispersion vehicle and method	Endpoints investigated	Findings and Conclusions	*Ref*
				SWCNT and bacterial infection with Listeria monocytogenes (LM)	decreased phagocytosis Failure to clear LM led to continued elevation in major chemokines and acute phase cytokines into the later course of infection Co-exposure also led to increased levels of bronchoalveolar lavage neutrophils, alveolar macrophages, lymphocytes and lactate dehydrogenase Enhanced acute inflammation and pulmonary injury with delayed bacterial clearance after SWCNT exposure may lead to increased susceptibility of lung infection in exposed populations	
MWCNT (purified and unpurified; different lengths)	*In vitro*	Human alveolar type II epithelium (A549)	Suspension in sterile water + 0.25% arabig gum using sonication	Cytotoxicity Cell uptake	All materials efficiently internalized in cells MWCNT were more toxic than other NP; toxicity not dependent on length or impurities	[209]
f-SWCNT f-MWCNT	*In vivo*	Mouse (BALB/c)	Suspension in PBS	Intravenous injection Biodistribution (30min, 3h, 24h) Urine analysis (18h)	Water-soluble and 111In-labeled DTPA-SWCNT followed a rapid first-order clearance from the blood through renal excretion without any toxic side effects Intact nanotubes were found in urine	[397]
MWCNT	*In vitro*	Murine alveolar		Cyotoxicity	Cytotoxicity did not appear to be associated with specific	[169]

CNT type	*In vitro/in vivo*	Model	Dispersion vehicle and method	Endpoints investigated	Findings and Conclusions	*Ref*
		macrophages			particle morphologies	
SWCNT	*In vivo* *In vitro*	Bacteria Rat cells Human lymphocytes		Bacterial mutagenicity Genotoxicity	No increase in urinary mutagenicity in rats as studied using the Ames assay No genotoxicity in the micronucleus and sister chromatid exchange assays Mitotic inhibition and cytotoxicity observed in human lymphocyte culture	[249]
MWCNT	*In vivo*	Mouse (male p53(+/-))	Suspension in 0.5% methyl cellulose followed by Tween80 addition, sonication and homogenizing	Intraperitoneal injection of a single dose Carcinogenicity	Induction of mesothelioma Possibility that carbon-made fibrous or rod-shaped micrometer particles may share carcinogenic mechanisms postulated for asbestos	[202]
CNT (purified)	*In vitro*	Blood neutrophils		Cytotoxicity Inflammation	Significant increases in superoxide anion and TNF-α production following cell contact for 1h while cell viability was decreasing	[218]
ArcD SWCNT (different sizes)	*In vivo*	Estuarine meiobenthic copepod (Amphiasus tenuiremis)		Aquatic toxicity Life-cycle effects	Very low toxicity of purified SWCNT, adverse effects only at unrealistic concentrations of 10 μg/ml Copepods ingested SWCNT which formed clusters in the gut and was eventually incorporated in a morphologically altered state into fecal pellets	[393]
SWCNT	*In vitro*	Human dermal fibroblasts	Dispersion in water using short-	Cytotoxicity	SWCNT most effective in reducing cell viability following 5 days exposure	[52]

CNT type	*In vitro/in vivo*	Model	Dispersion vehicle and method	Endpoints investigated	Findings and Conclusions	*Ref*
MWCNT (all purified)		(HDF)	term sonication	Cell adhesion Protein expression	Only SWCNT caused significant decreases in cell adhesion ability and colony formation Cytotoxicty of refined SWCNT from 30 min exposure on No cytotoxicity of unrefined SWCNT Cells detached from substrate and attached to SWCNT bundles instead Following exposure to unrefined SWCNT appearance of ruffles on cell membranes, less homogeneous distribution of p-cadherin and FAK together with nuclei movement towards regions of SWCNT attachement and more random and irregulat distribution of actin Fibronectin, laminin and collagen IV expression was strongly, focal adhesion and cell-cell adhesion protein expression slightly decreased Decrease in protein cyclin D2 No change in B-actin	
SWCNT (laser ablation; pristine)	*In vivo*	Rats (male Crl:CD® (SD)IGS BR)	Suspension in PBS + 1% Tween80	Intratracheal instillation 24h, 1 week, 1 and 3 months exposures	Exposure to high doses produced mortality within 24h post-instillation Pulmonary inflammation with non-dose-dependent granulomas Mechanical blockage of upper airways Foreign tissue body reaction	[179]

CNT type	*In vitro/in vivo*	Model	Dispersion vehicle and method	Endpoints investigated	Findings and Conclusions	*Ref*
SWCNT (purified and un-purified)	*In vitro*	Mesothelioma cells (MSTO-211H)	Dispersion in water + Tween80 followed by sonication and centrifugation	Dispersion effects Cytotoxicity Cell proliferation	All CNT fractions significantly decreased cell activity and proliferation in a dose-dependent manner Suspended CNT-bundles were less cytotoxic than asbestos Rope-like agglomerates induced more pronounced cytotoicity than asbestos Effects seemed to be independent of catalyst residues	[227]
CVD MWCNT	*In vitro*	Humen epidermal keratinocytes (HEK)	Dispersion in culture medium	Protein expression	Altered expression of 36 and 106 proteins following 24h and 48h exposure, respectively Downregulation of 67% of these proteins Alteration of proteins associated with metabolism, cell signaling and stress Effects on the expression of cytoskeletal elements and vesicular trafficking components Identification of proteins reflected a complex cellular response to MWCNT	[224]
SWCNT (non-purified and purified)	*In vitro*	Human alveolar type II epithelium (A549)	Storage in 1% SDS followed by acetone precipitation, resuspension in beidistilled water, sedimentation, centrifugation and culture medium	Cytotoxicity Dye interaction	Interaction between SWCNT and MTT dye No interaction between SWCNT and WST-1 or LDH assay No reduction in mitochondrial viability or membrane integrity No apoptosis or necrosis	[210]

CNT type	*In vitro/in vivo*	Model	Dispersion vehicle and method	Endpoints investigated	Findings and Conclusions	*Ref*
			suspension		No loss in MMP Cellular take-up of SWCNT bundles Accumulation of FAK and actin filaments near SWCNT which adhered onto the cells Cells seemed to detach from culture dish and grow out of plain which could be a possible explanation of granuloma formation seen in vivo.	
SWCNT	*In vitro*	Alveolar epithelial cells		Alveolar epithelial barrier properties Cytotoxicity	Transmonolyer resistance decreased significantly after SWCNT exposure with subsequent recovery No increases in LDH release	[211]
ArcD SWCNT (purified)	*In vivo*	Mouse (male CD-ICR)	Suspension in 1% Tween80	Intravenous injection Biodistribution Long-term accumulation	Long-term retention of SWCNT in mice (> 3 months) Low toxicity Long-term accumulation in liver, lung and spleen Changes in organ indices and serum biochemical parameters Slight inflammation and inflammatory cell infiltration in the lung as seen in histological studies No changes in serum immunological indicators No apoptosis in main organs	[197]

CNT type	*In vitro/in vivo*	Model	Dispersion vehicle and method	Endpoints investigated	Findings and Conclusions	*Ref*
					Toxicity believed to be due to oxidative stress (decreased glutathione and malondialdehyde (MDA) levels)	
SWCNT	*In vitro*	Primary mouse embryo fibroblasts		Cytotoxicity Oxidative stress Genotoxicity	SWCNT less effective in inducing intracellular oxidative stress than ZnO nanoparticles Oxidative stress may be a key route of nanoparticle cytotoxicity SWCNT induced more DNA damage than ZnO as determined by the Comet assay	[246]
Carbon nanofibers (Hat stacked)	*In vivo*	Rats (male Wistar)	Clusters	Implantation into subcutaneous tissue (thoracic region) 1 and 4 weeks exposure to 2 bilateral implants/rat	Normal process of inflammation for foreign bodies without severe inflammatory response observed No acute toxicity in the subcutaneous tissue No inhibition of wound healing Water solubility and characteristic structure composed (were phagocytosed and deliminated)	[191]
f-SWCNT	*In vitro*	Human epidermal keratinocytes (HEK)	Culture medium or pluronic F127 surfactant dispersion	Cytotoxicity Inflammation Ultrastructural changes Dispersion effects	Dose-dependent decrease in cell viability Low concentrations (0.005 μg/ml) have no effect on IL-6 or IL-8 following 1 – 48h exposures; higher doses (50 μg/ml) caused increased IL-6 and IL-8 response No effects on TNF-α, IL-10 or IL-1β Localization of f-SWCNT within intracytoplasmic vacuoles Surfactant treatment resulted in improved dispersion and	[225]

CNT type	*In vitro/in vivo*	Model	Dispersion vehicle and method	Endpoints investigated	Findings and Conclusions	*Ref*
					decreased toxicity	
MWCNT	*In vitro*	Mouse embryonic stem cells (ES)		Genotoxicity	Accumulation in mouse ES Induction of apoptosis Activation of tumour suppressor protein p53 Increased expression of base excision repair protein 8-oxoguanine-DNA glycosylase 1 (OGG1), double strand break repair protein Rad 51, phosphorylation of H2AX histone, SUMO modification of XRCC4 Increased mutation frequency based on the endogenous molecular marker adenine phosphoribosyltransferase (Aprt) Carful evaluation of genotoixicty of nanomaterials needed even for those materials that have been demonstrated to have limited or no toxicity at the cellular level	[247]

Table C.2: Literature review on frequently employed dispersion vehicles for CNT

Dsipersion Vehicle	***Reference***
Cell culture medium	[31, 48, 49, 50, 52, 54, 56, 151, 210, 213, 222, 224, 225, 229, 255, 257, 330, 284, 285]
PBS/saline	[181, 183, 185, 186, 192, 193, 194, 199, 207, 330, 373]
Distilled water/aqueous suspension	[5, 52, 82, 189, 212, 226, 231, 248, 389]
Tween	[113, 173, 175, 179, 197, 223, 227, 330]
Pluronic surfactant	[187, 196, 212, 215, 221, 223, 225]
Sodium dodecylsulfate (SDS)	[174, 235, 236]
DMSO	[167, 169, 228]
Serum	[176, 214, 330]
Triton X-100	[217, 223, 227]
Bovine serum albumin (BSA)	[201, 240]
DPPC	[240, 385]
Air	[139, 188]
BALF	[240]
Gelatine suspension	[204]
Tetrahydrofuran (THF)	[216]
Dimethylformamide	[205]
Serum and plasma wetting	[217]
Trifluoroactic acid	[394]
Polysulfane	[219]
Biomolecule dispersion	[11]
Arabic gum	[209]
Methyl cellulose and Tween	[202]
Natural organic matter	[395]

Table C.3: Literature review on cellular uptake of nanoparticles

NP	Cell type	Uptake	Method	*Reference*
SWCNT	A549	Yes	TEM	[210]
SWCNT	A549	No	TEM	[56]
SWCNT	Macrophages	Yes	TEM, EELS	[216]
SWCNT	A549, HEK293, HeLa, 3T3, 3T6, CHO, Jurkat, MOD-k	Yes	TEM, LSM	[250]
SWCNT	HaCaT	No	TEM, SEM	[31]
SWCNT	HF	No	TEM	[52]
MWCNT	HEK	Yes	TEM, EDS	[50]
SWCNT	Macrophages	Yes	Near-INF	[196]
f-MWCNT	HeLa	Yes	TEM	[396]
SWCNT	Macrophages	Yes	CLSM	[213]
f-SWCNT	Splenocytes	Yes	CLSM	[248]

Appendix D

Supplementary material for Chapter 6

Table D.1: Overview of experiments carried out as part of Chapter 6

Endpoint	Cell line	Particle type	Stimulus						Exposure time [h]
			No	*TNF*	*DPPC*	*DPPC +TNF*	*LPS*	*DPPC +LPS*	
Viability	A549-IL8	H							6
									24
									48
		A							6
									24
									48
	A549-IL6	H							6
									24
									48
		A							6
									24
									48
	A549-TNF-α	H							6
									24
									48
		A							6
									24
									48
	A549-NF-κB	H							6
									24
									48
		A							6
									24
									48
	A549	H							6
									24
									48
		A							6
									24
									48
	NHBE	H							6
									24
									48
		A							6
									24
									48
Promoter activation	A549-IL8	H							6
									24
									48
		A							6
									24
									48
	A549-IL6	H							6
									24
									48
		A							6
									24
									48

	A549-TNF-α	H							6
									24
									48
		A							6
									24
									48
	A549-NF-κB	H							6
									24
									48
		A							6
									24
									48
IL-8 protein release	A549-IL8	H							6
									24
									48
		A							6
									24
									48
	A549	H							6
									24
									48
		A							6
									24
									48
	NHBE	H							6
									24
									48
		A							6
									24
									48
IL-6 protein release	A549-IL8	H							6
									24
									48
		A							6
									24
									48
	NHBE	H							6
									24
									48
		A							6
									24
									48
MCP-1 protein release	A549-IL8	H							6
									24
									48
		A							6
									24
									48

D

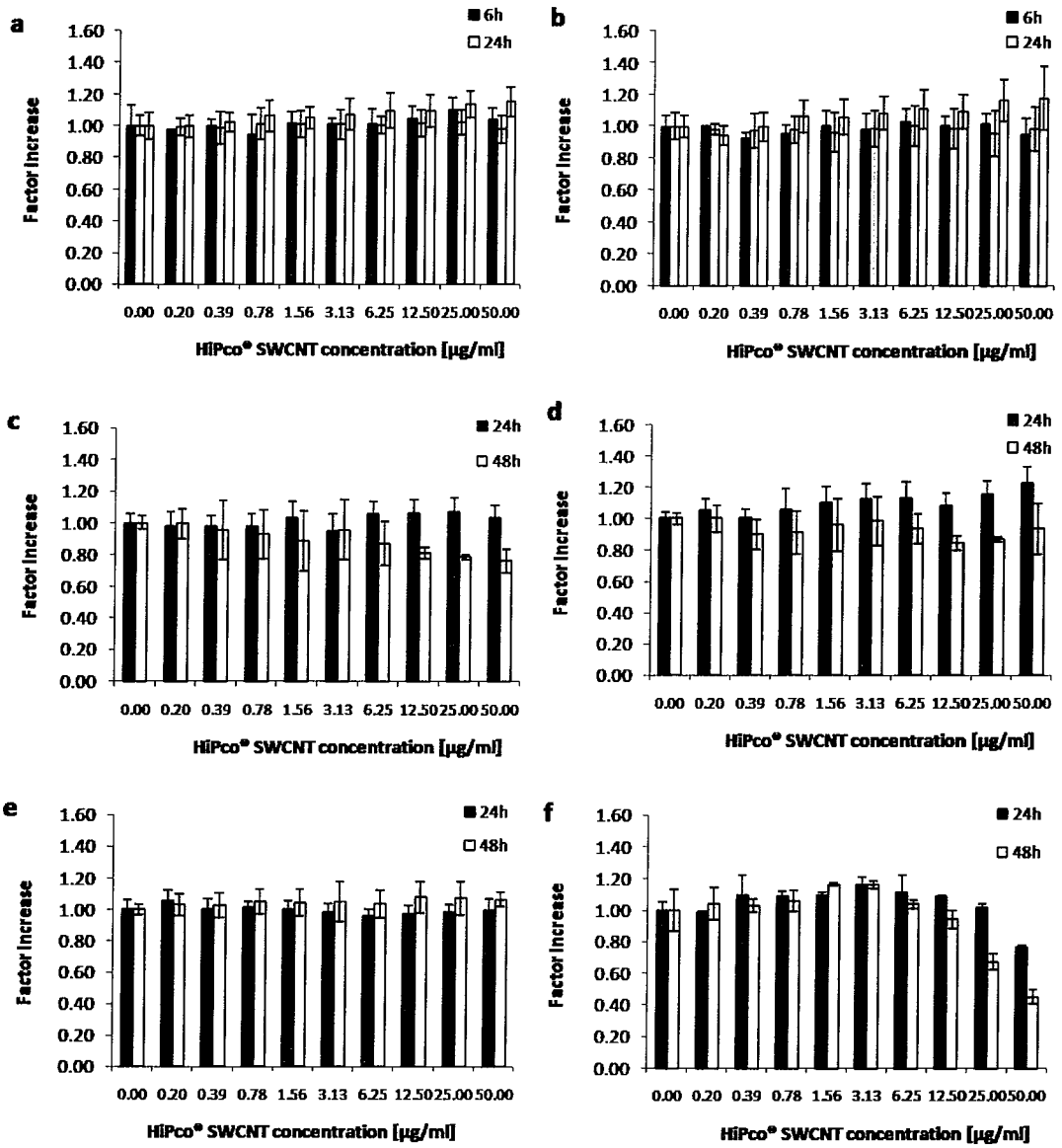

Figure D.1: A549-IL8 cell viability following 6h, 24h and 48h exposure to HiPco® SWCNT dispersed in a. culture medium, b. culture medium +TNF-α stimulation, c. DPPC, d. DPPC + TNF-α stimulation, e. culture medium +LPS, f. culture medium +TNF-α + LPS

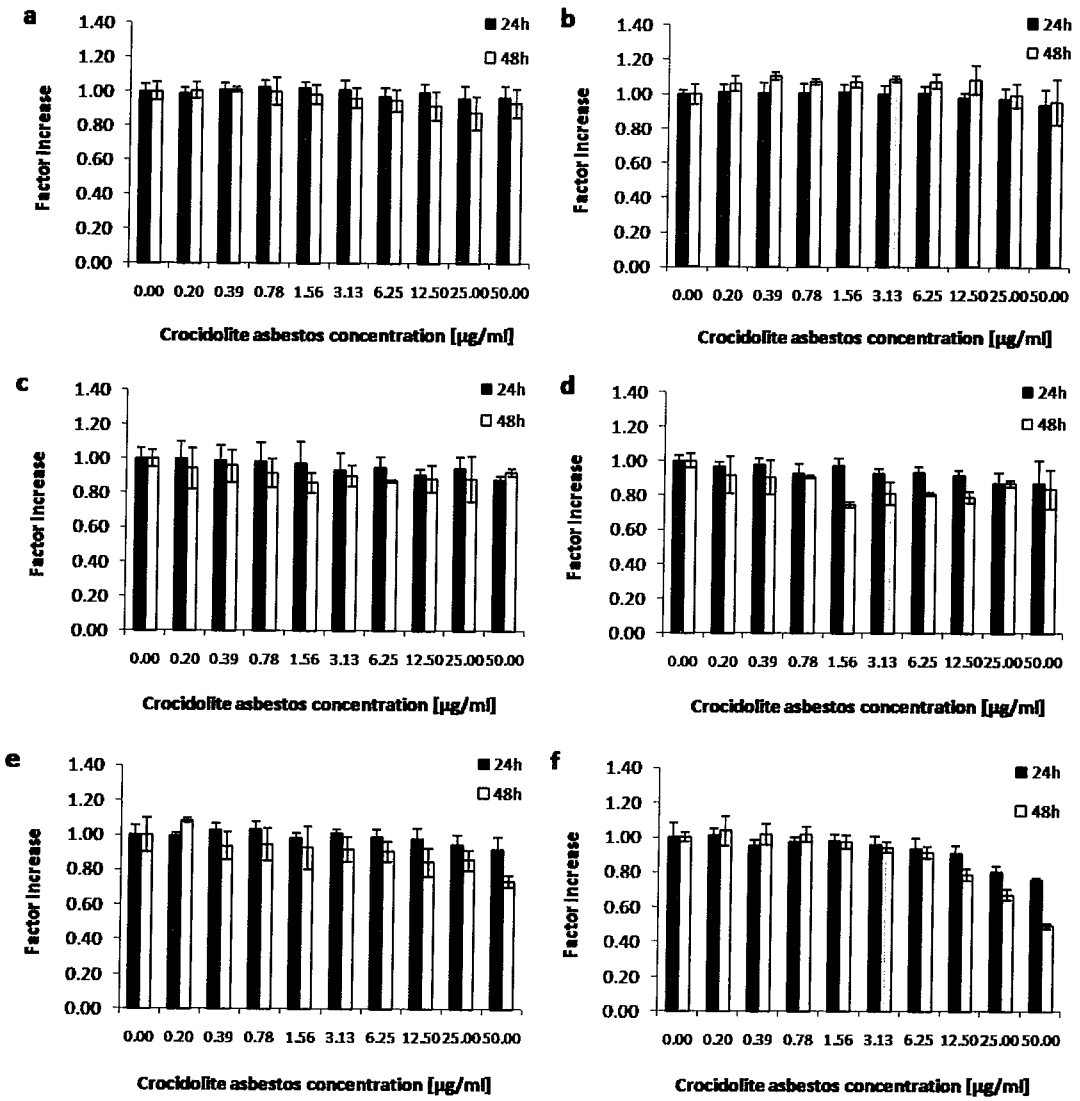

Figure D.2: A549-IL8 cell viability following 24h and 48h exposure to Crocidolite asbestos dispersed in a. culture medium, b. culture medium +TNF-α stimulation, c. DPPC, d. DPPC + TNF-α stimulation, e. culture medium +LPS, f. culture medium +TNF-α + LPS

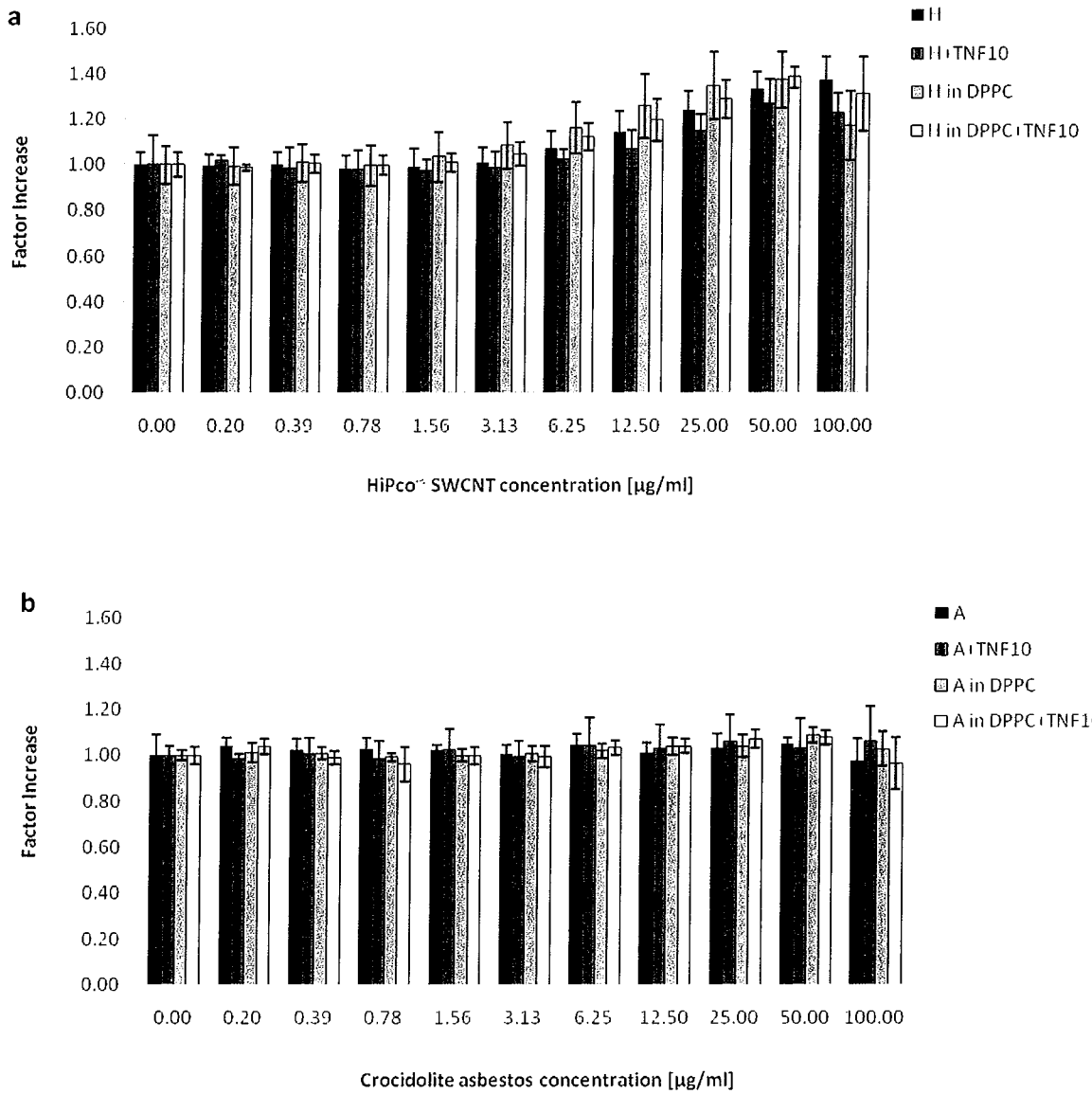

Figure D.3: NHBE cell viability following exposure to HiPco® SWCNT (a) and crocidolite asbestos (b) for 24 h.

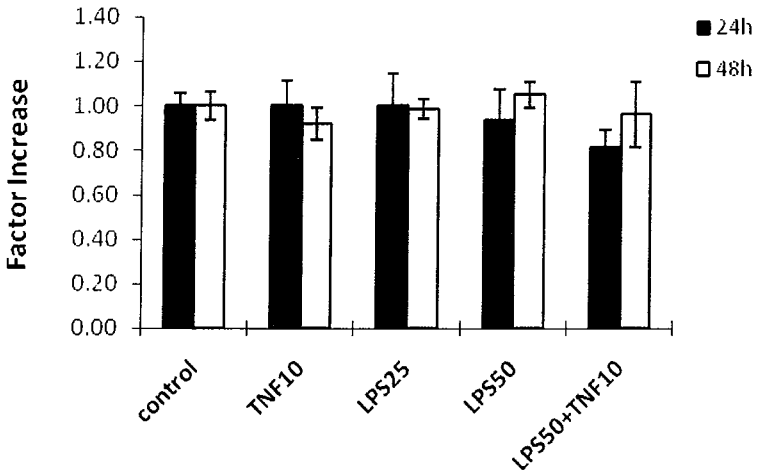

Figure D.4: Cell viability of A549-IL8 cells following 24 and 48h exposure to rh-TNF-α and/or LPS-PA.

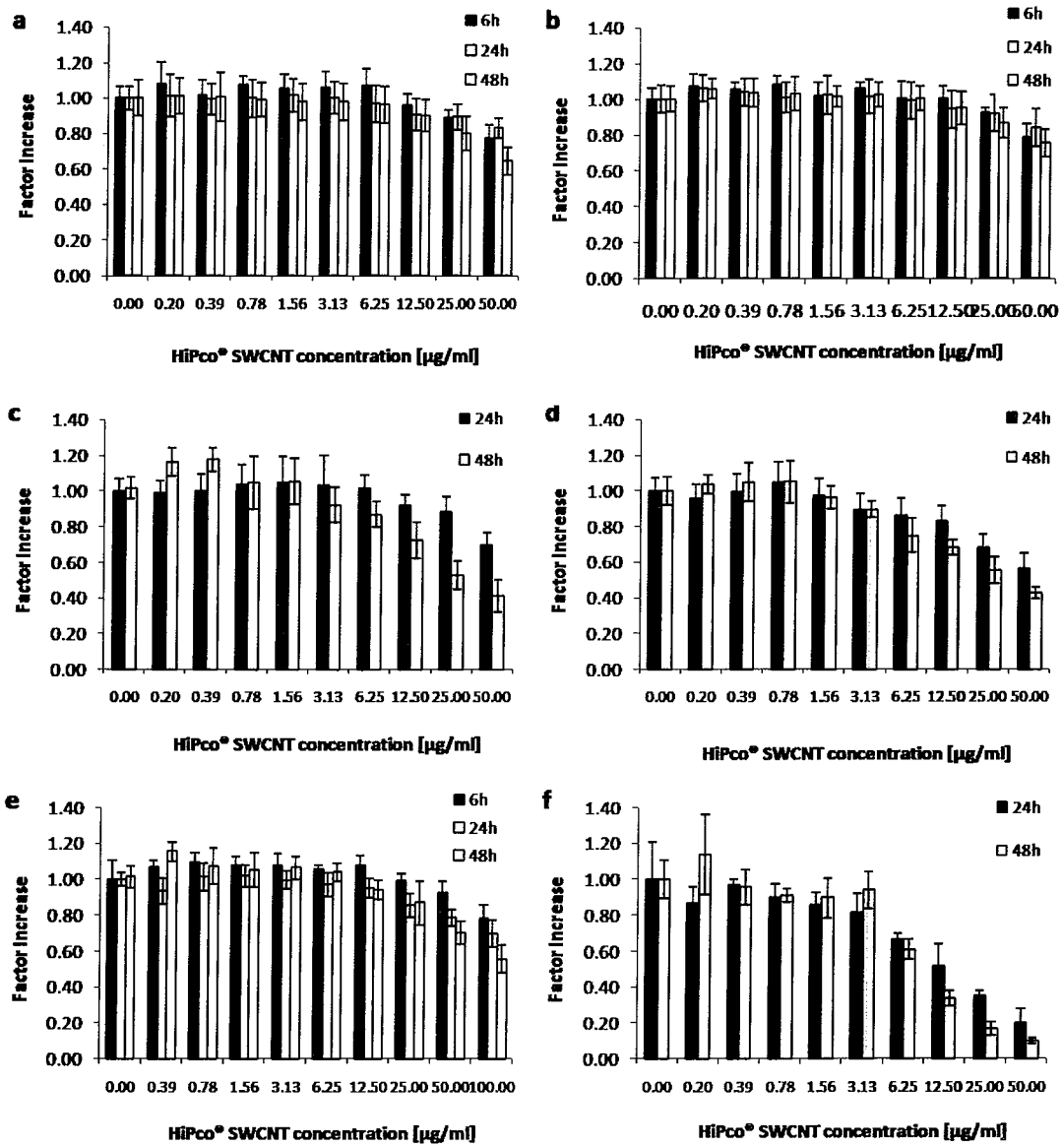

Figure D.5: IL-8 promoter activation following 6h, 24h and 48h exposure to HiPco® SWCNT dispersed in a. culture medium, b. culture medium +TNF-α stimulation, c. DPPC, d. DPPC + TNF-α stimulation, e. culture medium +LPS, f. culture medium +TNF-α + LPS

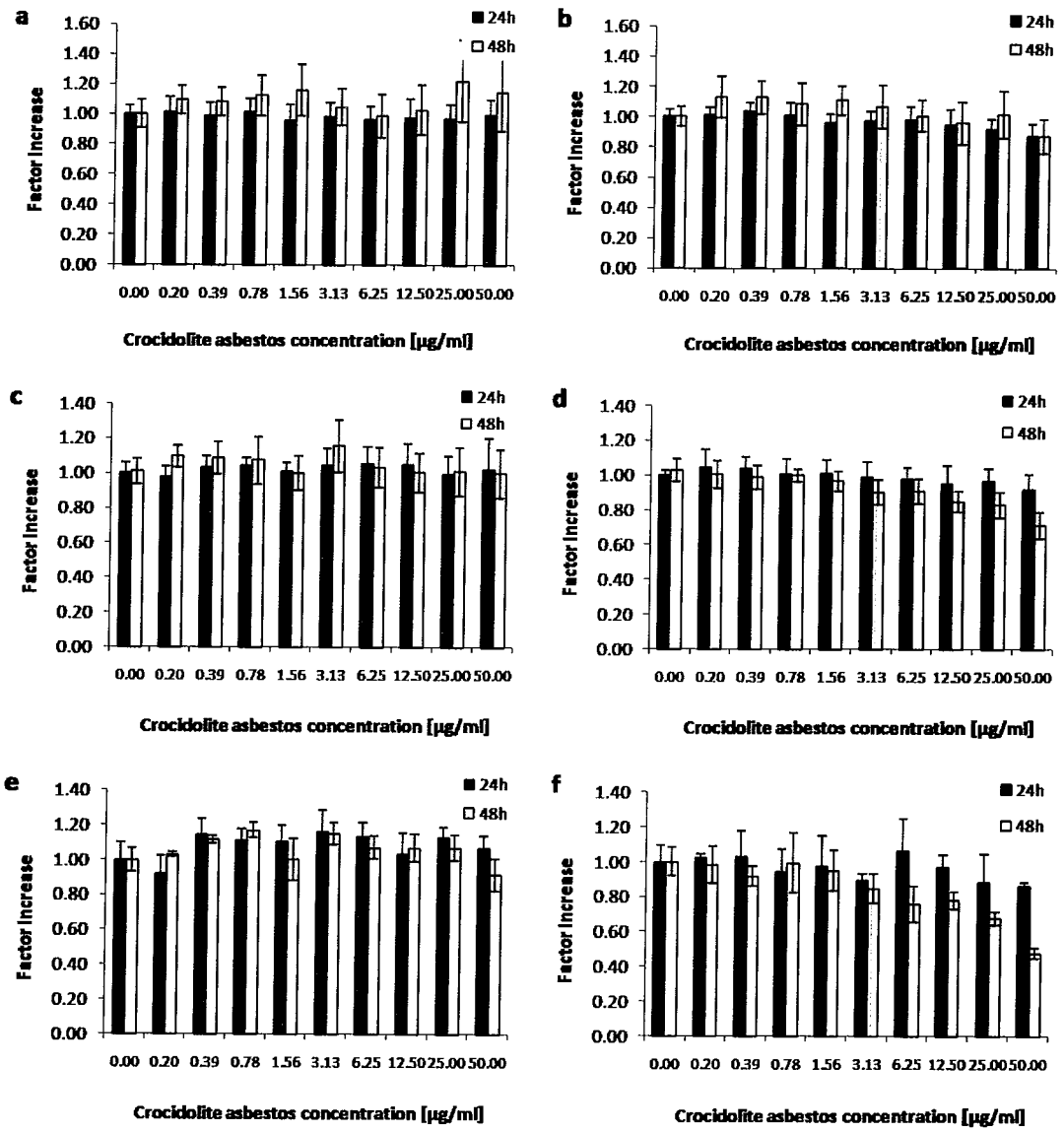

Figure D.6: IL-8 promoter activation following 6h, 24h and 48h exposure to Crocidolite asbestos dispersed in a. culture medium, b. culture medium +TNF-α stimulation, c. DPPC, d. DPPC + TNF-α stimulation, e. culture medium +LPS, f. culture medium +TNF-α + LPS

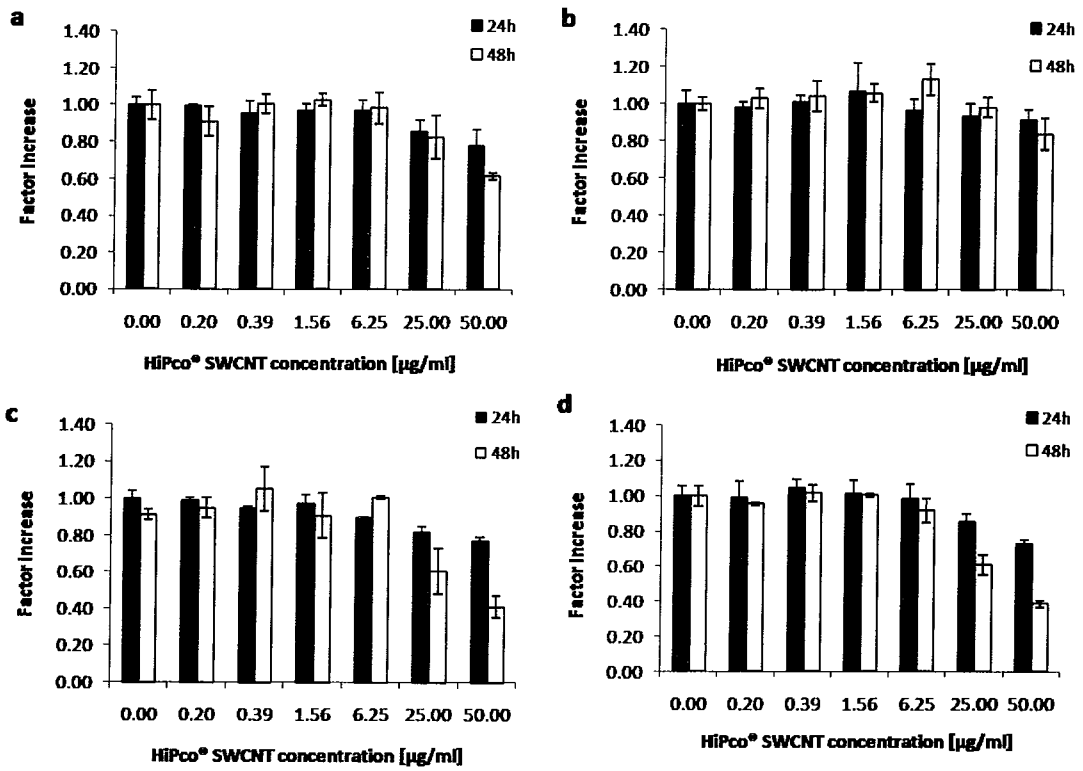

Figure D.7: IL-8 release by A549-IL8 cells following 24h and 48h exposure to HiPco® SWCNT dispersed in a. culture medium, b. culture medium +TNF-α stimulation, c. DPPC, d. DPPC + TNF-α stimulation

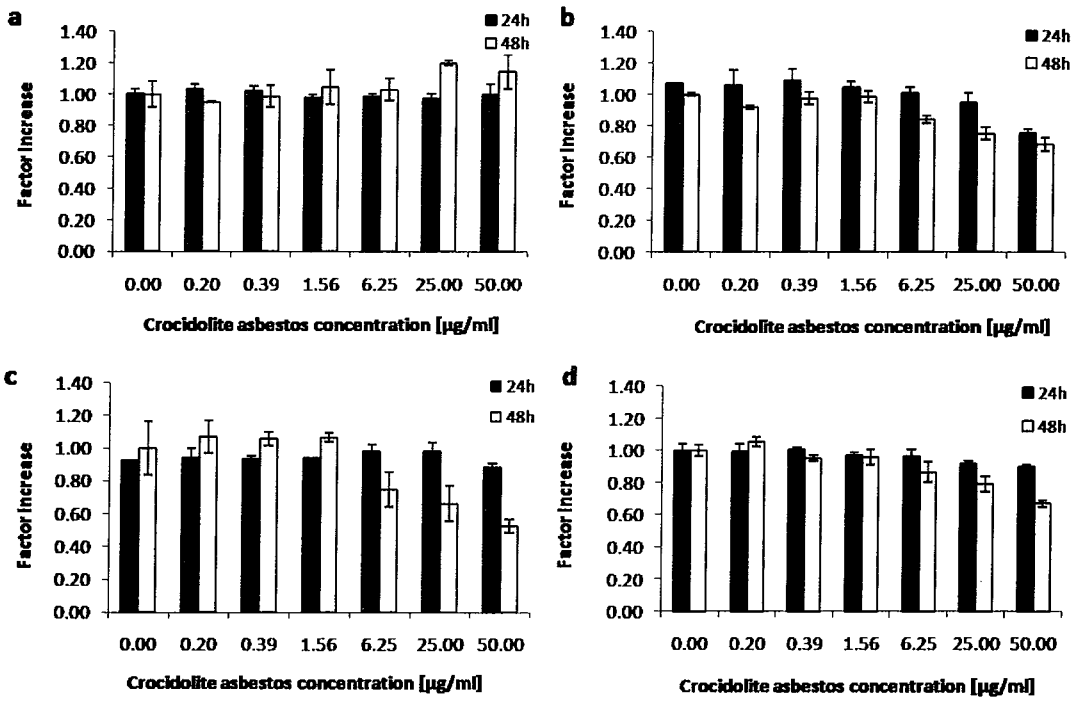

Figure D.8: IL-8 release by A549-IL8 cells following 24h and 48h exposure to Crocidolite asbestos dispersed in a. culture medium, b. culture medium +TNF-α stimulation, c. DPPC, d. DPPC + TNF-α stimulation

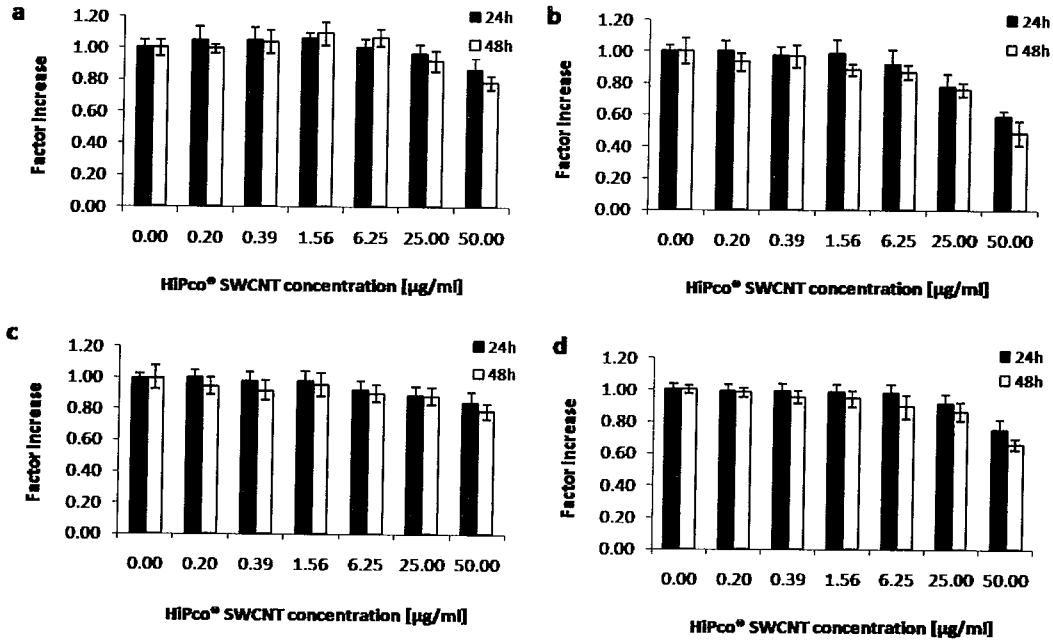

Figure D.9: IL-8 release by NHBE cells following 24h and 48h exposure to HiPco® SWCNT dispersed in a. culture medium, b. culture medium +TNF-α stimulation, c. DPPC, d. DPPC + TNF-α stimulation

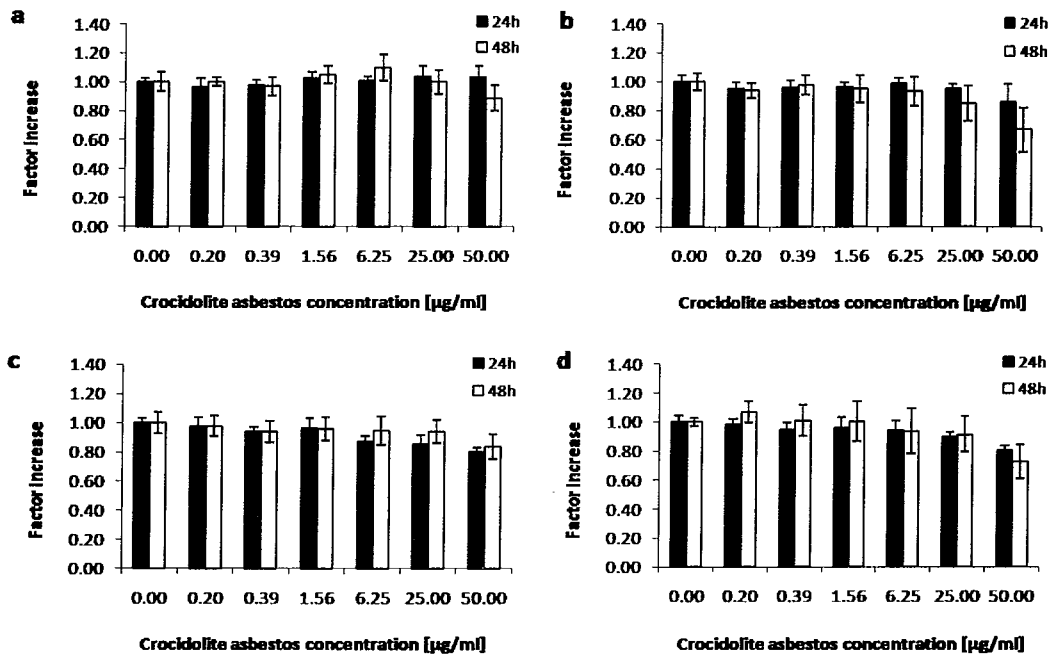

Figure D.10: IL-8 release by NHBE cells following 24h and 48h exposure to Crocidolite asbestos dispersed in a. culture medium, b. culture medium +TNF-α stimulation, c. DPPC, d. DPPC + TNF-α stimulation

Appendix E

Supplementary material for Chapter 7

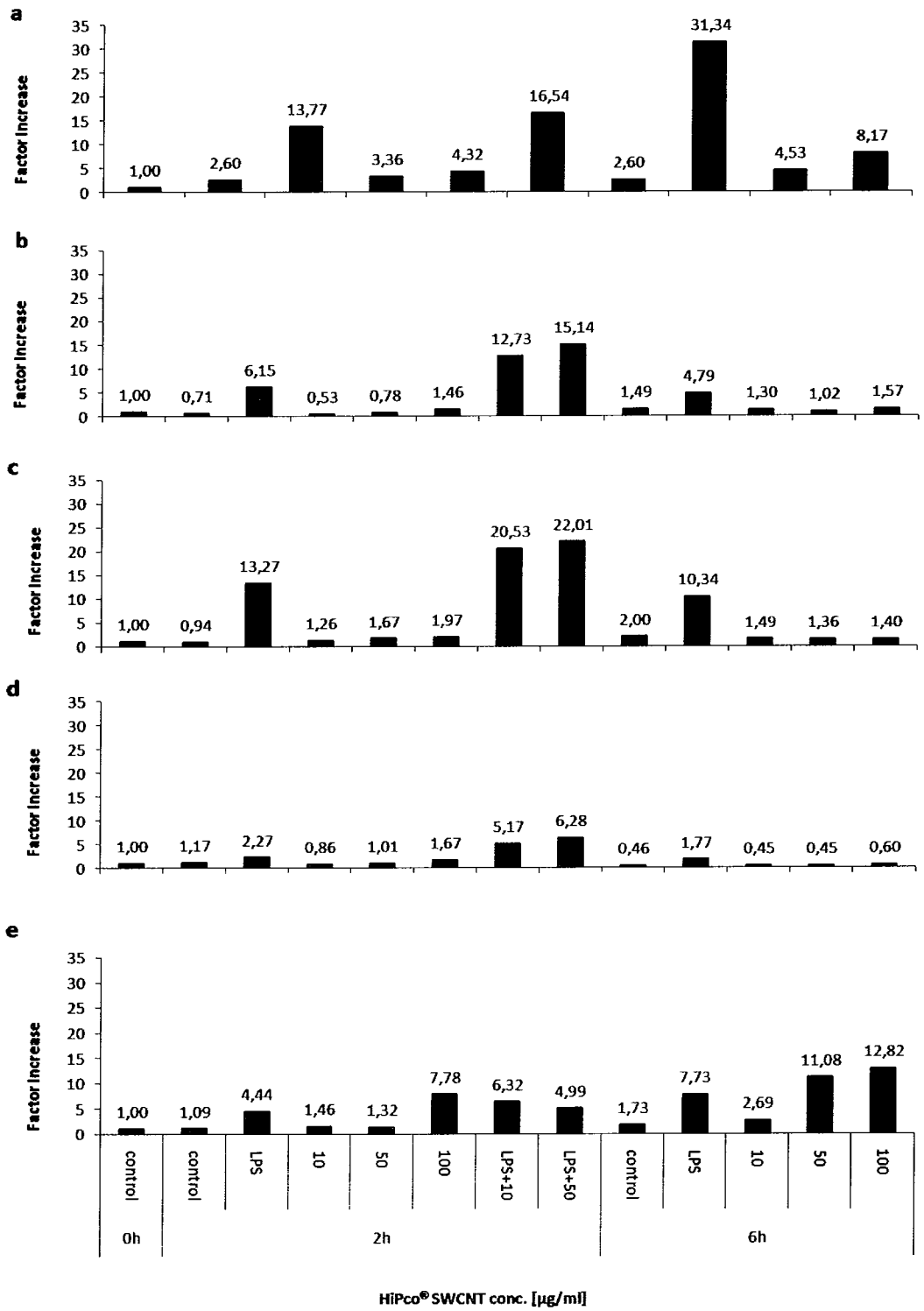

Figure E.1: Changes in IL-8 mRNA expression following exposure of MdM from donor a –e to HiPco® SWCNT for 2 h and 6 h.

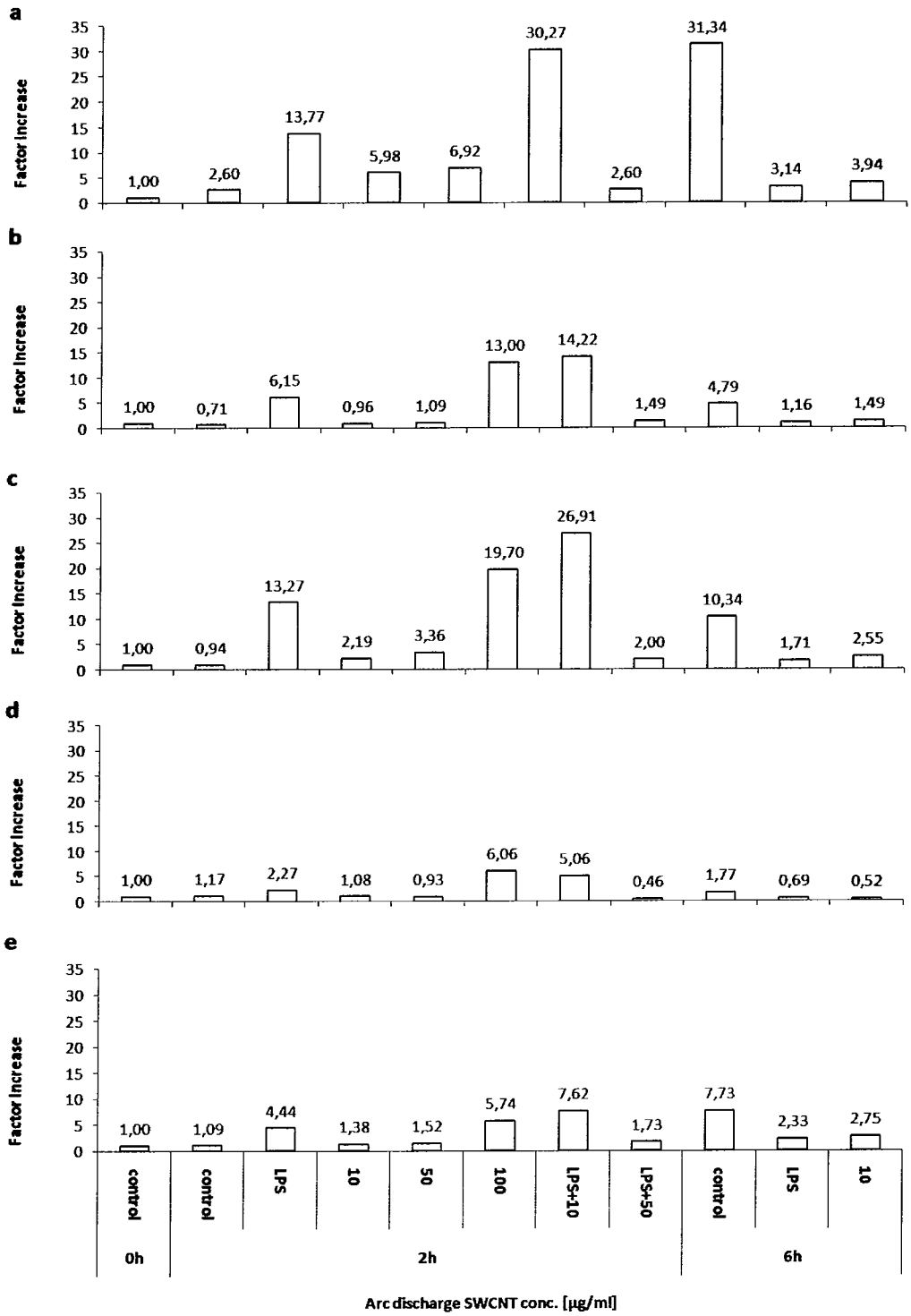

Figure E.2: Changes in IL-8 mRNA expression following exposure of MdM from donor a –e to ArcD SWCNT for 2 h and 6 h.

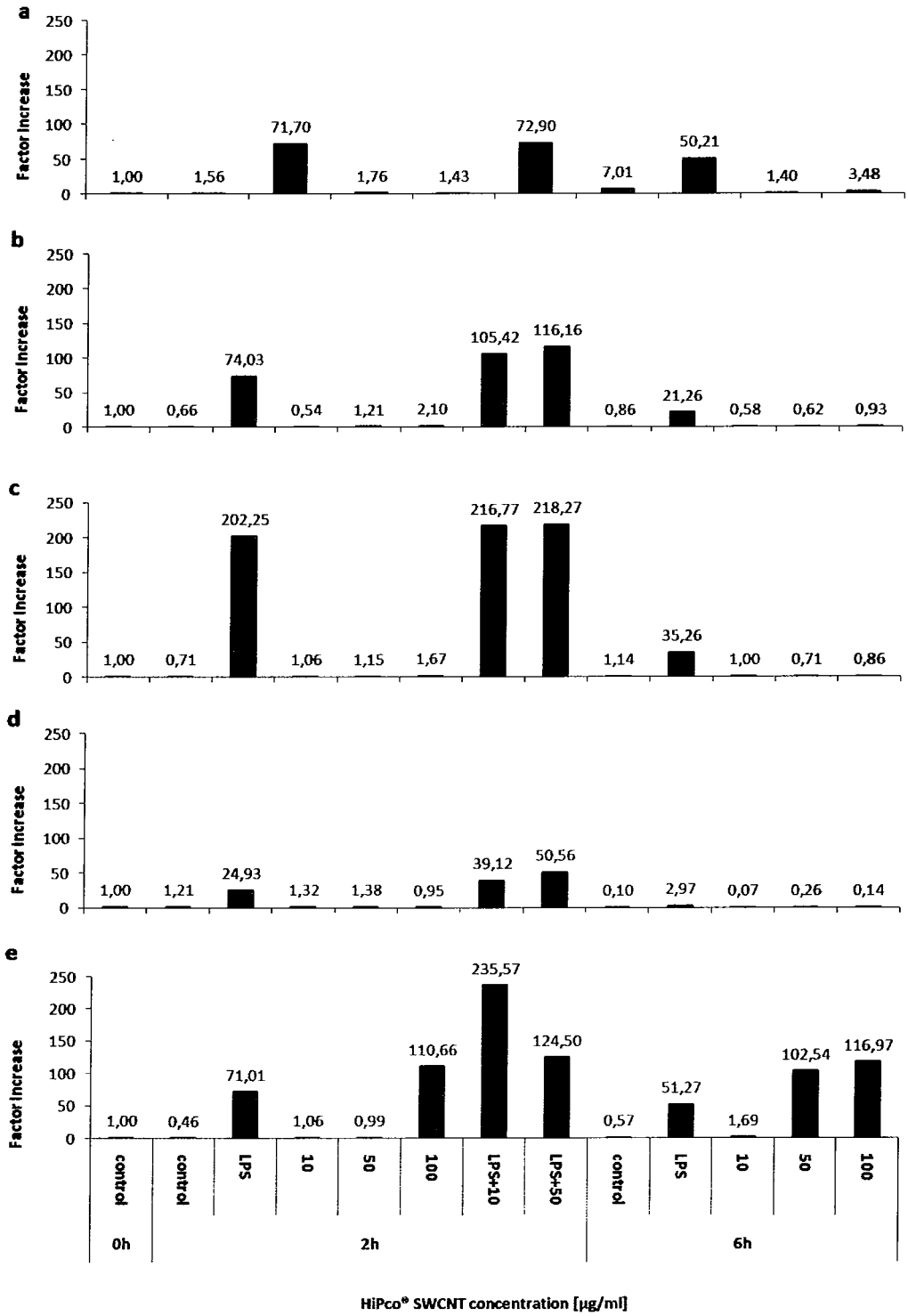

Figure E.3: Changes in COX-2 mRNA expression following exposure of MdM from donor a - e to HiPco® SWCNT for 2 h and 6 h.

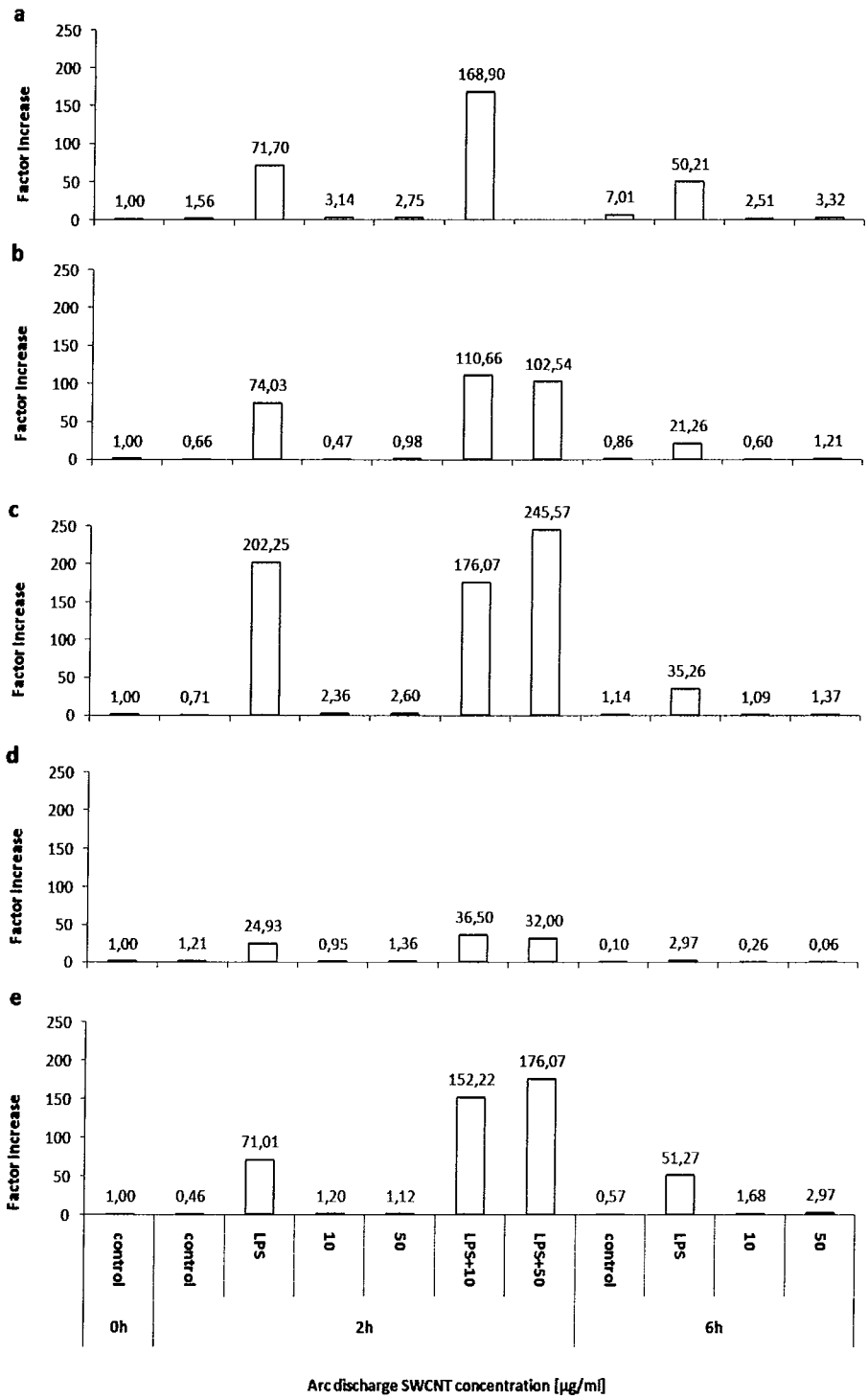

Figure E.4: Changes in COX-2 mRNA expression following exposure of MdM from donor a - e to ArcD SWCNT for 2 h and 6 h.

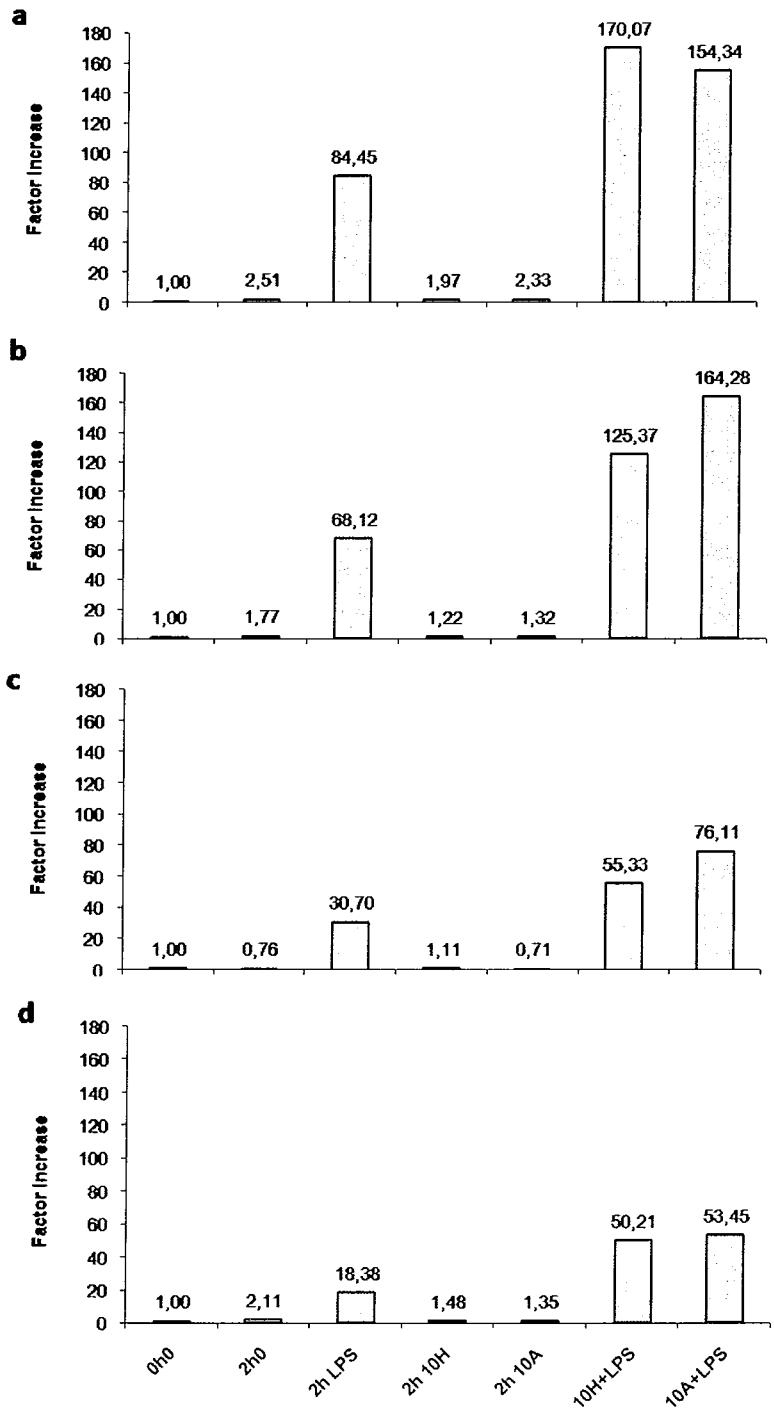

Figure E.5: Effects of HiPco® (H) and ArcD (A) SWCNT exposure on TNF-α mRNA expression of MdM cells from donor a - d following 2 h exposure.

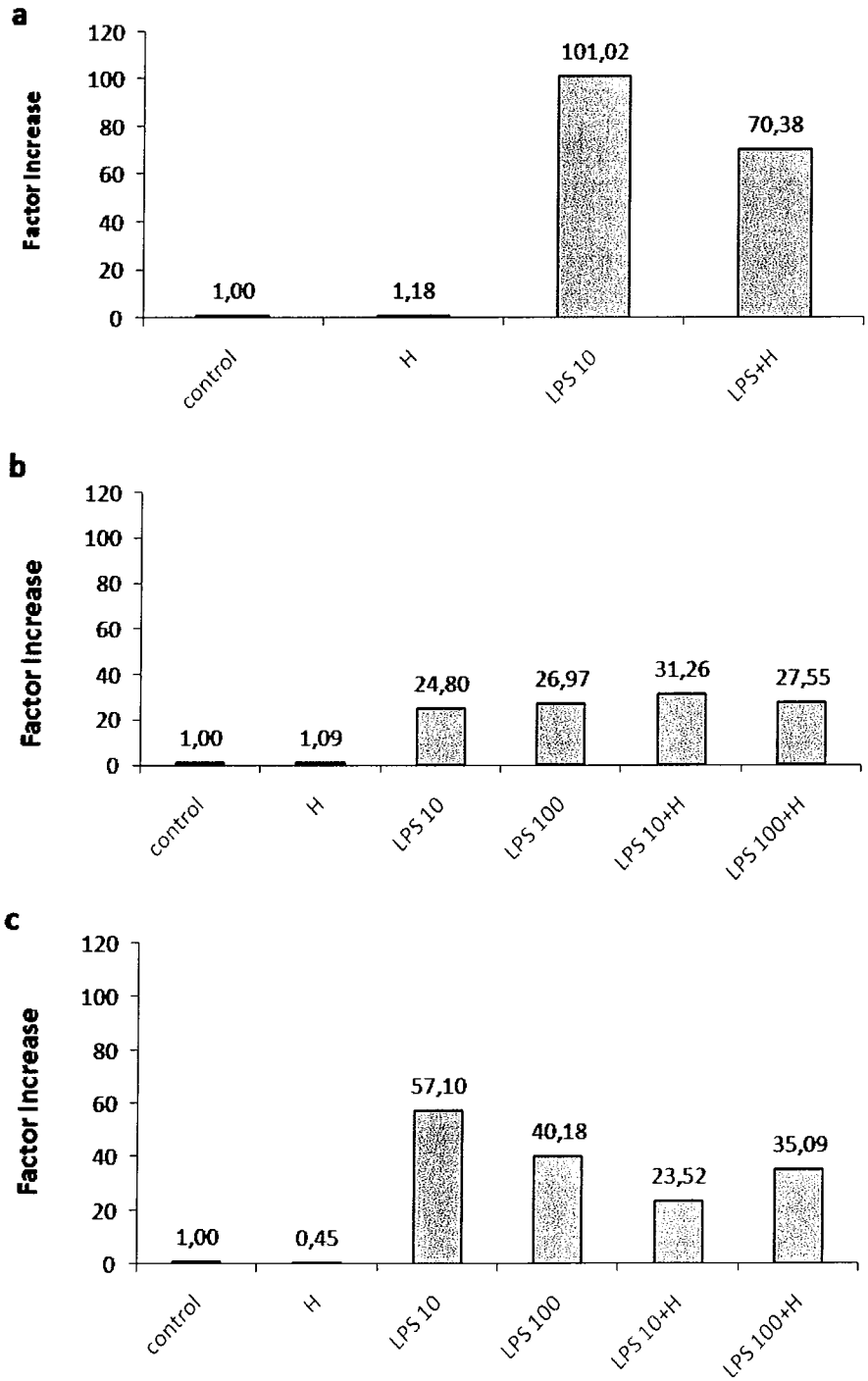

Figure E.6: Intracellular TNF-α protein following exposure of MdM cells derived from donors a - c for 6 h to 50 μg /ml of HiPco® SWCNT (H) with and without co-stimulation with LPS (10 ng/ml and 100 ng/ml) as measured by flow cytometry.

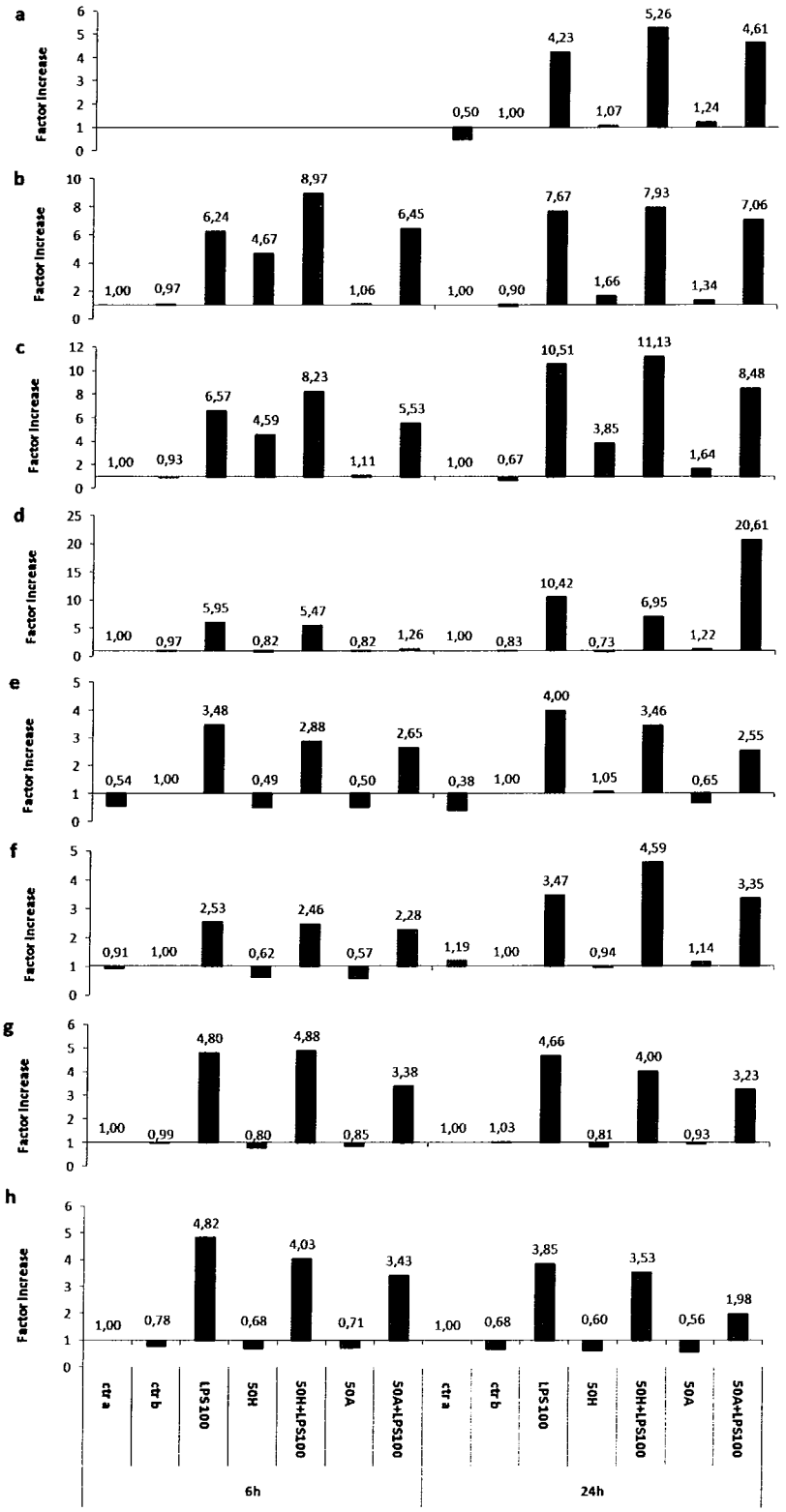

Figure E.7: IL-8 protein release by MdM cells derived from donors a - h following 6 h and 24 h exposure to 50 µg/ml HiPco® (H) or ArcD (A) SWCNT with or without co-stimulation with 100 µg/ml LPS.

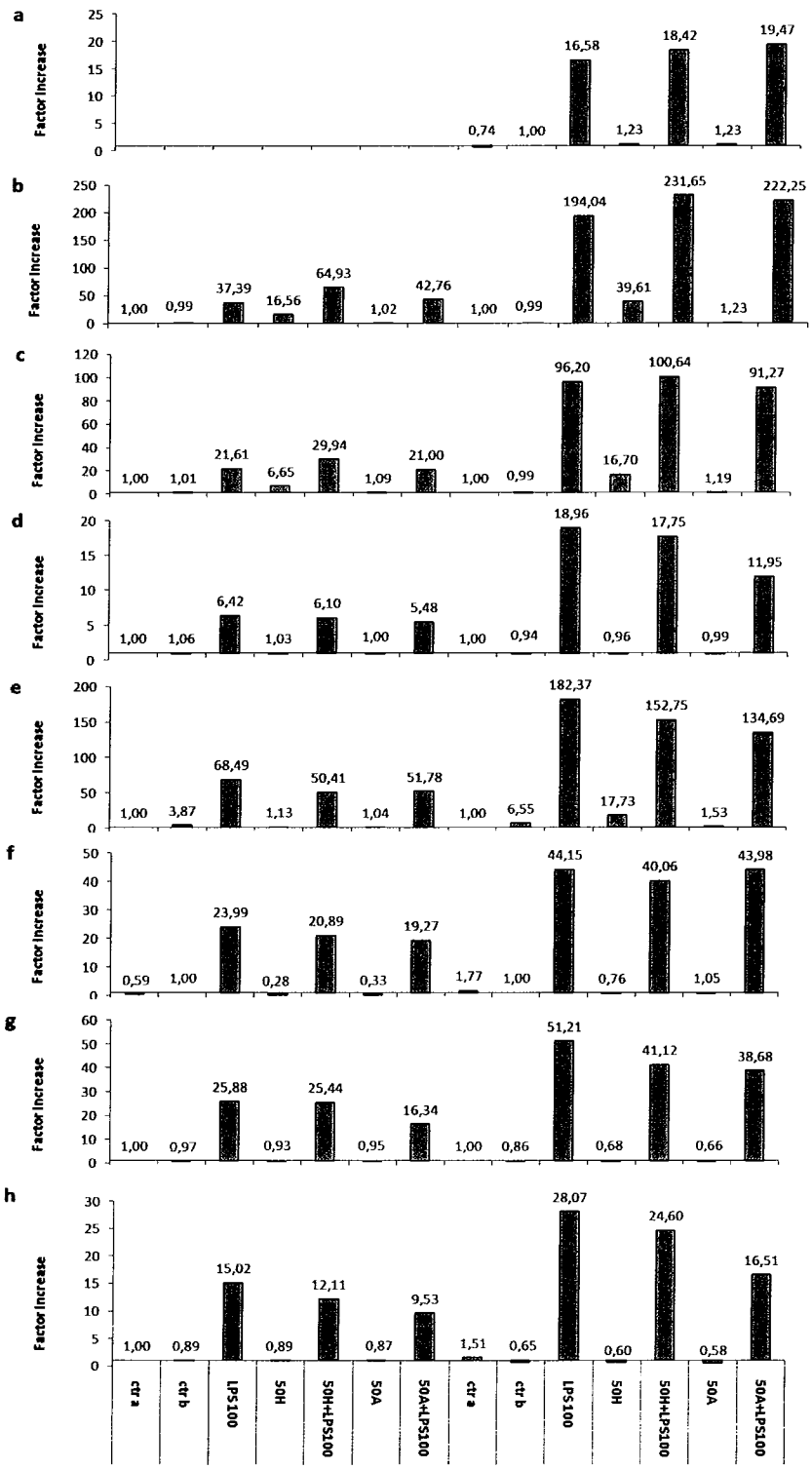

Figure E.8: IL-6 protein release by MdM cells derived from donors a - h following 6 h and 24 h exposure to 50 µg/ml HiPco® (H) or ArcD (A) SWCNT with or without co-stimulation with 100 µg/ml LPS.

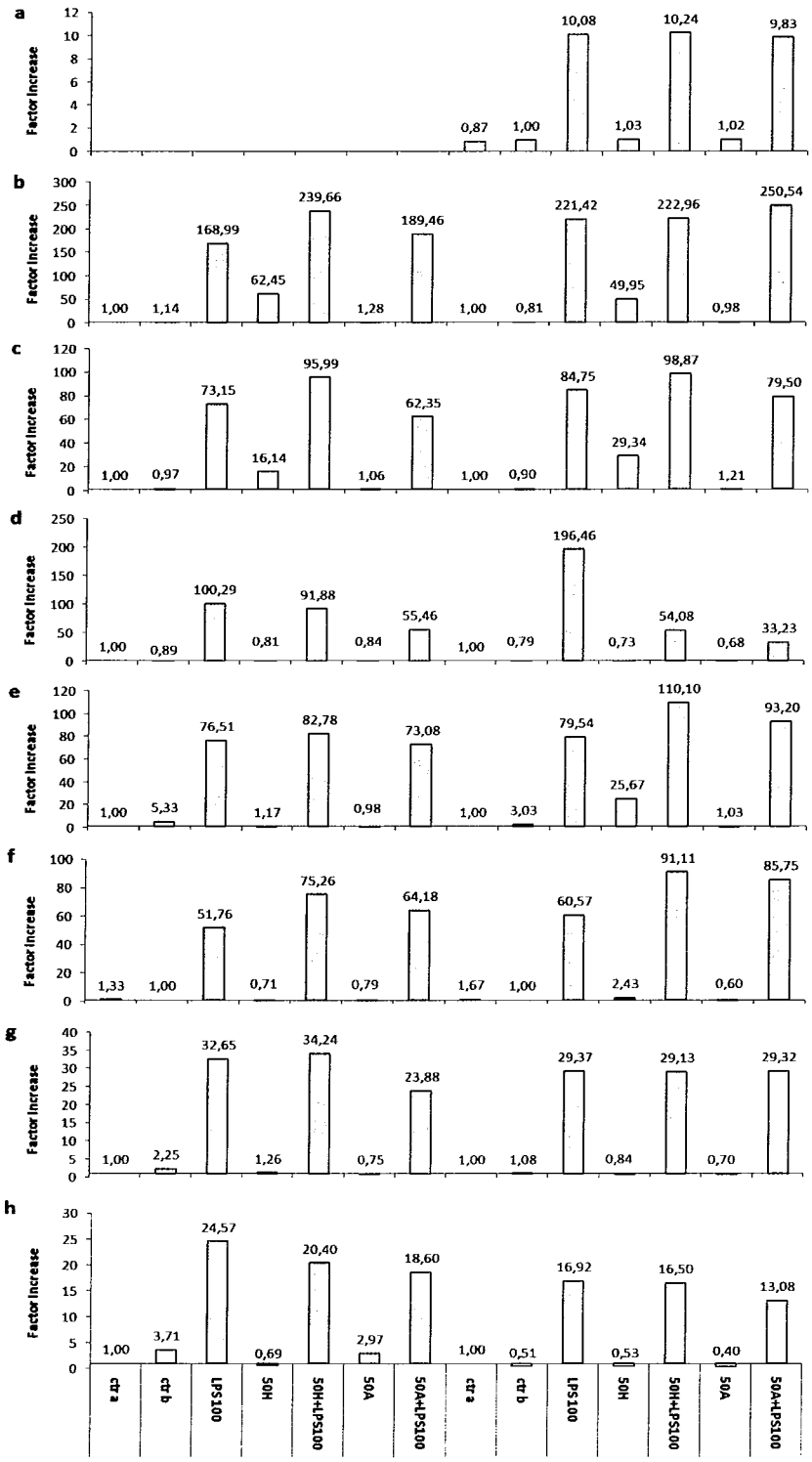

Figure E.9: TNF-α protein release by MdM cells derived from donors a - h following 6 h and 24 h exposure to 50 µg/ml HiPco® (H) or ArcD (A) SWCNT with or without co-stimulation with 100 µg/ml LPS.

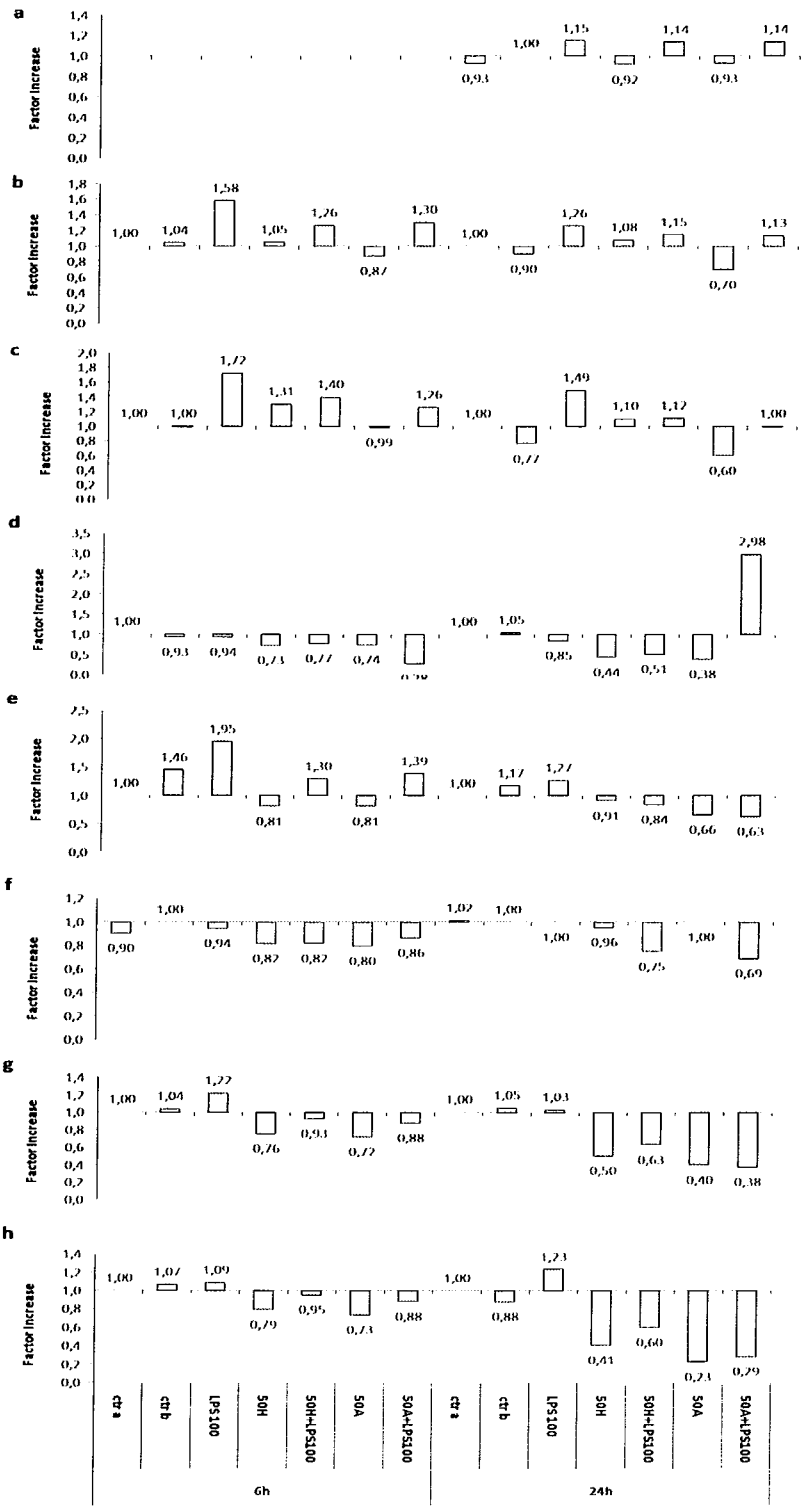

Figure E.10: MCP-1 protein release by MdM cells derived from donors a - h following 6 h and 24 h exposure to 50 µg/ml HiPco® (H) or ArcD (A) SWCNT with or without co-stimulation with 100 µg/ml LPS.